



University of Natural Resources and Life Sciences
Department of Biotechnology
Institute of Applied Microbiology (IAM)

Anti-idiotypic antibody Ab2/3H6
A humanization concept evaluated for
mouse monoclonal antibodies in
therapeutic application

Doctoral Thesis

Submitted by
DI Alexander Mader

Supervisor: Univ.Prof.Dr.DI Kunert Renate

Vienna, August 2011



I Acknowledgements

First I would like to thank professor emeritus Herman Katinger and current head of department Karola Vorauer-Uhl for giving me the opportunity to do my doctoral thesis at the Institute of Applied Microbiology (IAM).

I would also like to acknowledge Renate Kunert for supervision and guidance through the last 3.5 years and to carry on working in this very interesting field.

Further I would like to thank our cell culture technicians Willi Steinfellner as well as Martina Hofbauer and Thomas Sterovsky from Polymun for giving hints and advice in animal cell culture techniques.

I do not want to forget “Chief” Ingo from Polymun for “borrowing” ELISA reagents and Boris Ferko who arranged the rabbit trials.

I would like to mention the “Baculo group”, especially Stefan Gross for sharing instruments and reagents as well as having a good time at occasional social events.

I would also like to acknowledge many colleagues from IAM and Polymun for the pleasant atmosphere at the institute. Thanks to (in alphabetical order) Andreas Maccani, Christian Leitner, David Reinhart, Georg “Schurli” Hinterkörner, Heribert “Q” Quendler, Johannes “Jogi” Pichler, Juan Antonio Hernandez-Bort, Lukas Fliedl, Marion Tschernutter, Matthias “Hackl-Schorsch” Hackl, Stefan “Bleistift” Beisteiner, Veronika Chromikova, and many more ...

I would also like to acknowledge the Austrian Science Fond (FWF) who financed this thesis.

Last, but not least, I would like to thank my girlfriend Jenny for support and having an open ear for me.

Finally, I would like to apologize to those who I forgot to mention. Sorry and thank you too.

II Abstract

Despite decades of intense research no HIV-1 vaccine has been developed so far. The HIV-1 envelope protein harbors several conserved epitopes that are recognized by broadly neutralizing antibodies. One of these neutralizing sites, the MPER region of gp41, is targeted by one of the most potent and broadly neutralizing antibodies, 2F5. Different vaccination strategies and a lot of efforts have been undertaken to induce MPER neutralizing antibodies but little success has been achieved so far. Anti-idiotypic antibodies could represent an alternative vaccination approach in human therapy. The anti-idiotypic antibody Ab2/3H6 was generated in mouse and is directed against the human monoclonal antibody 2F5. Ab2/3H6 is supposed to mimic the antigen recognition site of 2F5 making it a putative candidate for HIV-1 vaccine purposes.

In order to reduce immunogenicity of therapeutic proteins, humanization methods have been developed since more than two decades. The mouse variable regions of Ab2/3H6 were subjected to three different humanization approaches, namely resurfacing, complementarity determining region (CDR)-grafting and superhumanization. Four different humanized Ab2/3H6 variants were developed and characterized for their binding affinity to 2F5 in comparison to the chimeric Ab2/3H6. The resurfaced and the 'conservative' CDR-grafted variants showed similar binding properties to 2F5 when compared to the chimeric version, while the 'aggressive' CDR-grafted antibody showed reduced affinity and the superhumanized type lost its binding ability. Immunogenicity analysis by bioinformatical prediction tools revealed that the humanization methods applied to Ab2/3H6 reduced potential immunogenic epitopes. These results revealed that humanization methods were successfully applied to Ab2/3H6.

Further in a proof-of-concept study, Ab2/3H6 was expressed as antibody fragment fusion protein with C-terminally attached immune-modulators and used for immunization of rabbits to induce HIV-1 antibodies. Collected antisera were affinity purified indicating that only a little amount of the total rabbit IgG fraction contained specific antibodies. The characterization of the induced anti-anti-idiotypic antibodies showed specificity for the HIV-1 envelope protein gp140 and the linear epitope of 2F5 GGGELDKWASL. Interestingly only those rabbits immunized with immunogens fused with the immune-modulators developed the HIV-1 specific antibodies. Despite specificity for the linear epitope and the truncated HIV-1 envelope protein these antibodies were not able to exhibit any virus neutralization activities. These results suggest that Ab2/3H6 alone might not be suitable as a vaccine, but the combination with other immunogens could be beneficial for induction of HIV-1 nAbs.

Keywords: HIV-1 / vaccine / humanization / anti-idiotypic / immunization study

III Zusammenfassung

Trotz intensiver Forschung in den letzten Jahrzehnten ist noch immer kein HIV-1 Impfstoff in Sicht. Wie auch bei andere Viren befinden sich auf dem HIV-1 Hüllprotein konservierte Epitope, die neutralisierende Antikörper induzieren können. Eines dieser neutralisierenden Epitope ist die MPER Region des gp41, welche von dem neutralisierenden Antikörper 2F5 erkannt wird. In der Vergangenheit wurden verschiedenste Impfstrategien erprobt um MPER neutralisierende Antikörper zu generieren, allerdings ohne den großen Durchbruch zu erzielen. Der Gebrauch von anti-idiotypischen Antikörpern in humaner Therapie stellt eine alternative Impfstrategie dar. Der in Maus generierte anti-idiotypische Antikörper Ab2/3H6 ist gegen den humanen monoklonalen Antikörper 2F5 gerichtet und soll erwartungsgemäß die Antigen Erkennungsstelle von 2F5 widerspiegeln. Daher gehört Ab2/3H6 zu möglichen HIV-1 Impfstoffkandidaten.

Um therapeutische Proteine in der Humanmedizin besser nutzbar zu machen, sollten diese möglichst wenig immunogen sein. Aus diesem Grund wurden vor mehr als 20 Jahren Humanisierungsstrategien entwickelt. In dieser Studie wurden an dem von der Maus abstammenden variablen Regionen des Antikörpers Ab2/3H6 drei verschiedene Humanisierungsansätze (Resurfacing, CDR-grafting, Superhumanization) angewandt. Vier verschiedene humanisierte Ab2/3H6 Antikörper Varianten wurden entwickelt und ihre Bindungsaffinität zu 2F5 wurde im Vergleich zu der chimären Version des Ab2/3H6 charakterisiert. Das Bindungsverhalten zu 2F5 war bei der „Resurfaced“ sowie der „conservative CDR-grafted“ Variante vergleichbar mit dem chimären Ab2/3H6, während der „aggressive CDR-grafted“ Antikörper ein reduziertes Bindungsverhalten und die „Superhumanized“ Version keine Binding zu 2F5 zeigte. Die Immunogenität der humanisierten Ab2/3H6 Antikörper wurde mit Hilfe von bioinformatischen Programmen bestimmt, welche vorhersagen, dass potentielle immunogene Epitope reduziert werden konnten. Zusammenfassend wurde hier erfolgreich die Humanisierung des Antikörpers Ab2/3H6 gezeigt.

In einer weiteren Studie wurden versucht HIV-1 spezifische Antikörper in Hasen zu induzieren. Zu diesem Zwecke wurden Antikörper Fragmente des Antikörpers Ab2/3H6 mit Immunmodulatoren am C-terminalen Ende fusioniert und den Hasen intraperitoneal sowie intramuskulär appliziert. Nach der Isolierung der IgG Fraktion aus den Antiseren der Hasen wurde festgestellt, dass spezifische Antikörper nur in geringen Mengen in dieser Fraktion enthalten sind. Die Charakterisierung dieser induzierten anti-anti-idiotypischen Antikörper zeigte spezifische Bindungen gegen das HIV-1 Hüllprotein gp140 und das lineare Epitop von 2F5 GGGELDKWASL. Interessanterweise wurden nur bei jenen Hasen HIV-1 spezifische Antikörper gebildet denen die immunmodulatorischen Fusionsproteine verabreicht wurden.

Trotz dieser Spezifität gegen das lineare Epitop und gp140 zeigten diese induzierten Antikörper keine Virus Neutralisierungsaktivität. Zusammenfassend wurde hier gezeigt, dass Ab2/3H6 alleine nicht als Impfstoff geeignet ist, aber die Verabreichung in Kombination mit anderen Immunogenen könnte Vorteilhaft für die Induktion von HIV-1 neutralisierenden Antikörpern sein.

Schlüsselwörter: HIV-1 / Impfstoff / Humanisierung / anti-idiotyp / Immunisierungsstudie

IV Abbreviations

AIDS	- Acquired Immune Deficiency Syndrome
HIV	- Human Immunodeficiency Virus
μ	- specific growth rate
aas	- amino acids
Abs	- Antibodies
bnAbs	- broadly neutralizing Antibodies
CDRs	- Complementarity Determining Regions
CHO	- Chinese Hamster Ovary
CMV	- Cytomegalovirus
CRFs	- Circulating Recombinant Forms
dhfr	- dehydrofolate reductase
DNA	- Deoxiribonucleic Acid
ELISA	- Enzyme-linked Immunosorbant Assay
Fabs	- Fragment antibodies
FRs	- Framework regions
GI	- Germinality Index
HAART	- Highly Active Antiretroviral Therapy
HACA	- Human Anti-Chimeric Antibody
HAMA	- Human Anti-Mouse Antibody
HARA	- Human Anti-Rat Antibody
HBS	- HEPES Buffered Saline
HC	- Heavy Chain
HLA	- Human Leukocyte Antigen
IgG1	- Immunoglobulin G class 1
IL15	- Interleukin 15
LC	- Light Chain
mAb	- monoclonal Antibody
MD	- Molecular Dynamics (simulation)
MHC	- Major Histocompatibility Complex
MPER	- Membrane Proximal External Region
MTX	- Methotrexate
neoR	- neomycin phosphotransferase
NMR	- Nuclear Magnet Resonance

- NNRTIs** - Non-Nucleoside Reverse Transcription Inhibitors
- NRTIs** - Nucleoside Reverse Transcription Inhibitors
- PEI** - Polyethylenimine
- RNA** - Ribonucleic Acid
- RT** - Reverse Transcriptase
- SDRs** - Specific Determining Regions
- SDS-PAGE** - Sodium Dodecylsulfate - Polyacrylamide Gel Electrophoreses
- SIV** - Simian Immunodeficiency Virus
- SV40** - Simian Virus 40
- TT** - Tetanus Toxin
- vH** - variable Heavy chain
- vL** - variable Light chain
- VLPs** - Virus Like Particles

V Table of content

I	ACKNOWLEDGEMENTS	2
II	ABSTRACT.....	3
III	ZUSAMMENFASSUNG.....	4
IV	ABBREVIATIONS	6
V	TABLE OF CONTENT.....	8
1	INTRODUCTION	10
1.1	HIV AND AIDS.....	10
1.2	HIV-1	11
1.2.1	<i>Virus structure</i>	11
1.2.2	<i>Replication cycle</i>	12
1.2.3	<i>The glycoproteins</i>	13
1.2.4	<i>MPER</i>	15
1.3	HIV-1 THERAPY	16
1.4	HIV-1 VACCINE RESEARCH.....	16
1.4.1	<i>Obstacles in vaccine development</i>	17
1.4.2	<i>Vaccine concepts</i>	17
1.4.2.1	Live Attenuated vaccines.....	18
1.4.2.2	Killed vaccines.....	18
1.4.2.3	Sub-unit vaccines	19
1.4.2.4	Virus like particles.....	20
1.4.2.5	Recombinant vector vaccines.....	20
1.4.2.6	Novel concepts.....	21
1.5	BROADLY NEUTRALIZING HIV ANTIBODIES	22
1.5.1	<i>gp120 specific antibodies</i>	23
1.5.2	<i>gp41 specific antibodies</i>	24
1.6	ANTI-IDIOTYPIC ANTIBODIES.....	26
1.6.1	<i>Ab2/3H6</i>	27
1.7	HUMANIZATION OF THERAPEUTIC ANTIBODIES.....	28
1.7.1	<i>Rational humanization approaches</i>	29
1.7.1.1	CDR-grafting	29
1.7.1.2	Resurfacing.....	30
1.7.1.3	Superhumanization.....	30
1.7.2	<i>Empirical humanization approaches</i>	31

1.7.2.1	Framework libraries	31
1.7.2.2	Framework shuffling	31
1.7.2.3	Humanengineering.....	31
2	AIMS AND RATIONAL OF THE PRESENT THESIS	32
3	TOPICS OF THE THESIS	33
3.1	HUMANIZATION OF AB2/3H6.....	33
3.1.1	<i>CDR-graft of Ab2/3H6</i>	33
3.1.2	<i>Superhumanization of Ab2/3H6</i>	35
3.1.3	<i>Resurfacing of Ab2/3H6</i>	37
3.1.4	<i>Generation of stable cell lines of humanized Ab2/3H6 variants</i>	40
3.1.5	<i>Affinity purification of chimeric and humanized Ab2/3H6 variants</i>	43
3.1.6	<i>Binding characteristics of humanized Ab2/3H6 variants</i>	44
3.1.6.1	The Mix/Match approach	44
3.1.7	<i>Molecular simulation of humanized Ab2/3H6 variants</i>	47
3.1.8	<i>Immunogenicity of humanized Ab2/3H6 variants</i>	47
3.1.8.1	Z-score, G-score and germinality index (GI)	47
3.1.8.2	B-cell and T-cell epitope prediction.....	49
3.2	THE HUMORAL IMMUNE RESPONSE OF AB2/3H6	57
3.2.1	<i>Development of Ab2/3H6 antibody fragment fusion proteins</i>	57
3.2.2	<i>Immunization of rabbits with Ab2/3H6Fab variants</i>	58
3.2.3	<i>Humoral immune response of Ab2/3H6Fab variants in rabbits</i>	58
4	OUTLOOK.....	60
4.1	CONCLUDING REMARKS ON HUMANIZATION OF AB2/3H6	60
4.2	THE POTENTIAL OF AB2/3H6 TO BE USED AS AN HIV-VACCINE.....	61
5	REFERENCES	64
6	FIGURE AND TABLE REFERENCES	89
7	SELECTED PUBLICATIONS	90

1 Introduction

1.1 HIV and AIDS

In 1981 Gottlieb et al. described the first time the clinical picture of an unknown disease which becomes manifested in opportunistic infections and development of cancer combined with reduction of CD4⁺ T-cells in human patients (Gottlieb et al. 1981). This disease should go down in history as acquired immunodeficiency syndrome (AIDS). Two years later the human immunodeficiency virus (HIV), a retrovirus was isolated from the blood of patients suffering from AIDS (Barré-Sinoussi et al. 1983; Levy et al. 1984; Popovic et al. 1984).

The AIDS epidemic remains one of the biggest unsolved health problems worldwide with devastating impact on infected individuals, in different local, social and economic situation. In 2009 33.3 million people were living with HIV, 2.6 million became newly infected and 1.8 million died because of AIDS. Since the outbreak of the pandemic approximately 25 million people died of AIDS related disease (UNAIDS 2010).

HIV is divided into two genetically distinct groups (HIV-1 and HIV-2) which originated from independent transmission events from chimpanzee and the sootey mangabey (Gao et al. 1999). Worldwide, the dominating form is HIV-1 which can be further clustered into four subgroups, M (major), O (outlier), N (non M; non O) (Stebbing and Moyle 2003) and a recently a newly discovered strain was designated group P (pending) (Plantier et al. 2009). The majority of all infections worldwide belong to group M which is further divided into genetically distinct clades A-D, F-H, J, K (Stebbing and Moyle 2003) and circulating recombinant forms (CRFs) resulting of recombination events within different clades (Burke 1997). This classification (Figure 1) is entirely predicted on genotypes and is regularly subjected to changes as new HIV genetic subtypes and CRFs will be discovered in the future due to the strong recombination and mutation ability of HIV-1.

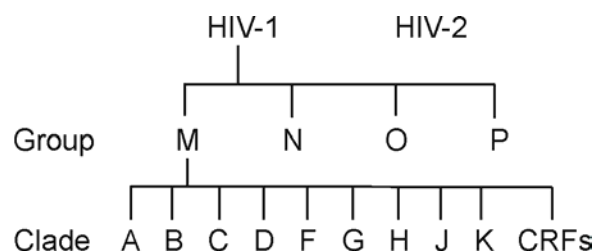


Figure 1. Classification of HIV-1

1.2 HIV-1

1.2.1 Virus structure

The HI-virus is classified as family retroviridae, genus lentivirus. It has an average particle size of 145 nm (Briggs et al. 2003) and consists of nine genes (Table I). Figure 2 represents a schematic graphic of an HIV-1 particle. It is composed of two copies of positive single-stranded ribonucleic acid (RNA) molecules associated with the protein p7, the enzymes reverse transcriptase and integrase. The core is surrounded by a cone-shaped box made up of protein p24. The whole virus particle is enveloped by a lipid membrane of host cell origin which is stabilized by the matrix protein p17 (Table I). The envelope of the virus includes the membrane-spanning gp41 and surface glycoprotein gp120 which are non-covalently associated and presented as a trimeric form in the mature virus (Earl et al. 1990).

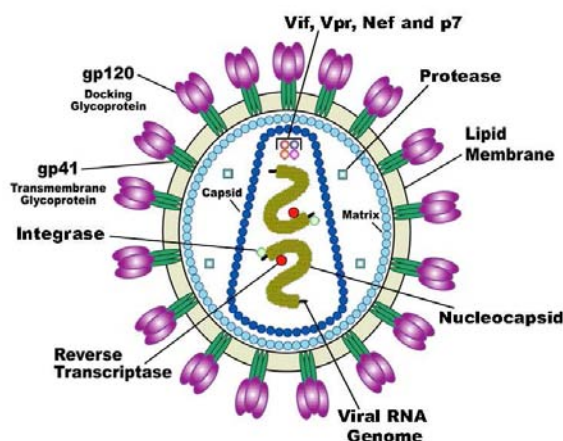


Figure 2. Schematic representation of a HIV-1 particle

Table I. Summary of genes of the HIV-1 genome

gene (protein)	name	Function
gag (pr55)	group specific antigen	encodes for matrix protein (p17), capsid (p24), nucleocapsid protein (p7),
pol (pr160)	polymerase	encodes for protease (p10), reverse transcriptase (p66/p51), integrase (p32)
env (gp160)	envelope	encodes for surface protein (gp120), transmembrane protein (gp41)
tat (p14)	transcriptional transactivator	increases transcription of HIV-1 RNA
rev (p19)	regulator of virion gene expression	transport of HIV-1 mRNA from nucleus into cytoplasm
nef (p27)	negative regulator	pathogen factor, downregulates MHC-I and MHC-II
vif (p27)	viral infectivity factor	disrupts antiviral activity of APOBEC
vpr (p15)	viral protein r	cell cycle arrest, import into nucleus
vpu (p16)	viral protein u	viral budding, release of virions from the cell

1.2.2 Replication cycle

The main target cells of HIV-1 are CD4⁺ T cells, macrophages, monocytes and dendritic cells. Entry of the virus begins with high-affinity attachment of gp120 to CD4 (Figure 3, step 1). Upon binding conformational changes of gp120 allows the chemokine binding domains of gp120 to interact with the chemokine receptor (either CXCR4 or CCR5) of the target cell. This brings the two membranes in closer proximity which allows gp41 to penetrate the cell membrane (Chan and Kim 1998; Wyatt and Sodroski 1998; Selvarajah et al. 2008) (Figure 3, step 2). After membrane fusion the viral single stranded RNA is released into the cytoplasm and transcribed into double stranded deoxyribonucleic acid (DNA) by reverse transcriptase (Figure 3, step 3). The viral DNA transcript is transported into the cell nucleus and is integrated into the host genome by the enzyme integrase (Zheng et al. 2005) (Figure 3, step 4). The provirus either remains dormant in a latent state or initiates replication. Upon viral replication, the integrated provirus is transcribed into messenger RNA which is exported from the nucleus into the cytoplasm, where it is translated into viral proteins which gather at lipid rafts (Mañes et al. 2000; Mañes et al. 2003)(Figure 3, step 5). The final step of the viral cycle starts with proteolytic cleavage of the newly synthesized polyprotein gp160 into the two glycoproteins gp41 and gp120. These are transported to the plasma membrane along with the HIV RNA where they are assembled into virions (Gelderblom et al. 1987)(Figure 3, step 6). Maturation occurs either in the forming bud or in the immature virion after it buds from the host cell by the action of viral protease (Barouch et al. 2000) (Figure 3, step 7).

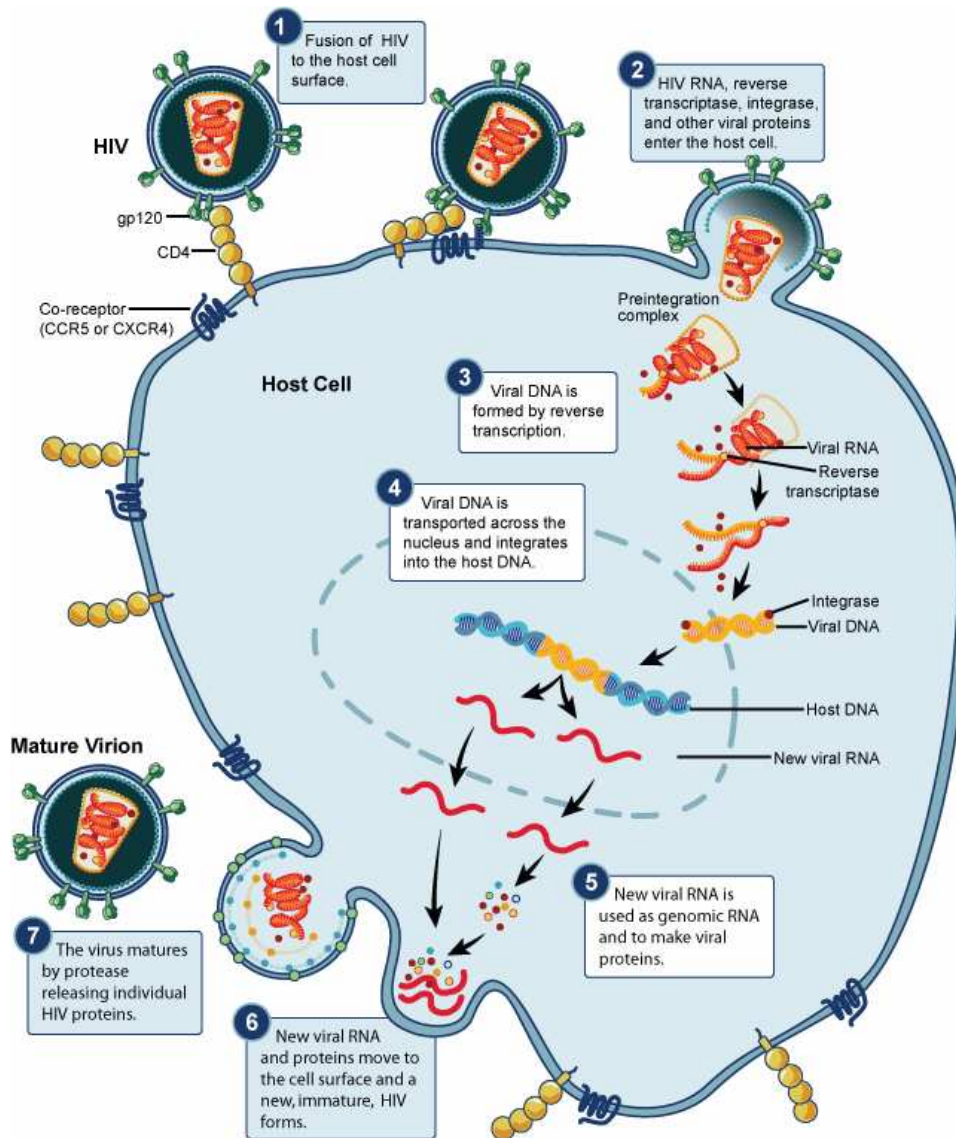


Figure 3. The HIV replication cycle. Refer to text for details.

1.2.3 The glycoproteins

As described in 1.2.2 the envelope protein is synthesized as a precursor (gp160) which trimerizes and is cleaved into two non-covalently associated fragments, the receptor binding fragment gp120 and the fusion fragment gp41. Three copies of each fragment make up the mature viral spike, which contributes to the only antigens on the virion surface (Allan et al. 1985; Veronese et al. 1985). After binding to the primary receptor (CD4) and the coreceptor (CCR5 or CXCR4) gp120 induces large conformational changes resulting in dissociation of gp120 and triggering a cascade of refolding events in gp41 (Harrison 2005; 2008).

Gp120 itself consists of five variable regions (V1–V5) in between more conserved regions (Blouin et al. 1996). V1–V4 form exposed loops anchored at their bases by disulphide bonds (Leonard et al. 1990). The glycoprotein is highly glycosylated, displaying both N-linked and O-linked glycans. The role of O-linked glycans concerning the viral phenotype of both HIV and simian immunodeficiency virus (SIV) is still not fully understood (Chackerian et al. 1997; Huang et al. 1997). In contrast, N-linked glycans have been intensively characterized and the number of sites found in the HIV-1 env gp120 region is around 25 with considerable variation in HIV strains. These sugar moieties are involved in various activities such as metabolism, transport, structural maintenance of the cell and protein, protein folding, recognition of particular cell types and adhesion to other cells (Zhang et al. 2004). The variable regions V1, V2, V4 and V5 are known for rapid shifts in length, number and localization of glycosylation sites (Zhang et al. 2004; Blay et al. 2006). The variable loops shield the more conserved receptor binding regions (Wyatt et al. 1998) which became only accessible upon structural change when the CD4-gp120 binding takes place (Zhang et al. 1999; Rits-Volloch et al. 2006). The N-linked glycosylation of viral envelope proteins, form a "glycan shield", which is one of the major mechanisms for blocking or minimizing virus neutralizing antibody response (Wei et al. 2003). This special glycoprotein configuration promotes viral persistence and immune evasion.

Gp41 consists of three major domains (Figure 4): the extracellular domain or ectodomain, the transmembran domain and the cytoplasmic tail (Gabuzda et al. 1992). During the fusion process gp41 adopts different distinct conformational states. Upon binding of gp120 to the coreceptor, the N-terminal fusion peptide of gp41 translocates and inserts into the target cell membrane. This extended conformation of the protein is referred to as the 'prehairpin intermediate' (Chan and Kim 1998). Further rearrangements involve folding back of the C-terminal heptad repeat 2 region of gp41 into a hairpin conformation, creating a six-helix bundle, which places the fusion peptide and the transmembrane segment at the same end of the molecule. This irreversible refolding of gp41 enables approaching of the viral and the host cell membranes (Chan et al. 1997; Weissenhorn et al. 1997). The conformational differences among these states are so diverse that each of them probably presents its distinct antigenic surfaces to the immune system.

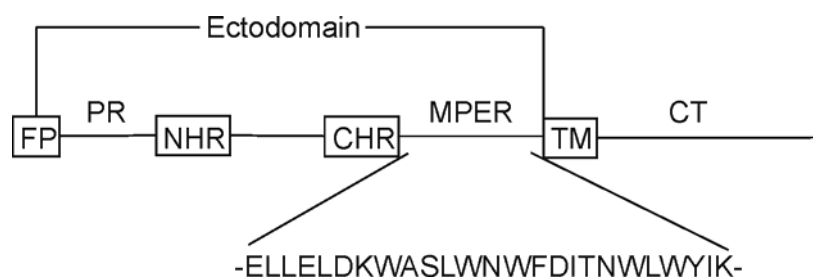


Figure 4. Schematic representation of gp41 domains. **FP:** fusion peptide; **PR:** polar region; **NHR:** N-terminal heptad repeat; **CHR:** C-terminal heptad repeat; **MPER:** membrane proximal external region; **TM:** transmembrane domain; **CT:** cytoplasmic domain

1.2.4 MPER

The membrane proximal external region (MPER) is a tryptophan-rich, 24 amino acids long region, located at the C-terminal end of the gp41 ectodomain (Figure 4). It is crucial for the proper functioning of gp41 as a fusion protein (Salzwedel et al. 1999) but the exact mechanism on how the MPER is involved in the fusion process is still unclear. The MPER is highly conserved, and contains epitopes that are recognized by three HIV-1 broadly neutralizing antibodies (bnAbs) making it very attractive as a vaccine target (Muster et al. 1993; Purtscher et al. 1994; Salzwedel et al. 1999; Zwick et al. 2001).

The actual structure of the MPER is not definitely solved. It was originally predicted as an α -helical structure (Gallaher et al. 1989), which was confirmed by three independent crystallographic studies of this region (Chan et al. 1997; Tan et al. 1997; Weissenhorn et al. 1997) and later supported by nuclear magnet resonance (NMR) structure studies (Schibli et al. 2001; Biron et al. 2005). However structural determination of monoclonal antibody (mAb) 2F5 with a 7-mer peptide ELDKWAS (Pai et al. 2000) and with a 17-mer peptide, EKNEQELLELDKWASLW (Ofek et al. 2004), revealed that this region of the MPER forms an extended conformation with a distinct β -turn. It is thought that these structural differences in the MPER could be related to the overall gp41 structural changes that occur during fusion and the possibility that the MPER undergoes a structural transition during fusion from an extended conformation to a helical structure (Barbato et al. 2003). These observations support the idea of MPER flexibility (Granseth et al. 2005) which could be the reason for its poor immunogenicity in neutralization studies (Ofek et al. 2004; Cardoso et al. 2005; Luo et al. 2006; Phogat et al. 2008).

1.3 HIV-1 therapy

Currently there is no cure available for HIV infection. Without therapy, the average survival time after infection is estimated to be nine to 11 years, depending on the HIV subtype (UNAIDS 2010). Death normally occurs from opportunistic infections or malignancies associated with the progressive failure of the immune system (Lawn 2004), within a year after the individual develops AIDS symptoms (Morgan et al. 2002). The development of highly active antiretroviral therapy (HAART) reduced the death rate from AIDS related diseases by 80 %, and raised the life expectancy for a newly diagnosed HIV-infected person to 20–50 years (Knoll et al. 2007; Collaboration 2008).

Current HAART therapeutics are combinations consisting of at least three drugs belonging to two types of antiretroviral agents. These classes are two nucleoside analogue reverse transcriptase inhibitors (NRTIs) plus either a protease inhibitor (PIs) or a non-nucleoside reverse transcriptase inhibitor (NNRTIs). Other classes of drugs such as entry inhibitors or integrase inhibitors provide treatment options for patients infected with viruses already resistant to common therapies. More than 20 HIV-1 treatment drugs have been approved¹ by the FDA until to date and more than ten are in clinical trial phase II/III².

However HAART neither cures the patient nor removes all symptoms and if the treatment is stopped, often highly HAART-resistant HIV-1 levels return (Martinez-Picado et al. 2000; Dybul et al. 2002). In general HAART improves health and quality of life of HIV-infected individuals and leads to a significant reduction in HIV-associated morbidity and mortality in the developed world (Chêne et al. 2003; Wood et al. 2003). However, anti-retroviral drugs are expensive, and infected individuals in developing countries do not have access to medications and treatments for HIV and AIDS. Research to improve current treatments includes decreasing side effects of current drugs, further simplifying drug regimens to improve efficiency, and determining the best sequence of regimens to manage drug resistance. Unfortunately, only a vaccine is thought to be able to control the pandemic. This is because a vaccine would be cheaper and being affordable for developing countries since it would not require daily treatment (Ferrantelli et al. 2004).

1.4 HIV-1 Vaccine research

Despite intense research in the last 25 years, an effective HIV-1 vaccine is still not available. HIV-1 has turned out to employ various strategies to avoid elicitation of neutralizing antibodies as well as to evade the few that might have evolved during infection. In the following paragraphs the main obstacles in HIV-1 vaccine development will be addressed.

¹ www.fda.org

² www.clinicaltrials.gov

1.4.1 Obstacles in vaccine development

One of the major evasion strategies of HIV-1 is its high mutation rate. Retroviral reverse transcriptase (RT) does not have an exonuclease proof reading activity and for HIV-1 RT it has been found that up to ten errors per genome and replication cycle are incorporated in vivo (Preston et al. 1988; Roberts et al. 1988). Because of the extremely high replication rate of 10×10^9 virions per day (Perelson et al. 1996) the virus undergoes a rapid evolution in an infected patient. Although only a small number of new and functional virions result from the high mutational rate, enough mutants are generated to escape the humoral immune response or chemotherapeutical pressure (Burton et al. 2005). Furthermore the defective and non infectious particles overload the immune system by displaying irrelevant epitopes (Poignard et al. 2003) leading to exhaustion and immunosenescence of the immune system (Gotch et al. 2001; Appay and Rowland-Jones 2002).

A common feature of all retroviruses is the integration of the transcribed viral DNA into the host cell genome. The provirus stays latent for extended periods of time and duplicates in parallel to cellular division. In this state the virus is invisible for the immune system. HIV-1 integrates rather fast into the genome of the host cell and establishes latency within days to weeks after infection. Therefore the time window of opportunity where HIV-1 remains vulnerable to eradication through the immune system is very short (Chun et al. 1998).

Another evasion mechanism of HIV-1 is its invisibility from the host immune system by acquisition of host cell derived proteins during budding from the host cell membrane. Some of these proteins (CD55 and CD59) are known to protect the virus from the immune complementary system (Stoiber et al. 1996). Additionally the virus surface is covered with unspecifically bound serum proteins (McMichael 1998).

However, the most accessible molecules for stimulation of the host immune system are the envelope proteins gp120 and gp41 (Montero et al. 2008). But the immunogenicity of several potential conserved and neutralizing epitopes is impeded either by the heavy glycosylation which forms a shield silencing the immunogenic protein or by the structural changes of the envelope trimer which adopts a quaternary conformation that effectively shields neutralization-sensitive domains (Rusert et al. 2011).

1.4.2 Vaccine concepts

So far protective immunity to HIV-1 has only been achieved by a passive immunization strategy in animal models by infusion of bnAbs (Mascola et al. 1999; Baba et al. 2000; Mascola et al. 2000; Hofmann-Lehmann et al. 2001a; Hofmann-Lehmann et al. 2001b).

Although these studies provided proof-of-concept of the protective effects of bnAbs an active and effective prophylactic vaccine will be the most elegant and safe way to fight the global HIV pandemic.

In 1987 the first phase I trial of an HIV-1 vaccine was conducted (Ezzell 1987). Since then more than 60 candidates have been tested in over 200 phase I/II trials and three phase III trials worldwide³. These vaccine candidates can be clustered into groups, aiming to induce bnAbs, typically using soluble recombinant proteins or focusing on the stimulation of CD8⁺ T-cell response, using viral vectors. Currently research aims at both strategies, the humoral and the cell-mediated immune response by heterologous prime/boost regimes (Ross et al. 2010). Despite this enormous number of HIV vaccines tested, only six trials reached the clinical efficiency stage IIb/III. Unfortunately, the most promising candidates, the vaccine AIDSVAX (monomeric HIV-1 gp120, aimed to induce Env-specific antibody responses) sponsored by VaxGen and Merck's Step Study (replication incompetent recombinant adenovirus 5 vector expression HIV-1 gag, pol, nef, aimed to elicit HIV-1 specific cellular immune responses) failed (Flynn et al. 2005; Pitisuttithum et al. 2006; Buchbinder et al. 2008; Corey et al. 2009). The recently conducted phase III trial RV144 (Rerks-Ngarm et al. 2009), a combination based on the canarypox vaccine ALVAC HIV (Sanofi-Pasteur) for priming and the AIDSVAX B/E (VaxGen) for boosting demonstrated that the vaccine regimen was safe and modestly effective in preventing HIV infection (Ross et al. 2010). These results indicate that protective immunity can be elicited through vaccination.

1.4.2.1 Live Attenuated vaccines

The use of live attenuated SIV as vaccine has shown great potential in monkey trials (Koff et al. 2006). Unfortunately, the attenuated virus reverted to virulence and caused disease over time in vaccinated animals (Chakrabarti et al. 2003; Hofmann-Lehmann et al. 2003). Similarly, some of the human long-term non-progressors of the Sydney Blood Bank Cohort, infected with a naturally attenuated HIV-1 variant progressed to AIDS (Churchill et al. 2006) and long-term cell culture studies showed that attenuated HIV-1 regained substantial replication capacity by acquiring compensatory changes in the viral genome (Berkhout et al. 1999). These results highlight the genetic instability and evolutionary capacity of attenuated SIV/HIV strains, which pose a serious safety risk for any future experimentation with live-attenuated HIV vaccines in humans (Berkhout and Paxton 2009). Nonetheless, the research in this field of vaccine design continues and novel strategies using single-cycle virus vaccines (Evans et al. 2005; Falkensammer et al. 2009) or conditionally live SIV/HIV variants (Das et al. 2004) were developed but have to be further evaluated.

1.4.2.2 Killed vaccines

One of the first vaccines to be tested in the HIV-1 field was a formalin inactivated whole SIV virus, which appeared successful when tested in an macaque model (Murphey-Corb et al. 1989) but later it turned out that the protective response was a consequence of wrong

³ www.iavireport.org/trails-db/

experimental design. The vaccine and challenge virus stocks had been propagated on human cells and the protective immune response in macaques was directed toward human major histocompatibility complex (MHC) proteins that were incorporated into viral membranes (Stott 1991; Carmichael and Sissons 1995). Another example of a killed vaccine was Remune, a γ -radiated and propiolacton inactivated HIV-1 virion with a clade A Env and clade G gag. This vaccine however had no effect in terms of CD4+ T cell count stabilization or decreasing viremia (Peters 2001). The concern that virus inactivation might not be 100 % complete and that killed HIV-1 vaccines might infect healthy volunteers as well as that certain viral purification methods leads to depletion of envelope proteins from the virus surface were major issues. Despite the mentioned disappointments, refined inactivation and purification protocols are under development (Sheppard 2005).

1.4.2.3 Sub-unit vaccines

These types of vaccines contain only the antigens needed to stimulate the immune system. At the beginnings sub-units had to be purified from natural virus. In present days all the relevant structures are prepared recombinantly making them safe regarding infectivity and pathogenicity. A major drawback of recombinant sub-unit vaccines is that only the humoral immune response of the immune system is triggered. Therefore the antigen of interest has to be formulated appropriately and administered in combination with potential adjuvants.

In case of HIV the viral envelope proteins gp160, gp120, and gp41 were used as sub-unit vaccine candidates. Recombinant gp160 expressed in Vero cells (Barrett et al. 1989) was able to elicit anti-HIV Abs in goats and induce T-helper (Th) 1 memory cells in chimpanzees (Mannhalter et al. 1995). Further heterologous prime boost regime in mice in which recombinant Vaccinia virus carrying HIV-1 env gene and gp160 was used for priming and only gp160 for subsequent boosting showed HIV-1 specific Ab and T-cell responses (Brühl et al. 1998). The following phase II clinical study using gp160 could not prove any beneficial effects (Pontesilli et al. 1998).

As already mentioned in 1.4.2 one of the biggest and most promising clinical trials (AIDSVAX) using recombinant monomeric gp120 failed probably due to the limited protective immunogenicity of the monomeric glycoprotein. Therefore current efforts aim to mimic the native structure of gp120 or gp41 in its trimeric form (Parren and Burton 2001), which is rather challenging because of the instability of the HIV-1 spike.

The introduction of disulfide bonds to covalently link gp120 and gp41, and the incorporation of trimerization motifs into the gp41 ectodomain, has been employed to stabilize recombinant trimers (Phogat and Wyatt 2007). Although none of these recombinant trimers accurately mimic the native HIV-1 spike, and only a few of them elicit Abs that neutralize heterologous isolates moderately (Beddows et al. 2005; Kothe et al. 2007; Kang et al. 2009). In this context it has been reported that bnAbs bind to an intermediate conformation of gp41 which

is supposed to be only exposed during the fusion event (Fouts et al. 2002). Therefore HIV-1 glycoprotein complexes with CD4 and CCR5 or CXCR4 were evaluated and found to elicit broad neutralization activity in macaques (Fouts et al. 2002). Compared to monomeric glycoproteins the immunocomplexes have a superior antibody response in mice (Xiao et al. 2003).

Although none of the mentioned immunogens has led to a breakthrough, recent work in elucidation of the structures of native HIV-1 trimers by cryoelectron tomographic (Zhu et al. 2006; Liu et al. 2008), as well as the isolation of new broadly neutralizing trimer-specific Abs (Walker et al. 2009), will eventually lead to a better understanding in the design of recombinant trimers, mimicking the native HIV-1 spike.

1.4.2.4 Virus like particles

As describes in 1.4.2.1 the use of live-attenuated viruses are currently not considered as safe for HIV-1 vaccine development due to the risk of mutation and reversion into a pathogenic form. An alternative could be the use of virus-like particles (VLPs). VLPs form infectious virions, are usually highly immunogenic and induce Ab responses in the absence of adjuvant but are non-pathogenic because the absence of a viral genome. Further VLP-based immunogens are able to present native trimers on the surface. However, due to the instability of the HIV-1 spike, non-functional forms of envelope glycoproteins are also integrated on the surface of VLPs displaying irrelevant epitopes (Poignard et al. 2003). A comparative immunogenicity study of VLPs showed that the binding activity of immunized sera was primarily focused on non-functional forms of envelope glycoproteins (Crooks et al. 2007). Additionally, the low number of native spikes on the surface of HIV-1 reduces the elicitation of Abs against native structures. Strategies to overcome these hurdles have been employed, including pseudotyping HIV-1 with heterologous envelopes (Marsac et al. 2002; Kuate et al. 2006), truncating the cytoplasmic tail of gp41 to increase Env expression (Poon et al. 2005), and generating VLPs with cleavage-defective Env to prevent gp120-gp41 dissociation (Crooks et al. 2007). Recently Ye et al showed that modified chimeric protein hemagglutinin/gp41 (HA/gp41) formed more stable trimers in VLPs with high reactivity to mAbs 2F5 and 4E10. Immunization of guinea pigs using the HA/gp41 VLPs induced Abs against the HIV gp41 at higher levels than immunization with standard HIV-1 as well as exhibited HIV-1 neutralization activity (Ye et al. 2011). However, none of these approaches have induced potent heterologous antibody responses in non-human primate models.

1.4.2.5 Recombinant vector vaccines

Vector vaccines are genetically modified viruses and bacteria, expressing either the antigen of interest by itself or deliver the gene encoding the antigen to cells. The most important vectors used in the HIV field are adenovirus serotype 5 and 35 (Barouch et al. 2000), adeno-

associated virus (AAV) (Xin et al. 2001), canyopox virus (Montefiori et al. 2001; Li et al. 2005), modified Vaccinia virus Ankara (MVA) and New York Vaccinia virus (NYVAC) (Verschoor et al. 1999), Venezuela equine encephalitis virus (VEE) (Perri et al. 2003) and others. Recombinant vectors are able to trigger humoral as well as cellular immune responses. A major drawback in this field was the failure of Merck's phase IIb clinical trial (STEP and Phambili), in which adenovirus serotype 5 expressing clade B gag, pol and nef was tested in healthy individuals (Sekaly 2008), showing that uncircumcised vaccines with pre-existing Abs against adenovirus 5 might be at a higher risk of HIV infection than those in the control group (Buchbinder et al. 2008).

A different approach that essentially bypasses immunization was suggested by Lewis *et al.* In a proof-of-concept study, the IgG1 b12 gene was delivered into mouse muscle using an adeno-associated virus (AAV) vector. The expressed Ab molecules established neutralization activity in the sera for over 6 months (Lewis et al. 2002). Later, this approach was evaluated in a non-human primate model by delivering neutralizing immunoadhesins (antigen-binding variable domains of fragment Abs (Fabs) fused to the Fc fragment of a rhesus IgG2 molecule) into macaques. The immunoadhesins were expressed in the macaque muscle myofibers, and serum neutralization activity was sustained for over 1 year including protection against SIV challenge in six out of nine monkeys (Johnson et al. 2009). Another study using lentiviral vector encoding mAb 2G12 showed inhibition of in-vivo HIV infection in a humanized mouse model (Joseph et al. 2010).

1.4.2.6 Novel concepts

Peptide vaccines are short epitopes containing between eight and 30 amino acids. They are usually less immunogenic than proteins and require the use of strong adjuvants or carrier proteins (Boberg et al. 2007; Boberg et al. 2008). A recently completed clinical trial (ANRS VAC18) using a mixture of five synthetic lipopeptides (LIPO-5) containing sequences of gag, pol, and nef cytotoxic T-lymphocyte epitopes induced CD8 and CD4 T-cell responses and was safe in all vaccines (Salmon-Céron et al. 2010).

DNA vaccines are based on plasmid DNA which per se is not highly immunogenic and is usually rapidly degraded prior to cellular uptake. Therefore, plasmid DNA is often combined with recombinant proteins or viral vectors in heterologous prime boost vaccination strategies (Buonaguro et al. 2007; Peters et al. 2007; Kutzler and Weiner 2008). The introduction and improvements of in-vitro electroporation makes plasmid DNA a stand-alone vaccine candidate (Bodles-Brakhop et al. 2009). This has been tested in non-human primate experiments which showed that electroporation-mediated DNA delivery increases the scale, quality and longevity of the immune response as well as reduces the peak viral load on challenge (Hirao et al. 2008; Martinon et al. 2009). For human therapy, the only HIV-1 phase I clinical trial regarding electroporation mediated delivery of DNA indicated that this kind of

vaccine is well tolerated and could elicit T-cell responses against HIV antigens (Dolter et al. 2011; Vasan et al. 2011).

Liposomes are self-assembly systems which have been recognized as potent adjuvants for vaccines and as carrier molecules for antigens (Allison and Gregoriadis 1974; Alving et al. 1995; Storm et al. 1998). Research in the early 90ies revealed the potential of this approach in the field of HIV (Thibodeau et al. 1989; Cornet et al. 1990; Cornet et al. 1992). Since then several groups have employed liposomal delivery of antigens in candidate HIV vaccines with more or less success (Sakaue et al. 2003; Grundner et al. 2005; Singh and Bisen 2006). In an approach conducted at our institute Quendler et al. showed that presentation of the MPER in a lipid membrane environment is not sufficient to induce neutralizing 2F5 or 4E10 like Ab response (Quendler 2008). However, a similar approach using liposomes containing phosphatidylinositol-4-phosphate (PIP) and the MPER showed that anti-MPER Abs with some HIV neutralization activity could be elicited in mice (Matyas et al. 2009).

1.5 Broadly neutralizing HIV antibodies

During the course of HIV-1 infection Env specific Abs are generated within weeks after infection but are mostly ineffective (Wei et al. 2003). Nevertheless, in some cases cross-clade reactive Abs capable of neutralizing heterologous virus are developed and several of them with broadly neutralizing activity have been isolated so far (Figure 5; Table 2). Some of these bnAbs (2F5, 2G12, b12) were able to completely block infection by chimeric SIV/HIV virus in macaques after passive transfer (Baba et al. 2000; Mascola et al. 2000; Parren et al. 2001). Therefore, one of the main goals of HIV vaccine design is identify epitopes that are able to induce bnAbs with similar potency to those already characterised.

bnAb	epitope specificity	neutralization		reference
		breadth ¹	potency ²	
2F5	Gp41 MPER	60	2,3	Muster T et al. 1993
4E10	Gp41 MPER	98	3,2	Stiegler G et al. 2001
Z13	Gp41 MPER	n.a.	n.a.	Zwick MB et al. 2001
2G12	Gp120 glycan	32	2,4	Trkola A et al. 1996
b12	Gp120 CD4	41	1,8	Burton DR et al. 1994
VRC01, VRC02	Gp120 CD4	91	0,34 0,32	Wu X et al. 2010
VRC03	Gp120 CD4	57	0,45	Wu X et al. 2010
HJ16	Gp120 CD4	36	8	Corti D et al. 2010
PG9, PG16	Gp120 V2,V3	79, 73	0,22 0,15	Walker LM et al. 2009
CH01-CH04	Gp120 V2,V3	35, 45	0,46 1,1	Bonsignori M et al. 2010

¹Breadth is defined as the percent of primary isolates neutralized with an IC50 < 50 µg/ml

²potency is defined as the mean IC50 value (µg/ml) within the group of viruses neutralized with IC50 values <50 µg/ml

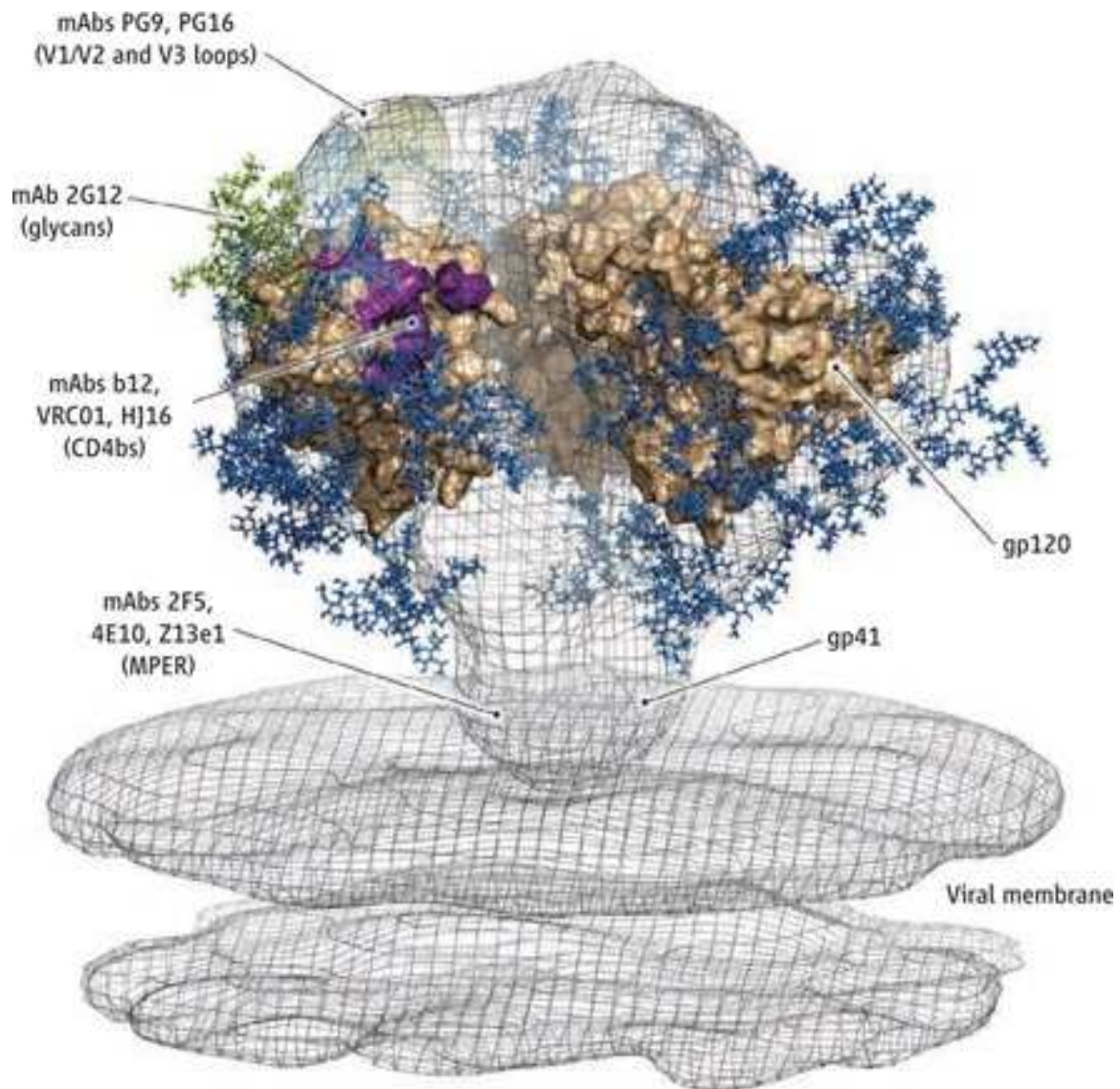


Figure 5. bnAbs target epitopes on the viral envelope spike at the surface of HIV-1.

1.5.1 gp120 specific antibodies

The solvent accessible area of gp120 is decorated by a dense array of carbohydrates, the so-called “glycan shield”, that masks conserved epitopes (Bolmstedt et al. 1996; McCaffrey et al. 2004). This “glycan shield” is poorly immunogenic, because different glycans can exist at a single site (Rudd and Dwek 1997) and the fact that the glycans are produced by the host glycosylation machinery and are seen as self-antigens (Zhu et al. 2000). However a few antibodies that are directed against epitopes of gp120 have been identified and will be discussed in the following paragraph.

The **mAb 2G12** was isolated from peripheral blood lymphocytes derived from HIV-1 infected donors (Buchacher et al. 1994). It recognizes a cluster of conserved mannose glycans on the surface of gp120 (Trkola et al. 1996) and poses an unusual structure at the Ab binding site

resulting from domain swapping (Calarese et al. 2003). Crystal structure of mAb 2G12 in complex with various oligomannosides revealed the dimerisation of the variable heavy chain via domain swapping creating a novel VH-VH interface in addition to the conventional VH-VL sites (Calarese et al. 2003; Calarese et al. 2005). Mab 2G12 neutralizes a broad spectrum of HIV-isolates in vitro (Trkola et al. 1995; Binley et al. 2004) and shows protection against infection in a monkey model (Mascola et al. 2000) and exerts selection pressure on virus in humans (Trkola et al. 2005).

The **mAb b12** (Burton et al. 1994) targets the CD4 binding site. Only the heavy chain of b12 interacts with gp120, with each of the three heavy-chain complementarity-determining regions (CDRs) making extensive contact (Zhou et al. 2007).

b12 is able protect macaques against vaginal challenge from pathogenic simian–human immunodeficiency virus (SHIV) (Parren et al. 2001).

The **mAbs VRC01, -02, and -03** (Wu et al. 2010) have been recently isolated from HIV-1 positive donors with CD4 binding site neutralization activity (Li et al. 2007). They bind to the CD4 binding site in a similar way like the primary CD4 receptor (Zhou et al. 2010). VRC01 and -02 are supposed to be offspring from the same clone and neutralize over 90 % of HIV-1 isolates, whereas VRC03 has a weaker neutralization activity (Wu et al. 2010).

Another panel of recently isolated mAbs are **PG9 and PG16**, both isolated from African HIV infected donors, which neutralize a large multiclade panel of HIV-1 isolates (Walker et al. 2009). The epitopes recognized by PG9 and PG16 are primarily located in conserved regions of the V2 and V3 loops of gp120. PG9 and PG16 bind predominantly to the same residues, although PG16 is more sensitive to V3 loop substitutions than PG9. Deglycosylation of gp120 abolished binding of PG9, which suggested that glycans are important, directly or indirectly, in forming the epitope. Additionally PG9 and PG16 require the presence of an Asp₁₆₀ within the V2 loop for neutralization activity (Robinson et al. 2010).

1.5.2 gp41 specific antibodies

The gp41 glycoprotein consists of several immunogenic regions (see 1.2.3 Figure 4). Reports on antibody reactivity to the PR, NHR, CHR, and CT domain indicate the potential of these regions as targets for vaccine design (Montero et al. 2008) but the major focus on elicitation of gp41 antibodies lies in the MPER region. Thus, in this paragraph only antibodies targeting the MPER will be described. The MPER region is weakly immunogenic and only three bnAbs have been identified so far.

The **mAb 2F5** was originally isolated as IgG3 by immortalizing human peripheral blood lymphocytes from blood of HIV-1-positive volunteers (Buchacher et al. 1994). The broadly

neutralizing 2F5 epitope has been initially mapped to the linear MPER sequence ELDKWA (aa 662 to 667) (Muster et al. 1993) and was later expanded to a longer 17-mer epitope (aa 655 to 671) (Parker et al. 2001; Tian et al. 2002; Barbato et al. 2003; Menendez et al. 2004). In a site-directed mutagenesis study Zwick et al. demonstrated that only the residues DKW are essential for mAb 2F5 binding (Zwick et al. 2005). These findings were confirmed by crystal structure analysis of mAb 2F5 Fab in complex with short synthetic peptides (Ofek et al. 2004; Bryson et al. 2009). Another unusual structural feature of mAb 2F5 is its long (22 amino acids) CDR-H3 loop (Kunert et al. 1998). The hydrophobic apex of the loop remains largely unbound but mutagenesis studies revealed that substitution of Trp at the tip of the loop decreases affinity to gp41, the linear epitope and neutralization activity (Zwick et al. 2004). Therefore the CDR-H3 loop may be involved in further interactions and/or is needed to remain the overall structure of the mAb 2F5. It has been also suggested that the hydrophobic loop may interact with the membrane and in consequence facilitate MPER binding (Ofek et al. 2004). Lorizate et al. found out that in the native or prefusion state of gp41 the MPER and the FP are located at the same end of the ectodomain suggesting that the natural epitope of mAb 2F5 may include more than the core DKW (Lorizate et al. 2006b). This hypothesis is based on the fact that different viruses bearing the DKW core have shown resistance to mAb 2F5 neutralization (Bures et al. 2002). Further mAb 2F5 is polyreactive, binding self-antigens like whole cell and cardiolipin (Haynes et al. 2005a). Haynes et al. suggested that mAb 2F5 initially binds to the membrane and in a second step to the MPER (Haynes et al. 2005b). This hypothesis is fostered by observations that mAb 2F5 binds to its liposomes conjugated epitope in a two step binding model whereas the interaction with the linear epitope followed a Langmuir 1:1 model (Alam et al. 2007).

The **mAb 4E10** was isolated in the same manner like mAb 2F5 (Buchacher et al. 1994). In comparison to mAb 2F5 it neutralizes a broader range of HIV-1 isolates (Binley et al. 2004; Mehandru et al. 2004). MAb 4E10 binds to the linear epitope NWFDIT (aa 671 to 676) just C-terminal to the ELDKWA sequence (Zwick et al. 2001). As with mAb 2F5 the six amino acids (aa) do not resemble the whole epitope; mAb 4E10 additionally binds to the FP at the N-terminus of gp41 and the MPER epitope (Hager-Braun et al. 2006). Mutagenesis studies revealed that Trp₆₇₂, Phe₆₇₃, and Thr₆₇₆ in the core epitope are essential for mAb 4E10 binding (Brunel et al. 2006) but for neutralization activity, additional to Trp₆₇₂ and Phe₆₇₃, Trp₆₈₀ outside of the core epitope is needed (Zwick et al. 2005). Crystallographic analysis revealed some interesting feature like the relatively long CDR-H3 loop (18 aa), but if this loop is important for neutralization is still unknown (Cardoso et al. 2007).

The **mAb fragment Z13** was isolated using a Fab phage-display library made from bone marrow of an HIV-1 positive individual (Zwick et al. 2001). MAb Fab Z13 overlaps the mAb

4E10 epitope NWF₆₇₁₋₆₇₇ (aa 671 to 677) but does not bind to gp41 from HIV-1 isolate IIB because of different amino acid composition in the core epitope (NWF₆₇₁₋₆₇₇) suggesting that Asp₆₇₄ is crucial for interaction. Further the neutralization capacity of mAb Fab Z13 is weaker than those of mAb 2F5 and mAb 4E10 (Zwick et al. 2001). mAb Fab Z13e1, an improved version of mAb Fab Z13 was developed by random mutation on CDR-L3 enhancing affinity to the MPER and increasing its neutralization potential (Nelson et al. 2007).

1.6 Anti-idiotypic antibodies

An anti-idiotypic Ab is an Ab directed against the antigen specific determinant of another Ab or T-cell receptor. Niels K. Jerne postulated 'The Network Theory of the Immune System', in which he presented the observation that Abs (Ab1) can elicit anti-idiotypic Abs (Ab2) directed against the paratope of the Ab1 (Jerne 1974). The cascade then continues, with the generation of anti-anti-idiotypic Abs (Ab3) that recognize Ab2 (Figure 6) (Shoenfeld 1995). These Ab2s are expected to mimic the initial antigen (Jerne et al. 1982; Fields et al. 1995).

Ab2s can be clustered into three groups: the Ab2 α are conventional Abs that recognize idiotopes distinct from the antigen-combining site on primary Ab1; Ab2 β are internal image antibodies that recognize epitopes within the antigen-combining site and that resemble the antigen of Ab1; and Ab2 γ recognize epitopes within the antigen-combining site, but do not resemble the nominal antigen (Pan et al. 1995).

The most important group of Ab2s are the internal image Abs (Ab2 β) which are directed against the binding site of the elicited Abs and can, in their paratope, structurally and/or functionally mimic the original antigen, or more precisely, the epitope of the original antigen (Izadyar et al. 1993; Poljak 1994; Kolesnikov et al. 2000; Ponomarenko et al. 2007; Vani et al. 2007). Thus, internal image Abs has a potential as antigen for the development of active vaccines. Such an approach is especially useful when the antigens are infectious, toxic, difficult to isolate and purify, or weakly immunogenic.

Until to date, anti-idiotypic Abs have been mainly developed as potential vaccines for cancer immunotherapy and significant success has been achieved using anti-Id vaccines mimicking tumor-associated antigens in animal studies (Lee and Ge 2010; Wang et al. 2010; Ladjemi et al. 2011; Ramos et al. 2011) as well as in clinical trials (Hurvitz and Timmerman 2005; Inogès et al. 2006; de Cerio et al. 2007).

For the development of an HIV vaccine the anti-idiotypic approach was only considered by a few groups. Sperlagh et al produced Ab2s against an anti-HIV Ab targeting gp120 in rabbits. The Ab2 induced Ab3s in rats that showed binding reactivity to native gp120 but failed to induce virus-neutralizing (Sperlagh et al. 1994). The Ab2 1F7, a mAb raised against IgG pooled from HIV-infected humans, recognizes human Abs against HIV gag, pol and env and

macaque Abs against SIV gag and env (Müller et al. 1991). Treatment of SHIV-infected macaques with 1F7 increases the breadth and potency of HIV-neutralizing Abs, presumably through anti-idiotypic suppression of dominant B cell clones (Müller et al. 1998). 1F7 has been shown previously to induce apoptosis of a subset of CD8+ T cells from HIV-infected individuals, suggesting that it interacts with both T and B cells (Müller et al. 1995). This was confirmed by Grant et al demonstrating that 1F7 selectively inhibits cytotoxic T cells activated in HIV-1 infection (Grant et al. 2000). Burioni et al developed two Ab2s (P1 and P2) which recognize the idiotype of the broadly neutralizing anti-CD4bs human mAb b12, thus mimicking the CD4bs epitope. P1 and P2 Fabs were able to induce anti-gp120 response in rabbits and rabbits sera show the ability to neutralize two HIV-1 strains (HXB2 and MN) in an Env-pseudotype neutralization assay (Burioni et al. 2008).

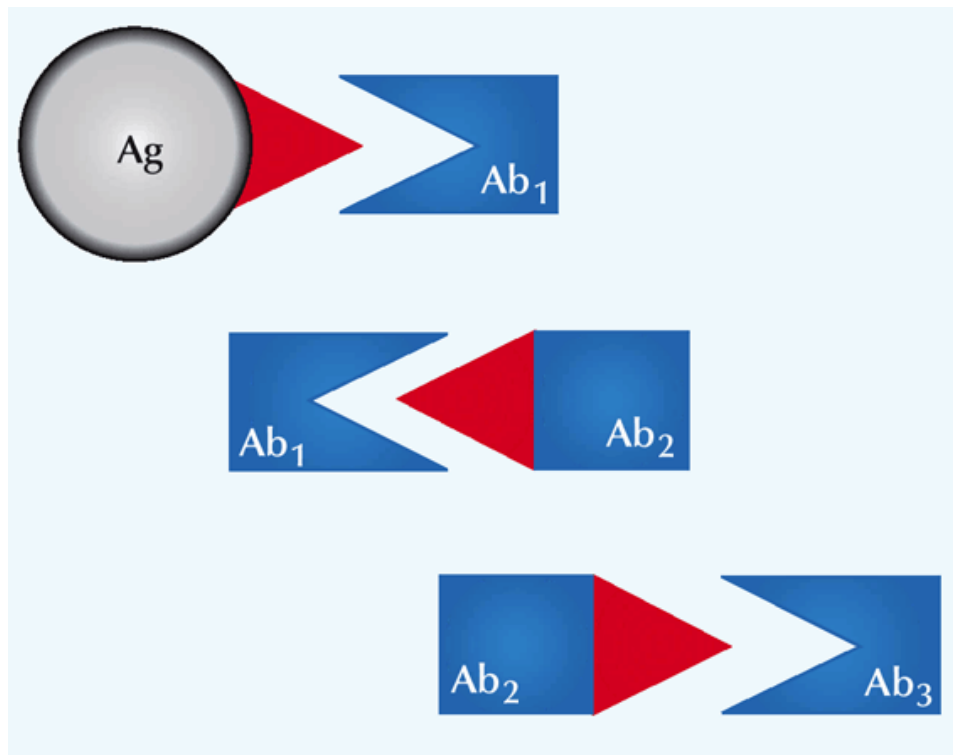


Figure 6. The Network Theory of the Immune system

1.6.1 Ab2/3H6

The anti-idiotypic Ab Ab2/3H6 was developed at our institute by immunization of mice with mAb 2F5 Fab (Kunert et al. 2002). The hybridoma derived mouse Ab2/3H6 IgG was able to block the binding of mAb 2F5 to the synthetic epitope (ELDKWA) and to gp160 in an enzyme-linked immunosorbent competition assay. Ab2/2H6 diminished the neutralizing potency of mAb 2F5 in an in-vitro HIV neutralization assay. Further Ab2/3H6 Fab fragments were able of inducing a mAb 2F5-specific response in B6D2F1 mice applying a simple prime-

boost immunization (Kunert et al. 2002). Gach et al successfully chimerized and recombinantly expressed the Ab2/3H6 as IgG and Fab molecules in CHO cells (Gach et al. 2007a) as well as in pichia pastoris (Gach et al. 2007b). During these studies a glycosylation site was found in the CDR2 of the Ab2/3H6 heavy chain which had no effect on the biological function of the Ab (Gach et al. 2007b). Further structural analysis revealed that the two proline residues in the CDR-H3 loop (P₁₁₃ and P₁₁₆) do not contribute to mAb 2F5 interaction while the tyrosine at the apex of the loop (Y₁₁₁) is critical for binding to mAb 2F5 (Gach et al. 2008a). Additional immunization studies in guinea pigs using whole Ab2/3H6 IgG or Fab fragments did not lead to expected results because the immune sera competed against mAb 2F5 for the binding to ELDKWA indicating that the Ab2/3H6 IgG1 had not been entirely cleared from other guinea pig immune system molecules (Gach et al. 2008b).

To get a deeper insight into the interaction between Ab2/3H6 and mAb 2F5 the crystal structure of both Fab fragments in complex was solved (Bryson et al. 2008). The conclusion of this study was that Ab2/3H6 Fab binds to mAb 2F5 Fab' via a helix-like protrusion formed by residues (58^H)RYSPSLNTRL(67^H) of the mAb 2F5 Fab' variable domain which is proximal to but not overlapping with the core (DKW) epitope-binding pocket of mAb 2F5. Therefore Ab2/3H6 was defined as Ab2 γ class (Bryson et al. 2008). However as mentioned in 1.5.2 the complete epitope of mAb 2F5 has not been identified so far, therefore Ab2/3H6 is still of therapeutic interest as an anti-idiotypic HIV-1 vaccine.

1.7 Humanization of therapeutic antibodies

The invention of hybridoma technology (Köhler and Milstein 1975) allowed the production of single specific Abs in large volume bioreactors. This technology however is largely limited to the production of murine or rat derived Abs. During the 1980s 80 % of all mAbs in clinical development were of mouse origin (Nelson et al. 2010). However mouse derived Abs in human therapy have been associated with short serum half life and the risk to trigger anti-mouse Ab (HAMA) or human anti-rat Ab (HARA) responses (Waldmann and Hale 2005; Presta 2008). In first approaches chimeric variants of the Abs were engineered (Morrison et al. 1984) generating molecules with approximately 70 % human content (Figure 7) which retained the specificity of the parental Ab but were still able to elicit anti-chimeric Ab (HACA) responses (Hwang and Foote 2005). Two years later Jones et al successfully grafted mouse CDRs onto a human framework (FR) which resulted in the first humanized Ab (Figure 7) (Jones et al. 1986). Since then, the number of mouse Abs in clinical use dropped during the 2000s to 7 % (Nelson et al. 2010). Further improvements in Ab development resulted in fully human Abs derived from phage display approaches using human libraries, transgenic

animals or very recently the development of naïve human B cell libraries that can be screened against any antigen (Duvall et al. 2011).

In this paragraph the focus will be laid on the description of selected humanization methods. In general humanization methods can be divided in “rational” approaches and “empirical” methods. The first are defined by creating only a few carefully designed humanized variants that are expressed and further optimized while the second is characterized by development of large libraries of humanized variants and screening of them for the best binding variants.

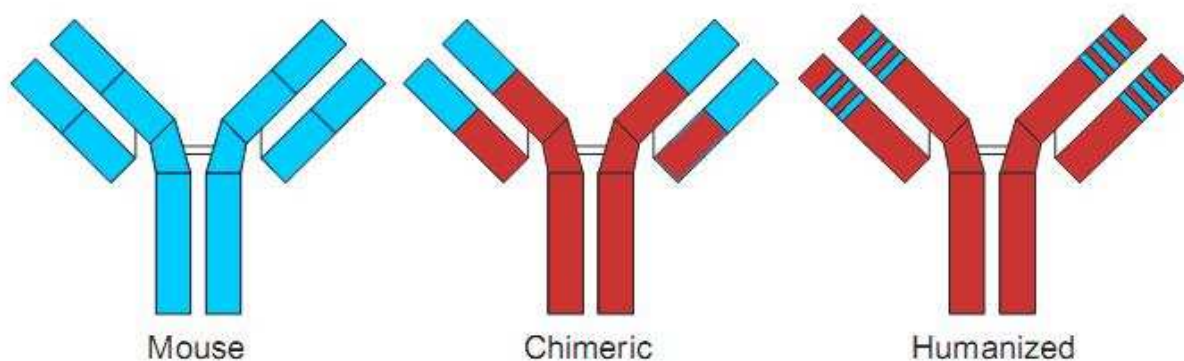


Figure 7. Humanization of murine Abs. (blue) mouse residues; (red) human residues

1.7.1 Rational humanization approaches

1.7.1.1 CDR-grafting

CDR-grafting was developed by Jones et al to reduce immunogenicity of Abs (Jones et al. 1986). In a first proof of concept the heavy chain (HC) CDRs of the murine anti-hapten Ab B1-8 were grafted on the HC of the human Ab NEWM. The humanized HC was then combined with the murine B1-8 light chain (LC) resulting in a specific functional hybrid Ab. Based on these findings, two years later the therapeutic Ab for treatment of B-cell lymphocytic leukemia, CamPath® (Alemtuzumab) was humanized (Riechmann et al. 1988). The classical CDR-graft approach starts with definition of the CDRs. The best way to identify the residues in contact with the antigen is to resolve the crystal structure of the Ab complexed with the antigen or by alanin scanning mutagenesis (Fuh et al. 2006). If the crystal structure is not available CDRs are selected according to sequence variability (Wu and Kabat 1970), structural variability (Chothia et al. 1989), contact definition (MacCallum et al. 1996) or specific determining regions (SDRs) (Padlan et al. 1995). The next step is the selection of the human acceptor FR. Initial works used known human Ab structures (fixed FR approach) regardless their homology to the mouse Ab (Jones et al. 1986; Riechmann et al. 1988). The best-fit method relies on the human sequence displaying the highest homology to the non-human Ab (Queen et al. 1989) whereas others used human consensus FR

sequences (Carter et al. 1992; Presta et al. 1993). Regardless of the chosen method, human germline genes are favoured today because they lack somatic mutations and are therefore supposed to be less immunogenic (Neuberger and Milstein 1995). A major factor of CDR-grafting is the decrease or loss of affinity because of incompatibilities between mouse CDRs and human FR, which makes backmutations indispensable (Saldhana 2007). These backmutations have to be defined individually for each Ab and each aa position even if Abs have a high sequence identity or similar antigen specificity (Rosok et al. 1996). In some cases, backmutations at known critical positions are counterproductive (Caldas et al. 2000; Gonzales et al. 2003). The majority of Abs have been humanized using this method.

1.7.1.2 Resurfacing

This approach was proposed by Pedersen et al who analyzed twelve Abs of known structure to identify a set of solvent accessible residues within the FRs (Pedersen et al. 1994). Later the analysis of solvent accessible residues was optimized by using a computer model instead of sequence analysis (Staelens et al. 2006). Resurfacing retains the non-exposed residues of the non-human Ab. Only surface residues in the non-human Ab are changed to human residues. Since resurfacing does not change the residues in the core of the Ab, the expectation is to eliminate potential B-cell epitopes, while retaining the structural conformation of the CDRs. Unfortunately T-cell epitopes are not considered using this method. A couple of Abs have been humanized using this approach (Roguska et al. 1994; Roguska et al. 1996; O'Connor et al. 1998; Delagrave et al. 1999; Chiu et al. 2011) and one of them the Ab conjugate huC242-DM1 (Cantuzumab mertasine) showed no anti-globulin response in a clinical trial (Rodon et al. 2008).

1.7.1.3 Superhumanization

In contrast to CDR-grafting, which relies on comparison of the non-human and the human FR regions, the superhumanization approach is based on comparison of the CDRs (Tan et al. 2002). In a first step the canonical structure classes (Chothia and Lesk 1987) of the murine Ab are analyzed. Then functional human germline genes with the same or closely related canonical structures to the mouse sequence are selected. Those with the highest identity within the CDRs are chosen as acceptor FR. CDRs are grafted onto the acceptor FR and in contrast to CDR-grafting, no backmutations should be necessary. The superhumanized Ab by Tan et al reduced affinity 30-fold but retained biological activity (Tan et al. 2002). Only a few Abs are reported to be humanized using this approach (Hwang et al. 2005; Hu et al. 2007).

1.7.2 Empirical humanization approaches

1.7.2.1 Framework libraries

This method is basically a CDR-grafting approach but instead of creating few back mutations in the frameworks, combinatorial libraries of a large number of variants are constructed. The residues targeted for mutagenesis were buried residues critical to maintain the canonical structures. Phage display panning of the library leads to selection of the FRs that best supports the grafted CDRs (Rosok et al. 1996; Baca et al. 1997; Rader et al. 2000; Son et al. 2004).

1.7.2.2 Framework shuffling

Dall'Acqua et al combined whole FRs with the non-human CDRs. These constructed libraries were screened for binding in a two step process, first isolating the humanized variable light (vL) followed by variable heavy (vH) chain (Dall'Acqua et al. 2005). Instead of using the mentioned two step approach also a one step FR shuffling approach was reported (Damschroder et al. 2007).

1.7.2.3 Humaneering

This method allows for isolation of Abs that are over 90 % identical to human germline gene antibodies. First the aas required for antigen binding (minimum specificity determinants) are identified experimentally. In a next step these potential essential non-human aas are integrated into human FRs and sequentially replaced by human residues. These libraries are then assessed for binding (Almagro and Fransson 2008).

2 Aims and rational of the present thesis

Despite intense research in the last decades there is still no HIV-1 vaccine available. The identification of bnAbs binding to highly conserved epitopes on the MPER region of the gp41 envelope protein has attracted this region as target for vaccine development. One of these Abs is the mAb 2F5 which broadly and potently neutralizes primary HIV-1 isolates. The specific induction of 2F5 like broadly nAbs against the MPER is a major goal for Ab-based HIV-1 vaccine strategies but has been only of limited success so far. In the past, approaches to elicit 2F5-like Abs were based on using synthetic peptide epitopes of the MPER with or without other antigens or in context with membranes to simulate the original HIV-1 antigen. An alternative method to induce bnAbs is the anti-idiotypic approach. The anti-idiotypic Ab Ab2/3H6 developed at our institute has been intensively characterized and is estimated to mimic the epitope of mAb 2F5. Ab2/3H6 therefore would be of great therapeutic interest as an anti-Id HIV-1 vaccine. Former immunization studies with the anti-idiotyp were performed in mice or guinea pigs. The results were promising but due to the limited amount of sera obtained from these small animals further characterizations could not be performed.

Here we present in a first part of the project the humanization of Ab2/3H6. The induced Ab3 should theoretically be directed against the paratope of the Ab2/3H6 which is resembled by the CDRs. In contrast, Ab3 immune responses against the FR regions do not contribute to the anticipated effect and should be prevented. Therefore the aim of the humanization approach is to reduce immunogenicity of FR regions and thus drive the Ab3 immune response towards the paratope of the Ab2/3H6, which is expected to be structurally similar to the mAb 2F5 HIV-1 epitope. We applied three different humanization approaches to the mouse derived Ab2/3H6 and analyzed the newly generated proteins in comparison to the chAb2/3H6.

In a second part of the project we did the final proof of concept and tested if Ab2/3H6 is able to induce Ab3s in rabbits. To improve the potency of Ab2/3H6 we designed fusion proteins consisting of Ab2/3H6 Ab fragments and C-terminally attached immune stimulatory cytokine interleukin 15 (IL15) or the so-called “promiscuous” T-cell epitopes from tetanus toxin (TT) to induce T-cell responses against the virus. The fusion proteins of Ab2/3H6 Fabs with the IL15 and alternatively an epitope of TT were recombinantly expressed in CHO cells. Rabbits were immunized with the different Ab2/3H6 Fabs and the humoral immune response as well as the neutralization potency of the obtained Ab3s was evaluated.

3 Topics of the thesis

3.1 Humanization of Ab2/3H6

As mentioned in section 1.7 a therapeutic Ab should be as human as possible to maintain the therapeutic effect. To prevent immunological side effects or drug degradation during therapy it should not induce the generation of anti mouse immune reactions HAMA. In case of an anti-idiotypic antibody vaccine, immunogenicity is desired to stimulate the immune system. Hence only the CDRs of Ab2/3H6 which are expected to mimic the gp41 epitope of mAb 2F5 should elicit an immune reaction and other domains of the Ab like the FRs should not be detected by the immune system. Therefore we postulate that humanization of the FRs of Ab2/3H6 will direct the immune response towards the CDRs.

Humanization of an Ab is not trivial. Every molecule behaves differently and not every approach can be transferred to another Ab without the need for modifications (see section 1.7 for a general view on humanization methods). To evaluate which approach fits best for Ab2/3H6 three different rational methods were evaluated.

3.1.1 CDR-graft of Ab2/3H6

The workflow for CDR-grafting Ab2/3H6 is depicted in figure 8. The aa sequence of Ab2/3H6 vH and vL was numbered and CDRs were defined according to Kabat et al (Wu and Kabat 1970). To keep the approach as close as possible to the classical method described by Jones et al (Jones et al. 1986) an existing human Ab was used as acceptor FR. An identity search of Ab2/3H6 variable regions in the UniProt database⁴ revealed that the human Ab sequence EU had the highest identity. The alignment of the vH and vL regions of human Ab EU and murine Ab2/3H6 are shown in section 6.1 (selected publications: Mader et al. 2010). In total 70 aas were identified (36 aas in the FR of Ab2/3H6 vL and 34 aas in the FR of Ab2/3H6 vH) that differed from the acceptor FR sequence. Normally the human FRs are not compatible with the mouse CDRs, resulting in reduction or complete loss of binding to the antigen. Thus backmutations have to be introduced to restore binding affinity (see section 1.7.1). In the beginning of the 1990ies intense research on Ab sequences and structures showed that certain FR residues contribute significantly to the conformation of the CDRs (Riechmann et al. 1988; Chothia et al. 1989; Queen et al. 1989; Co et al. 1991; Foote and Winter 1992) or are directly involved in antigen binding (Mian et al. 1991). These findings were summarized by Adair, Athwal and Emtage (Adair et al. 2003) and were considered for CDR-grafting of Ab2/3H6.

⁴ www.uniprot.org

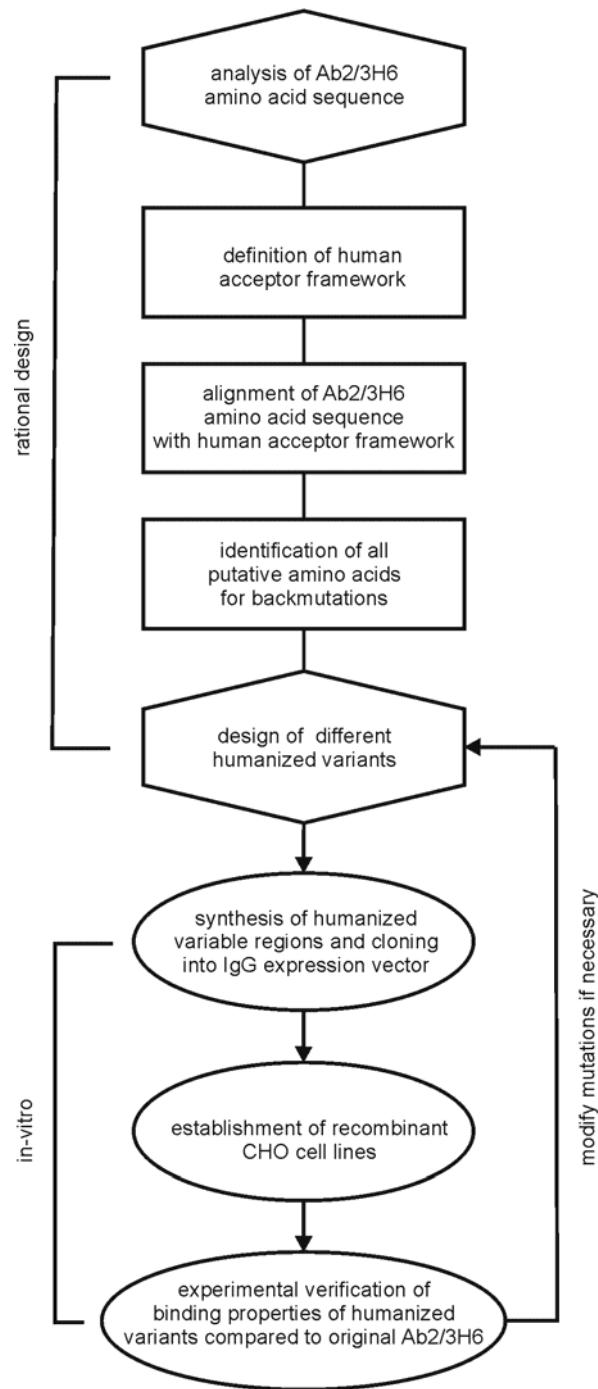


Figure 8. Workflow for CDR-grafting Ab2/3H6

According to the patent of Adair et al 22 potential backmutation sites in the Ab2/3H6 vH and 13 in the Ab2/3H6 vL were identified to be necessary. From these 35 putative aas ten in Ab2/3H6 vH and five in the Ab2/3H6 vL are at probable critical positions for remaining the correct and original CDR conformation. In the light of this analysis two variants of CDR-grafted humanized Ab2/3H6 were designed. In the so-called conservative graft (GC3H6), all potential aas were backmutated to mouse and in the so-called aggressive graft (GA3H6), only the critical residues were substituted to the murine aas in the human acceptor FRs. A

detailed table of the FR backmutations in the CDR-grafted variants is provided in section 6.1 (selected publication: Mader et al. 2010).

After design of the GC3H6 and GA3H6 vH as well as vL regions, cDNAs were synthesized by Genearth (Regensburg, Germany) and inserted into a plasmid vector containing a human IgG1 HC leader/constant region under the control of the SV40 promoter and a dehydrofolate reductase (dhfr) cassette (Figure 9A) or inserted into a plasmid vector containing a human kappa LC leader/constant region under the control of the CMV promoter and neomycin phosphotransferase (neoR) cassette (Figure 9B). These plasmids were used to generate stable CHO cell lines (see section 3.4).

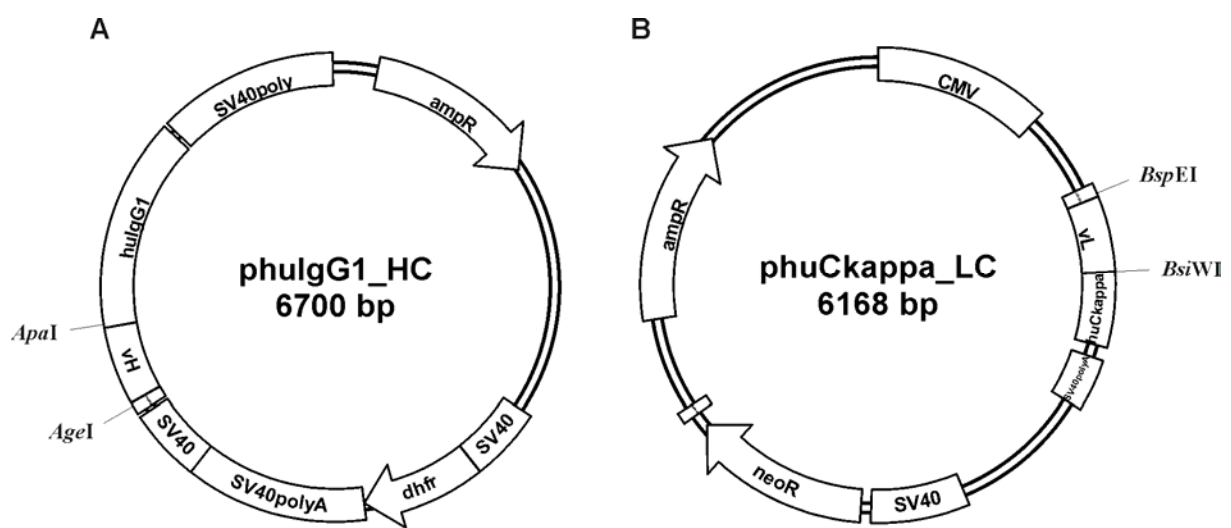


Figure 9. Plasmid map of mammalian expression vectors for expression of **(A)** humanized Ab2/3H6 HC and **(B)** humanized Ab2/3H6 LC. All synthesized Ab2/3H6 vH and vL variants were cloned into the expression vector using the displayed restriction sites.

3.1.2 Superhumanization of Ab2/3H6

As depicted in figure 10 this approach starts with analysis of Ab2/3H6 sequence regarding definition of the CDRs and the canonical structure classes. CDRs were defined in the same manner like in the CDR-graft approach (section 3.1) and canonical structure classes were identified using an automated online tool provided by Dr Andrew C.R. Martin's laboratory⁵. The human germline vH/J_H and vK/J_K gene sequences were extracted from the V-Base database⁶. For the vH region six and the vL region 23 human germline sequences with the same canonical structure class as the Ab2/3H6 were identified. In the same manner the six J_H and five J_K regions were extracted. These sequences were pairwise aligned with Ab2/3H6 and the sequence with the best residue to residue match in the CDRs was defined as

⁵ <http://www.bioinf.org.uk/abs/chothia.html>

⁶ <http://vbase.mrc-cpe.cam.ac.uk/>

acceptor FR. A table showing the canonical structure classes of Ab2/3H6 and the defined human germline acceptor FR IGHV1-f*01/JH4 for the vH and IGKV5-2*01/JK2 for the vL is provided in section 6.1 (selected publications: Mader et al. 2010).

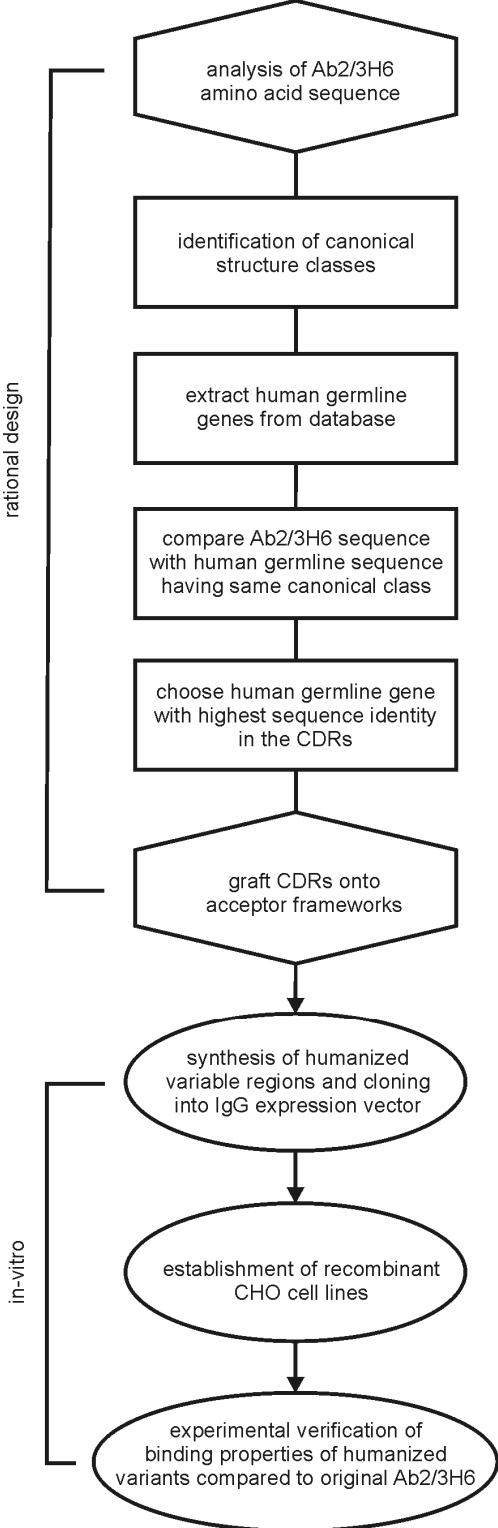


Figure 10. Workflow for superhumanizing Ab2/3H6

As mentioned in section 1.7.1 the difference between CDR-grafting and Superhumanization is that only the CDRs were compared for highest sequence identity while ignoring the FRs. The sequence identity of Ab2/3H6 CDRs to IGHV1-f*01/JH4 CDRs is 80 % identity in CDR-H1, and 31 % identity in CDR-H2 while identity to IGKV5-2*01/JK2 CDRs is 64 % in CDR-L1, 43 % in CDR-L2, and 77 % in CDR-L3. The alignments of Ab2/3H6 CDRs to the defined human germline acceptor FR CDRs is provided in section 6.1 (selected publications: Mader et al. 2010). Because it is proposed that no backmutations are required to maintain the conformation of the murine CDRs in the human FR using this method, the Ab2/3H6 CDRs are simply grafted into the defined acceptor FR to obtain the superhumanized Ab2/3H6 variant (SH3H6). The genes of SH3H6 vH as well as vL were synthesized by Geneart (Regensburg, Germany) and inserted into a plasmid vector containing a human IgG1 HC leader/constant region under the control of the SV40 promoter and a dhfr cassette (Figure 9A) or inserted into a plasmid vector containing a human kappa LC leader/constant region under the control of the CMV promoter and neoR cassette (Figure 9B). These plasmids were used to generate stable CHO cell lines (see section 3.4)

3.1.3 Resurfacing of Ab2/3H6

The workflow for resurfacing Ab2/3H6 is depicted in figure 11. This method is based on analysis of a molecular computer model of the mouse Ab. Therefore the outcome of resurfacing depends on an accurate model. The best accurate model would be the crystal structure of Ab2/3H6. Unfortunately the crystal structure of Ab2/3H6 (Bryson et al. 2008) was not available at the beginning of this humanization project. Thus, homology modeling by the web-based antibody modeling server WAM⁷ (Whitelegg and Rees 2000) was used to generate a molecular computer model of our anti-idiotypic Ab. Briefly, the WAM server blasted the sequence of Ab2/3H6 against the Protein Data Bank (PDB)⁸ to find a crystal structure which had the highest identity to the Ab. In case of Ab2/3H6 the crystal structure used as template for homology modeling was 2GJJ (Hu et al. 2008). Afterwards the program predicted the side chains of the loops using CONGEN iterative algorithm (Brucoleri and Karplus 1987). The CDR-H3 loop of Ab2/3H6 is relatively long (13 amino acids) and was predicted with Valence Force Field (VFF) side-chain energy screen (Dauber-Osguthorpe et al. 1988). Finally, after energy minimization the predicted model was downloaded from the server and used for the resurfacing approach. All further analysis and manipulation of the molecular model of Ab2/3H6 were done using the Swiss Pdb Viewer software (Guex and Peitsch 1997). Pedersen et al defined that side chains of aas that are 30 % exposed at the surface of the protein are accessible for other molecules (Pedersen et al. 1994). Therefore the threshold for identification of surface expose residues was set to that value resulting in 34

⁷ <http://antibody.bath.ac.uk/wam1.html>

⁸ <http://www.pdb.org/>

aas (16 in the FR of vH and 16 in the FR of vL) that were exposed in Ab2/3H6 (Figure 12). Human germline gene sequence IGHV1-3*01 with 64.9 % identity to the murine vH region and IGKV5-2*01 with 63.2 % identity to the vL of Ab2/3H6 were defined as corresponding human germline residues. In the vH FR of the mouse Ab only three surface exposed aas differed from the human germline sequence and were substituted to the human version (Gln^{H5}Val, Thr^{H14}Pro, and His^{H41}Pro). In case of vL seven residues were adapted to the corresponding human germline aas (Ser^{L10}Phe, Leu^{L11}Met, Ile^{L15}Pro, Glu^{L17}Asp, Arg^{L45}Ile, Ser^{L60}Pro, and Gly^{L100}Gln). Using the Swiss Pdb Viewer program, these mutations were manually inserted; side chains were rotated for stable side chain conformation and then subjected to energy minimization using the GROMOS 43B1 force field (van Gunsteren et al. 1996) provided with the software. After in-silico analysis of the homology model of the humanized Ab2/3H6 variant additional buried aas had to be changed to the human counterpart to stabilize the molecule (Table II) resulting in the humanized resurfaced Ab2/3H6 (RS3H6) variant. To determine conformational changes in the CDRs of Ab2/3H6 compared to RS3H6 the two homology models were superimposed. The overlay picture of the CDRs of the two Ab versions is provided in section 6.1 (selected publications: Mader et al. 2010) revealing that the overall CDR conformation between the mouse and humanized Ab had been conserved. The only difference that could be observed is the Tyr^{H53} in the CDR-H2 loop of RS3H6 that had a different side chain conformation. The rotation of the Tyr^{H53} side chain in the RS3H6 model showed that there is only a minor energy difference between these two conformations suggesting that Tyr^{H53} will be flexible and exist in both conformations and might therefore not influence the correct CDR-H2 folding and antigen binding properties. The genes of RH3H6 VH as well as VL were synthesized by Genesart (Regensburg, Germany) and inserted into a plasmid vector containing a human IgG1 HC leader/constant region under the control of the SV40 promoter and a dhfr cassette (Figure 9A) or inserted into a plasmid vector containing a human kappa LC leader/constant region under the control of the CMV promoter and neoR cassette (Figure 9B). These plasmids were used to generate stable CHO cell lines (see section 3.4).

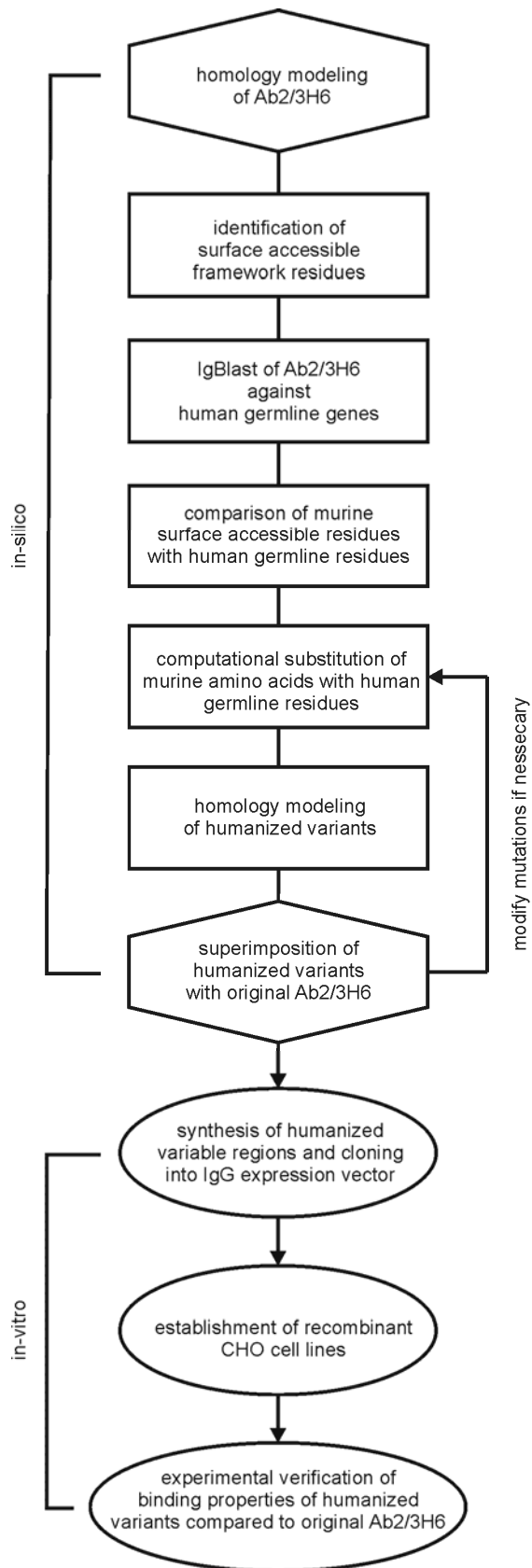


Figure 11. Workflow for resurfacing of Ab2/3H6

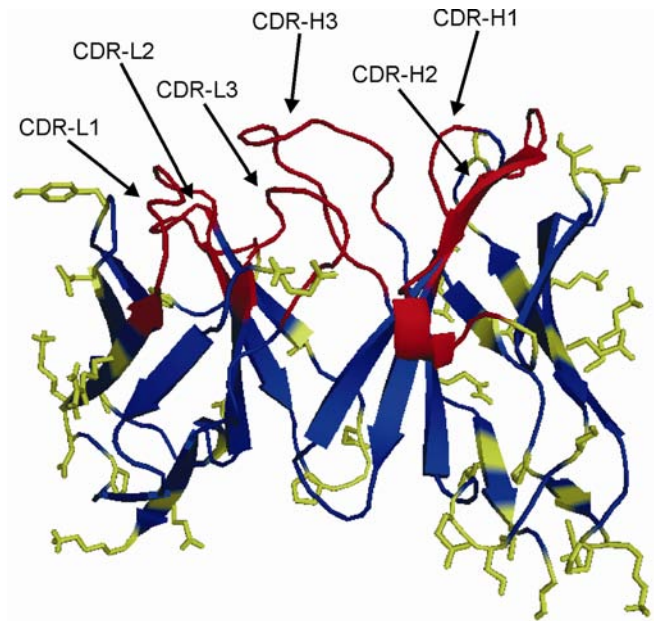


Figure 12. Homology model of Ab2/3H6. The CDRs are in red; the buried regions in blue; the surface exposed areas in green. Only the exposed side chains are displayed in the ribbon model.

Table II. Buried aas substitutions in the resurfaced Ab2/3H6 antibody

Position (Kabat numbering)	Modification	remarks
H1	Insertion of Gln	Missing amino acid in position H1 in the original Ab2/3H6 sequence
H40	Ser >> Ala	Ser ^{H41} might clash with Pro ^{H41}
L13	Met >> Ala	Additional H-bonds were formed between Met ^{L13} and Glu ^{L105} as well as Lys ^{L107}
L14	Ser >> Thr	Ser ^{L14} might clash with Asp ^{L17}

3.1.4 Generation of stable cell lines of humanized Ab2/3H6 variants

Mammalian expression vectors described in figure 9 were used for co-transfection of CHO dhfr negative cells [CHO DUKX; ATCC CRL-9096; (Urlaub and Chasin 1980). Briefly 2.5 µg of each plasmid (HC and LC) were incubated with 50 µg Polyethylenimine (PEI) in a total volume of 400 µl HEPES buffered saline buffer (HBS). The transfection mix was then added to 1×10^6 cells grown in ProCHO5 medium supplemented with glutamine, hypoxanthine and thymidine and incubated for four hours at 37 °C 7 % CO₂. After change of medium to remove the remaining PEI-DNA complexes, cells were incubated over night. The next day the transfected CHO cells were transferred into ProCHO5 medium supplemented with glutamine and geneticin (G418) and plated into 96 well plates at a density of 10000 cells per well for selection of positive clones. A description on the establishment of recombinant stable CHO cell lines producing humanized Ab2/3H6 variants is shown in figure 13.

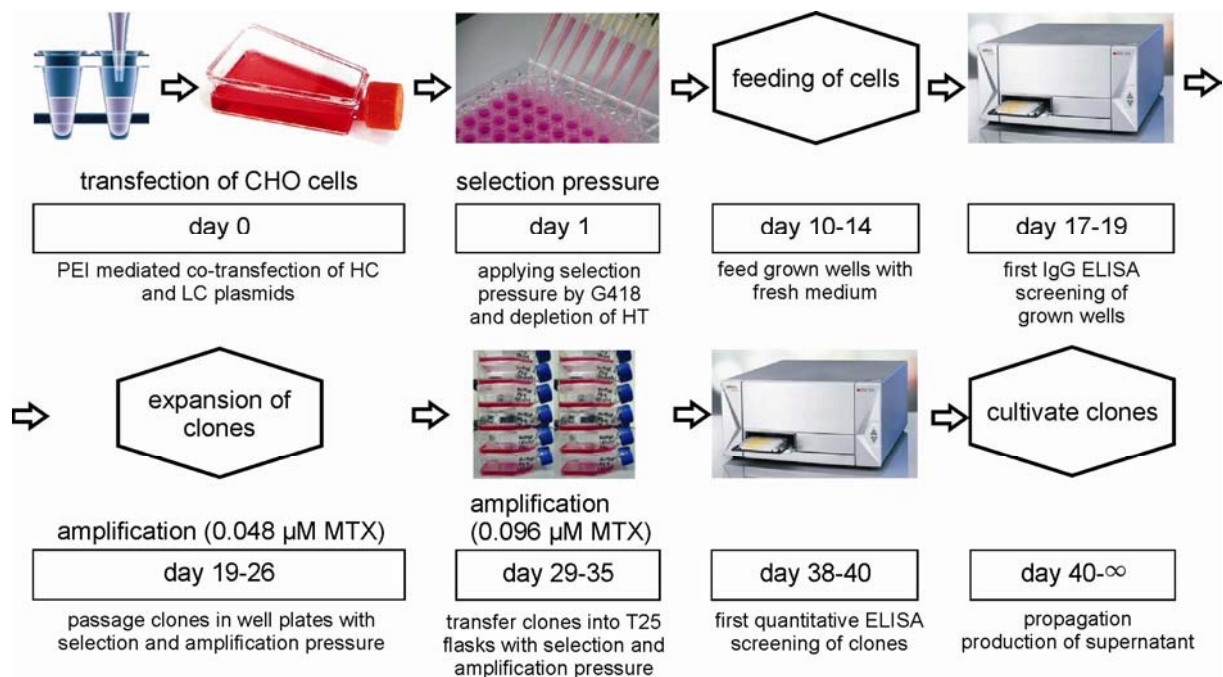


Figure 13. Workflow for generation of recombinant CHO cell lines producing humanized Ab2/3H6 variants

The selection of transfected CHO clones resulted in 85 % - 100 % grown wells in the 96 well selection plates. After IgG screening using an anti-huGamma/anti-huKappa chain sandwich ELISA the 12 best producing clones from each transfection were selected for expansion and amplification using methotrexate (MTX). These best producers were propagated, transferred into T25 flasks, further amplified and quantitatively screened for immunoglobulin secretion in the above mentioned ELISA. After this first quantitative screening the best four producing clones from each humanized Ab2/3H6 variant were further propagated and tested for growth performance and production as well as used for production of culture supernatant for

subsequent Ab purification. Selected cell culture data for the recombinant CHO cell lines producing humanized Ab2/3H6 variants are summarized in table III.

Table III. Summary of initial screenings of recombinant CHO cell lines producing humanized Ab2/3H6 variants

recombinant CHO cell line producing	96 well selection plate		T25 1 st quantitative screening		T25 2 nd quantitative screening	
	grown wells [%]	qualitative screening [$\mu\text{g/ml}$]	Titer [$\mu\text{g/ml}$]	qp ¹ [pg/cell/day]	Titer [$\mu\text{g/ml}$]	qp ¹ [pg/cell/day]
RS3H6	99	0.1 - 0.2	0.33 - 0.75	0.23 - 0.55	0.47 - 0.98	0.33 - 0.52
SH3H6	99	0.05 - 0.2	0.15 - 0.43	0.13 - 0.30	0.16 - 0.50	0.11 - 0.28
GA3H6	100	0.1 - 0.2	0.44 - 0.79	0.64 - 1.41	0.45 - 1.39	0.19 - 0.91
GC3H6	85	0.1 - 0.2	0.56 - 0.63	0.46 - 0.66	0.85 - 1.44	0.49 - 0.72

¹calculated with end cell number

The best producing CHO clones from each humanized Ab2/3H6 variant was tested in a six days static batch culture (Table IV). The obtained titers in this batch experiments were sufficient for subsequent purification of humanized Abs, thus no further gene amplification or stabilizing sub-cloning steps were considered. Further, these clones were used for production of supernatant in Spinner flasks as well as Roller bottles. The production process was run over two weeks splitting the cells twice a week and collecting the supernatant. Samples were taken at every passage step and analyzed for specific growth rate, specific productivity and absolute Ab concentrations. No significant differences between cultivation in Spinner flasks or Roller bottles were observed. The total Ab titer was in a similar range for different recombinant CHO clone. However the specific growth rate (μ) was slightly better in the Roller bottles. The results of these cultivation experiments are visualized in figure 14 and summarized in table V.

Table IV. Six days batch of best producing humanized Ab2/3H6 variants CHO clones from 2nd T25 screening

recombinant CHO cell line producing	T80			T175		
	Titer [$\mu\text{g/ml}$]	qp ¹ [pg/cell/day]	μ [d^{-1}]	Titer [$\mu\text{g/ml}$]	qp ¹ [pg/cell/day]	μ [d^{-1}]
RS3H6/A4	1.85	0.97	0.08	1.00	0.44	0.13
SH3H6/C2	2.40	0.92	0.18	1.80	0.78	0.14
GA3H6/D10	1.90	0.97	0.09	2.30	1.05	0.12
GC3H6/D3	2.10	0.82	0.16	2.00	0.96	0.10

¹calculated with cell days

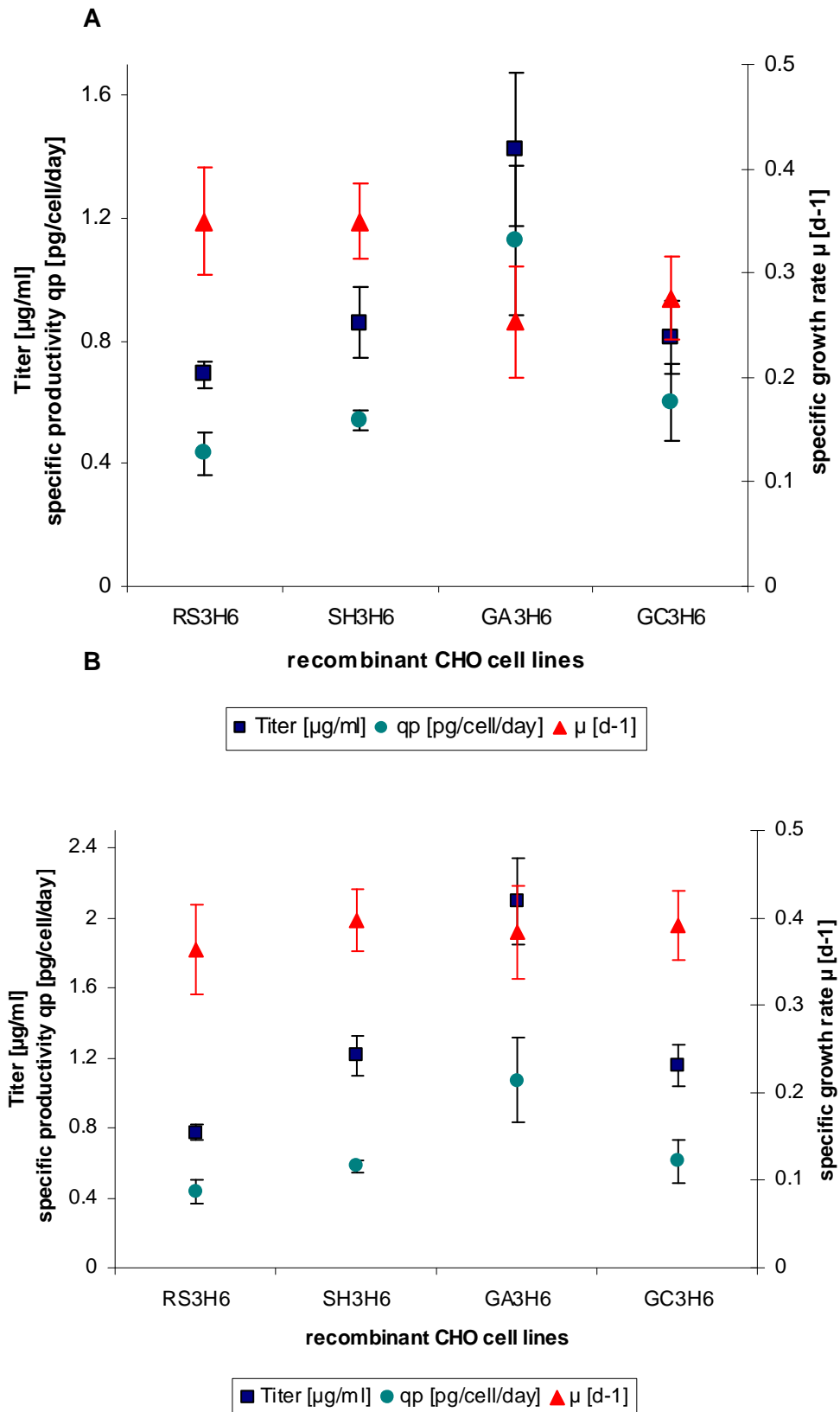


Figure 14. Cultivation of selected CHO clones producing humanized Ab2/3H6 variants in **(A)** Spinner flasks and **(B)** Roller bottles. For each recombinant clone the mean value of total antibody titer, specific productivity (qp), and specific growth rate (μ) determined during two weeks of cultivation is displayed in the graph. Error bars represent the standard deviation [n=4 for **(A)** and n=5 for **(B)**].

Table V. Two weeks cultivation of selected CHO clones producing humanized Ab2/3H6 variants in **(A)** Spinner flasks and **(B)** Roller bottles

A Cultivation in Spinner flasks

passage number	RS3H6			SH3H6			GA3H6			GC3H6		
	Titer	μ	qp	Titer	μ	qp	Titer	μ	qp	Titer	μ	qp
	[$\mu\text{g/ml}$]	[d^{-1}]	[pg/cell]	[$\mu\text{g/ml}$]	[d^{-1}]	[pg/cell/day]	[$\mu\text{g/ml}$]	[d^{-1}]	[pg/cell/day]	[$\mu\text{g/ml}$]	[d^{-1}]	[pg/cell/day]
1	0.70	0.33	0.42	0.95	0.34	0.55	1.11	0.23	0.85	0.65	0.24	0.48
2	0.65	0.42	0.43	0.89	0.40	0.58	1.44	0.27	1.25	0.91	0.33	0.67
3	0.67	0.34	0.35	0.91	0.32	0.52	1.72	0.19	1.02	0.89	0.27	0.51
4	0.74	0.30	0.53	0.70	0.34	0.52	1.42	0.32	1.39	0.79	0.26	0.74

B Cultivation in Roller bottles

passage number	RS3H6			SH3H6			GA3H6			GC3H6		
	Titer	μ	qp	Titer	μ	qp	Titer	μ	qp	Titer	μ	qp
	[$\mu\text{g/ml}$]	[d^{-1}]	[pg/cell]	[$\mu\text{g/ml}$]	[d^{-1}]	[pg/cell/day]	[$\mu\text{g/ml}$]	[d^{-1}]	[pg/cell/day]	[$\mu\text{g/ml}$]	[d^{-1}]	[pg/cell/day]
1	0.72	0.40	0.33	1.39	0.43	0.60	1.68	0.37	0.90	1.08	0.35	0.62
2	0.82	0.43	0.28	1.54	0.39	0.53	2.91	0.40	0.99	1.51	0.41	0.57
3	0.80	0.43	0.43	0.92	0.45	0.51	1.69	0.46	0.91	0.86	0.40	0.55
4	0.73	0.21	0.53	1.18	0.40	0.71	2.01	0.29	1.30	1.04	0.55	0.64
5	0.80	0.34	0.59	1.04	0.32	0.55	2.19	0.40	1.25	1.27	0.25	0.66

During the two weeks production process two liters supernatant of each CHO clone was harvested resulting in a total amount of 1 – 2 mg / l recombinant humanized Ab2/3H6 variant, respectively. The recombinant cell line producing the chimeric Ab2/3H6 (Gach et al. 2007a) was used as reference material in all analyses. Supernatant of this cell line was produced in the same way as for the humanized variants.

3.1.5 Affinity purification of chimeric and humanized Ab2/3H6 variants

The purification process is described in detail in section 6.1 (selected publications: Mader et al. 2010). The chromatogram in figure 15A shows a typical protein A affinity purification run which was the same for purification of all Ab2/3H6 IgG variants resulting in 1.5 – 3.5 mg purified Ab for each variant. The purity achieved using affinity purification was > 90 % and was verified with SDS-PAGE and Western Blot (figure 15B).

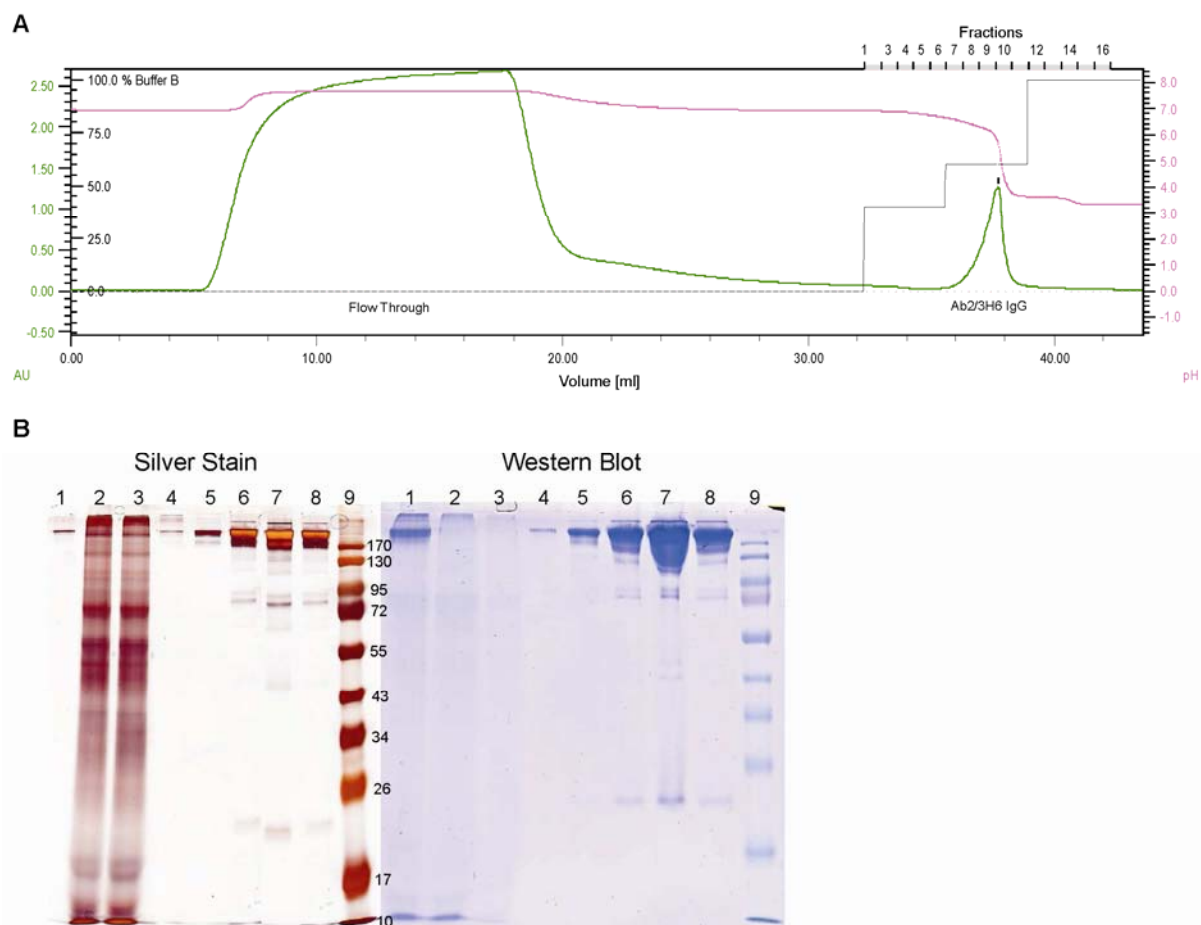


Figure 15. In panel **A** a typical chromatogram of a protein A affinity purification run is shown. The green curve is the absorbance units at 280 nm. All host cell proteins and impurities did not bind to the column and are represented by the large Flow Through peak. The bound IgG were eluted with pH 4.0 (pink curve). In panel **B** the Silver Stain and Western Blot (anti- κ) of this purification run are shown. Lane 1: CHO supernatant; Lane 2: Flow Through; Lane 3: Wash; Lane 4-8: elution fractions; Lane 9: marker

3.1.6 Binding characteristics of humanized Ab2/3H6 variants

The purified IgGs of all Ab2/3H6 variants were tested for their binding capacity in a bio-layer interferometry assay with the Octet QK and in a competition ELISA. The results of these experiments are provided in section 6.1 (selected publications: Mader et al. 2010). In summary the humanized Ab2/3H6 variants RS3H6, GC3H6 showed the same affinity, GA3H6 had a 2-fold loss in affinity and SH3H6 lost the ability to bind mAb 2F5 in comparison to chimeric Ab2/3H6.

3.1.6.1 The Mix/Match approach

Additionally to the expression of the fully humanized variants in stable CHO cell lines, so called Ab2/3H6 mix/match versions were transiently expressed in HEK293F cells (Invitrogen). These mix/match Abs contained a humanized HC or LC and the corresponding chimeric HC or LC (i.e. RS3H6 HC with chAb2/3H6 LC or RS3H6 LC with chAb2/3H6 HC did

not change binding properties; data not shown). The binding properties of different Ab2/3H6 mix/match variants were tested in competition assay and are shown in figure 16. The aggressively grafted LC (GALC) in combination with chAb2/3H6 HC showed the same decreased competition effect (red open triangle) as GA3H6 in comparison to the chimeric Ab2/3H6. This indicated that probably the LC of the GA3H6 version is responsible for the 2-fold loss in binding affinity of GA3H6 to mAb 2F5 since GAHC in combination with chLC showed identical as Ab2/3H6. In contrast the conservatively grafted LC (GCLC) in combination with chAb2/3H6 HC had similar properties as the original Ab2/3H6.

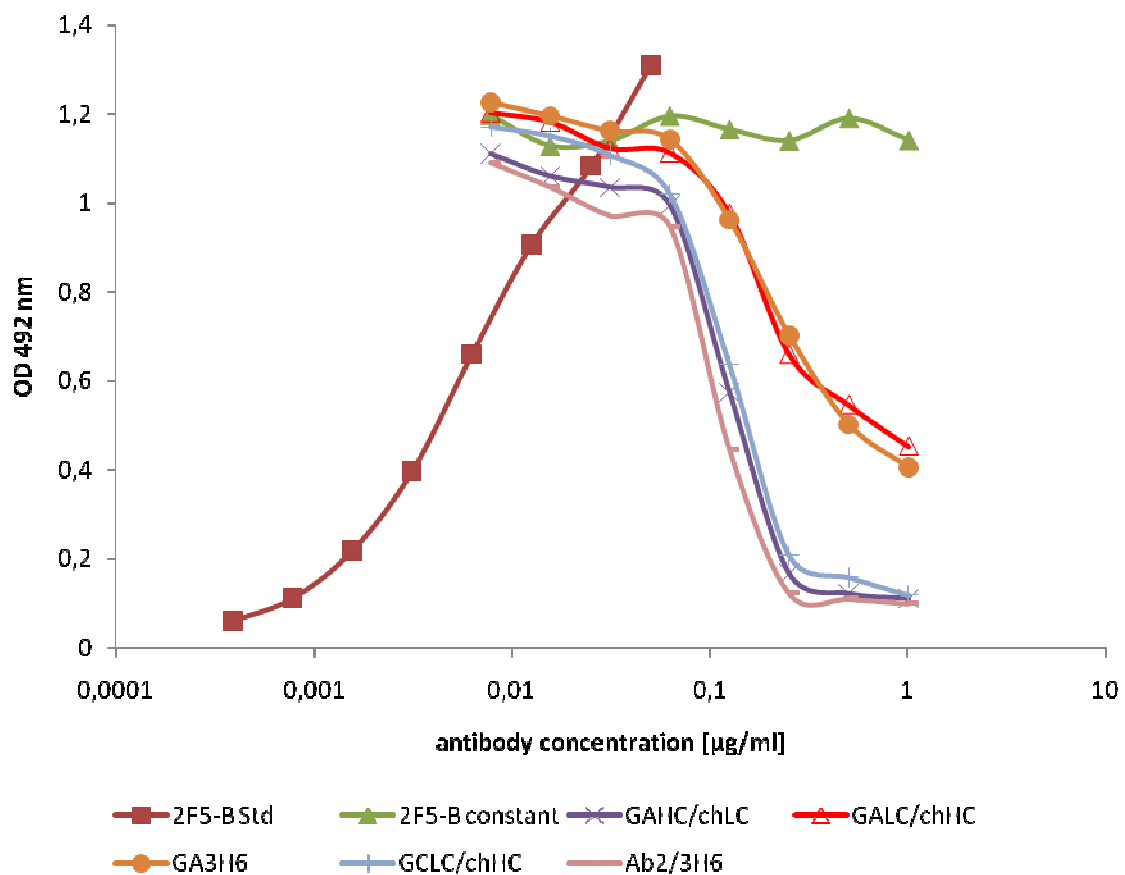


Figure 16. Competition assay of Ab2/3H6 mix/match variants.

Therefore an additional CDR-grafted humanized form of Ab2/3H6, containing the aggressively grafted HC and the conservatively grafted LC was developed. The stable CHO cell line of this version termed “graft mix Ab2/3H6” (GM3H6) was established in the same way as described in 3.4. Binding properties of GM3H6 were determined. The IC50 and aK-values calculated from the competition ELISA (figure 17) shows that the GM3H6 version had the same binding properties as the chimeric Ab2/3H6.

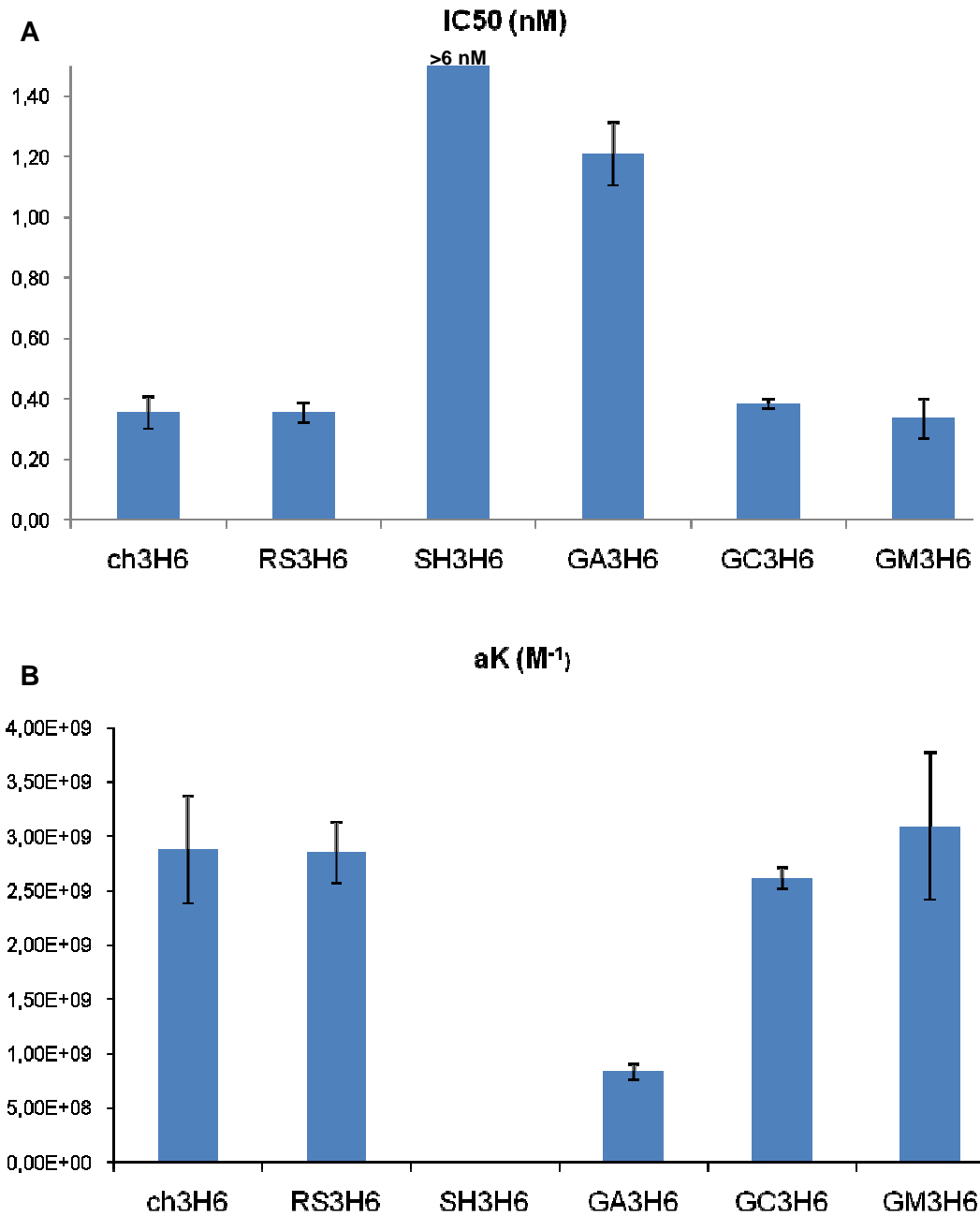


Figure 17. Binding properties of humanized Ab2/3H6 variants in comparison to chimeric Ab2/3H6. Panel **A**: IC₅₀ values are calculated from the Ab2/3H6 concentration required for 50 % inhibition of maximal binding in competitive ELISA. Panel **B**: aK values are calculated as the reciprocal value of the Ab2/3H6 concentration required to inhibit 50 % of the maximal binding in a competitive ELISA. The columns represent the mean values including the standard deviations by error bars of four independent experiments (n=4).

3.1.7 Molecular simulation of humanized Ab2/3H6 variants

Performing in-vitro binding studies revealed that the superhumanized Ab2/3H6 variant lost binding to mAb 2F5 (see section 3.1.6). To elucidate the molecular nature of the lost interaction collaboration with the Institute of Molecular Modeling and Simulation was started. With molecular dynamics (MD) simulation, not only the structural differences between models but also differences in their fluctuations and dynamics can be monitored. De Ruiter et al performed MD simulations of the murine Ab2/3H6 in solution and bound to mAb 2F5 as well as of the different humanized Ab2/3H6 models to gain more insights in the differences between these models (section 6.2 selected publications: deRuiter et al. 2011). The simulation of the SH3H6 in comparison with the original Ab2/3H6 showed that the TyrH54^{SH3H6} sidechain is not available for hydrogen bonding with mAb 2F5 (de Ruiter et al. 2011) as it is shown in the crystal structure of the complex between mAb 2F5 and Ab2/3H6 (Bryson et al. 2008). On the other hand TyrH103^{SH3H6} is more flexible resulting in clashes with backbone atoms of mAb 2F5 and therefore needs to move to a less favorable orientation (de Ruiter et al. 2011).

3.1.8 Immunogenicity of humanized Ab2/3H6 variants

After the discovery that murine Abs are likely to induce HAMA in therapy, humanization strategies were developed to circumvent this phenomenon. Today humanized or fully human Ab therapeutics are considered to be safe. However in the last years immunogenicity regarding human(ized) Abs became a controversial topic (Barbosa and Celis 2007; De Groot and Scott 2007; Getts et al. 2010; Harding et al. 2010).

Therefore, immunogenicity assessment of a human therapeutic is required by the regulatories (EMEA 2007) and is considered to be done in pre-clinical and clinical studies. To estimate the potential of a human therapeutic to be immunogenic, bioinformatical tools have been developed in the last decades and by steadily improving the algorithms and screening capacity by increasing computational power these tools gain more and more attention (Brusic et al. 2004; De Groot and Moise 2007; Zhang et al. 2008; El-Manzalawy and Honavar 2010; Wang et al. 2011).

In this paragraph some of the freely available online tools are described in the context with the humanization of Ab2/3H6.

3.1.8.1 Z-score, G-score and germinality index (GI)

The Z-score has been defined by Abhinandan et al for analysis of “the degree of humanness” of Ab sequences (Abhinandan and Martin 2007). They extracted data sets of human Abs from the Kabat database⁹ and calculated mean sequence identities and standard deviations. In general, the Z-score simply indicates how many standard deviations below or above the

⁹ <http://www.kabatdatabase.com>

mean of a certain value is. A human sequence should have a Z-score around zero therefore they suggest that their method can be used for predicting Ab immunogenicity.

The G-score (Thullier et al. 2010) is an improvement or extension to the above described Z-score. The difference is that instead of data sets of human Abs, germline variable genes were used which were retrieved from the NCBI database¹⁰. Z-score and G-score analysis for the humanized Ab2/3H6 variants in comparison with chimeric Ab2/3H6 had been done using an automated online tool provided by Dr Andrew C.R. Martin's laboratory^{11,12}. Another method to calculate the "humanness" was proposed by Pelat et al (Pelat et al. 2008). The so-called germinality index (GI) is the ratio of non-human residues in the FR to human germline residues calculated from the closest human germline. In general, the GI simply indicated how related a FR is to the most identical human germline sequence. A GI of one is 100 % human germline. The obtained Z-score, G-score and GI values are summarized in table VI. The Z- and G-scores of the humanized Ab2/3H6 HCs are all lower than that of the chimeric version indicating that humanization of the HCs leads to more human like Ab HCs in all Ab2/3H6 variants. Interestingly the RS3H6 and SH3H6 LC have higher Z-score values indicating that they are less human than the chimeric Ab2/3H6 variant. The RS3H6 LC had six human aa substitutions in the FR and the SH3H6 LC consists of a complete human germline FR, thus the Z- and G-score should be lower compared to the chimeric LC. Therefore, the human germline FR IGKV5-2*01/Jk2 used for acceptor framework in the superhumanization approach was analyzed revealing a Z-score of -3.173 and a G-score of -3.448. The Z-score calculation proposed by Abhinadan et al. is based on average similarity to the human repertoire represented by a set of human antibodies. In case of human kappa light chain this set resembles 645 human sequences.

Table VI. Z-score of Ab2/3H6 variants

antibody variants	Z-score		G-score		GI
	HC	LC	HC	LC	
chAb2/3H6	-1.533	-3.177	-2.3	-3.659	0.669
RS3H6	-0.928	-3.566	-1.567	-3.885	0.740
SH3H6	-0.605	-3.525	0.408	-3.892	1
GA3H6	-0.267	-1.706	0.161	-1.979	0.834
GC3H6	-1.037	-2.372	1.179	2.419	0.768
GM3H6	-0.267	-2.372	0.161	2.419	0.812

In case of the G-score it seemed that the IGKV5-2*01 germline gene was not implemented in the extracted data sets. This could be because the IGKV5-2*01 is very rare. A blast search

¹⁰ <http://www.ncbi.nlm.nih.gov/>

¹¹ <http://www.bioinf.org.uk/abs/gscore/>

¹² <http://www.bioinf.org.uk/abs/shab/>

against the non-redundant Gene Bank showed that very few human Ab sequences are deposited that match the IGKV5-2*01 germline gene and a search against the pdb database revealed that the crystal structure of an existing Ab that is most identical to that germline gene has only an identity of 66 %. The GI values indicate that every Ab2/3H6 variant has been improved towards germline like FRs, which might result in a reduced immunogenicity because human germline FRs do not have somatic hypermutations and should therefore be less immunogenic (Shearman et al. 1991).

In the light of these findings Z- and G-score analysis might in our case not be the right tool for predicting antigenicity especially in the case of the kappa light chains used in this humanization approach. The GI value just indicates that the Ab2/3H6 variants are now closer to the human germline.

3.1.8.2 B-cell and T-cell epitope prediction

Identification and characterization of B-cell epitopes is one of the key steps in epitope-driven vaccine design. There are two classes of B-cell epitopes: linear (continuous or sequential) epitopes or conformational (discontinuous) epitopes. Linear epitopes are short peptides that correspond to a contiguous aas sequence fragment of a protein (Barlow et al. 1986; Langeveld et al. 2001). In contrast conformational epitopes are composed of aas that are not contiguous in primary sequence, but due to folding of the protein resemble a 3-dimensional structural epitope.

Although the majority of B-cell epitopes are thought to be conformational in nature (Walter 1986), most experimental as well as computational methods focus on mapping linear B-cell epitopes (Flower 2007). However, in the past few years, there is increasing interest in methods for predicting conformational B-cell epitopes (El-Manzalawy and Honavar 2010). Unfortunately, the conformation-dependent nature of antigen-Ab binding complicates the problem of B-cell epitope prediction. Hence, B-cell epitope prediction is less tractable than T-cell epitope prediction (Korber et al. 2006). In a preliminary study a couple of prediction programs (reviewed in (El-Manzalawy and Honavar 2010)) were tested with the homology models of the Ab2/3H6 variants. Only with Ellipro¹³, a freely available conformational B-cell epitope predictor developed by Ponomarenko et al. it was possible to get a prediction (Ponomarenko et al. 2008). Briefly, the homology model pdb-files from our Ab2/3H6, RS3H6, GA3H6 and SH3H6 variants were submitted for prediction to the Ellipro server. With the homology model data the server predicts linear B-cell epitopes (Table VII) as well as conformational epitopes (Figure 18).

¹³ http://tools.immuneepitope.org/tools/ElliPro/iedb_input

Table VII. Linear B-cell epitope prediction using Ellipro

Ab2/3H6					
epitopes vH	number aas	score	epitopes vL	number aas	score
SIGYGSSPPFPY	12	0.755	EIKRA	5	0.848
QSHGKSL	7	0.753	KPGEPPR	7	0.761
DTSSN	5	0.694	SDNLPYT	7	0.695
GPELVKTGAS	10	0.691	GYGTD	5	0.661
NSLTSE	6	0.679	TSTDIDD	7	0.644
EVQLQ	5	0.648	ETTV	4	0.642
KASGYSFTDY	10	0.569	PASLSMSIGEK	11	0.631
CYTGATNYSQKFKGK	15	0.568	GNTLRPGVPSR	11	0.631
			ENMLSE	6	0.581

RS3H6					
epitopes vH	number aas	score	epitopes vL	number aas	score
SIGYGSSPPFPY	12	0.756	EIKRT	5	0.817
QAPGQSL	7	0.749	KPGEPP I	7	0.743
DTSSN	5	0.696	SDNLPYT	7	0.725
GPELVKPGAS	10	0.693	STDIDD	6	0.703
NSLTSE	6	0.674	AFMSATPGDK	10	0.673
CYTGATNYSQKFKGK	15	0.593	GYGTD	5	0.646
KASGYSFTDY	10	0.557	GNTLRPGVPPR	11	0.628
			ENMLSE	6	0.543

GA3H6					
epitopes vH	number aas	score	epitopes vL	number aas	score
SIGYGSSPP	9	0.854	EVKRT	5	0.879
APGQGL	6	0.802	QKPGKAPK	8	0.712
DTSTN	5	0.711	SDNLPYMF	8	0.702
GAEVKKPGSS	10	0.678	STDIDDD	7	0.645
SSLRSE	6	0.631	PSTLSASVGDR	11	0.618
CYTGATNYAQKFOGR	15	0.614	SDGNTLRPGVPSR	13	0.607
SGYTFTDY	8	0.549	SGTE	4	0.596
			SSLQPD	6	0.563

SH3H6					
epitopes vH	number aas	score	epitopes vL	number aas	score
DTSTD	5	0.777	KPGEAA	6	0.798
QAPGKGL	7	0.732	SDNLPYT	7	0.706
SIGYGSSPPFPY	12	0.713	PAFMSATPGDK	11	0.693
GAEVKKPGAT	10	0.688	YGTD	4	0.668
YSQKFKGR	8	0.629	STDIDDD	7	0.645
VTVS	4	0.618	DGNTLRPGIPPR	12	0.615
KVSGYTFTDY	10	0.602	NNIESE	6	0.592
CYTGA	5	0.602			
SSLRSED T	8	0.591			

B-cell epitopes inside the CDRs are in **bold** and **gray shaded**

The program predicted in the original Ab2/3H6 Ab 11 linear B-cell epitopes in the FRs and six in the CDRs. According to the prediction a reduction of two linear epitopes in the RS3H6, GA3H6 and SH3H6 variant could be achieved with the different humanization approaches. The conformational B-cell epitope prediction for the original AB2/3H6 by Ellipro is visualized in figure 18. Most of the B-cell epitopes overlap or cover the CDR regions, but also conformational B-cell epitopes were predicted for the FR1, FR2 and FR3 regions of the vH as well as vL respectively. However, according to accessibility coloring not all the predicted B-cell epitope residues are accessible (blue color indicates buried aas). In total seven conformational epitopes were predicted for Ab2/3H6, RS3H6 and GA3H6. For SH3H6 only 6 epitopes were predicted. The predicted epitopes in all variants were attributed to the same epitopes. Only the number of residues per epitope and the prediction score differed slightly, but according to this prediction method no reduction in conformational B-cell epitopes were achieved by our humanization study.

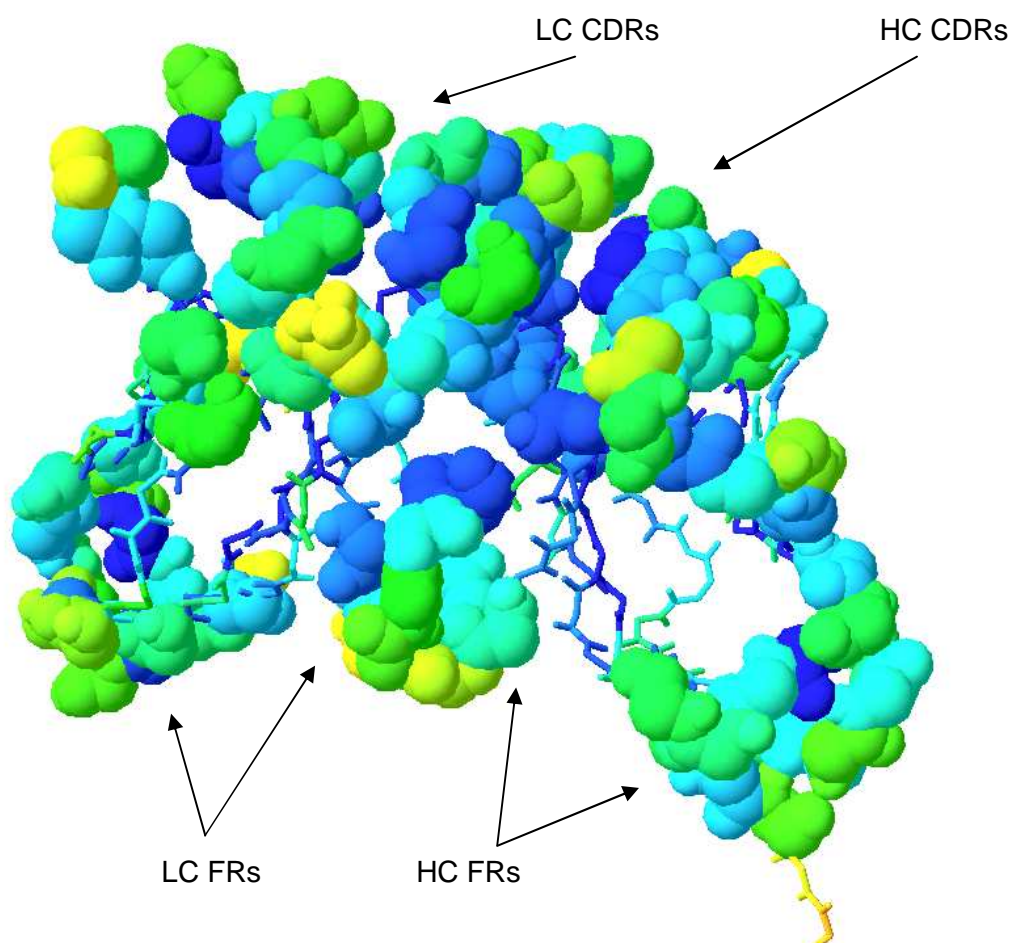


Figure 18. Conformational B-cell epitope prediction by Ellipro server. The model of Ab2/3H6 was colored according to accessibility. Green/Yellow: accessible; Blue: buried.

The amount of T cell epitopes in a protein is one of the factors that contribute to immunogenicity. The binding strength of T cell epitopes to MHC molecules is a key determinant in T cell epitope immunogenicity (De Groot and Martin 2009). Thus, the fate of a protein drug may be determined by its constituent 9-mers and their corresponding MHC/HLA binding affinities. One approach to measuring the potential immunogenicity of a protein is to parse protein sequences into overlapping 9- or 15-mer peptide frames, and to search for potential T cell epitopes by estimating the HLA binding potential of these short sequences, *in silico*, to eight common class II HLA alleles that “cover” the majority of human genetic backgrounds (Southwood et al. 1998).

T cells recognize linear epitopes derived from proteins that are processed by APCs. Briefly, antigenic proteins are broken down by proteolytic enzymes in the APC. During this process very large numbers of peptide fragments are produced. Any one of these fragments could be a T cell epitope, but only about 2% of all the fragments generated have the right aas sequence that allow them to bind in the MHC binding groove and be presented on the surface of the APC. One of the critical determinants of immunogenicity is the strength of T cell epitope binding to MHC molecules (Lazarski et al. 2005). Peptides binding with higher affinity to MHC as well as peptides that bind to clusters of different HLA alleles are more likely to be displayed on the cell surface where they can be recognized by TCRs.

In this study the freely available prediction tool NetMHCIIpan2.1¹⁴ (Nielsen et al. 2010) was used. For this analysis the original Ab2/3H6, GA3H6 and SH3H6 were considered. The results of the NetMHCIIpan prediction is summarized in table VIII. In total 51 epitopes for Ab2/3H6, 50 epitopes for GA3H6 and 52 epitopes for SH3H6 were predicted. The results were evaluated according following parameters: strong binders have a predicted affinity lower 50 nM; weak binders have a predicted affinity lower 500 nM; epitopes that react with multiple HLA-alleles are more likely to be T-cell epitopes. According to this defined parameters the epitopes reacting with four or more HLA-alleles were considered to be potential T-cell epitopes. Ab2/3H6 therefore had 16 potential T-cell epitopes whereas six overlap or cover the CDRs, GA3H6 had 13 potential epitopes with eight inside or overlapping the CDRs and SH3H6 had 11 predicted T-cell epitopes with seven contributing to CDR regions. According to T-cell prediction the amount of T-cell epitopes in the FRs of GA3H6 could be reduced by 50 % and of SH3H6 by 60 % in comparison to the original Ab2/3H6.

¹⁴ <http://www.cbs.dtu.dk/services/NetMHCIIpan/>

Table VIII. T-cell epitope analysis using NetMHCIIpan2.1

Ab2/3H6								
Sequence (vH):	VQLQQSGPELVKGTGASVKISCKASGYSFTDYFMHWVKQSHGKSLDWIGYINCYTGATNYSQKFKGKATFT VDTSSNTAYMQFNLSLTSEDSAVYYCARTSIGYGSSPPFPYWGQGLVTVSA							
epitope sequence	DRB1*0101	DRB1*0301	DRB1*0401	DRB1*0701	DRB1*0801	DRB1*1101	DRB1*1301	DRB1*1501
CYTGATNYS						489.79		
DYFMHWVKQ	408.85							
FKGKATFTV	67.42		411.85	131.14	329.49	388.8		
FMHWVKQSH								277.05
FNSLTSEDS	5.75		8.22	44.38	219.66	132.21		350.86
FTDYFMHWV								166.77
FTVDTSSNT	217.87	305.79	22.11	173.48				
GYSFTDYFM								449.85
IGYGSSPPF	205.44							471.86
INCYTGATN								333.78
LQQSGPELV	72.07			201.27			161.95	
LVKTGASVK					311.22			331.01
SCKASGYSF	492.55			422.01				
SVKISCKAS					337.64			
TAYMQFNLS	159.57							
TFTVDTSSN					402.93			
VDTSSNTAY							312.93	
VKISCKASG					63.98	144.83	161.32	
VKQSHGKSL	64.7			36.11			157.03	362.78
VKTGASVKI	31.86			32.58			47.45	376.41
VYYCARTSI					264.61	429.23		
WIGYINCYT	401.99							355.49
WVKQSHGKS	44.62				18.38	21.18		
YCARTSIGY					450.73			
YFMHWVKQS	76.38		396.17	158.33	20.25	22.93		180.33
YGSSPPFPY	244.19			292.74				
YINCYTGAT	125.54		310.91		412.42			
YMQFNLSLT	26.05		25.19	233.28	388.89	193.44		205.57
YSFTDYFMH				267.56	467.36	367.41		191.71
YSQKFKGKA	482.58				119.28	93.82		
YTGATNYSQ	62.69		28.49	170.44		471.23		
YWGQGLVTV	29.68		249.64					
YYCARTSIG	13.65		32.64	76.93	30.84	29.94		214.93
Sequence (vL):	ETTVTQSPASLSMSIGKVTIRCITSTDDIDDMNYYQQKPGEPRLLI SDGNTLRPGVPSRFSSSGYGTD FVFTIENMLSEDVADYYCLQSDNLPYTFGGGTNLEIK							
epitope sequence	DRB1*0101	DRB1*0301	DRB1*0401	DRB1*0701	DRB1*0801	DRB1*1101	DRB1*1301	DRB1*1501
CLQSDNLPY		187.53					173.11	
EKVTIRCIT					256.64			
FGGGTNLEI			436					

FVFTIENML	43.55		116.7	34.99			404.5	448.08
IENMLSEVD	40.96						266.66	
IRCITSTDI	179.18		349.18	49.99	90.46		213.87	
LISDGNTLR		9.48	57.15					
LLISDGNTL	71.3			181.78			23.4	414.56
LRPGVPSRF	91.34						294.18	
LSEVDADYY		147.89						
LSMSIGEKV	24.17			35.44			53.18	485.96
MLSEVDADY		140.69	403.25				213.13	
VFTIENMLS			111.23		489.6		276.25	
VTIRCITST					231.04			
VTQSPASLS	22.86		195.96	123.31	245.14		243.17	
YCLQSDNLP	423.7		87.4					
YQKPGPEPP	114.83							
YTFGGTNL	55.51			281.8				
YYCLQSDNL	13.1		59.83	130.78				369.62

GA3H6								
Sequence (vH):	QVQLVQSGAEVKKPGSSVKVSKASGYTFDYMHWVRQAPGQGLEWIGYINCYTGATNYAQKFGQGRVTIT VDTSTNTAYMELSSLRSEDYAFYFCARTSIGYSSPPFPYWGQGLVTVSS							
epitope sequence	DRB1*0101	DRB1*0301	DRB1*0401	DRB1*0701	DRB1*0801	DRB1*1101	DRB1*1301	DRB1*1501
CYTGATNYA	49.25			252.16				
DYFMHWVRQ	347.43							
FMHWVRQAP						183.05		
FQGRVTITV	173.45			128.28	270.2			
FTDYFMHWV								195.82
FYFCARTSI	289.7			196.63	163.48	26.14		
IGYSSPPF	205.44							471.86
INCYTGATN	108.74			392.49				306.28
ITVDTSTNT		254.17	156.54		296.2		102.38	
LRSEDYAFY	111.17	173.7	94.75				480.21	
LSSLRSEDY	69.64			403.31				
LVQSGAEVK	119.94			365.04			383.08	
MHWVRQAPG					76.12			
RVTITVDTS					234.53			
TAFYFCART								490.87
TAYMELSSL	183.92							
TITVDTSTN			229.71		266.69			
VDTSTNTAY			416.91				165.76	
VKVSCKASG					104.47	307.12	432.39	
VRQAPGQGL	30.43			197.72			234.79	
VTITVDTST					248.72			
WIGYINCYT	359.84							307.05
WVRQAPGQG					218.53			
YAKFGQGRV	182.67				408.16	360.55		

YFCARTSIG	8.8		28.97	39.12	22.23	16.77		194.05
YFMHWVRQA	47.75			98.13	29.75	50.04		128.81
YGSSPPFPY	244.19			292.74				
YINCYTGAT	130.58		284.91		405.37			
YMELSSLRS	7.93		41.64	163.81	309.26	110.97		360.43
YTFDYFMH				215.39	394.5	334.07		227.25
YTGATNYAQ	54.78		25.54	333.7				
YWGGQTLVT	36.16		288.78					

Sequence (vL):	DTQVTQSPSTLSASVGDRVTITCITSTDIDDDMNWYQQKPGKAPKLLISDGNTLRPGVPSRFISSGS GTEFTLTISSLQDDFADYYCLQSDNLPYMGQGTKVEVK							
epitope sequence	DRB1*0101	DRB1*0301	DRB1*0401	DRB1*0701	DRB1*0801	DRB1*1101	DRB1*1301	DRB1*1501
CLQSDNLPY							105.85	
EFTLTISL	420.74			324.59				
FISSGSGTE	279.04			176.58				
FTLTISLQ	30.43		21.1	25.46	138.46	304.8		
ITCITSTDI	395.57			53.53	162.82		368.32	
LISDGNTLR		9.54	55.33					
LLISDGNTL	68.59			160.55			22.49	389.22
LQSDNLPYM		70.27						
LRPGVPSRF	59.53	469.54					199.42	
LSASVGDRV	234.36			120.6			108.26	
RFISSGSGT	436.96							
VTITCITST					320			
VTQSPSTLS	99.23		166.53	133.35	271.41			
WYQQKPGKA	34.58				473.14	316.2		
YCLQSDNLP	282.89		73.24					
YMGQGTKV	9.24			142.61		348.32		492.57
YQKPGKAP	381.99							
YYCLQSDNL	10.8		51.91	88.19				297.05

SH3H6								
Sequence (vH):	EVQLVQSGAEVKKPGATVKISKVSGYFTDYFMHWVQAPGKGLEWVMGYINCYTGATNYSQKFKGRVTIT ADTSTDYAYMELSSLRSEDYAVYCATTSIGYSSPPFPYWGQTLVTVSS							
epitope sequence	DRB1*0101	DRB1*0301	DRB1*0401	DRB1*0701	DRB1*0801	DRB1*1101	DRB1*1301	DRB1*1501
ATVKISKV						345.64		
CYTGATNYS						489.79		
FKGRVTITA	125.94		371.94	322.15	75.76	148.71		
FTDYFMHWV								246.36
IGYSSPPF	240.52							
INCYTGATN								381.83
ITADTSTDY		105.16	98.35				212.09	
LRSEDYAVY		139.19	151.17				423.94	
LSSLRSEDY	72.2			389.75				
LVQSGAEVK	184.26			499.07			417.91	
MHWVQAPG					137.7			

SCKVSGYTF				407.77				
TAYMELSSL	255.03							
TVKISCKVS					471.84			
VKISCKVSG					99.04	240.53	264.39	
VQQAPGKGL	18.52			197.72				441.94
VTITADTST					429.02			
VYYCATTSI	388.58			38.84				
WMGYINCYT	406.59							419.97
WVQQAPGKG	17.68					344.8		
YCATTSIGY				116.2				
YFMHWVQQA	72.98		470.72	198.7	160.68	240.39		
YGSSPPFPY	244.19			337.34				
YINCYTGAT	125.75		343.93		476.53			
YMELSSLRS	9.34		53.78	238.67	474.48	137.22		497.84
YSQKFKGRV	455.13			499.26	145.57	114.47		
YTFDYFMH				247.09				311.22
YTGATNYSQ	62.69		28.49	170.44		471.23		
YWGGTLVT	36.16		288.78					
YYCATTSIG	19.56		20.29		142.9	124.56		434.51
Sequence (vL): ETTLTQSPAFMSATPGDKVNISCITSTDDIDDMNWWYQKPGEEAIFIIQDGNTLRPGIPPRFSGSGY GTDFTLTINNIESEDAAYFCLQSDNLPYTFGQGTKLEIK								
epitope sequence	DRB1*0101	DRB1*0301	DRB1*0401	DRB1*0701	DRB1*0801	DRB1*1101	DRB1*1301	DRB1*1501
CLQSDNLPY		179.82					135.24	
DFTLTINNI	234.75						90.18	
FCLQSDNLP	295.22		29.24					
FIIQDGNTL	11.46		55.71	184.69			26.91	182.73
FMSATPGDK	20.88	469.55	92.8	51.97	363.27	174.65		
FTLTINNIE	273.64		106.4	108.9	460.08			
IESEDAAYY	243.09						176.05	
IFIIQDGNT					388.44			
IIQDGNTLR		16.98					18.51	
INNIESEDA	350.26							
ISCITSTDI				94.07	345.69		300.05	
LRPGIPPRF	209.6							
LTINNIESE							171.49	
LTQSPAFMS	30.68		125.13	64.4	282.77			
PAFMSATPG	100.82							
TLTQSPAFM							451.25	
WYQKPGEA	32.42							
YFCLQSDNL	8.66		28.74	62.58	346.62	227.89		176.08
YGTDFTLTI	366.85		105.18	241.22				
YQKPGEAA	17.63							
YTFGQTKL	9.44			57.19		348.82		
YYFCLQSDN						303.22		

Values < 50 (strong binders); <500 (weak binders)

3.2 The humoral immune response of Ab2/3H6

In previous studies Gach et al. demonstrated that Ab2/3H6 is able to inhibit the binding of mAb 2F5 to its synthetic epitope ELDKWASL (Gach et al. 2007a) and induces anti-anti-idiotypic Abs in a mouse (Gach et al. 2008a) as well as in a guinea pig immunization study (Gach et al. 2008b). These results were quite promising but in these former studies only binding assays against gp160 or gp41 and the linear epitope ELDKWASL were performed. Further the obtained amounts of reactive sera from these animals were quantitatively insufficient to perform further analysis.

To verify the previous results and proof the claim that Ab2/3H6 is capable to induce neutralizing anti-HIV-1 Abs a prime / boost immunization regime in rabbits was set up.

3.2.1 Development of Ab2/3H6 antibody fragment fusion proteins

To improve the potency of Ab2/3H6, fusion proteins consisting of Ab2/3H6 Fab with C-terminally attached polypeptides were designed (Figure 19). These polypeptides should stimulate the immune system by eliciting B- and T-cell responses against the antigen and therefore increasing the generation of anti-anti-idiotypic Abs in-vivo.

One of these immune stimulatory polypeptides is the cytokine interleukin 15 (IL15) which has a wide range of biological activities including activation and proliferation of CD8+ T-cells and natural killer T-cells, the maintenance of CD8+ memory cells, and the differentiation and maturation of B cells (Waldmann 2006; Rodrigues and Bonorino 2009).

Other immunostimulatory peptides are the so-called “promiscuous” T-cell epitopes from tetanus toxin (TT) (Panina-Bordignon et al. 1989; Kaumaya et al. 1993). Previous studies showed that co-immunization with the T-cell epitope from TT increased the production of HIV-1 nAbs in a macaque prime/boost study (Benferhat et al. 2009).

Therefore we designed fusion proteins of Ab2/3H6 Fabs with the IL15 and alternatively an epitope of TT, respectively. For details on generation of the expression plasmids refer to section 7 (selected publications: Mader et al. 2011 submitted).

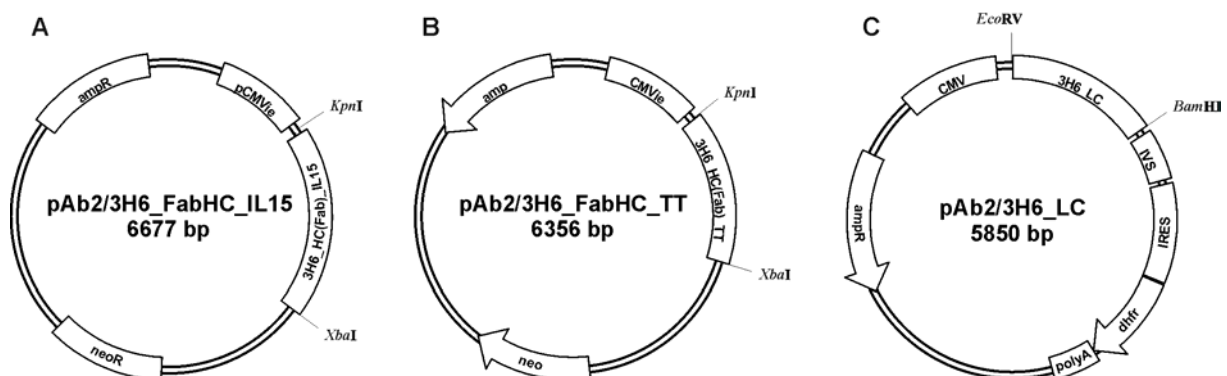


Figure 19. Plasmid map of **A** Ab2/3H6FabHC-IL15 **B** Ab2/3H6FabHC-TT and **C** Ab2/3H6LC

Stable recombinant CHO cell lines producing Ab2/3H6^{Fab}-IL15 or Ab2/3H6^{Fab}-TT were developed in the same way as described in section 3.1.4. The only difference was that the CHO clones for Ab2/3H6^{Fab}-IL15 were additionally amplified with 0.19 μ M MTX to increase the total Ab content in the supernatant. Table IX summarizes selected cell culture data for the recombinant CHO cell lines producing the Ab2/3H6^{Fab} fusion variants.

Table IX. Summary cell line development for Ab2/3H6^{Fab} fusion variants

recombinant CHO cell line producing	96 well selection plate		T25 1 st quantitative screening		T25 2 nd quantitative screening		Spinner cultivation ³		
	grow n wells [%]	screening [μ g/ml]	Titer [μ g/ml]	qp ¹ [pg/cell/day]	Titer [μ g/ml]	qp ¹ [pg/cell/day]	mean Titer [μ g/ml]	mean μ [d ⁻¹]	mean qp ² [pg/cell/day]
Ab2/3H6 ^{Fab} -IL15	97	0.2 - 0.4	0.9 - 1.7	0.8 - 1.7	2.7 - 7.7	2.4 -3.1	6.1 (1.2)	0.3 (0.01)	4.9 (0.5)
Ab2/3H6 ^{Fab} -TT	90	0.2 - 0.4	2.3 -13.0	n.a.	3.9 - 12.4	1.7 - 2.9	17.2 (4.4)	0.2 (0.01)	12.3 (2.7)

¹calculated with end cell number

²calculated with cell days

³two weeks spinner cultivation of selected clone (mean value with standard deviation in brackets n=4)

The purification of Ab2/3H6^{Fab} variants was done by anion exchange chromatography and a subsequent size exclusion polishing step. For details about the purification process refer to section 7 (selected publications: Mader et al. 2011 submitted).

3.2.2 Immunization of rabbits with Ab2/3H6Fab variants

In collaboration with the Institute of Small Farm Animals, Animal Production Research Center, Nitra (Slovakia) an immunization study in New Zealand white rabbits was initiated. Purified Ab2/3H6^{Fab}, -IL15, and -TT preparations were used for the immunisation of six rabbits (groups of two rabbits per preparation). The animals were immunised subcutaneously and intramuscularly with 0.1 mg of purified Ab2/3H6^{Fab} proteins emulsified in complete Freund's adjuvant and boosted two times with the same Fab preparations in incomplete Freund's adjuvant at three-week intervals. Pre-immune sera were collected one day prior the first immunization step. Terminal bleeding and sera preparation were done ten days after the third immunisation step.

3.2.3 Humoral immune response of Ab2/3H6Fab variants in rabbits

Pre-immune and immune sera of all rabbits were analyzed by ELISA for total rabbit IgG, Ab2/3H6^{Fab} specific Abs as well as reactivity against HIV-1 epitopes. For details refer to section 7 (selected publications: Mader et al. 2011 submitted). Briefly, immunization with the

Ab2/3H6^{Fab} fusion proteins did not lead to a significant increase in total rabbit IgG titers and binding specificity for Ab2/3H6^{Fab} was in all samples at a similar level. Binding specificity of the immune sera towards the linear epitope ELDKWASL as well as against the recombinant gp140 protein UG37 (Jefferis et al. 2004) could not be determined by ELISA because the pre-immune control showed strong cross reactivity. To eliminate unspecific reactions in subsequent analysis IgG was purified from each rabbit sera using a Protein A affinity purification step (refer to section 7: selected publications: Mader et al. 2011 submitted). Western Blot assay using mAb 2F5 as control and a purified rabbit IgG pool showed binding against the HIV-1 protein UG37 (Figure 20).

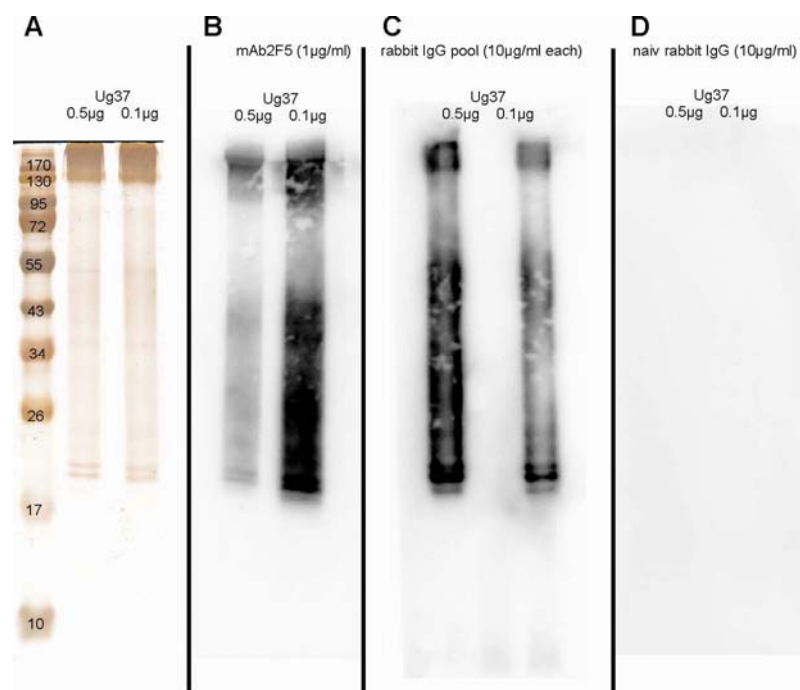


Figure 20. **A** SDS-PAGE of recombinant UG37 **B** Western Blot of UG37 detected with mAb 2F5 as primary and anti-huIgG- γ -chain-AP as secondary antibody **C** Western Blot of UG37 detected with purified rabbit IgG pool of Ab2/3H6^{Fab}-IL15 immunized rabbits as primary and anti-rabbitIgG-AP as secondary antibody **D** Western Blot of UG37 detected with purified rabbit IgG pool of pre-immune sera as primary and anti-rabbitIgG-AP as secondary antibody. All blots were visualized with NBT/BCIP.

Subsequent ELISA binding studies revealed that all the purified rabbit IgG had similar binding reactivity against Ab2/3H6^{Fab} but only three of them showed specificity against the HIV-1 epitopes of UG37 (refer to section 7: selected publications: Mader et al. 2011 submitted). To further characterize the induced anti-anti-idiotypic Abs an Ab3 affinity purification protocol was developed. For details about the Ab3 affinity purification process refer to section 7 (selected publications: Mader et al. 2011 submitted). Briefly, an UG37/GGGELDKWASL coupled column was prepared and batches of previous purified

rabbit IgG fractions containing anti-HIV-1 Abs were applied, unbound IgG was washed off and UG37/GGGELDKWASL specific Abs were eluted using low pH buffer. The results of this purification step revealed that only less than 1 % of the total rabbit IgG fraction contained Ab3s (refer to section 7: selected publications: Mader et al. 2011 submitted). The affinity enriched purified Ab3s were further tested for specificity to UG37 and GGGELDKWASL in ELISA as well as in a biolayer interferometry assay. The Ab3 fraction showed a 10-fold stronger binding to UG37 than to the linear epitope GGGELDKWASL and an approximately 7-fold weaker binding affinity to UG37 than the mAb 2F5 (refer to section 7: selected publications: Mader et al. 2011 submitted). To investigate the neutralization potency of the purified gp140 binding Ab3 fraction a TZM-bl Env-pseudotyped virus assay against the HIV-1 SF162 Env clone was performed. Unfortunately, the purified Ab3s failed to neutralize the pseudotyped virus.

4 Outlook

4.1 Concluding remarks on humanization of Ab2/3H6

In the last 20 years, rational and empirical humanization methods have been developed (Almagro and Fransson 2008) but there is still no generally applicable method available which can be used to eliminate potential immunogenic sites while keeping the specificity of the Ab. Each Ab has to be analyzed separately and different methods have to be tested in each particular case to obtain a humanized variant that features the same affinity and biological activity as the parental Ab.

Three different state of the art humanization approaches have been applied to the muAb2/3H6. The humanized Ab2/3H6 variants RS3H6, GC3H6 showed the same affinity but GA3H6 had a two-fold loss in affinity to mAb 2F5 in comparison to chAb2/3H6. SH3H6 lost the ability to bind mAb 2F5 completely demonstrating this approach as not suitable for humanization of Ab2/3H6.

Despite of this disappointment, the superhumanization approach is quite promising because it leads to a humanized Ab with a complete human germline FR and therefore immunogenicity is expected to be minimal because the remaining murine residues lie only inside the CDRs. In order to elucidate the lost interaction we applied molecular dynamics (MD) simulation to our humanized Ab2/3H6 variants. The MD simulation of the SH3H6 in comparison with the original Ab2/3H6 showed that the TyrH54^{SH3H6} sidechain is not flexible enough to form a hydrogen bond with the antigen mAb 2F5 as it is shown in the crystal structure of 2F5/3H6. In contrast TyrH103^{SH3H6} is more flexible as in the original Ab2/3H6 resulting in clashes with backbone atoms of mAb 2F5 and therefore tends to move to a less favorable orientation (de Ruyter et al. 2011). If the predictions from MD simulation will help to

restore the binding affinity of SH3H6, needs to be investigated in a future project.

Further the humanized Ab2/3H6 variants were subjected to immunogenicity B- and T-cell epitope screening by bioinformatical prediction methods. The relating B-cell epitope prediction showed no significant differences between the Ab2/3H6 variants, but T-cell epitope prediction revealed a more than 50% reduction of potential T-cell epitopes in GA3H6 and SH3H6 version.

Concluding on this study we have compared the biochemical and immunochemical properties of different humanization variants of the mouse derived Ab2/3H6 experimentally as well as with bioinformatical methods. Thereby we found identical behaviour of the conservatively grafted version and similar binding potential of the aggressively grafted variant while the superhumanized version lost completely binding activity. Both humanization approaches transfer mouse CDRs to human FRs with differences in selection of the human FRs. During grafting the most identical FR is used as acceptor while in the superhumanization approach structural similarities are most important for decision of FRs. According to our bioinformatical immunogenicity prediction studies, both the CDR-graft as well as the superhumanization approach induced a reduction of possible T-cell epitopes in the FRs. In the light of this evaluation humanization of Ab2/3H6 using the classical CDR-graft approach or alternatively the resurfacing method generated humanized Ab variants that retained similar binding affinity to mAb 2F5 while the superhumanization approach failed. In regulatory terms the CDR-graft would be favourable because the majority of humanized Abs approved by the FDA are CDR-grafted. It is generally accepted that none of all described and also applied methods in this work may claim to be generally applicable for all individual mouse Abs. The implementation of MD simulation to the humanization process showed promising results which will lead in the right direction for developing a generalized humanization method, but this has to be evaluated in a future project.

4.2 The potential of Ab2/3H6 to be used as an HIV-vaccine

The global HIV pandemic is still expanding and thus the development of a preventive vaccine is of high priority. One approach is to elicit bnAbs against the MPER region that resemble similar potency as the mAb 2F5. In previous studies MPER-containing proteins (Kim et al. 2007; Zhang et al. 2009) or MPER-containing peptides (Ho et al. 2002; Joyce et al. 2002; Wang et al. 2005) failed to elicit bnAbs, eventually due to the poor immunogenicity of the MPER (Montero et al. 2008). It was suggested that the native gp41 exodomain is structurally more complex than represented by the linear epitope (Menendez et al. 2004; Lorizate et al. 2006a) and thus incorrect conformation of MPER-based peptide immunogens result in suboptimal presentation of neutralizing epitopes (Ofek et al. 2004; Cardoso et al. 2005). Additionally, a so far unidentified part of a second epitope has been considered (Julien et al.

2008). This possible second epitope could be an alpha-helix turn C-terminal of the core epitope DKW (Bryson et al. 2009) or associated membrane regions (Alam et al. 2009; Ofek et al. 2010; Scherer et al. 2010) which interact with the long CDR-H3 loop of mAb 2F5. This rather complex neutralizing epitope calls for an alternative vaccine approach like anti-idiotypic Abs. In previous studies Gach et al. demonstrated that Ab2/3H6 is able to inhibit the binding of mAb 2F5 to its synthetic epitope ELDKWA and induces Ab3s (2F5-like Abs) in a mouse immunization study (Gach et al. 2007a; Gach et al. 2008a). However, in these former studies only binding assays against gp160 and the linear epitope ELDKWA were performed. To get a deeper insight into the binding mechanism of Ab2/3H6 to mAb 2F5 co-crystallization of Ab2/3H6 in complex with mAb 2F5 was performed. This study revealed that Ab2/3H6 only partly overlaps with the HIV-1 epitope on mAb 2F5 but does not center on the core epitope binding site of mAb 2F5. Thus the Ab was classified as a gamma-class anti-idiotypic Ab (Bryson et al. 2008). However, since mAb 2F5 crystals were generated with a small peptide of the MPER only, the exact binding mechanism of mAb 2F5 to HIV remains elusive and the most critical paratope responsible for the neutralization activity of mAb 2F5 might not be identified yet.

In a “proof-of-concept” study an anti-idiotypic network approach was used to induce 2F5-like Abs. Ab2/3H6^{Fab} fusion proteins containing the molecular adjuvant IL15 or a “promiscuous” T-cell epitope of TT were administered in a rabbit prime/boost regime. The induced affinity purified Ab3s showed significant binding to the HIV-1 protein UG37 as well as to the synthetic linear epitope of mAb 2F5. However, the amount of HIV-1 specific Ab3s induced with this approach was rather low compared to induced ab3s specific for Ab2/3H6^{Fab}. Since the neutralization assays failed to indicate that nAbs were generated in rabbits, we favor the hypothesis of a second epitope that is responsible for the neutralization potency of mAb 2F5. Additionally the long H3 loop of mAb 2F5 indicates that the Ab has experienced intensive somatic mutagenesis and it is questionable if a seven week prime/boost schedule can represent the maturation of the human immune system.

To conclude on this study, Ab2/3H6 shows the ability to induce Abs against the HIV-1 envelope protein UG37 as well as the synthetic epitope of mAb 2F5. Despite the induced Ab3s were not able to inhibit infection of TZM-bl cells in an Env-pseudotyped neutralization assay Ab2/3H6 at least mimicks part of the epitope of mAb 2F5 as demonstrated by ELISA and bio-layer interferometry affinity measurements.

After decades of intense research regarding the induction of 2F5-like Abs a potent immunogen that is able to induce bn 2F5-like Abs is still missing. Deciphering the complete and correct mechanism on how mAb 2F5 prevents gp41 to fuse with the host cell membrane is the major task in developing HIV-1 vaccines able to induce broadly neutralizing anti-MPER Abs. Unfortunately, the anti-idiotypic approach using Ab2/3H6 does not lead to the desired

outcome. Therefore Ab2/3H6 alone is not suitable as a vaccine, but the combination with other immunogens or the use of membranes as adjuvants (Maeso et al. 2011) might be beneficial for induction of HIV nAbs.

5 References

Abhinandan, K. and Martin, A. (2007) Analyzing the "degree of humanness" of antibody sequences. *J Mol Biol* **369**, 852-862.

Adair, J., Athwal, D. and Emtage, J. (2003) Humanised antibodies. US patent 7262050.

Alam, S.M., McAdams, M., Boren, D., Rak, M., Scarce, R.M., Gao, F., Camacho, Z.T., Gewirth, D., Kelsoe, G., Chen, P. and Haynes, B.F. (2007) The role of antibody polyspecificity and lipid reactivity in binding of broadly neutralizing anti-HIV-1 envelope human monoclonal antibodies 2F5 and 4E10 to glycoprotein 41 membrane proximal envelope epitopes. *J Immunol* **178**, 4424-4435.

Alam, S.M., Morelli, M., Dennison, S.M., Liao, H.X., Zhang, R., Xia, S.M., Rits-Volloch, S., Sun, L., Harrison, S.C., Haynes, B.F. and Chen, B. (2009) Role of HIV membrane in neutralization by two broadly neutralizing antibodies. *Proc Natl Acad Sci U S A* **106**, 20234-20239.

Allan, J.S., Coligan, J.E., Barin, F., McLane, M.F., Sodroski, J.G., Rosen, C.A., Haseltine, W.A., Lee, T.H. and Essex, M. (1985) Major glycoprotein antigens that induce antibodies in AIDS patients are encoded by HTLV-III. *Science* **228**, 1091-1094.

Allison, A.G. and Gregoriadis, G. (1974) Liposomes as immunological adjuvants. *Nature* **252**, 252.

Almagro, J. and Fransson, J. (2008) Humanization of antibodies. *Front Biosci* **13**, 1619-1633.

Alving, C.R., Koulchin, V., Glenn, G.M. and Rao, M. (1995) Liposomes as carriers of peptide antigens: induction of antibodies and cytotoxic T lymphocytes to conjugated and unconjugated peptides. *Immunol Rev* **145**, 5-31.

Appay, V. and Rowland-Jones, S.L. (2002) Premature ageing of the immune system: the cause of AIDS? *Trends Immunol* **23**, 580-585.

Baba, T.W., Liska, V., Hofmann-Lehmann, R., Vlasak, J., Xu, W., Ayehunie, S., Cavacini, L.A., Posner, M.R., Katinger, H., Stiegler, G., Bernacky, B.J., Rizvi, T.A., Schmidt, R., Hill, L.R., Keeling, M.E., Lu, Y., Wright, J.E., Chou, T.C. and Ruprecht, R.M. (2000) Human neutralizing monoclonal antibodies of the IgG1 subtype protect against mucosal simian-human immunodeficiency virus infection. *Nat Med* **6**, 200-206.

Baca, M., Presta, L.G., O'Connor, S.J. and Wells, J.A. (1997) Antibody humanization using monovalent phage display. *J Biol Chem* **272**, 10678-10684.

Barbato, G., Bianchi, E., Ingallinella, P., Humi, W.H., Miller, M.D., Ciliberto, G., Cortese, R., Bazzo, R., Shiver, J.W. and Pessi, A. (2003) Structural analysis of the epitope of the anti-HIV antibody 2F5 sheds light into its mechanism of neutralization and HIV fusion. *J Mol Biol* **330**, 1101-1115.

Barbosa, M.D. and Celis, E. (2007) Immunogenicity of protein therapeutics and the interplay between tolerance and antibody responses. *Drug Discov Today* **12**, 674-681.

Barlow, D.J., Edwards, M.S. and Thornton, J.M. (1986) Continuous and discontinuous protein antigenic determinants. *Nature* **322**, 747-748.

Barouch, D.H., Santra, S., Schmitz, J.E., Kuroda, M.J., Fu, T.M., Wagner, W., Bilska, M., Craiu, A., Zheng, X.X., Krivulka, G.R., Beaudry, K., Lifton, M.A., Nickerson, C.E., Trigona, W.L., Punt, K., Freed, D.C., Guan, L., Dubey, S., Casimiro, D., Simon, A., Davies, M.E., Chastain, M., Strom, T.B., Gelman, R.S., Montefiori, D.C., Lewis, M.G., Emini, E.A., Shiver, J.W. and Letvin, N.L. (2000) Control of viremia and prevention of clinical AIDS in rhesus monkeys by cytokine-augmented DNA vaccination. *Science* **290**, 486-492.

Barrett, N., Mitterer, A., Mundt, W., Eibl, J., Eibl, M., Gallo, R.C., Moss, B. and Dörner, F. (1989) Large-scale production and purification of a vaccinia recombinant-derived HIV-1 gp160 and analysis of its immunogenicity. *AIDS Res Hum Retroviruses* **5**, 159-171.

Barré-Sinoussi, F., Chermann, J.C., Rey, F., Nugeyre, M.T., Chamaret, S., Gruest, J., Dauterive, C., Axler-Blin, C., Vézinet-Brun, F., Rouzioux, C., Rozenbaum, W. and Montagnier, L. (1983) Isolation of a T-lymphotropic retrovirus from a patient at risk for acquired immune deficiency syndrome (AIDS). *Science* **220**, 868-871.

Beddows, S., Schülke, N., Kirschner, M., Barnes, K., Franti, M., Michael, E., Ketas, T., Sanders, R.W., Maddon, P.J., Olson, W.C. and Moore, J.P. (2005) Evaluating the immunogenicity of a disulfide-stabilized, cleaved, trimeric form of the envelope glycoprotein complex of human immunodeficiency virus type 1. *J Virol* **79**, 8812-8827.

Benferhat, R., Martinon, F., Krust, B., Le Grand, R. and Hovanessian, A.G. (2009) The CBD1 peptide corresponding to the caveolin-1 binding domain of HIV-1 glycoprotein gp41 elicits neutralizing antibodies in cynomolgus macaques when administered with the tetanus T helper epitope. *Mol Immunol* **46**, 705-712.

Berkhout, B. and Paxton, W.A. (2009) HIV vaccine: it may take two to tango, but no party time yet. *Retrovirology* **6**, 88.

Berkhout, B., Verhoef, K., van Wamel, J.L. and Back, N.K. (1999) Genetic instability of live, attenuated human immunodeficiency virus type 1 vaccine strains. *J Virol* **73**, 1138-1145.

Binley, J.M., Wrinn, T., Korber, B., Zwick, M.B., Wang, M., Chappey, C., Stiegler, G., Kunert, R., Zolla-Pazner, S., Katinger, H., Petropoulos, C.J. and Burton, D.R. (2004) Comprehensive cross-clade neutralization analysis of a panel of anti-human immunodeficiency virus type 1 monoclonal antibodies. *J Virol* **78**, 13232-13252.

Biron, Z., Khare, S., Quadt, S.R., Hayek, Y., Naider, F. and Anglistter, J. (2005) The 2F5 epitope is helical in the HIV-1 entry inhibitor T-20. *Biochemistry* **44**, 13602-13611.

Blay, W.M., Gnanakaran, S., Foley, B., Doria-Rose, N.A., Korber, B.T. and Haigwood, N.L. (2006) Consistent patterns of change during the divergence of human immunodeficiency virus type 1 envelope from that of the inoculated virus in simian/human immunodeficiency virus-infected macaques. *J Virol* **80**, 999-1014.

Blouin, J., Guzman, E. and Foley, B. (1996) **Global variation in the HIV-1 V3 region.** In *Human Retroviruses and AIDS: A Compilation and Analysis of Nucleic Acid and Amino Acid Sequences* eds. Myers, G., Korber, B., Foley, B., Jeang, K.-T., Mellors, J. and Wain-

Hobson, S. pp.p. III77-III201. Theoretical Biology and Biophysics Group, Los Alamos National Laboratory, Los Alamos, NM.

Boberg, A., Dominici, S., Brave, A., Hallermalm, K., Hinkula, J., Magnani, M. and Wahren, B. (2007) Immunization with HIV protease peptides linked to syngeneic erythrocytes. *Infect Agent Cancer* **2**, 9.

Boberg, A., Gaunitz, S., Bråve, A., Wahren, B. and Carlin, N. (2008) Enhancement of epitope-specific cellular immune responses by immunization with HIV-1 peptides genetically conjugated to the B-subunit of recombinant cholera toxin. *Vaccine* **26**, 5079-5082.

Bodles-Brakhop, A.M., Heller, R. and Draghia-Akli, R. (2009) Electroporation for the delivery of DNA-based vaccines and immunotherapeutics: current clinical developments. *Mol Ther* **17**, 585-592.

Bolmstedt, A., Sjölander, S., Hansen, J.E., Akerblom, L., Hemming, A., Hu, S.L., Morein, B. and Olofsson, S. (1996) Influence of N-linked glycans in V4-V5 region of human immunodeficiency virus type 1 glycoprotein gp160 on induction of a virus-neutralizing humoral response. *J Acquir Immune Defic Syndr Hum Retrovirol* **12**, 213-220.

Briggs, J.A., Wilk, T., Welker, R., Kräusslich, H.G. and Fuller, S.D. (2003) Structural organization of authentic, mature HIV-1 virions and cores. *EMBO J* **22**, 1707-1715.

Bruccoleri, R. and Karplus, M. (1987) Prediction of the folding of short polypeptide segments by uniform conformational sampling. *Biopolymers* **26**, 137-168.

Brunel, F.M., Zwick, M.B., Cardoso, R.M., Nelson, J.D., Wilson, I.A., Burton, D.R. and Dawson, P.E. (2006) Structure-function analysis of the epitope for 4E10, a broadly neutralizing human immunodeficiency virus type 1 antibody. *J Virol* **80**, 1680-1687.

Brusic, V., Bajic, V.B. and Petrovsky, N. (2004) Computational methods for prediction of T-cell epitopes--a framework for modelling, testing, and applications. *Methods* **34**, 436-443.

Bryson, S., Julien, J., Isenman, D., Kunert, R., Katinger, H. and Pai, E. (2008) Crystal structure of the complex between the F(ab)' fragment of the cross-neutralizing anti-HIV-1 antibody 2F5 and the F(ab) fragment of its anti-idiotypic antibody 3H6. *J Mol Biol* **382**, 910-919.

Bryson, S., Julien, J.P., Hynes, R.C. and Pai, E.F. (2009) Crystallographic definition of the epitope promiscuity of the broadly neutralizing anti-human immunodeficiency virus type 1 antibody 2F5: vaccine design implications. *J Virol* **83**, 11862-11875.

Brühl, P., Kerschbaum, A., Eibl, M.M. and Mannhalter, J.W. (1998) An experimental prime-boost regimen leading to HIV type 1-specific mucosal and systemic immunity in BALB/c mice. *AIDS Res Hum Retroviruses* **14**, 401-407.

Buchacher, A., Predl, R., Strutzenberger, K., Steinfellner, W., Trkola, A., Purtscher, M., Gruber, G., Tauer, C., Steindl, F. and Jungbauer, A. (1994) Generation of human monoclonal antibodies against HIV-1 proteins; electrofusion and Epstein-Barr virus transformation for peripheral blood lymphocyte immortalization. *AIDS Res Hum Retroviruses* **10**, 359-369.

Buchbinder, S.P., Mehrotra, D.V., Duerr, A., Fitzgerald, D.W., Mogg, R., Li, D., Gilbert, P.B., Lama, J.R., Marmor, M., Del Rio, C., McElrath, M.J., Casimiro, D.R., Gottesdiener, K.M., Chodakewitz, J.A., Corey, L., Robertson, M.N. and Team, S.S.P. (2008) Efficacy assessment of a cell-mediated immunity HIV-1 vaccine (the Step Study): a double-blind, randomised, placebo-controlled, test-of-concept trial. *Lancet* **372**, 1881-1893.

Buonaguro, L., Devito, C., Tornesello, M.L., Schröder, U., Wahren, B., Hinkula, J. and Buonaguro, F.M. (2007) DNA-VLP prime-boost intra-nasal immunization induces cellular and humoral anti-HIV-1 systemic and mucosal immunity with cross-clade neutralizing activity. *Vaccine* **25**, 5968-5977.

Bures, R., Morris, L., Williamson, C., Ramjee, G., Deers, M., Fiscus, S.A., Abdool-Karim, S. and Montefiori, D.C. (2002) Regional clustering of shared neutralization determinants on primary isolates of clade C human immunodeficiency virus type 1 from South Africa. *J Virol* **76**, 2233-2244.

Burioni, R., Mancini, N., De Marco, D., Clementi, N., Perotti, M., Nitti, G., Sassi, M., Canducci, F., Shvela, K., Bagnarelli, P., Mascola, J.R. and Clementi, M. (2008) Anti-HIV-1 response elicited in rabbits by anti-idiotypic monoclonal antibodies mimicking the CD4-binding site. *PLoS One* **3**, e3423.

Burke, D.S. (1997) Recombination in HIV: an important viral evolutionary strategy. *Emerg Infect Dis* **3**, 253-259.

Burton, D.R., Pyati, J., Koduri, R., Sharp, S.J., Thornton, G.B., Parren, P.W., Sawyer, L.S., Hendry, R.M., Dunlop, N. and Nara, P.L. (1994) Efficient neutralization of primary isolates of HIV-1 by a recombinant human monoclonal antibody. *Science* **266**, 1024-1027.

Burton, D.R., Stanfield, R.L. and Wilson, I.A. (2005) Antibody vs. HIV in a clash of evolutionary titans. *Proc Natl Acad Sci U S A* **102**, 14943-14948.

Calarese, D., Scanlan, C., Zwick, M., Deechongkit, S., Mimura, Y., Kunert, R., Zhu, P., Wormald, M., Stanfield, R., Roux, K., Kelly, J., Rudd, P., Dwek, R., Katinger, H., Burton, D. and Wilson, I. (2003) Antibody domain exchange is an immunological solution to carbohydrate cluster recognition. *Science* **300**, 2065-2071.

Calarese, D.A., Lee, H.K., Huang, C.Y., Best, M.D., Astronomo, R.D., Stanfield, R.L., Katinger, H., Burton, D.R., Wong, C.H. and Wilson, I.A. (2005) Dissection of the carbohydrate specificity of the broadly neutralizing anti-HIV-1 antibody 2G12. *Proc Natl Acad Sci U S A* **102**, 13372-13377.

Caldas, C., Coelho, V., Rigden, D., Neschich, G., Moro, A. and Brígido, M. (2000) Design and synthesis of germline-based hemi-humanized single-chain Fv against the CD18 surface antigen. *Protein Eng* **13**, 353-360.

Cardoso, R., Zwick, M., Stanfield, R., Kunert, R., Binley, J., Katinger, H., Burton, D. and Wilson, I. (2005) Broadly neutralizing anti-HIV antibody 4E10 recognizes a helical conformation of a highly conserved fusion-associated motif in gp41. *Immunity* **22**, 163-173.

Cardoso, R.M., Brunel, F.M., Ferguson, S., Zwick, M., Burton, D.R., Dawson, P.E. and Wilson, I.A. (2007) Structural basis of enhanced binding of extended and helically

constrained peptide epitopes of the broadly neutralizing HIV-1 antibody 4E10. *J Mol Biol* **365**, 1533-1544.

Carmichael, A.J. and Sissons, J.G. (1995) Vaccines against HIV. *QJM* **88**, 77-79.

Carter, P., Presta, L., Gorman, C., Ridgway, J., Henner, D., Wong, W., Rowland, A., Kotts, C., Carver, M. and Shepard, H. (1992) Humanization of an anti-p185HER2 antibody for human cancer therapy. *Proc Natl Acad Sci U S A* **89**, 4285-4289.

Chackerian, B., Rudensey, L.M. and Overbaugh, J. (1997) Specific N-linked and O-linked glycosylation modifications in the envelope V1 domain of simian immunodeficiency virus variants that evolve in the host alter recognition by neutralizing antibodies. *J Virol* **71**, 7719-7727.

Chakrabarti, L.A., Metzner, K.J., Ivanovic, T., Cheng, H., Louis-Virelizier, J., Connor, R.I. and Cheng-Mayer, C. (2003) A truncated form of Nef selected during pathogenic reversion of simian immunodeficiency virus SIVmac239Deltanef increases viral replication. *J Virol* **77**, 1245-1256.

Chan, D.C., Fass, D., Berger, J.M. and Kim, P.S. (1997) Core structure of gp41 from the HIV envelope glycoprotein. *Cell* **89**, 263-273.

Chan, D.C. and Kim, P.S. (1998) HIV entry and its inhibition. *Cell* **93**, 681-684.

Chiu, W.C., Lai, Y.P. and Chou, M.Y. (2011) Humanization and characterization of an anti-human TNF- α murine monoclonal antibody. *PLoS One* **6**, e16373.

Chothia, C. and Lesk, A. (1987) Canonical structures for the hypervariable regions of immunoglobulins. *J Mol Biol* **196**, 901-917.

Chothia, C., Lesk, A., Tramontano, A., Levitt, M., Smith-Gill, S., Air, G., Sheriff, S., Padlan, E., Davies, D. and Tulip, W. (1989) Conformations of immunoglobulin hypervariable regions. *Nature* **342**, 877-883.

Chun, T.W., Engel, D., Berrey, M.M., Shea, T., Corey, L. and Fauci, A.S. (1998) Early establishment of a pool of latently infected, resting CD4(+) T cells during primary HIV-1 infection. *Proc Natl Acad Sci U S A* **95**, 8869-8873.

Churchill, M.J., Rhodes, D.I., Learmont, J.C., Sullivan, J.S., Wesselingh, S.L., Cooke, I.R., Deacon, N.J. and Gorry, P.R. (2006) Longitudinal analysis of human immunodeficiency virus type 1 nef/long terminal repeat sequences in a cohort of long-term survivors infected from a single source. *J Virol* **80**, 1047-1052.

Chêne, G., Sterne, J.A., May, M., Costagliola, D., Ledergerber, B., Phillips, A.N., Dabis, F., Lundgren, J., D'Arminio Monforte, A., de Wolf, F., Hogg, R., Reiss, P., Justice, A., Leport, C., Staszewski, S., Gill, J., Fatkenheuer, G., Egger, M.E. and Collaboration, A.T.C. (2003) Prognostic importance of initial response in HIV-1 infected patients starting potent antiretroviral therapy: analysis of prospective studies. *Lancet* **362**, 679-686.

Co, M., Deschamps, M., Whitley, R. and Queen, C. (1991) Humanized antibodies for antiviral therapy. *Proc Natl Acad Sci U S A* **88**, 2869-2873.

Collaboration, A.T.C. (2008) Life expectancy of individuals on combination antiretroviral therapy in high-income countries: a collaborative analysis of 14 cohort studies. *Lancet* **372**, 293-299.

Corey, L., McElrath, M.J. and Kublin, J.G. (2009) Post-step modifications for research on HIV vaccines. *AIDS* **23**, 3-8.

Cornet, B., Decroly, E., Thines-Sempoux, D., Ruyschaert, J.M. and Vandenbranden, M. (1992) Properties of HIV membrane reconstituted from its recombinant gp160 envelope glycoprotein. *AIDS Res Hum Retroviruses* **8**, 1823-1831.

Cornet, B., Vandenbranden, M., Cogniaux, J., Giurgea, L., Dekegel, D. and Ruyschaert, J.M. (1990) Virosomes reconstituted from human immunodeficiency virus proteins and lipids. *Biochem Biophys Res Commun* **167**, 222-231.

Crooks, E.T., Moore, P.L., Franti, M., Cayanan, C.S., Zhu, P., Jiang, P., de Vries, R.P., Wiley, C., Zharkikh, I., Schülke, N., Roux, K.H., Montefiori, D.C., Burton, D.R. and Binley, J.M. (2007) A comparative immunogenicity study of HIV-1 virus-like particles bearing various forms of envelope proteins, particles bearing no envelope and soluble monomeric gp120. *Virology* **366**, 245-262.

Dall'Acqua, W., Damschroder, M., Zhang, J., Woods, R., Widjaja, L., Yu, J. and Wu, H. (2005) Antibody humanization by framework shuffling. *Methods* **36**, 43-60.

Damschroder, M.M., Widjaja, L., Gill, P.S., Krasnoperov, V., Jiang, W., Dall'Acqua, W.F. and Wu, H. (2007) Framework shuffling of antibodies to reduce immunogenicity and manipulate functional and biophysical properties. *Mol Immunol* **44**, 3049-3060.

Das, A.T., Verhoef, K. and Berkhout, B. (2004) A conditionally replicating virus as a novel approach toward an HIV vaccine. *Methods Enzymol* **388**, 359-379.

Dauber-Osguthorpe, P., Roberts, V., Osguthorpe, D., Wolff, J., Genest, M. and Hagler, A. (1988) Structure and energetics of ligand binding to proteins: Escherichia coli dihydrofolate reductase-trimethoprim, a drug-receptor system. *Proteins* **4**, 31-47.

de Cerio, A.L., Zabalegui, N., Rodríguez-Calvillo, M., Inogés, S. and Bendandi, M. (2007) Anti-idiotypic antibodies in cancer treatment. *Oncogene* **26**, 3594-3602.

De Groot, A.S. and Martin, W. (2009) Reducing risk, improving outcomes: bioengineering less immunogenic protein therapeutics. *Clin Immunol* **131**, 189-201.

De Groot, A.S. and Moise, L. (2007) Prediction of immunogenicity for therapeutic proteins: state of the art. *Curr Opin Drug Discov Devel* **10**, 332-340.

De Groot, A.S. and Scott, D.W. (2007) Immunogenicity of protein therapeutics. *Trends Immunol* **28**, 482-490.

de Ruiter, A., Mader, A., Kunert, R. and Oostenbrink, C. (2011) Molecular Simulations to Rationalize Humanized Ab2/3H6 Activity. *Australian Journal of Chemistry* **64**, 900-909.

Delagrave, S., Catalan, J., Sweet, C., Drabik, G., Henry, A., Rees, A., Monath, T. and Guirakhoo, F. (1999) Effects of humanization by variable domain resurfacing on the antiviral activity of a single-chain antibody against respiratory syncytial virus. *Protein Eng* **12**, 357-362.

Dolter, K.E., Evans, C.F., Ellefsen, B., Song, J., Boente-Carrera, M., Vittorino, R., Rosenberg, T.J., Hannaman, D. and Vasan, S. (2011) Immunogenicity, safety, biodistribution and persistence of ADVAX, a prophylactic DNA vaccine for HIV-1, delivered by in vivo electroporation. *Vaccine* **29**, 795-803.

Duvall, M., Bradley, N. and Fiorini, R.N. (2011) A novel platform to produce human monoclonal antibodies: The next generation of therapeutic human monoclonal antibodies discovery. *MAbs* **3**, 203-208.

Dybul, M., Fauci, A.S., Bartlett, J.G., Kaplan, J.E., Pau, A.K. and HIV, P.o.C.P.f.T.o. (2002) Guidelines for using antiretroviral agents among HIV-infected adults and adolescents. *Ann Intern Med* **137**, 381-433.

Earl, P.L., Doms, R.W. and Moss, B. (1990) Oligomeric structure of the human immunodeficiency virus type 1 envelope glycoprotein. *Proc Natl Acad Sci U S A* **87**, 648-652.

El-Manzalawy, Y. and Honavar, V. (2010) Recent advances in B-cell epitope prediction methods. *Immunome Res* **6 Suppl 2**, S2.

EMA (2007) Guideline of immunogenicity assessment of biotechnology-derived therapeutic proteins ed. (CHMP), C.F.M.P.F.H.U. p.18.

Evans, D.T., Bricker, J.E., Sanford, H.B., Lang, S., Carville, A., Richardson, B.A., Piatak, M., Lifson, J.D., Mansfield, K.G. and Desrosiers, R.C. (2005) Immunization of macaques with single-cycle simian immunodeficiency virus (SIV) stimulates diverse virus-specific immune responses and reduces viral loads after challenge with SIVmac239. *J Virol* **79**, 7707-7720.

Ezzell, C. (1987) Trials of vaccine against AIDS to begin in humans. *Nature* **328**, 747.

Falkensammer, B., Rubner, B., Hiltgartner, A., Wilflingseder, D., Stahl Hennig, C., Kuate, S., Uberla, K., Norley, S., Strasak, A., Racz, P. and Stoiber, H. (2009) Role of complement and antibodies in controlling infection with pathogenic simian immunodeficiency virus (SIV) in macaques vaccinated with replication-deficient viral vectors. *Retrovirology* **6**, 60.

Ferrantelli, F., Cafaro, A. and Ensoli, B. (2004) Nonstructural HIV proteins as targets for prophylactic or therapeutic vaccines. *Curr Opin Biotechnol* **15**, 543-556.

Fields, B., Goldbaum, F., Ysern, X., Poljak, R. and Mariuzza, R. (1995) Molecular basis of antigen mimicry by an anti-idiotope. *Nature* **374**, 739-742.

Flower, D.R. (2007) Immunoinformatics and the in silico prediction of immunogenicity. An introduction. *Methods Mol Biol* **409**, 1-15.

Flynn, N., Forthal, D., Harro, C., Judson, F., Mayer, K., Para, M. and Group, r.H.V.S. (2005) Placebo-controlled phase 3 trial of a recombinant glycoprotein 120 vaccine to prevent HIV-1 infection. *J Infect Dis* **191**, 654-665.

Foote, J. and Winter, G. (1992) Antibody framework residues affecting the conformation of the hypervariable loops. *J Mol Biol* **224**, 487-499.

Fouts, T., Godfrey, K., Bobb, K., Montefiori, D., Hanson, C.V., Kalyanaraman, V.S., DeVico, A. and Pal, R. (2002) Crosslinked HIV-1 envelope-CD4 receptor complexes elicit broadly cross-reactive neutralizing antibodies in rhesus macaques. *Proc Natl Acad Sci U S A* **99**, 11842-11847.

Fuh, G., Wu, P., Liang, W.C., Ultsch, M., Lee, C.V., Moffat, B. and Wiesmann, C. (2006) Structure-function studies of two synthetic anti-vascular endothelial growth factor Fabs and comparison with the Avastin Fab. *J Biol Chem* **281**, 6625-6631.

Gabuzda, D.H., Lever, A., Terwilliger, E. and Sodroski, J. (1992) Effects of deletions in the cytoplasmic domain on biological functions of human immunodeficiency virus type 1 envelope glycoproteins. *J Virol* **66**, 3306-3315.

Gach, J., Quendler, H., Strobach, S., Katinger, H. and Kunert, R. (2008a) Structural analysis and in vivo administration of an anti-idiotypic antibody against mAb 2F5. *Mol Immunol* **45**, 1027-1034.

Gach, J., Quendler, H., Weik, R., Katinger, H. and Kunert, R. (2007a) Partial humanization and characterization of an anti-idiotypic antibody against monoclonal antibody 2F5, a potential HIV vaccine? *AIDS Res Hum Retroviruses* **23**, 1405-1415.

Gach, J.S., Maurer, M., Hahn, R., Gasser, B., Mattanovich, D., Katinger, H. and Kunert, R. (2007b) High level expression of a promising anti-idiotypic antibody fragment vaccine against HIV-1 in *Pichia pastoris*. *J Biotechnol* **128**, 735-746.

Gach, J.S., Quendler, H., Ferko, B., Katinger, H. and Kunert, R. (2008b) Expression, purification, and in vivo administration of a promising anti-idiotypic HIV-1 vaccine. *Mol Biotechnol* **39**, 119-125.

Gallaher, W.R., Ball, J.M., Garry, R.F., Griffin, M.C. and Montelaro, R.C. (1989) A general model for the transmembrane proteins of HIV and other retroviruses. *AIDS Res Hum Retroviruses* **5**, 431-440.

Gao, F., Bailes, E., Robertson, D.L., Chen, Y., Rodenburg, C.M., Michael, S.F., Cummins, L.B., Arthur, L.O., Peeters, M., Shaw, G.M., Sharp, P.M. and Hahn, B.H. (1999) Origin of HIV-1 in the chimpanzee *Pan troglodytes*. *Nature* **397**, 436-441.

Gelderblom, H.R., Hausmann, E.H., Ozel, M., Pauli, G. and Koch, M.A. (1987) Fine structure of human immunodeficiency virus (HIV) and immunolocalization of structural proteins. *Virology* **156**, 171-176.

Getts, D.R., Getts, M.T., McCarthy, D.P., Chastain, E.M. and Miller, S.D. (2010) Have we overestimated the benefit of human(ized) antibodies? *MAbs* **2**, 682-694.

- Gonzales, N., Padlan, E., De Pascalis, R., Schuck, P., Schlom, J. and Kashmiri, S. (2003) Minimizing immunogenicity of the SDR-grafted humanized antibody CC49 by genetic manipulation of the framework residues. *Mol Immunol* **40**, 337-349.
- Gotch, F.M., Imami, N. and Hardy, G. (2001) Candidate vaccines for immunotherapy in HIV. *HIV Med* **2**, 260-265.
- Gottlieb, M.S., Schroff, R., Schanker, H.M., Weisman, J.D., Fan, P.T., Wolf, R.A. and Saxon, A. (1981) Pneumocystis carinii pneumonia and mucosal candidiasis in previously healthy homosexual men: evidence of a new acquired cellular immunodeficiency. *N Engl J Med* **305**, 1425-1431.
- Granseth, E., von Heijne, G. and Elofsson, A. (2005) A study of the membrane-water interface region of membrane proteins. *J Mol Biol* **346**, 377-385.
- Grant, M., Smaill, F., Muller, S., Kohler, H. and Rosenthal, K. (2000) The anti-idiotypic antibody 1F7 selectively inhibits cytotoxic T cells activated in HIV-1 infection. *Immunol Cell Biol* **78**, 20-27.
- Grundner, C., Li, Y., Louder, M., Mascola, J., Yang, X., Sodroski, J. and Wyatt, R. (2005) Analysis of the neutralizing antibody response elicited in rabbits by repeated inoculation with trimeric HIV-1 envelope glycoproteins. *Virology* **331**, 33-46.
- Guex, N. and Peitsch, M. (1997) SWISS-MODEL and the Swiss-PdbViewer: an environment for comparative protein modeling. *Electrophoresis* **18**, 2714-2723.
- Hager-Braun, C., Katinger, H. and Tomer, K.B. (2006) The HIV-neutralizing monoclonal antibody 4E10 recognizes N-terminal sequences on the native antigen. *J Immunol* **176**, 7471-7481.
- Harding, F.A., Stickler, M.M., Razo, J. and DuBridg, R.B. (2010) The immunogenicity of humanized and fully human antibodies: residual immunogenicity resides in the CDR regions. *MAbs* **2**, 256-265.
- Harrison, S.C. (2005) Mechanism of membrane fusion by viral envelope proteins. *Adv Virus Res* **64**, 231-261.
- Harrison, S.C. (2008) Viral membrane fusion. *Nat Struct Mol Biol* **15**, 690-698.
- Haynes, B.F., Fleming, J., St Clair, E.W., Katinger, H., Stiegler, G., Kunert, R., Robinson, J., Scearce, R.M., Plonk, K., Staats, H.F., Ortel, T.L., Liao, H.X. and Alam, S.M. (2005a) Cardiolipin polyspecific autoreactivity in two broadly neutralizing HIV-1 antibodies. *Science* **308**, 1906-1908.
- Haynes, B.F., Moody, M.A., Verkoczy, L., Kelsoe, G. and Alam, S.M. (2005b) Antibody polyspecificity and neutralization of HIV-1: a hypothesis. *Hum Antibodies* **14**, 59-67.
- Hirao, L.A., Wu, L., Khan, A.S., Satishchandran, A., Draghia-Akli, R. and Weiner, D.B. (2008) Intradermal/subcutaneous immunization by electroporation improves plasmid vaccine delivery and potency in pigs and rhesus macaques. *Vaccine* **26**, 440-448.

Ho, J., MacDonald, K.S. and Barber, B.H. (2002) Construction of recombinant targeting immunogens incorporating an HIV-1 neutralizing epitope into sites of differing conformational constraint. *Vaccine* **20**, 1169-1180.

Hofmann-Lehmann, R., Rasmussen, R.A., Vlasak, J., Smith, B.A., Baba, T.W., Liska, V., Montefiori, D.C., McClure, H.M., Anderson, D.C., Bernacky, B.J., Rizvi, T.A., Schmidt, R., Hill, L.R., Keeling, M.E., Katinger, H., Stiegler, G., Posner, M.R., Cavacini, L.A., Chou, T.C. and Ruprecht, R.M. (2001a) Passive immunization against oral AIDS virus transmission: an approach to prevent mother-to-infant HIV-1 transmission? *J Med Primatol* **30**, 190-196.

Hofmann-Lehmann, R., Vlasak, J., Rasmussen, R.A., Smith, B.A., Baba, T.W., Liska, V., Ferrantelli, F., Montefiori, D.C., McClure, H.M., Anderson, D.C., Bernacky, B.J., Rizvi, T.A., Schmidt, R., Hill, L.R., Keeling, M.E., Katinger, H., Stiegler, G., Cavacini, L.A., Posner, M.R., Chou, T.C., Andersen, J. and Ruprecht, R.M. (2001b) Postnatal passive immunization of neonatal macaques with a triple combination of human monoclonal antibodies against oral simian-human immunodeficiency virus challenge. *J Virol* **75**, 7470-7480.

Hofmann-Lehmann, R., Vlasak, J., Williams, A.L., Chenine, A.L., McClure, H.M., Anderson, D.C., O'Neil, S. and Ruprecht, R.M. (2003) Live attenuated, nef-deleted SIV is pathogenic in most adult macaques after prolonged observation. *AIDS* **17**, 157-166.

Hu, S., Zhu, Z., Li, L., Chang, L., Li, W., Cheng, L., Teng, M. and Liu, J. (2008) Epitope mapping and structural analysis of an anti-ErbB2 antibody A21: Molecular basis for tumor inhibitory mechanism. *Proteins* **70**, 938-949.

Hu, W., Chau, D., Wu, J., Jager, S. and Nagata, L. (2007) Humanization and mammalian expression of a murine monoclonal antibody against Venezuelan equine encephalitis virus. *Vaccine* **25**, 3210-3214.

Huang, X., Barchi, J.J., Lung, F.D., Roller, P.P., Nara, P.L., Muschik, J. and Garrity, R.R. (1997) Glycosylation affects both the three-dimensional structure and antibody binding properties of the HIV-1IIIB GP120 peptide RP135. *Biochemistry* **36**, 10846-10856.

Hurvitz, S. and Timmerman, J. (2005) Current status of therapeutic vaccines for non-Hodgkin's lymphoma. *Curr Opin Oncol* **17**, 432-440.

Hwang, W., Almagro, J., Buss, T., Tan, P. and Foote, J. (2005) Use of human germline genes in a CDR homology-based approach to antibody humanization. *Methods* **36**, 35-42.

Hwang, W. and Foote, J. (2005) Immunogenicity of engineered antibodies. *Methods* **36**, 3-10.

Inogès, S., Rodríguez-Calvillo, M., Zabalegui, N., Lòpez-Dìaz de Cerio, A., Villanueva, H., Soria, E., Suárez, L., Rodríguez-Caballero, A., Pastor, F., García-Muñoz, R., Panizo, C., Pèrez-Calvo, J., Melero, I., Rocha, E., Orfao, A., Bendandi, M., group, G.E.d.L.T.A.d.M.O.s. and group, P.p.e.E.y.T.d.H.M.s. (2006) Clinical benefit associated with idiotypic vaccination in patients with follicular lymphoma. *J Natl Cancer Inst* **98**, 1292-1301.

Izadyar, L., Friboulet, A., Remy, M.H., Roseto, A. and Thomas, D. (1993) Monoclonal anti-idiotypic antibodies as functional internal images of enzyme active sites: production of a catalytic antibody with a cholinesterase activity. *Proc Natl Acad Sci U S A* **90**, 8876-8880.

Jeffs, S.A., Goriup, S., Kebble, B., Crane, D., Bolgiano, B., Sattentau, Q., Jones, S. and Holmes, H. (2004) Expression and characterisation of recombinant oligomeric envelope glycoproteins derived from primary isolates of HIV-1. *Vaccine* **22**, 1032-1046.

Jerne, N. (1974) Towards a network theory of the immune system. *Ann Immunol (Paris)* **125C**, 373-389.

Jerne, N., Roland, J. and Cazenave, P. (1982) Recurrent idiotopes and internal images. *EMBO J* **1**, 243-247.

Johnson, P.R., Schnepf, B.C., Zhang, J., Connell, M.J., Greene, S.M., Yuste, E., Desrosiers, R.C. and Clark, K.R. (2009) Vector-mediated gene transfer engenders long-lived neutralizing activity and protection against SIV infection in monkeys. *Nat Med* **15**, 901-906.

Jones, P., Dear, P., Foote, J., Neuberger, M. and Winter, G. (1986) Replacing the complementarity-determining regions in a human antibody with those from a mouse. *Nature* **321**, 522-525.

Joseph, A., Zheng, J.H., Chen, K., Dutta, M., Chen, C., Stiegler, G., Kunert, R., Follenzi, A. and Goldstein, H. (2010) Inhibition of in vivo HIV infection in humanized mice by gene therapy of human hematopoietic stem cells with a lentiviral vector encoding a broadly neutralizing anti-HIV antibody. *J Virol* **84**, 6645-6653.

Joyce, J.G., Humi, W.M., Bogusky, M.J., Garsky, V.M., Liang, X., Citron, M.P., Danzeisen, R.C., Miller, M.D., Shiver, J.W. and Keller, P.M. (2002) Enhancement of alpha -helicity in the HIV-1 inhibitory peptide DP178 leads to an increased affinity for human monoclonal antibody 2F5 but does not elicit neutralizing responses in vitro. Implications for vaccine design. *J Biol Chem* **277**, 45811-45820.

Julien, J.P., Bryson, S., Nieva, J.L. and Pai, E.F. (2008) Structural details of HIV-1 recognition by the broadly neutralizing monoclonal antibody 2F5: epitope conformation, antigen-recognition loop mobility, and anion-binding site. *J Mol Biol* **384**, 377-392.

Kang, Y.K., Andjelic, S., Binley, J.M., Crooks, E.T., Franti, M., Iyer, S.P., Donovan, G.P., Dey, A.K., Zhu, P., Roux, K.H., Durso, R.J., Parsons, T.F., Maddon, P.J., Moore, J.P. and Olson, W.C. (2009) Structural and immunogenicity studies of a cleaved, stabilized envelope trimer derived from subtype A HIV-1. *Vaccine* **27**, 5120-5132.

Kaumaya, P.T., Kobs-Conrad, S., Seo, Y.H., Lee, H., VanBuskirk, A.M., Feng, N., Sheridan, J.F. and Stevens, V. (1993) Peptide vaccines incorporating a 'promiscuous' T-cell epitope bypass certain haplotype restricted immune responses and provide broad spectrum immunogenicity. *J Mol Recognit* **6**, 81-94.

Kim, M., Qiao, Z., Yu, J., Montefiori, D. and Reinherz, E.L. (2007) Immunogenicity of recombinant human immunodeficiency virus type 1-like particles expressing gp41 derivatives in a pre-fusion state. *Vaccine* **25**, 5102-5114.

Knoll, B., Lassmann, B. and Temesgen, Z. (2007) Current status of HIV infection: a review for non-HIV-treating physicians. *Int J Dermatol* **46**, 1219-1228.

Koff, W.C., Johnson, P.R., Watkins, D.I., Burton, D.R., Lifson, J.D., Hasenkrug, K.J., McDermott, A.B., Schultz, A., Zamb, T.J., Boyle, R. and Desrosiers, R.C. (2006) HIV vaccine design: insights from live attenuated SIV vaccines. *Nat Immunol* **7**, 19-23.

Kolesnikov, A.V., Kozyr, A.V., Alexandrova, E.S., Koralewski, F., Demin, A.V., Titov, M.I., Avalle, B., Tramontano, A., Paul, S., Thomas, D., Gabibov, A.G. and Friboulet, A. (2000) Enzyme mimicry by the antiidiotypic antibody approach. *Proc Natl Acad Sci U S A* **97**, 13526-13531.

Korber, B., LaBute, M. and Yusim, K. (2006) Immunoinformatics comes of age. *PLoS Comput Biol* **2**, e71.

Kothe, D.L., Decker, J.M., Li, Y., Weng, Z., Bibollet-Ruche, F., Zammit, K.P., Salazar, M.G., Chen, Y., Salazar-Gonzalez, J.F., Moldoveanu, Z., Mestecky, J., Gao, F., Haynes, B.F., Shaw, G.M., Muldoon, M., Korber, B.T. and Hahn, B.H. (2007) Antigenicity and immunogenicity of HIV-1 consensus subtype B envelope glycoproteins. *Virology* **360**, 218-234.

Kuate, S., Stahl-Hennig, C., Stoiber, H., Nchinda, G., Floto, A., Franz, M., Sauermann, U., Bredl, S., Deml, L., Ignatius, R., Norley, S., Racz, P., Tenner-Racz, K., Steinman, R.M., Wagner, R. and Uberla, K. (2006) Immunogenicity and efficacy of immunodeficiency virus-like particles pseudotyped with the G protein of vesicular stomatitis virus. *Virology* **351**, 133-144.

Kunert, R., Rüker, F. and Katinger, H. (1998) Molecular characterization of five neutralizing anti-HIV type 1 antibodies: identification of nonconventional D segments in the human monoclonal antibodies 2G12 and 2F5. *AIDS Res Hum Retroviruses* **14**, 1115-1128.

Kunert, R., Weik, R., Ferko, B., Stiegler, G. and Katinger, H. (2002) Anti-idiotypic antibody Ab2/3H6 mimics the epitope of the neutralizing anti-HIV-1 monoclonal antibody 2F5. *AIDS* **16**, 667-668.

Kutzler, M.A. and Weiner, D.B. (2008) DNA vaccines: ready for prime time? *Nat Rev Genet* **9**, 776-788.

Köhler, G. and Milstein, C. (1975) Continuous cultures of fused cells secreting antibody of predefined specificity. *Nature* **256**, 495-497.

Ladjemi, M.Z., Chardes, T., Corgnac, S., Garambois, V., Morisseau, S., Robert, B., Bascoul-Mollevi, C., Ait Arsa, I., Jacot, W., Pouget, J.P., Pelegrin, A. and Navarro-Teulon, I. (2011) Vaccination with human anti-trastuzumab anti-idiotype scFv reverses HER2 immunological tolerance and induces tumor immunity in MMTV.f.huHER2(Fo5) mice. *Breast Cancer Res* **13**, R17.

Langeveld, J.P., Martinez-Torrecedrada, J., Boshuizen, R.S., Melen, R.H. and Ignacio Casal, J. (2001) Characterisation of a protective linear B cell epitope against feline parvoviruses. *Vaccine* **19**, 2352-2360.

Lawn, S.D. (2004) AIDS in Africa: the impact of coinfections on the pathogenesis of HIV-1 infection. *J Infect* **48**, 1-12.

Lazarski, C.A., Chaves, F.A., Jenks, S.A., Wu, S., Richards, K.A., Weaver, J.M. and Sant, A.J. (2005) The kinetic stability of MHC class II:peptide complexes is a key parameter that dictates immunodominance. *Immunity* **23**, 29-40.

Lee, G. and Ge, B. (2010) Inhibition of in vitro tumor cell growth by RP215 monoclonal antibody and antibodies raised against its anti-idiotypic antibodies. *Cancer Immunol Immunother* **59**, 1347-1356.

Leonard, C.K., Spellman, M.W., Riddle, L., Harris, R.J., Thomas, J.N. and Gregory, T.J. (1990) Assignment of intrachain disulfide bonds and characterization of potential glycosylation sites of the type 1 recombinant human immunodeficiency virus envelope glycoprotein (gp120) expressed in Chinese hamster ovary cells. *J Biol Chem* **265**, 10373-10382.

Levy, J.A., Hoffman, A.D., Kramer, S.M., Landis, J.A., Shimabukuro, J.M. and Oshiro, L.S. (1984) Isolation of lymphocytopathic retroviruses from San Francisco patients with AIDS. *Science* **225**, 840-842.

Lewis, A.D., Chen, R., Montefiori, D.C., Johnson, P.R. and Clark, K.R. (2002) Generation of neutralizing activity against human immunodeficiency virus type 1 in serum by antibody gene transfer. *J Virol* **76**, 8769-8775.

Li, M., Gao, F., Mascola, J.R., Stamatatos, L., Polonis, V.R., Koutsoukos, M., Voss, G., Goepfert, P., Gilbert, P., Greene, K.M., Bilska, M., Kothe, D.L., Salazar-Gonzalez, J.F., Wei, X., Decker, J.M., Hahn, B.H. and Montefiori, D.C. (2005) Human immunodeficiency virus type 1 env clones from acute and early subtype B infections for standardized assessments of vaccine-elicited neutralizing antibodies. *J Virol* **79**, 10108-10125.

Li, Y., Migueles, S.A., Welcher, B., Svehla, K., Phogat, A., Louder, M.K., Wu, X., Shaw, G.M., Connors, M., Wyatt, R.T. and Mascola, J.R. (2007) Broad HIV-1 neutralization mediated by CD4-binding site antibodies. *Nat Med* **13**, 1032-1034.

Liu, J., Bartesaghi, A., Borgnia, M.J., Sapiro, G. and Subramaniam, S. (2008) Molecular architecture of native HIV-1 gp120 trimers. *Nature* **455**, 109-113.

Lorizate, M., Cruz, A., Huarte, N., Kunert, R., Pérez-Gil, J. and Nieva, J.L. (2006a) Recognition and blocking of HIV-1 gp41 pre-transmembrane sequence by monoclonal 4E10 antibody in a Raft-like membrane environment. *J Biol Chem* **281**, 39598-39606.

Lorizate, M., Gómara, M.J., de la Torre, B.G., Andreu, D. and Nieva, J.L. (2006b) Membrane-transferring sequences of the HIV-1 Gp41 ectodomain assemble into an immunogenic complex. *J Mol Biol* **360**, 45-55.

Luo, M., Yuan, F., Liu, Y., Jiang, S., Song, X., Jiang, P., Yin, X., Ding, M. and Deng, H. (2006) Induction of neutralizing antibody against human immunodeficiency virus type 1 (HIV-1) by immunization with gp41 membrane-proximal external region (MPER) fused with porcine endogenous retrovirus (PERV) p15E fragment. *Vaccine* **24**, 435-442.

MacCallum, R.M., Martin, A.C. and Thornton, J.M. (1996) Antibody-antigen interactions: contact analysis and binding site topography. *J Mol Biol* **262**, 732-745.

Maeso, R., Huarte, N., Julien, J.P., Kunert, R., Pai, E.F. and Nieva, J.L. (2011) Interaction of Anti-HIV Type 1 Antibody 2F5 with Phospholipid Bilayers and Its Relevance for the Mechanism of Virus Neutralization. *AIDS Res Hum Retroviruses*.

Mannhalter, J.W., Fischer, M.B., Wolf, H.M., Küpcü, Z., Barrett, N., Dorner, F., Eder, G. and Eibl, M.M. (1995) Immunization of chimpanzees with recombinant gp160, but not infection with human immunodeficiency virus type 1, induces envelope-specific Th1 memory cells. *J Infect Dis* **171**, 437-440.

Marsac, D., Loirat, D., Petit, C., Schwartz, O. and Michel, M.L. (2002) Enhanced presentation of major histocompatibility complex class I-restricted human immunodeficiency virus type 1 (HIV-1) Gag-specific epitopes after DNA immunization with vectors coding for vesicular stomatitis virus glycoprotein-pseudotyped HIV-1 Gag particles. *J Virol* **76**, 7544-7553.

Martinez-Picado, J., DePasquale, M.P., Kartsonis, N., Hanna, G.J., Wong, J., Finzi, D., Rosenberg, E., Gunthard, H.F., Sutton, L., Savara, A., Petropoulos, C.J., Hellmann, N., Walker, B.D., Richman, D.D., Siliciano, R. and D'Aquila, R.T. (2000) Antiretroviral resistance during successful therapy of HIV type 1 infection. *Proc Natl Acad Sci U S A* **97**, 10948-10953.

Martinon, F., Kaldma, K., Sikut, R., Culina, S., Romain, G., Tuomela, M., Adojaan, M., Männik, A., Toots, U., Kivisild, T., Morin, J., Brochard, P., Delache, B., Tripiciano, A., Ensoli, F., Stanescu, I., Le Grand, R. and Ustav, M. (2009) Persistent immune responses induced by a human immunodeficiency virus DNA vaccine delivered in association with electroporation in the skin of nonhuman primates. *Hum Gene Ther* **20**, 1291-1307.

Mascola, J.R., Lewis, M.G., Stiegler, G., Harris, D., VanCott, T.C., Hayes, D., Louder, M.K., Brown, C.R., Sapan, C.V., Frankel, S.S., Lu, Y., Robb, M.L., Katinger, H. and Birx, D.L. (1999) Protection of Macaques against pathogenic simian/human immunodeficiency virus 89.6PD by passive transfer of neutralizing antibodies. *J Virol* **73**, 4009-4018.

Mascola, J.R., Stiegler, G., VanCott, T.C., Katinger, H., Carpenter, C.B., Hanson, C.E., Beary, H., Hayes, D., Frankel, S.S., Birx, D.L. and Lewis, M.G. (2000) Protection of macaques against vaginal transmission of a pathogenic HIV-1/SIV chimeric virus by passive infusion of neutralizing antibodies. *Nat Med* **6**, 207-210.

Matyas, G.R., Wiczorek, L., Beck, Z., Ochsenbauer-Jambor, C., Kappes, J.C., Michael, N.L., Polonis, V.R. and Alving, C.R. (2009) Neutralizing antibodies induced by liposomal HIV-1 glycoprotein 41 peptide simultaneously bind to both the 2F5 or 4E10 epitope and lipid epitopes. *AIDS* **23**, 2069-2077.

Mañes, S., del Real, G., Lacalle, R.A., Lucas, P., Gómez-Moutón, C., Sánchez-Palomino, S., Delgado, R., Alcamí, J., Mira, E. and Martínez-A, C. (2000) Membrane raft microdomains mediate lateral assemblies required for HIV-1 infection. *EMBO Rep* **1**, 190-196.

Mañes, S., del Real, G. and Martínez-A, C. (2003) Pathogens: raft hijackers. *Nat Rev Immunol* **3**, 557-568.

McCaffrey, R.A., Saunders, C., Hensel, M. and Stamatatos, L. (2004) N-linked glycosylation of the V3 loop and the immunologically silent face of gp120 protects human immunodeficiency virus type 1 SF162 from neutralization by anti-gp120 and anti-gp41 antibodies. *J Virol* **78**, 3279-3295.

McMichael, A.J. (1998) The original sin of killer T cells. *Nature* **394**, 421-422.

Mehandru, S., Wrin, T., Galovich, J., Stiegler, G., Vcelar, B., Hurley, A., Hogan, C., Vasan, S., Katinger, H., Petropoulos, C.J. and Markowitz, M. (2004) Neutralization profiles of newly transmitted human immunodeficiency virus type 1 by monoclonal antibodies 2G12, 2F5, and 4E10. *J Virol* **78**, 14039-14042.

Menendez, A., Chow, K.C., Pan, O.C. and Scott, J.K. (2004) Human immunodeficiency virus type 1-neutralizing monoclonal antibody 2F5 is multispecific for sequences flanking the DKW core epitope. *J Mol Biol* **338**, 311-327.

Mian, I., Bradwell, A. and Olson, A. (1991) Structure, function and properties of antibody binding sites. *J Mol Biol* **217**, 133-151.

Montefiori, D.C., Safrit, J.T., Lydy, S.L., Barry, A.P., Bilska, M., Vo, H.T., Klein, M., Tartaglia, J., Robinson, H.L. and Rovinski, B. (2001) Induction of neutralizing antibodies and gag-specific cellular immune responses to an R5 primary isolate of human immunodeficiency virus type 1 in rhesus macaques. *J Virol* **75**, 5879-5890.

Montero, M., van Houten, N.E., Wang, X. and Scott, J.K. (2008) The membrane-proximal external region of the human immunodeficiency virus type 1 envelope: dominant site of antibody neutralization and target for vaccine design. *Microbiol Mol Biol Rev* **72**, 54-84, table of contents.

Morgan, D., Mahe, C., Mayanja, B., Okongo, J.M., Lubega, R. and Whitworth, J.A. (2002) HIV-1 infection in rural Africa: is there a difference in median time to AIDS and survival compared with that in industrialized countries? *AIDS* **16**, 597-603.

Morrison, S., Johnson, M., Herzenberg, L. and Oi, V. (1984) Chimeric human antibody molecules: mouse antigen-binding domains with human constant region domains. *Proc Natl Acad Sci U S A* **81**, 6851-6855.

Murphey-Corb, M., Martin, L.N., Davison-Fairburn, B., Montelaro, R.C., Miller, M., West, M., Ohkawa, S., Baskin, G.B., Zhang, J.Y. and Putney, S.D. (1989) A formalin-inactivated whole SIV vaccine confers protection in macaques. *Science* **246**, 1293-1297.

Muster, T., Steindl, F., Purtscher, M., Trkola, A., Klima, A., Himmler, G., Rüber, F. and Katinger, H. (1993) A conserved neutralizing epitope on gp41 of human immunodeficiency virus type 1. *J Virol* **67**, 6642-6647.

Müller, S., Brams, P., Collins, H., Dorigo, O., Wang, H.-T. and Köhler, H. (1995) Apoptosis of CD4⁺ and CD8⁺ Cells from HIV-1 infected individuals: role of anti-idiotypic antibodies **4**, 229-238.

Müller, S., Margolin, D.H., Nara, P.L., Alvord, W.G. and Köhler, H. (1998) Stimulation of HIV-1-neutralizing antibodies in simian HIV-IIIB-infected macaques. *Proc Natl Acad Sci U S A* **95**, 276-281.

Müller, S., Wang, H.T., Kaveri, S.V., Chattopadhyay, S. and Köhler, H. (1991) Generation and specificity of monoclonal anti-idiotypic antibodies against human HIV-specific antibodies.

I. Cross-reacting idiotopes are expressed in subpopulations of HIV-infected individuals. *J Immunol* **147**, 933-941.

Nelson, A., Dhimolea, E. and Reichert, J. (2010) Development trends for human monoclonal antibody therapeutics. *Nat Rev Drug Discov* **9**, 767-774.

Nelson, J.D., Brunel, F.M., Jensen, R., Crooks, E.T., Cardoso, R.M., Wang, M., Hessel, A., Wilson, I.A., Binley, J.M., Dawson, P.E., Burton, D.R. and Zwick, M.B. (2007) An affinity-enhanced neutralizing antibody against the membrane-proximal external region of human immunodeficiency virus type 1 gp41 recognizes an epitope between those of 2F5 and 4E10. *J Virol* **81**, 4033-4043.

Neuberger, M.S. and Milstein, C. (1995) Somatic hypermutation. *Curr Opin Immunol* **7**, 248-254.

Nielsen, M., Justesen, S., Lund, O., Lundegaard, C. and Buus, S. (2010) NetMHCIIpan-2.0 - Improved pan-specific HLA-DR predictions using a novel concurrent alignment and weight optimization training procedure. *Immunome Res* **6**, 9.

O'Connor, S., Meng, Y., Rezaie, A. and Presta, L. (1998) Humanization of an antibody against human protein C and calcium-dependence involving framework residues. *Protein Eng* **11**, 321-328.

Ofek, G., McKee, K., Yang, Y., Yang, Z.Y., Skinner, J., Guenaga, F.J., Wyatt, R., Zwick, M.B., Nabel, G.J., Mascola, J.R. and Kwong, P.D. (2010) Relationship between antibody 2F5 neutralization of HIV-1 and hydrophobicity of its heavy chain third complementarity-determining region. *J Virol* **84**, 2955-2962.

Ofek, G., Tang, M., Sambor, A., Katinger, H., Mascola, J., Wyatt, R. and Kwong, P. (2004) Structure and mechanistic analysis of the anti-human immunodeficiency virus type 1 antibody 2F5 in complex with its gp41 epitope. *J Virol* **78**, 10724-10737.

Padlan, E.A., Abergel, C. and Tipper, J.P. (1995) Identification of specificity-determining residues in antibodies. *FASEB J* **9**, 133-139.

Pai, E., Klein, M., Chong, P. and Pedyczak, A. (2000) Fab'-epitope complex from the HIV-1 cross-neutralizing monoclonal antibody 2F5 ed. Patent, W.I.P.O. U.S. WO-00/61618.

Pan, Y., Yuhasz, S.C. and Amzel, L.M. (1995) Anti-idiotypic antibodies: biological function and structural studies. *FASEB J* **9**, 43-49.

Panina-Bordignon, P., Tan, A., Termijtelen, A., Demotz, S., Corradin, G. and Lanzavecchia, A. (1989) Universally immunogenic T cell epitopes: promiscuous binding to human MHC class II and promiscuous recognition by T cells. *Eur J Immunol* **19**, 2237-2242.

Parker, C.E., Deterding, L.J., Hager-Braun, C., Binley, J.M., Schülke, N., Katinger, H., Moore, J.P. and Tomer, K.B. (2001) Fine definition of the epitope on the gp41 glycoprotein of human immunodeficiency virus type 1 for the neutralizing monoclonal antibody 2F5. *J Virol* **75**, 10906-10911.

Parren, P.W. and Burton, D.R. (2001) The antiviral activity of antibodies in vitro and in vivo. *Adv Immunol* **77**, 195-262.

Parren, P.W., Marx, P.A., Hessel, A.J., Luckay, A., Harouse, J., Cheng-Mayer, C., Moore, J.P. and Burton, D.R. (2001) Antibody protects macaques against vaginal challenge with a pathogenic R5 simian/human immunodeficiency virus at serum levels giving complete neutralization in vitro. *J Virol* **75**, 8340-8347.

Pedersen, J., Henry, A., Searle, S., Guild, B., Roguska, M. and Rees, A. (1994) Comparison of surface accessible residues in human and murine immunoglobulin Fv domains. Implication for humanization of murine antibodies. *J Mol Biol* **235**, 959-973.

Pelat, T., Bedouelle, H., Rees, A.R., Crennell, S.J., Lefranc, M.P. and Thullier, P. (2008) Germline humanization of a non-human primate antibody that neutralizes the anthrax toxin, by in vitro and in silico engineering. *J Mol Biol* **384**, 1400-1407.

Perelson, A.S., Neumann, A.U., Markowitz, M., Leonard, J.M. and Ho, D.D. (1996) HIV-1 dynamics in vivo: virion clearance rate, infected cell life-span, and viral generation time. *Science* **271**, 1582-1586.

Perri, S., Greer, C.E., Thudium, K., Doe, B., Legg, H., Liu, H., Romero, R.E., Tang, Z., Bin, Q., Dubensky, T.W., Vajdy, M., Otten, G.R. and Polo, J.M. (2003) An alphavirus replicon particle chimera derived from venezuelan equine encephalitis and sindbis viruses is a potent gene-based vaccine delivery vector. *J Virol* **77**, 10394-10403.

Peters, B.S. (2001) The basis for HIV immunotherapeutic vaccines. *Vaccine* **20**, 688-705.

Peters, B.S., Jaoko, W., Vardas, E., Panayotakopoulos, G., Fast, P., Schmidt, C., Gilmour, J., Bogoshi, M., Omosa-Manyonyi, G., Dally, L., Klavinskis, L., Farah, B., Tarragona, T., Bart, P.A., Robinson, A., Pieterse, C., Stevens, W., Thomas, R., Barin, B., McMichael, A.J., McIntyre, J.A., Pantaleo, G., Hanke, T. and Bwayo, J. (2007) Studies of a prophylactic HIV-1 vaccine candidate based on modified vaccinia virus Ankara (MVA) with and without DNA priming: effects of dosage and route on safety and immunogenicity. *Vaccine* **25**, 2120-2127.

Phogat, S., Svehla, K., Tang, M., Spadaccini, A., Muller, J., Mascola, J., Berkower, I. and Wyatt, R. (2008) Analysis of the human immunodeficiency virus type 1 gp41 membrane proximal external region arrayed on hepatitis B surface antigen particles. *Virology* **373**, 72-84.

Phogat, S. and Wyatt, R. (2007) Rational modifications of HIV-1 envelope glycoproteins for immunogen design. *Curr Pharm Des* **13**, 213-227.

Pitisuttithum, P., Gilbert, P., Gurwith, M., Heyward, W., Martin, M., van Griensven, F., Hu, D., Tappero, J.W., Choopanya, K. and Group, B.V.E. (2006) Randomized, double-blind, placebo-controlled efficacy trial of a bivalent recombinant glycoprotein 120 HIV-1 vaccine among injection drug users in Bangkok, Thailand. *J Infect Dis* **194**, 1661-1671.

Plantier, J.C., Leoz, M., Dickerson, J.E., De Oliveira, F., Cordonnier, F., Lemée, V., Damond, F., Robertson, D.L. and Simon, F. (2009) A new human immunodeficiency virus derived from gorillas. *Nat Med* **15**, 871-872.

Poignard, P., Moulard, M., Golez, E., Vivona, V., Franti, M., Venturini, S., Wang, M., Parren, P.W. and Burton, D.R. (2003) Heterogeneity of envelope molecules expressed on primary human immunodeficiency virus type 1 particles as probed by the binding of neutralizing and nonneutralizing antibodies. *J Virol* **77**, 353-365.

Poljak, R.J. (1994) An idiotope--anti-idiotope complex and the structural basis of molecular mimicking. *Proc Natl Acad Sci U S A* **91**, 1599-1600.

Ponomarenko, J., Bui, H.H., Li, W., Fusseder, N., Bourne, P.E., Sette, A. and Peters, B. (2008) ElliPro: a new structure-based tool for the prediction of antibody epitopes. *BMC Bioinformatics* **9**, 514.

Ponomarenko, N.A., Pillet, D., Paon, M., Vorobiev, I.I., Smirnov, I.V., Adenier, H., Avalle, B., Kolesnikov, A.V., Kozyr, A.V., Thomas, D., Gabibov, A.G. and Friboulet, A. (2007) Anti-idiotypic antibody mimics proteolytic function of parent antigen. *Biochemistry* **46**, 14598-14609.

Pontesilli, O., Guerra, E.C., Ammassari, A., Tomino, C., Carlesimo, M., Antinori, A., Tamburrini, E., Prozzo, A., Seeber, A.C., Vella, S., Ortona, L. and Aiuti, F. (1998) Phase II controlled trial of post-exposure immunization with recombinant gp160 versus antiretroviral therapy in asymptomatic HIV-1-infected adults. VaxSyn Protocol Team. *AIDS* **12**, 473-480.

Poon, B., Hsu, J.F., Gudeman, V., Chen, I.S. and Grovit-Ferbas, K. (2005) Formaldehyde-treated, heat-inactivated virions with increased human immunodeficiency virus type 1 env can be used to induce high-titer neutralizing antibody responses. *J Virol* **79**, 10210-10217.

Popovic, M., Sarngadharan, M.G., Read, E. and Gallo, R.C. (1984) Detection, isolation, and continuous production of cytopathic retroviruses (HTLV-III) from patients with AIDS and pre-AIDS. *Science* **224**, 497-500.

Presta, L. (2008) Molecular engineering and design of therapeutic antibodies. *Curr Opin Immunol* **20**, 460-470.

Presta, L., Lahr, S., Shields, R., Porter, J., Gorman, C., Fendly, B. and Jardieu, P. (1993) Humanization of an antibody directed against IgE. *J Immunol* **151**, 2623-2632.

Preston, B.D., Poiesz, B.J. and Loeb, L.A. (1988) Fidelity of HIV-1 reverse transcriptase. *Science* **242**, 1168-1171.

Purtscher, M., Trkola, A., Gruber, G., Buchacher, A., Predl, R., Steindl, F., Tauer, C., Berger, R., Barrett, N. and Jungbauer, A. (1994) A broadly neutralizing human monoclonal antibody against gp41 of human immunodeficiency virus type 1. *AIDS Res Hum Retroviruses* **10**, 1651-1658.

Queen, C., Schneider, W., Selick, H., Payne, P., Landolfi, N., Duncan, J., Avdalovic, N., Levitt, M., Junghans, R. and Waldmann, T. (1989) A humanized antibody that binds to the interleukin 2 receptor. *Proc Natl Acad Sci U S A* **86**, 10029-10033.

Quendler, H. (2008) Development of an HIV-1 Vaccine based on Liposome Technology. In *Department of Biotechnology, institute of Applied Microbiology*. p.95: University of Natural Resources and Life Sciences, Vienna.

Rader, C., Ritter, G., Nathan, S., Elia, M., Gout, I., Jungbluth, A.A., Cohen, L.S., Welt, S., Old, L.J. and Barbas, C.F. (2000) The rabbit antibody repertoire as a novel source for the generation of therapeutic human antibodies. *J Biol Chem* **275**, 13668-13676.

Ramos, A.S., Parise, C.B., Travassos, L.R., Han, S.W., de Campos-Lima, P.O. and de Moraes, J.Z. (2011) The idiotype (Id) cascade in mice elicited the production of anti-R24 Id and anti-anti-Id monoclonal antibodies with antitumor and protective activity against human melanoma. *Cancer Sci* **102**, 64-70.

Reks-Ngarm, S., Pitisuttithum, P., Nitayaphan, S., Kaewkungwal, J., Chiu, J., Paris, R., Premisri, N., Namwat, C., de Souza, M., Adams, E., Benenson, M., Gurunathan, S., Tartaglia, J., McNeil, J., Francis, D., Stablein, D., Birx, D., Chunsuttiwat, S., Khamboonruang, C., Thongcharoen, P., Robb, M., Michael, N., Kunasol, P., Kim, J. and Investigators, M.-T. (2009) Vaccination with ALVAC and AIDSVAX to prevent HIV-1 infection in Thailand. *N Engl J Med* **361**, 2209-2220.

Riechmann, L., Clark, M., Waldmann, H. and Winter, G. (1988) Reshaping human antibodies for therapy. *Nature* **332**, 323-327.

Rits-Volloch, S., Frey, G., Harrison, S.C. and Chen, B. (2006) Restraining the conformation of HIV-1 gp120 by removing a flexible loop. *EMBO J* **25**, 5026-5035.

Roberts, J.D., Bebenek, K. and Kunkel, T.A. (1988) The accuracy of reverse transcriptase from HIV-1. *Science* **242**, 1171-1173.

Robinson, J.E., Franco, K., Elliott, D.H., Maher, M.J., Reyna, A., Montefiori, D.C., Zolla-Pazner, S., Gorny, M.K., Kraft, Z. and Stamatatos, L. (2010) Quaternary epitope specificities of anti-HIV-1 neutralizing antibodies generated in rhesus macaques infected by the simian/human immunodeficiency virus SHIVSF162P4. *J Virol* **84**, 3443-3453.

Rodon, J., Garrison, M., Hammond, L., de Bono, J., Smith, L., Forero, L., Hao, D., Takimoto, C., Lambert, J., Pandite, L., Howard, M., Xie, H. and Tolcher, A. (2008) Cantuzumab mertansine in a three-times a week schedule: a phase I and pharmacokinetic study. *Cancer Chemother Pharmacol* **62**, 911-919.

Rodrigues, L. and Bonorino, C. (2009) Role of IL-15 and IL-21 in viral immunity: applications for vaccines and therapies. *Expert Rev Vaccines* **8**, 167-177.

Roguska, M., Pedersen, J., Henry, A., Searle, S., Roja, C., Avery, B., Hoffee, M., Cook, S., Lambert, J., Blättler, W., Rees, A. and Guild, B. (1996) A comparison of two murine monoclonal antibodies humanized by CDR-grafting and variable domain resurfacing. *Protein Eng* **9**, 895-904.

Roguska, M., Pedersen, J., Keddy, C., Henry, A., Searle, S., Lambert, J., Goldmacher, V., Blättler, W., Rees, A. and Guild, B. (1994) Humanization of murine monoclonal antibodies through variable domain resurfacing. *Proc Natl Acad Sci U S A* **91**, 969-973.

Rosok, M., Yelton, D., Harris, L., Bajorath, J., Hellström, K., Hellström, I., Cruz, G., Kristensson, K., Lin, H., Huse, W. and Glaser, S. (1996) A combinatorial library strategy for the rapid humanization of anticarcinoma BR96 Fab. *J Biol Chem* **271**, 22611-22618.

Ross, A.L., Br ave, A., Scarlatti, G., Manrique, A. and Buonaguro, L. (2010) Progress towards development of an HIV vaccine: report of the AIDS Vaccine 2009 Conference. *Lancet Infect Dis* **10**, 305-316.

Rudd, P.M. and Dwek, R.A. (1997) Glycosylation: heterogeneity and the 3D structure of proteins. *Crit Rev Biochem Mol Biol* **32**, 1-100.

Rusert, P., Krarup, A., Magnus, C., Brandenberg, O.F., Weber, J., Ehler, A.K., Regoes, R.R., G unthard, H.F. and Trkola, A. (2011) Interaction of the gp120 V1V2 loop with a neighboring gp120 unit shields the HIV envelope trimer against cross-neutralizing antibodies. *J Exp Med* **208**, 1419-1433.

Sakaue, G., Hiroi, T., Nakagawa, Y., Someya, K., Iwatani, K., Sawa, Y., Takahashi, H., Honda, M., Kunisawa, J. and Kiyono, H. (2003) HIV mucosal vaccine: nasal immunization with gp160-encapsulated hemagglutinating virus of Japan-liposome induces antigen-specific CTLs and neutralizing antibody responses. *J Immunol* **170**, 495-502.

Saldhana, J. (2007) Molecular Engineering I: Humanization. In *Handbook of therapeutic antibodies* ed. Dubel, S.: Wiley-VCH, Weinheim.

Salmon-C eron, D., Durier, C., Desaint, C., Cuzin, L., Surenaud, M., Hamouda, N.B., Leli evre, J.D., Bonnet, B., Pialoux, G., Poizot-Martin, I., Aboulker, J.P., L evy, Y., Launay, O. and group, A.V.t. (2010) Immunogenicity and safety of an HIV-1 lipopeptide vaccine in healthy adults: a phase 2 placebo-controlled ANRS trial. *AIDS* **24**, 2211-2223.

Salzwedel, K., West, J.T. and Hunter, E. (1999) A conserved tryptophan-rich motif in the membrane-proximal region of the human immunodeficiency virus type 1 gp41 ectodomain is important for Env-mediated fusion and virus infectivity. *J Virol* **73**, 2469-2480.

Scherer, E.M., Leaman, D.P., Zwick, M.B., McMichael, A.J. and Burton, D.R. (2010) Aromatic residues at the edge of the antibody combining site facilitate viral glycoprotein recognition through membrane interactions. *Proc Natl Acad Sci U S A* **107**, 1529-1534.

Schibli, D.J., Montelaro, R.C. and Vogel, H.J. (2001) The membrane-proximal tryptophan-rich region of the HIV glycoprotein, gp41, forms a well-defined helix in dodecylphosphocholine micelles. *Biochemistry* **40**, 9570-9578.

Sekaly, R.P. (2008) The failed HIV Merck vaccine study: a step back or a launching point for future vaccine development? *J Exp Med* **205**, 7-12.

Selvarajah, S., Puffer, B.A., Lee, F.H., Zhu, P., Li, Y., Wyatt, R., Roux, K.H., Doms, R.W. and Burton, D.R. (2008) Focused dampening of antibody response to the immunodominant variable loops by engineered soluble gp140. *AIDS Res Hum Retroviruses* **24**, 301-314.

Shearman, C.W., Pollock, D., White, G., Hehir, K., Moore, G.P., Kanzy, E.J. and Kurrel, R. (1991) Construction, expression and characterization of humanized antibodies directed against the human alpha/beta T cell receptor. *J Immunol* **147**, 4366-4373.

Sheppard, H.W. (2005) Inactivated- or killed-virus HIV/AIDS vaccines. *Curr Drug Targets Infect Disord* **5**, 131-141.

Shoenfeld, Y. (1995) Idiotypic network, pathogenic autoantibodies and autoimmunity. *Clin Exp Immunol* **101 Suppl 1**, 26-28.

Singh, S.K. and Bisen, P.S. (2006) Adjuvanticity of stealth liposomes on the immunogenicity of synthetic gp41 epitope of HIV-1. *Vaccine* **24**, 4161-4166.

Son, J.H., Lee, U.H., Lee, J.J., Kwon, B., Kwon, B.S. and Park, J.W. (2004) Humanization of agonistic anti-human 4-1BB monoclonal antibody using a phage-displayed combinatorial library. *J Immunol Methods* **286**, 187-201.

Southwood, S., Sidney, J., Kondo, A., del Guercio, M.F., Appella, E., Hoffman, S., Kubo, R.T., Chesnut, R.W., Grey, H.M. and Sette, A. (1998) Several common HLA-DR types share largely overlapping peptide binding repertoires. *J Immunol* **160**, 3363-3373.

Sperlagh, M., Hoxie, J., Maruyama, H., Stefano, K., Gonzales-Scarano, F., Prewett, M., Liang, S., Matsushita, S. and Herlyn, D. (1994) Polyclonal antiidiotypic antibodies mimicking gp120 of HIV-1. *Viral Immunol* **7**, 61-69.

Staelens, S., Desmet, J., Ngo, T., Vauterin, S., Pareyn, I., Barbeaux, P., Van Rompaey, I., Stassen, J., Deckmyn, H. and Vanhoorelbeke, K. (2006) Humanization by variable domain resurfacing and grafting on a human IgG4, using a new approach for determination of non-human like surface accessible framework residues based on homology modelling of variable domains. *Mol Immunol* **43**, 1243-1257.

Stebbing, J. and Moyle, G. (2003) The clades of HIV: their origins and clinical significance. *AIDS Rev* **5**, 205-213.

Stoiber, H., Pintér, C., Siccardi, A.G., Clivio, A. and Dierich, M.P. (1996) Efficient destruction of human immunodeficiency virus in human serum by inhibiting the protective action of complement factor H and decay accelerating factor (DAF, CD55). *J Exp Med* **183**, 307-310.

Storm, G., ten Kate, M.T., Working, P.K. and Bakker-Woudenberg, I.A. (1998) Doxorubicin entrapped in sterically stabilized liposomes: effects on bacterial blood clearance capacity of the mononuclear phagocyte system. *Clin Cancer Res* **4**, 111-115.

Stott, E.J. (1991) Anti-cell antibody in macaques. *Nature* **353**, 393.

Tan, K., Liu, J., Wang, J., Shen, S. and Lu, M. (1997) Atomic structure of a thermostable subdomain of HIV-1 gp41. *Proc Natl Acad Sci U S A* **94**, 12303-12308.

Tan, P., Mitchell, D., Buss, T., Holmes, M., Anasetti, C. and Foote, J. (2002) "Superhumanized" antibodies: reduction of immunogenic potential by complementarity-determining region grafting with human germline sequences: application to an anti-CD28. *J Immunol* **169**, 1119-1125.

Thibodeau, L., Chagnon, M., Flamand, L., Oth, D., Lachapelle, L., Tremblay, C. and Montagnier, L. (1989) [Role of liposomes in the presentation of HIV envelope glycoprotein and the immune response in mice]. *C R Acad Sci III* **309**, 741-747.

Thullier, P., Huish, O., Pelat, T. and Martin, A.C. (2010) The humanness of macaque antibody sequences. *J Mol Biol* **396**, 1439-1450.

Tian, Y., Ramesh, C.V., Ma, X., Naqvi, S., Patel, T., Cenizal, T., Tiscione, M., Diaz, K., Crea, T., Arnold, E., Arnold, G.F. and Taylor, J.W. (2002) Structure-affinity relationships in the gp41 ELDKWA epitope for the HIV-1 neutralizing monoclonal antibody 2F5: effects of side-chain and backbone modifications and conformational constraints. *J Pept Res* **59**, 264-276.

Trkola, A., Kuster, H., Rusert, P., Joos, B., Fischer, M., Leemann, C., Manrique, A., Huber, M., Rehr, M., Oxenius, A., Weber, R., Stiegler, G., Vcelar, B., Katinger, H., Aceto, L. and Günthard, H.F. (2005) Delay of HIV-1 rebound after cessation of antiretroviral therapy through passive transfer of human neutralizing antibodies. *Nat Med* **11**, 615-622.

Trkola, A., Pomales, A., Yuan, H., Korber, B., Maddon, P., Allaway, G., Katinger, H., Barbas, C.r., Burton, D. and Ho, D. (1995) Cross-clade neutralization of primary isolates of human immunodeficiency virus type 1 by human monoclonal antibodies and tetrameric CD4-IgG. *J Virol* **69**, 6609-6617.

Trkola, A., Purtscher, M., Muster, T., Ballaun, C., Buchacher, A., Sullivan, N., Srinivasan, K., Sodroski, J., Moore, J.P. and Katinger, H. (1996) Human monoclonal antibody 2G12 defines a distinctive neutralization epitope on the gp120 glycoprotein of human immunodeficiency virus type 1. *J Virol* **70**, 1100-1108.

UNAIDS (2010) *Global Report: UNAIDS Report on the Global AIDS Epidemic: 2010*.

Urlaub, G. and Chasin, L. (1980) Isolation of Chinese hamster cell mutants deficient in dihydrofolate reductase activity. *Proc Natl Acad Sci U S A* **77**, 4216-4220.

van Gunsteren, W.F., Billeter, S.R., Eising, A.A., Huenenberger, P.H., Krueger, P., Mark, A.E., Scott, W.R.P. and Tiron, I.G. (1996) *Biomolecular Simulation: The GROMOS96 Manual and User Guide*. VdF: Hochschulverlag AG, Zuerich, Switzerland.

Vani, J., Justin, J., Nagasuma, R.C., Nayak, R. and Shaila, M.S. (2007) Peptidomimics of antigen are present in variable region of heavy and light chains of anti-idiotypic antibody and function as surrogate antigen for perpetuation of immunological memory. *Mol Immunol* **44**, 3345-3354.

Vasan, S., Hurley, A., Schlesinger, S.J., Hannaman, D., Gardiner, D.F., Dugin, D.P., Boente-Carrera, M., Vittorino, R., Caskey, M., Andersen, J., Huang, Y., Cox, J.H., Tarragona-Fiol, T., Gill, D.K., Cheeseman, H., Clark, L., Dally, L., Smith, C., Schmidt, C., Park, H.H., Kopycinski, J.T., Gilmour, J., Fast, P., Bernard, R. and Ho, D.D. (2011) In vivo electroporation enhances the immunogenicity of an HIV-1 DNA vaccine candidate in healthy volunteers. *PLoS One* **6**, e19252.

Veronese, F.D., DeVico, A.L., Copeland, T.D., Oroszlan, S., Gallo, R.C. and Sarngadharan, M.G. (1985) Characterization of gp41 as the transmembrane protein coded by the HTLV-III/LAV envelope gene. *Science* **229**, 1402-1405.

Verschoor, E.J., Mooij, P., Oostermeijer, H., van der Kolk, M., ten Haaft, P., Verstrepen, B., Sun, Y., Morein, B., Akerblom, L., Fuller, D.H., Barnett, S.W. and Heeney, J.L. (1999) Comparison of immunity generated by nucleic acid-, MF59-, and ISCOM-formulated human

immunodeficiency virus type 1 vaccines in Rhesus macaques: evidence for viral clearance. *J Virol* **73**, 3292-3300.

Waldmann, H. and Hale, G. (2005) CAMPATH: from concept to clinic. *Philos Trans R Soc Lond B Biol Sci* **360**, 1707-1711.

Waldmann, T.A. (2006) The biology of interleukin-2 and interleukin-15: implications for cancer therapy and vaccine design. *Nat Rev Immunol* **6**, 595-601.

Walker, L.M., Phogat, S.K., Chan-Hui, P.Y., Wagner, D., Phung, P., Goss, J.L., Wrin, T., Simek, M.D., Fling, S., Mitcham, J.L., Lehrman, J.K., Priddy, F.H., Olsen, O.A., Frey, S.M., Hammond, P.W., Kaminsky, S., Zamb, T., Moyle, M., Koff, W.C., Poignard, P., Burton, D.R. and Investigators, P.G.P. (2009) Broad and potent neutralizing antibodies from an African donor reveal a new HIV-1 vaccine target. *Science* **326**, 285-289.

Walter, G. (1986) Production and use of antibodies against synthetic peptides. *J Immunol Methods* **88**, 149-161.

Wang, J.J., Li, Y.H., Liu, Y.H., Song, J., Guo, F.J., Li, Y.L. and Li, G.C. (2010) The ability of human bispecific anti-idiotypic antibody to elicit humoral and cellular immune responses in mice. *Int Immunopharmacol* **10**, 707-712.

Wang, Y., Wu, W., Negre, N.N., White, K.P., Li, C. and Shah, P.K. (2011) Determinants of antigenicity and specificity in immune response for protein sequences. *BMC Bioinformatics* **12**, 251.

Wang, Z., Liu, Z., Cheng, X. and Chen, Y.H. (2005) The recombinant immunogen with high-density epitopes of ELDKWA and ELDEWA induced antibodies recognizing both epitopes on HIV-1 gp41. *Microbiol Immunol* **49**, 703-709.

Wei, X., Decker, J.M., Wang, S., Hui, H., Kappes, J.C., Wu, X., Salazar-Gonzalez, J.F., Salazar, M.G., Kilby, J.M., Saag, M.S., Komarova, N.L., Nowak, M.A., Hahn, B.H., Kwong, P.D. and Shaw, G.M. (2003) Antibody neutralization and escape by HIV-1. *Nature* **422**, 307-312.

Weissenhorn, W., Dessen, A., Harrison, S.C., Skehel, J.J. and Wiley, D.C. (1997) Atomic structure of the ectodomain from HIV-1 gp41. *Nature* **387**, 426-430.

Whitelegg, N. and Rees, A. (2000) WAM: an improved algorithm for modelling antibodies on the WEB. *Protein Eng* **13**, 819-824.

Wood, E., Hogg, R.S., Yip, B., Harrigan, P.R., O'Shaughnessy, M.V. and Montaner, J.S. (2003) Is there a baseline CD4 cell count that precludes a survival response to modern antiretroviral therapy? *AIDS* **17**, 711-720.

Wu, T.T. and Kabat, E.A. (1970) An analysis of the sequences of the variable regions of Bence Jones proteins and myeloma light chains and their implications for antibody complementarity. *J Exp Med* **132**, 211-250.

Wu, X., Yang, Z.Y., Li, Y., Hogerkorp, C.M., Schief, W.R., Seaman, M.S., Zhou, T., Schmidt, S.D., Wu, L., Xu, L., Longo, N.S., McKee, K., O'Dell, S., Louder, M.K., Wycuff, D.L., Feng, Y., Nason, M., Doria-Rose, N., Connors, M., Kwong, P.D., Roederer, M., Wyatt, R.T., Nabel, G.J. and Mascola, J.R. (2010) Rational design of envelope identifies broadly neutralizing human monoclonal antibodies to HIV-1. *Science* **329**, 856-861.

Wyatt, R., Kwong, P.D., Desjardins, E., Sweet, R.W., Robinson, J., Hendrickson, W.A. and Sodroski, J.G. (1998) The antigenic structure of the HIV gp120 envelope glycoprotein. *Nature* **393**, 705-711.

Wyatt, R. and Sodroski, J. (1998) The HIV-1 envelope glycoproteins: fusogens, antigens, and immunogens. *Science* **280**, 1884-1888.

Xiao, X., Phogat, S., Shu, Y., Phogat, A., Chow, Y.H., Wei, O.L., Goldstein, H., Broder, C.C. and Dimitrov, D.S. (2003) Purified complexes of HIV-1 envelope glycoproteins with CD4 and CCR5(CXCR4): production, characterization and immunogenicity. *Vaccine* **21**, 4275-4284.

Xin, K.Q., Urabe, M., Yang, J., Nomiya, K., Mizukami, H., Hamajima, K., Nomiya, H., Saito, T., Imai, M., Monahan, J., Okuda, K. and Ozawa, K. (2001) A novel recombinant adeno-associated virus vaccine induces a long-term humoral immune response to human immunodeficiency virus. *Hum Gene Ther* **12**, 1047-1061.

Ye, L., Wen, Z., Dong, K., Wang, X., Bu, Z., Zhang, H., Compans, R.W. and Yang, C. (2011) Induction of HIV Neutralizing Antibodies against the MPER of the HIV Envelope Protein by HA/gp41 Chimeric Protein-Based DNA and VLP Vaccines. *PLoS One* **6**, e14813.

Zhang, M., Gaschen, B., Blay, W., Foley, B., Haigwood, N., Kuiken, C. and Korber, B. (2004) Tracking global patterns of N-linked glycosylation site variation in highly variable viral glycoproteins: HIV, SIV, and HCV envelopes and influenza hemagglutinin. *Glycobiology* **14**, 1229-1246.

Zhang, M.Y., Wang, Y., Mankowski, M.K., Ptak, R.G. and Dimitrov, D.S. (2009) Cross-reactive HIV-1-neutralizing activity of serum IgG from a rabbit immunized with gp41 fused to IgG1 Fc: possible role of the prolonged half-life of the immunogen. *Vaccine* **27**, 857-863.

Zhang, Q., Wang, P., Kim, Y., Haste-Andersen, P., Beaver, J., Bourne, P.E., Bui, H.H., Buus, S., Frankild, S., Greenbaum, J., Lund, O., Lundegaard, C., Nielsen, M., Ponomarenko, J., Sette, A., Zhu, Z. and Peters, B. (2008) Immune epitope database analysis resource (IEDB-AR). *Nucleic Acids Res* **36**, W513-518.

Zhang, W., Canziani, G., Plugariu, C., Wyatt, R., Sodroski, J., Sweet, R., Kwong, P., Hendrickson, W. and Chaiken, I. (1999) Conformational changes of gp120 in epitopes near the CCR5 binding site are induced by CD4 and a CD4 miniprotein mimetic. *Biochemistry* **38**, 9405-9416.

Zheng, Y.H., Lovsin, N. and Peterlin, B.M. (2005) Newly identified host factors modulate HIV replication. *Immunol Lett* **97**, 225-234.

Zhou, T., Georgiev, I., Wu, X., Yang, Z.Y., Dai, K., Finzi, A., Kwon, Y.D., Scheid, J.F., Shi, W., Xu, L., Yang, Y., Zhu, J., Nussenzweig, M.C., Sodroski, J., Shapiro, L., Nabel, G.J.,

Mascola, J.R. and Kwong, P.D. (2010) Structural basis for broad and potent neutralization of HIV-1 by antibody VRC01. *Science* **329**, 811-817.

Zhou, T., Xu, L., Dey, B., Hessel, A.J., Van Ryk, D., Xiang, S.H., Yang, X., Zhang, M.Y., Zwick, M.B., Arthos, J., Burton, D.R., Dimitrov, D.S., Sodroski, J., Wyatt, R., Nabel, G.J. and Kwong, P.D. (2007) Structural definition of a conserved neutralization epitope on HIV-1 gp120. *Nature* **445**, 732-737.

Zhu, P., Liu, J., Bess, J., Chertova, E., Lifson, J.D., Grisé, H., Ofek, G.A., Taylor, K.A. and Roux, K.H. (2006) Distribution and three-dimensional structure of AIDS virus envelope spikes. *Nature* **441**, 847-852.

Zhu, X., Borchers, C., Bienstock, R.J. and Tomer, K.B. (2000) Mass spectrometric characterization of the glycosylation pattern of HIV-gp120 expressed in CHO cells. *Biochemistry* **39**, 11194-11204.

Zwick, M.B., Jensen, R., Church, S., Wang, M., Stiegler, G., Kunert, R., Katinger, H. and Burton, D.R. (2005) Anti-human immunodeficiency virus type 1 (HIV-1) antibodies 2F5 and 4E10 require surprisingly few crucial residues in the membrane-proximal external region of glycoprotein gp41 to neutralize HIV-1. *J Virol* **79**, 1252-1261.

Zwick, M.B., Komori, H.K., Stanfield, R.L., Church, S., Wang, M., Parren, P.W., Kunert, R., Katinger, H., Wilson, I.A. and Burton, D.R. (2004) The long third complementarity-determining region of the heavy chain is important in the activity of the broadly neutralizing anti-human immunodeficiency virus type 1 antibody 2F5. *J Virol* **78**, 3155-3161.

Zwick, M.B., Labrijn, A.F., Wang, M., Spencehauer, C., Saphire, E.O., Binley, J.M., Moore, J.P., Stiegler, G., Katinger, H., Burton, D.R. and Parren, P.W. (2001) Broadly neutralizing antibodies targeted to the membrane-proximal external region of human immunodeficiency virus type 1 glycoprotein gp41. *J Virol* **75**, 10892-10905.

6 Figure and Table references

Figure 1.: adapted from <http://www.avert.org/hiv-types.htm>

Figure 2.: from US National Institute of Health:
<http://www.niaid.nih.gov/factsheets/howhiv.htm>

Figure 3.: from AIDS 2009, Frank Lee, web book Creative Commons: <http://www.web-books.com/eLibrary/DN/B0/B22/05MHIV.html>

Figure 4.: adapted from: Montero, M., van Houten, N.E., Wang, X. and Scott, J.K. (2008)
The membrane-proximal external region of the human immunodeficiency virus type 1 envelope: dominant site of antibody neutralization and target for vaccine design. *Microbiol Mol Biol Rev* 72, 54-84

Figure 5.: Burton, D.R., Weiss, R.A. (2010) A boost for HIV vaccine design. *Science* 329, 770-773

Figure 6.: Shoenfeld, Y. (1995) Idiotypic network, pathogenic autoantibodies and autoimmunity. *Clin Exp Immunol* 101 Suppl 1, 26-28.

7 Selected publications

Mader, A., Kunert, R., (2010) Humanization strategies for an anti-idiotypic antibody mimicking HIV-1 gp41. *Protein Eng Des Sel* 23, 947-954.

de Ruiter, A., **Mader, A.**, Kunert, R. and Oostenbrink, C. (2011) Molecular Simulations to Rationalize Humanized Ab2/3H6 Activity. *Australian Journal of Chemistry* 64, 900-909.

Mader, A., Kunert R. Evaluation of the potency of the anti-idiotypic antibody Ab2/3H6 mimicking gp41 as a HIV-1 vaccine in a rabbit prime/boost study (Accepted with Revisions at PLOS One August 2011)

Humanization strategies for an anti-idiotypic antibody mimicking HIV-1 gp41

A. Mader and R. Kunert¹

Department of Biotechnology, Institute for Applied Microbiology, BOKU—
University of Natural Resources and Applied Life Sciences, Muthgasse 11,
A-1190 Vienna, Austria

¹To whom correspondence should be addressed.
E-mail: rene.kunert@boku.ac.at

Received June 21, 2010; revised September 3, 2010;
accepted September 30, 2010

Edited by Anthony Rees

Anti-idiotypic antibodies could represent an alternative vaccination approach in human therapy. The anti-idiotypic antibody Ab2/3H6 was generated in mouse and is directed against the human monoclonal antibody 2F5, which broadly and potently neutralizes primary HIV-1 isolates. Ab2/3H6 is able to mimic the antigen recognition site of 2F5 making it a putative candidate for HIV-1 vaccine purposes. In order to reduce immunogenicity of therapeutic proteins, humanization methods have been developed. The mouse variable regions of Ab2/3H6 were subjected to three different humanization approaches, namely resurfacing, complementarity determining region (CDR)-grafting and superhumanization. Four different humanized Ab2/3H6 variants were characterized for their binding affinity to 2F5 in comparison to the chimeric Ab2/3H6. The resurfaced and the ‘conservative’ CDR-grafted variants showed similar binding properties to 2F5 when compared to the chimeric version, while the ‘aggressive’ CDR-grafted antibody showed reduced affinity and the superhumanized type lost its binding ability. In this study, we developed humanized Ab2/3H6 variants that retained the same affinity as the parental antibody, and are therefore of potential interest for future clinical trials.

Keywords: 2F5/anti-idiotyp/HIV-1/humanization/vaccine

Introduction

More than 30 years ago, Niels K. Jerne postulated ‘The Network Theory of the Immune System’, in which he presented the observation that antibodies (Abs) can elicit anti-idiotypic Abs (Ab2) directed against the paratope of the first Ab (Jerne, 1974). These Ab2 are expected to mimic the initial antigen (Jerne *et al.*, 1982; Fields *et al.*, 1995). After contact with the immune system, Ab2 induce anti-anti-idiotypic Abs (Ab3) (Shoenfeld, 1995) similar in the capability to the first Ab. Therefore, Ab2 are potent as vaccines, which has been shown in recent clinical trials (Hurvitz and Timmerman, 2005; Park *et al.*, 2005; Inogès *et al.*, 2006).

For most infectious diseases including smallpox, diphtheria, tetanus, hepatitis A, hepatitis B, influenza and

others (Amanna *et al.*, 2008; Plotkin, 2008), conventional vaccines are able to induce a humoral immune response. This, however, has not been achieved for AIDS. During 30 years of research, attempts to develop a vaccine eliciting broadly neutralizing HIV-1 Abs have only been of limited success (Burton *et al.*, 2004; Flynn *et al.*, 2005; Haynes and Montefiori, 2006; Rerks-Ngarm *et al.*, 2009).

One of the most potent Ab identified so far is the monoclonal Ab (mAb) 2F5 (Trkola *et al.*, 1995), which binds with high affinity to a conserved site of the membrane-proximal external region (MPER) of the virus envelope glycoprotein gp41 (Stoiber *et al.*, 1997). It has been shown that mAb 2F5 broadly and potently neutralizes primary HIV-1 isolates (Purtscher *et al.*, 1994). The mouse-derived Ab2/3H6 (ABP04229, ABP04230) was developed at the Department of Biotechnology (Kunert *et al.*, 2002) and is directed against mAb 2F5. The chimeric version of Ab2/3H6 (chAb2/3H6) significantly inhibits the binding of mAb 2F5 to its synthetic epitope ELDKWA in an equimolar ratio and also decreases the *in vitro* neutralization potency of mAb 2F5 in a dose-related manner (Gach *et al.*, 2007). Ab2/3H6 is therefore expected to mimic the epitope of mAb 2F5 and is of great therapeutic interest as an anti-idiotypic vaccine against HIV.

However, since Ab2/3H6 originates from mouse, a human anti-mouse immune response (HAMA) (Sgro, 1995) or, in case of the chimeric version, a human anti-chimeric response (HACA) (Hwang and Foote, 2005) might be triggered when Ab2/3H6 is applied in human therapy; an effect that is required to be circumvented. Induced Ab3 should theoretically be directed against the paratope of the Ab2 which in case of Ab2/3H6 is composed of the complementarity determining regions (CDRs). In contrast, Ab3 immune responses against the framework regions (FR) do not contribute to the anticipated effect and should be prevented. Therefore, the aim of humanization approaches is to reduce immunogenicity of FR regions and thus drive the Ab3 immune response towards the paratope of the Ab2, which is structurally similar to the mAb 2F5 HIV-1 epitope. In the past 25 years, several humanization methods have been developed and applied to various murine Abs before entering clinical trails (reviewed in Almagro and Fransson, 2008). In the present study, we applied three different humanization approaches to the mouse-derived Ab2/3H6 (muAb2/3H6) and analysed the newly generated proteins in comparison to the chAb2/3H6. The results of our studies are discussed according to the existing literature.

Materials and methods

Humanization of Ab2/3H6

Resurfacing. The idea of resurfacing is that the immunogenicity of a protein is determined by the surface accessibility of amino acids (aa) and protruding residues (Novotný *et al.*,

1986). Therefore, a molecular model of muAb2/3H6 was generated by web-based Ab modelling software WAM (<http://antibody.bath.ac.uk/index.html>) (Whitelegg and Rees, 2000). This program predicts the side chains of the loops using 'CONGEN iterative algorithm' (Bruccoleri and Karplus, 1987). The CDR-H3 of Ab2/3H6 is relatively long with 13 aa. Therefore, we identified the structure of the loop with 'VFF side-chain energy screen' (Dauber-Osguthorpe *et al.*, 1988). The generated model of the murine Ab was used to identify surface accessible residues (Staelens *et al.*, 2006) with a threshold that was set to 30% (Pedersen *et al.*, 1994) using the Swiss Pdb Viewer Software (Guex and Peitsch, 1997). In a second step, the sequence of the muAb2/3H6 variable heavy (V_H) and light (V_L) chain was searched using IGBLAST against the human IgG germline database (NCBI; <http://www.ncbi.nlm.nih.gov/igblast/>). The stated surface residues were exchanged manually to those found on the selected human germline sequence and then subjected to energy minimization [GROMOS 43B1 force field; (van Gunsteren *et al.*, 1996)] using the software Swiss PDB Viewer program.

The resulting models were viewed and analysed with SwissPdb Viewer and PyMOL (<http://pymol.sourceforge.net/>). Based on this information, we superimposed the models of muAb2/3H6 and RS3H6 to determine changes in the loop structure.

CDR graft. During CDR grafting, the CDRs of the murine Ab are transferred to a human FR (Jones *et al.*, 1986). For CDR grafting, the fixed FR approach was chosen in which the closest related existing human Ab structure is used as acceptor FR. Therefore, the muAb2/3H6 V_H and V_L chain was searched against the UniProt database (www.uniprot.org). This procedure might lead to a reduction or complete loss of binding affinity because certain FR residues contribute significantly to the conformation of the CDRs (Chothia *et al.*, 1989; Foote and Winter, 1992) or are even directly involved in antigen binding (Mian *et al.*, 1991). This problem is solved by reintroducing the murine amino acids into the human FR at positions that are critical for CDR loop conformation (Riechmann *et al.*, 1988; Queen *et al.*, 1989; Co *et al.*, 1991; Foote and Winter, 1992). With this method, we generated two different CDR-graft variants, one 'conservative' graft (GC3H6) with various backmutations according to the mouse FR and one 'aggressive' graft (GA3H6) with less backmutations.

Superhumanization. The superhumanization approach is based on structural homologies between mouse and human CDRs. It is based on the axiom that if a mouse and human Ab have similar-structured CDRs, the human FR will also support the mouse CDRs, with retention of affinity. FR homology is not a factor and critical FR residues are not carried over from the mouse into the humanized Ab (Tan *et al.*, 2002; Hwang *et al.*, 2005). The comparison of CDRs which are structurally clustered into canonical structure classes was defined by Chothia and Lesk (1987). An automated determination of the Chothia canonical structure class from immunoglobulin sequences has been provided by Dr Andrew C.R. Martin's laboratory and is available online at <http://www.bioinf.org.uk/abs/chothia.html>.

In the next step, a human germline sequence with the same canonical structure class as the mouse Ab with the best

residue to residue match in the CDRs is defined as acceptor FR. Afterwards, mouse CDRs are grafted onto the chosen acceptor FR to create the superhumanized variant SH3H6.

Antibody expression

The genes of the V_H and V_L of the humanized Ab2/3H6 variants RS3H6, GC3H6, GA3H6 and SH3H6 were synthesized by Genart (Regensburg, Germany).

The synthetic V_H genes were inserted into the plasmid vector phuIgG1 containing a human IgG1 HC leader/constant region under the control of the SV40 promoter and a dihydrofolate reductase (dhfr) cassette. In parallel, the synthetic V_L genes were inserted into the plasmid vector phuCkappa containing a human kappa LC leader/constant region under the control of the CMV and a neomycin selection cassette. Similarly, the chAb2/3H6 was recombinantly expressed and used as reference material in all analyses (Gach *et al.*, 2007).

Stable cell lines were generated by cotransfection of corresponding HC and LC plasmids into CHO dhfr negative cells [ATCC CRL-9096; (Urlaub and Chasin, 1980)]. Clones were selected with Geneticin G418 (Fisher Scientific) and methotrexate (MTX) (Sigma) in combination with limiting dilution subcloning. Collected supernatants were concentrated by Stirred cell 8200 with UF Discs Ultracel RC 10 kD (Millipore) before purification.

Purification via affinity chromatography

Purification of all Ab2/3H6IgG1 variants was performed on a BioLogic Duo Flow chromatography system (Biorad). Ten millilitre concentrated animal cell culture supernatant was filtered through a 0.22 μ m syringe filter (Millipore) and diluted 1:2 in buffer A (100 mM Glycin, 100 mM NaCl, pH 7.0). The UNOsphere SUPra Mini cartridge column (Biorad) was equilibrated with 5 column volumes (cv) buffer A. Twenty millilitre of the concentrated sample were loaded onto the column using direct injection via the DuoFlow F40 pump at a flow rate of 1 ml/min corresponding to a linear velocity of 243.6 cm/h. The column was washed with buffer A until the optical density returned to base line. IgGs were eluted from the Protein A column using a three-step gradient of 40, 60 and 100% of buffer B (100 mM Glycin pH 3.5) in buffer A in 5 cv at a flow rate of 1.5 ml/min (364.4 cm/h). Quantification of Ab2/3H6IgG1 was done by quantitative double sandwich ELISA.

Antibody affinity

Bio-Layer Interferometry (BLI), a label-free technology, was used for measuring the interactions of Ab2/3H6IgG1 with mAb 2F5. Affinity measurements were performed with an Octet QK equipped with streptavidin (SA) biosensor tips (fortéBio, Menlo Park, CA, USA). The assay was performed at 30°C in 1× Kinetics assay buffer (fortéBio). Samples were agitated at 1000 rpm. Prior to analysis, SA sensors were humidified for 15 min. Tips were loaded with 1 μ g/ml of biotinylated mAb 2F5 (mAb2F5-B) for 80 s which typically resulted in capture levels of 0.7 to 0.8 nm within a row of eight tips. Ab2/3H6IgG1 variants were prepared in a 500 nM concentration. Association was monitored for 60 s. Data were processed and analysed using the Octet data analysis software 6.3 (fortéBio).

Competition ELISA

Apparent affinity constants (aK) of Ab2/3H6IgG1 variants were calculated by 505 residual binding of mAb2F5-B in a competition ELISA (Kunert *et al.*, 2000). Briefly, the synthetic peptide GGGELDKWASL was coated onto MaxiSorp 96-well plates (Nunc). Culture supernatant of the Ab2/3H6IgG1 variants was serially diluted and mixed with a constant amount of mAb2F5-B (50 ng/ml). The mixture and the serially diluted standard (mAb2F5-B; 100 ng/ml) were incubated for 1 h and afterwards transferred onto the pre-coated plates. Unbound mAb2F5-B was detected with horseradish-peroxidase labelled SA conjugate (Roche).

Results

Humanization of 3H6

Resurfacing. The human germline V_H sequence IGHV1-3*01 (64.9% identity to muAb2/3H6 V_H) and V_L kappa sequence IGKV5-2*01 (63.2% identity to muAb2/3H6 V_L) were defined as corresponding human germlines.

The model of the muAb2/3H6 was used to identify surface accessible residues. Single aa were substituted manually with human germline residues. The side chains were rotated manually to evaluate stable side-chain conformation and then subjected to energy minimization using the Swiss PDB Viewer program. Sixteen aa in the V_H of muAb2/3H6 were identified as surface accessible residues. Only three of them differed from the human germline sequence and were adapted to the human version (Gln^{H5}Val, Thr^{H14}Pro and His^{H41}Pro). Additionally, the missing residue Gln^{H1} was inserted and the buried Ser^{H40} was changed to the corresponding human Ala since the model revealed that Ser^{H40} might clash with Pro^{H41}. In case of muAb2/3H6 V_L , 7 out of 16 surface accessible aa differed from the human germline and were substituted to their corresponding aa (Ser^{L10}Phe, Leu^{L11}Met, Ile^{L15}Pro, Glu^{L17}Asp, Arg^{L45}Ile, Ser^{L60}Pro and Gly^{L100}Gln). The molecular model showed a possible clash between the introduced Asp^{L17} and the Ser^{L14} therefore, the buried Ser^{L14} was changed to Thr. Further, the model revealed that additional H-bonds were formed between the buried Met^{L13} and Glu^{L105} as well as Lys^{L107}. Thus Met^{L13} was changed to Ala.

Afterwards, the models of the mouse variable region and the resurfaced Ab2/3H6, named RS3H6, were superimposed to determine conformational changes in the loop regions. As depicted in Fig. 1, the RS3H6 CDRs coloured in red showed only minor differences in the loop structures in comparison to the muAb2/3H6 CDRs coloured in green. Additionally, we analysed the root-mean-square deviation (RMSD), which can be used as a measure for the similarity in three-dimensional structures (Maiorov and Crippen, 1994). High RMSD values mean dissimilar and zero means identical in conformation. RMSD cut-off values have been published for different applications proposing RMSD value <1.5 Å is suitable for defining antibody epitopes (Baker and Sali, 2001). The RMSD values of the CDR loop structures model of RS3H6 in comparison to Ab2/3H6 ranged from 0.50 to 1.34 Å indicating a similar conformation. The only difference between RS3H6 and muAb2/3H6 was observed in the loop of CDR-H2. Figure 1 shows conformational changes at position Y^{H53} resulting in an RMSD value of 2.213 Å. The

Y at position 53 in the RS3H6 variant has a different side-chain conformation in comparison to the muAb2/3H6 resulting in the higher RMSD value. The model of the CDR-H2 showed that different angles of the Y^{H53} side chain can be present in the loop. The formation seen in RS3H6 CDR-H2 has a slightly better energy minimum in comparison to the conformation seen in muAb2/3H6 CDR-H2 (data not shown). Due to this minor energy differences and the fact that surface exposed side chains are flexible in solution, we suppose that Y^{H53} will exist in both conformations and might not influence the correct CDR-H2 conformation.

CDR graft. The human Ab EU V_H (P01742.1) and V_L (P01598.1) sequences were defined as acceptor FR. The sequence of muAb2/3H6 V_H showed 53% identity to human Ab EU V_H and muAb2/3H6 V_L has 47% identity to EU V_L . We identified 36 aa in the FR of muAb2/3H6 V_H and 34 in the FR of muAb2/3H6 V_L that differed from the acceptor FR sequence. The alignment of muAb2/3H6 V_H and V_L sequences with their corresponding EU sequence is shown in Fig. 2.

In order to obtain a functional CDR-grafted Ab2/3H6 Ab, a so-called 'conservative' graft (GC3H6) harbouring back-mutations at all identified positions that might influence the CDR conformation was developed. In GC3H6, 22 aa in the V_H and 13 aa in the V_L FR were identified for backmutation (highlighted in grey in Fig. 2) and mutated in the human acceptor FR to their murine counterpart (Table I). As summarized in Table I the reasons for switching single aa are (i) influences on the structure of the antibody, (ii) contribution to the canonical structure class, (iii) regions of venier-zones, (iv) contribution of aa to the V_H/V_L interface or (v) lack of single positions in the EU antibody. In order to reduce the amount of backmutations, making the grafted Ab more humanlike, a so-called 'aggressive' graft (GA3H6) harbouring only backmutations at probable critical positions like venier-zones or regions contributing to the canonical structure classes was designed. This variant has only 10 backmutations in the V_H and 5 backmutations in the V_L (Table I).

Superhumanization. Canonical structure classes of muAb2/3H6 were identified as class 1-2 for V_H and class 2-1-1 for V_L (Table II) according to <http://www.bioinf.org.uk/abs/chothia.html>. Human germline V_H/J_H and V_k/J_k gene sequences were extracted from the V-Base database (<http://vbase.mrc-cpe.cam.ac.uk/>). Table II describes the structure classes of the muAb2/3H6 and the nearest related human germline V_H and V_L gene sequences. The human germline V_H sequence with the highest sequence identity in the CDRs representing the canonical structure class 1-2 is IGHV1-f*01 with 80% identity in CDR-H1, and 31% in CDR-H2. The J_H segment contributes a variable number of residues of CDR-H3. Therefore, J_H4 which has YFDY at position 100d-102 was chosen as the best match. The human germline V_k sequence with the highest sequence identity in the CDRs representing the canonical structure class 2-1-1 is IGKV5-2*01 with 64% identity in CDR-L1 and 43% in CDR-L2. The J_k segment encodes two residues of CDR-L3. J_k2 has YT at position 96–97 and was chosen as the best match. Afterwards, the muAb2/3H6 CDRs were grafted onto the above-defined human acceptor FR.

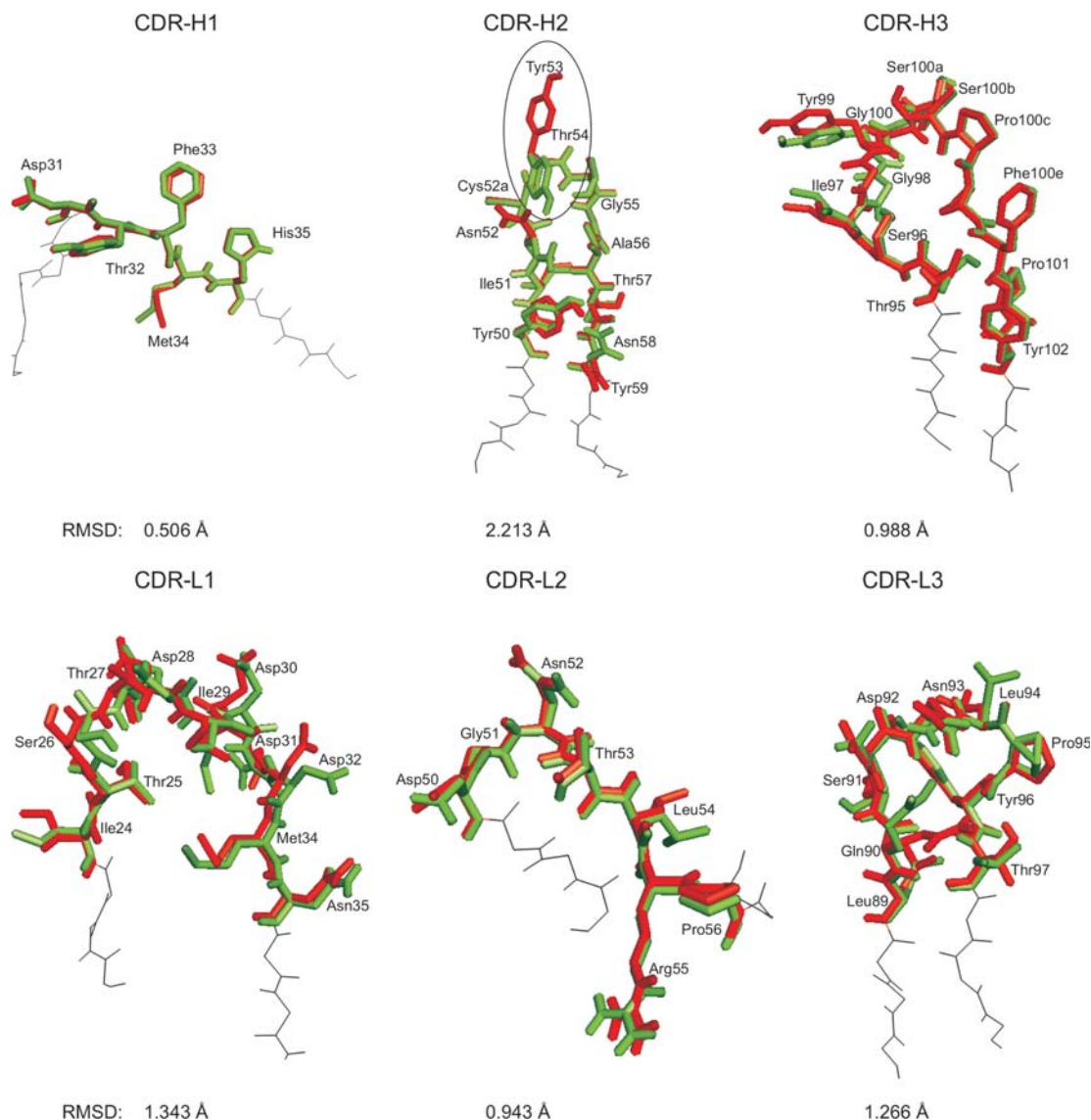


Fig. 1. Structure homology models of resurfaced Ab2/3H6 CDRs (red) versus mouse Ab2/3H6 CDRs (green).

The resulting Ab SH3H6 is composed of human germline FR regions and the original mouse CDRs, respectively. No murine FR residues were carried over to the humanized construct. Figure 3 shows sequence identities in the CDR regions between muAb2/3H6 and the nearest related human germline sequence, which was selected by identities with the same canonical structures to demonstrate similarity.

Binding properties of 3H6 humanization variants

The purified IgGs of all Ab2/3H6 variants were tested for their binding capacity with the Octet QK and in a competition ELISA. The binding of the Ab2/3H6IgG1 variants to mAb2F5 was determined in an affinity binding study using BLI. The binding curves (Fig. 4a) of RS3H6 and GC3H6 show a similar interaction with mAb2F5 as chAb2/3H6. The lower signal of GA3H6 indicates a lower affinity to its antigen, whereas SH3H6 shows no interaction. The binding rate (k_{obs}) calculated by the fortÉBio Octet QK software package is summarized in Fig. 4b. RS3H6, GC3H6 and chAb2/3H6 showed similar k_{obs} values ranging from 6.2×10^{-2} to $7.5 \times 10^{-2} \text{ s}^{-1}$ indicating the same affinity to

mAb2F5, whereas GA3H6 ($3.8 \times 10^{-2} \text{ s}^{-1}$) has a two-fold reduced affinity and SH3H6 does not bind to mAb2F5.

Further we compared the four humanized Ab2/3H6 variants and the chAb2/3H6 in a competition ELISA (Fig. 5). The optical density resulting from binding of mAb2F5 to its peptide epitope GGGELDKWASL is plotted versus the logarithm of the concentration of Ab2/3H6 preparations in the liquid phase. RS3H6 and GC3H6 showed a nearly identical behaviour of concentration-dependent mAb2F5 inhibition. Binding capacity of mAb2F5 to its peptide epitope (GGGELDKWASL) was reduced by 50% after incubation of mAb2F5 with a 5-fold excess of RS3H6, GC3H6 or chAb2/3H6. Besides, GA3H6 inhibited 50% mAb2F5 only with a 17-fold excess. In contrast, SH3H6 did not inhibit mAb2F5 binding to the solid phase even in an 80-fold excess. Table III summarizes the aK values calculated as the reciprocal value of the Ab2/3H6 concentration required to inhibit 50% of the maximal binding in a competitive ELISA. RS3H6 and GC3H6 showed similar aK values ($2.0 \times 10^9 \text{ M}^{-1}$) as the ch3H6 ($2.5 \times 10^9 \text{ M}^{-1}$), whereas GA3H6 had a reduced affinity ($7.1 \times 10^8 \text{ M}^{-1}$) compared to the

(a)

Kabat numbering	FR1			CDR1	FR2			CDR2																						
	1	10	20	30	40	50	52	a	60																					
EU	Q	V	Q	L	V	Q	S	G	E	V	K	K	P	G	S	S	V	K	M	S	C	K	A	S	G	E	F	S		
Mu3H6	-	V	Q	L	Q	Q	S	G	P	E	L	V	K	T	G	A	S	V	K	I	S	C	K	A	S	G	Y	S	F	T

Kabat numbering	FR3			CDR3	FR4																																																			
	70	80	82 abc	90	100 abcde	110																																																		
EU	G	R	T	T	T	A	D	E	S	T	N	T	A	Y	M	E	S	S	L	R	S	E	D	A	F	Y	C	A	G	-	-	-	G	Y	G	I	Y	S	P	E	E	Y	H	G	G	E	L	V	T	V	S					
Mu3H6	G	K	A	T	F	T	V	D	T	S	S	N	T	A	Y	M	Q	F	N	S	L	T	S	E	D	S	A	V	Y	Y	C	A	R	T	S	I	G	Y	G	S	S	P	P	P	P	Y	W	G	Q	G	T	L	V	T	V	S

(b)

Kabat numbering	FR1			CDR1	FR2			CDR2																																																
	1	10	20	30	40	50																																																		
EU	D	E	Q	M	T	Q	S	P	S	H	L	S	A	S	V	G	D	R	V	T	I	T	C	R	A	S	Q	S	I	N	T	W	L	A	W	Y	Q	Q	K	P	G	K	A	P	K	L	L	M	Y	K	A	S	S	L	E	S
Mu3H6	E	T	T	V	T	Q	S	P	A	S	L	S	M	S	I	G	E	K	V	T	I	R	C	I	T	S	T	D	I	D	D	D	M	N	W	Y	Q	Q	K	P	G	E	P	P	R	L	L	I	S	D	G	N	T	L	R	P

Kabat numbering	FR3			CDR3	FR4																																													
	60	70	80	90	100																																													
EU	G	V	P	S	R	F	I	S	G	E	G	T	E	F	T	T	I	S	S	L	Q	P	D	D	F	A	Y	Y	C	Q	Q	Y	N	S	D	S	K	M	F	G	Q	G	T	V	E	V	E	K		
Mu3H6	G	V	P	S	R	F	S	S	G	Y	G	T	D	F	V	F	T	I	E	N	M	L	S	E	D	V	A	D	Y	Y	C	L	Q	S	D	N	L	P	Y	T	F	G	G	G	T	N	L	E	I	K

Fig. 2. Alignment of heavy chain variable region (a) and light chain variable region (b) of human antibody EU and mouse antibody Ab2/3H6 for CDR grafting. Amino acids in the EU framework that were chosen for backmutations are highlighted in grey.

Table I. Framework backmutations in the CDR-grafted variants (GC3H6 and GA3H6)

Kabat numbering	Acceptor FR EU	Backmutation	
		GC3H6	GA3H6
H9 ^a	A	P	-
H20 ^a	V	I	-
H27 ^{b,c}	G	Y	Y
H28 ^c	T	S	-
H30 ^c	S	T	T
H38 ^d	R	K	-
H43 ^a	Q	K	-
H44 ^d	G	S	-
H46 ^{c,d}	E	D	-
H48 ^c	M	G	G
H67 ^c	V	A	-
H69 ^c	I	F	V
H71 ^{b,c}	A	V	V
H73 ^c	E	T	T
H82 ^a	L	F	-
H87 ^a	T	S	-
H91 ^d	F	Y	-
H94 ^{b,c}	G	R	R
H103 ^{c,d}	N	W	W
H105 ^a	G	Q	Q
H106 ^c	-	G	G
H107 ^c	-	T	T
L1 ^c	D	E	-
L2 ^{b,c}	I	T	T
L3 ^c	Q	T	-
L4 ^c	M	V	V
L10 ^a	T	S	-
L43 ^d	A	P	-
L45 ^d	K	R	-
L48 ^{b,c}	M	I	I
L64 ^{b,c}	G	S	S
L67 ^c	S	Y	-
L73 ^a	L	F	-
L85 ^a	T	D	D
L103 ^a	K	N	-

^aResidues that might have an influence on the protein structure.

^bResidues in close proximity or contributing to canonical structure class.

^cResidues in close contact or contributing to vernier zone.

^dResidues buried at the V_H/V_L interface.

^eResidues missing in the EU antibody.

Table II. Canonical structure class of mouse Ab2/3H6 and human germline variable heavy (IGHV1-f*01) and light chain (IGKV5-2*01)

CDR	Canonical structure class		
	mu3H6 V _H	IGHV1-f*01	Chothia definition
H1	1	1	H ²⁴ = A,V,G; H ²⁶ = G; H ²⁷ = F,Y; H ²⁹ = F; H ³⁴ = M,W,I; H ⁹⁴ = R,K H ⁵² = P,T,A; H ⁵⁵ = G,S; H ⁷¹ = A,T,L
H2	Similar 2 (H ⁵² = N; H ⁷¹ = V)	2	
L1	mu3H6 V _L Similar 2 (L ² = T; L ²⁵ = T; L ³³ = M)	IGKV5-2*01 Similar 2 (L ² = T; L ³³ = M)	L ² = I; L ²⁵ = A; L ²⁹ = V,I; L ³³ = L; L ⁷¹ = FY
L2	Similar 1 (L ⁶⁴ = S)	1	L ⁴⁸ = I; L ⁵¹ = A,T; L ⁵² = S,T; L ⁶⁴ = G
L3	1	1	L ⁹⁰ = Q,N,H; L ⁹⁵ = P

original Ab and SH3H6 lost the ability to inhibit mAb2F5 binding to its epitope. An equimolar amount of the negative control (unspecific human IgG) did not show interaction with mAb2F5.

Taken together, the results of the BLI and the competition ELISA assay show that RS3H6 and GC3H6 retained the same binding affinity and neutralizing potency as chAb2/3H6, while GA3H6 had a minor loss in its affinity and SH3H6 completely lost its binding ability to mAb2F5.

Discussion

In the past 20 years, rational and empirical humanization methods have been developed (reviewed in Almagro and Fransson, 2008), but there is still no generally applicable method available which can be used to eliminate potential immunogenic sites while keeping the specificity of the Ab. Each Ab has to be analysed separately and different methods have to be tested in each particular case to obtain a

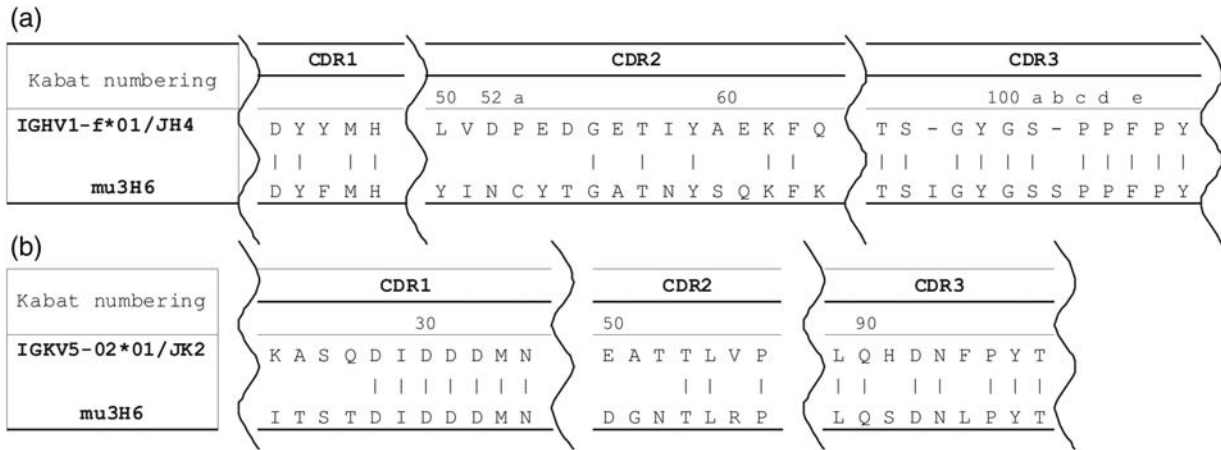


Fig. 3. Alignment of amino acid sequences of the heavy chain CDRs (a) and light chain CDRs (b) of human germline sequences IGHV1-f*01/JH4, IGKV5-02*01/JK2 and mouse antibody Ab2/3H6.

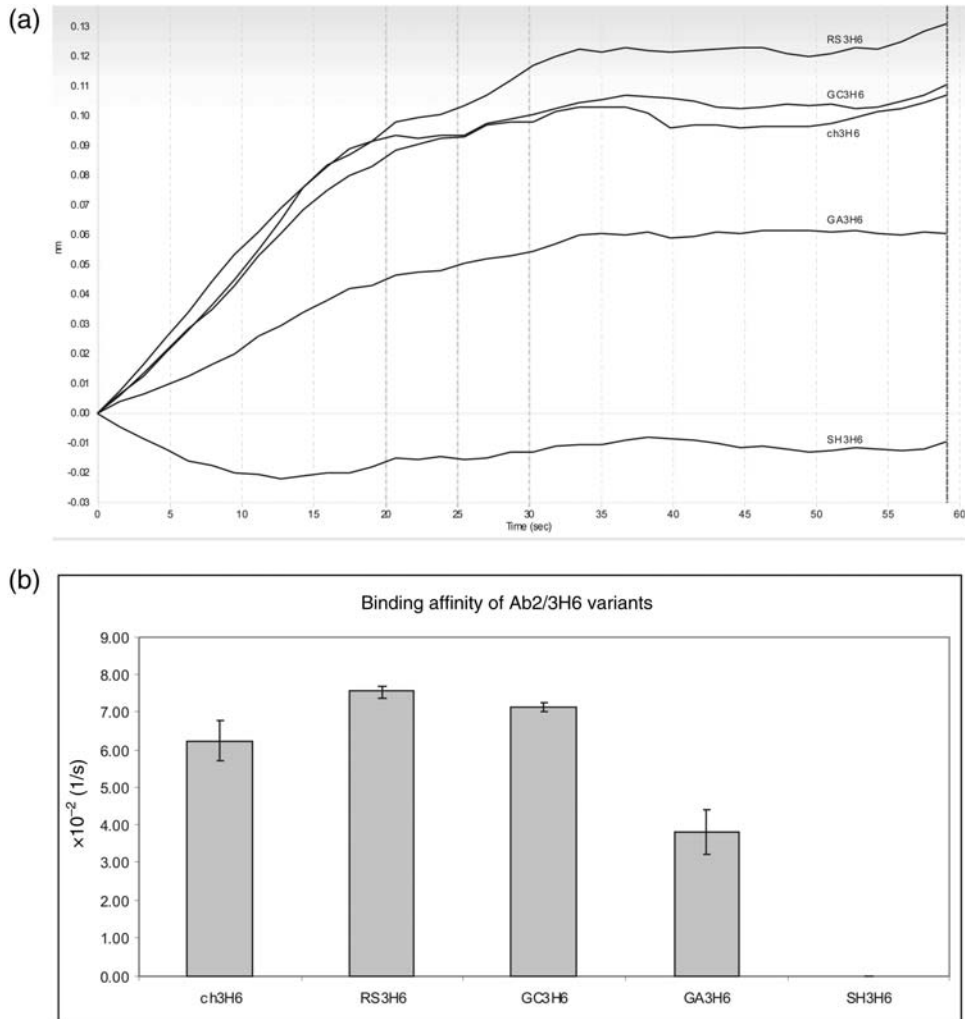


Fig. 4. Binding curves of Ab2/3H6IgG1 variants to mAb 2F5 (a) and comparison of the binding rate (k_{obs}) of the Ab2/3H6IgG1 variants (b).

humanized variant that features the same affinity and biological activity as the parental Ab.

Variable domain resurfacing emerged as an alternative to CDR grafting. The basic idea of this method is that only surface residues in the non-human Ab are able to induce HAMA and therefore only these few murine surface aa are

changed to human residues (Pedersen *et al.*, 1994; Roguska *et al.*, 1994). The resurfacing method is quite promising in terms of retaining antigen affinity because no changes are introduced to the protein core. Since resurfacing only changes the residues at the surface of the molecule, the expectation is to eliminate potential B-cell epitopes while

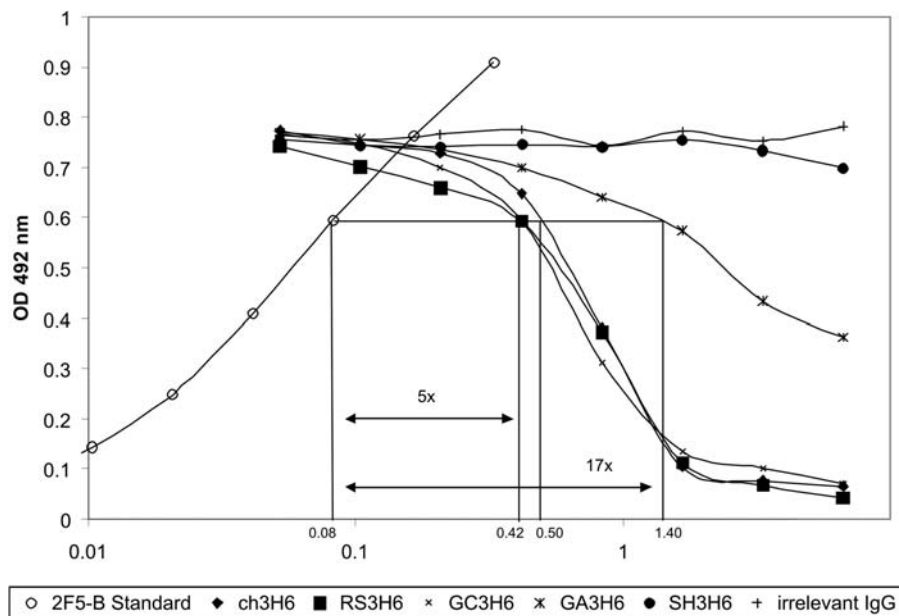


Fig. 5. Experimental determination of the apparent affinity constant (aK) of Ab2/3H6 variants.

Table III. aK values determined for different Ab2/3H6 preparations

3H6 variants	IC50 (nM)	aK (M^{-1})
ch3H6	0.5	2.5×10^9
RS3H6	0.4	2.0×10^9
GC3H6	0.4	2.0×10^9
GA3H6	1.4	7.1×10^8
SH3H6	No binding to 2F5	No binding to 2F5
Irrelevant IgG	No binding to 2F5	No binding to 2F5

IC50, 3H6 concentration required for 50% inhibition of maximal binding in competitive ELISA. aK = $1/IC_{50}$.

retaining the specificity resulting in an Ab that would show little or no immunogenicity when applied in human therapy. Unfortunately T-cell epitopes are not considered using this method. However, recent clinical evaluation of the resurfaced Ab conjugate huC242-DM1 (Cantuzumab mertansine) showed no anti-human globulin response in patients (Rodon *et al.*, 2008), proving that the resurfacing approach results in Abs with reduced immunogenicity when applied in human therapy.

The conventional method for humanization of a murine Ab is CDR grafting. This approach has been used for the majority of humanized Abs approved by the Food and drug Administration (FDA) including Herceptin[®] (trastuzumab) (Carter *et al.*, 1992), Campath[®] (alemtuzumab) (Riechmann *et al.*, 1988) or Xolair[®] (omalizumab) (Presta *et al.*, 1993). Commonly, affinity decreases after CDR grafting as a consequence of incompatibilities between non-human CDRs and human FRs. In order to circumvent this problem, backmutations have to be introduced to restore or prevent affinity losses. These backmutations have to be defined individually for each Ab and each aa positions even if Abs have a high sequence homology or similar antigen specificity (Rosok *et al.*, 1996). In some cases, backmutations at known critical positions are counterproductive (Caldas *et al.*, 2000; Gonzales *et al.*, 2003). Thus, introducing backmutations is

difficult and not always straight forward, which has been shown for the humanized Ab Xolair[®] (omalizumab) where 22 different variants were tested experimentally to determine the best version (Presta *et al.*, 1993) or Omnitarg[®] (pertuzumab) where 10 variants have been developed to obtain a humanized variant with the same affinity as the parental Ab (Adams *et al.*, 2006). More than 10 CDR grafted Abs for human therapies have been approved by the FDA to date. Clinical studies revealed that CDR grafted Abs have a reduced immunogenicity when applied in human therapy (Hwang and Foote, 2005).

Superhumanization is based on structural comparisons of CDRs in which a FR homology is irrelevant. Using this strategy, three Abs have already been successfully humanized in the past (Tan *et al.*, 2002; Hwang *et al.*, 2005; Hu *et al.*, 2007). This approach has the advantage over CDR grafting that only one version has to be created because it was postulated that the CDRs between Abs with the same canonical loop structure can be substituted without altering the conformation (Tan *et al.*, 2002). This leads to a humanized Ab with a complete human germline FR and therefore immunogenicity is expected to be minimal because the remaining murine residues lie inside the CDRs. Using this strategy, the murine anti-human CD28 Ab 9.3 was humanized resulting in a variant with a 30-fold loss in affinity but the biological activity was retained (Tan *et al.*, 2002). In an other case, the superhumanized form of the Ab D1.3 had a better affinity (6-fold loss in comparison to the murine variant) (Hwang *et al.*, 2005) than the CDR-grafted version (70-fold loss in affinity) (Foote and Winter, 1992).

To conclude on this study, the induction of neutralizing 2F5-like Abs is challenging and has not been achieved so far with conventional epitope vaccination approaches (Burton *et al.*, 2004). A possible reason might be that the mAb2F5 epitope is only weakly immunogenic. As part of the MPER, it is difficult to keep a stable and correct conformation when used as a conventional vaccine (Ofek *et al.*, 2004; Cardoso *et al.*, 2005). Therefore, an Ab2 vaccine approach would be a

promising alternative. In former studies, muAb2/3H6 was able to induce 2F5-like Abs in mice (Kunert *et al.*, 2002; Gach *et al.*, 2007). In order to use Ab2/3H6 in a clinical vaccination study, the reduction of its immunogenicity in the FRs is essential to reduce adverse effects.

We have applied three different state of the art humanization approaches to the muAb2/3H6. The humanized Ab2/3H6 variants RS3H6, GC3H6 showed the same affinity and GA3H6 had a 2-fold loss in affinity to mAb2F5 activity in comparison to chAb2/3H6. SH3H6 lost the ability to bind mAb2F5. This approach was not suitable for humanization of Ab2/3H6. We postulate that humanizing the FR of Ab2/3H6 will drive the immune response towards the paratope of the Ab2 and therefore enhance elicitation of Ab3 when administered during therapy. Affinity to mAb2F5 is therefore not the crucial factor in evaluating the best candidate for a clinical study. Our results show that the Ab2/3H6 variants RS3H6 and GA3H6 would be suitable candidates for further studies but due to regulatory reasons and the fact that the majority of humanized Abs approved by the FDA are CDR-grafted GA3H6 is the candidate of choice.

Acknowledgements

We thank Marion Tschernutter for critical discussion.

Funding

This work was supported by the Austrian Science Fund (FWF) [Project number: P20603-B13].

References

- Adams,C., Allison,D., Flagella,K., Presta,L., Clarke,J., Dybdal,N., McKeever,K. and Sliwkowski,M. (2006) *Cancer Immunol. Immunother.*, **55**, 717–727.
- Almagro,J. and Fransson,J. (2008) *Front. Biosci.*, **13**, 1619–1633.
- Amanna,I., Messaoudi,I. and Slifka,M. (2008) *Hum. Vaccin.*, **4**, 316–319.
- Baker,D. and Sali,A. (2001) *Science*, **294**, 93–96. doi: 10.1126/science.1065659.
- Bruccoleri,R. and Karplus,M. (1987) *Biopolymers*, **26**, 137–168.
- Burton,D., Desrosiers,R., Doms,R., *et al.* (2004) *Nat. Immunol.*, **5**, 233–236. doi: 10.1038/ni0304-233.
- Caldas,C., Coelho,V., Rigden,D., Neschich,G., Moro,A. and Brígido,M. (2000) *Protein Eng.*, **13**, 353–360.
- Cardoso,R., Zwick,M., Stanfield,R., Kunert,R., Binley,J., Katinger,H., Burton,D. and Wilson,I. (2005) *Immunity*, **22**, 163–173. doi: 10.1016/j.immuni.2004.12.011.
- Carter,P., Presta,L., Gorman,C., *et al.* (1992) *Proc. Natl Acad. Sci. USA*, **89**, 4285–4289.
- Chothia,C. and Lesk,A. (1987) *J. Mol. Biol.*, **196**, 901–917.
- Chothia,C., Lesk,A., Tramontano,A., *et al.* (1989) *Nature*, **342**, 877–883.
- Co,M., Deschamps,M., Whitley,R. and Queen,C. (1991) *Proc. Natl Acad. Sci. USA*, **88**, 2869–2873.
- Dauber-Osguthorpe,P., Roberts,V., Osguthorpe,D., Wolff,J., Genest,M. and Hagler,A. (1988) *Proteins*, **4**, 31–47.
- Fields,B., Goldbaum,F., Ysern,X., Poljak,R. and Mariuzza,R. (1995) *Nature*, **374**, 739–742. doi: 10.1038/374739a0.
- Flynn,N., Forthal,D., Harro,C., Judson,F., Mayer,K. and Para,M. and Group r.H.V.S. (2005) *J. Infect. Dis.*, **191**, 654–665. doi: 10.1086/428404.
- Foote,J. and Winter,G. (1992) *J. Mol. Biol.*, **224**, 487–499.
- Gach,J., Quendler,H., Weik,R., Katinger,H. and Kunert,R. (2007) *AIDS Res. Hum. Retroviruses*, **23**, 1405–1415.
- Gonzales,N., Padlan,E., De Pascalis,R., Schuck,P., Schlom,J. and Kashmiri,S. (2003) *Mol. Immunol.*, **40**, 337–349. doi: 10.1016/S0161589003001664.
- Guex,N. and Peitsch,M. (1997) *Electrophoresis*, **18**, 2714–2723.
- Haynes,B. and Montefiori,D. (2006) *Expert Rev. Vaccines*, **5**, 579–595. doi: 10.1586/14760584.5.4.579.
- Hu,W., Chau,D., Wu,J., Jager,S. and Nagata,L. (2007) *Vaccine*, **25**, 3210–3214.
- Hurvitz,S. and Timmerman,J. (2005) *Curr. Opin. Oncol.*, **17**, 432–440. doi: 10.1093/nci/djj358.
- Hwang,W. and Foote,J. (2005) *Methods*, **36**, 3–10. doi: 10.1016/j.jmeth.2005.01.001.
- Hwang,W., Almagro,J., Buss,T., Tan,P. and Foote,J. (2005) *Methods*, **36**, 35–42.
- Inogès,S., Rodríguez-Calvillo,M., Zabalegui,N., *et al.* (2006) *J. Natl Cancer Inst.*, **98**, 1292–1301. doi: 10.1093/jnci/djj358.
- Jerne,N. (1974) *Ann. Immunol. (Paris)*, **125C**, 373–389.
- Jerne,N., Roland,J. and Cazenave,P. (1982) *EMBO J.*, **1**, 243–247.
- Jones,P., Dear,P., Foote,J., Neuberger,M. and Winter,G. (1986) *Nature*, **321**, 522–525.
- Kunert,R., Steinfellner,W., Purtscher,M., Assadian,A. and Katinger,H. (2000) *Biotechnol. Bioeng.*, **67**, 97–103.
- Kunert,R., Weik,R., Ferko,B., Stiegler,G. and Katinger,H. (2002) *AIDS*, **16**, 667–668.
- Maiorov,V. and Crippen,G. (1994) *J. Mol. Biol.*, **235**, 625–634. doi: 10.1006/jmbi.1994.1017.
- Mian,I., Bradwell,A. and Olson,A. (1991) *J. Mol. Biol.*, **217**, 133–151.
- Novotný,J., Handschumacher,M., Haber,E., Bruccoleri,R., Carlson,W., Fanning,D., Smith,J. and Rose,G. (1986) *Proc. Natl Acad. Sci. USA*, **83**, 226–230.
- Ofek,G., Tang,M., Sambor,A., Katinger,H., Mascola,J., Wyatt,R. and Kwong,P. (2004) *J. Virol.*, **78**, 10724–10737. doi: 10.1128/JVI.78.19.10724-10737.2004.
- Park,I., Youn,J., Choi,I., Nahm,M., Kim,S. and Shin,J. (2005) *Infect. Immun.*, **73**, 6399–6406. doi: 10.1128/IAI.73.10.6399-6406.2005.
- Pedersen,J., Henry,A., Searle,S., Guild,B., Roguska,M. and Rees,A. (1994) *J. Mol. Biol.*, **235**, 959–973.
- Plotkin,S. (2008) *Clin. Infect. Dis.*, **47**, 401–409. doi: 10.1086/589862.
- Presta,L., Lahr,S., Shields,R., Porter,J., Gorman,C., Fendly,B. and Jardieu,P. (1993) *J. Immunol.*, **151**, 2623–2632.
- Purtscher,M., Trkola,A., Gruber,G., *et al.* (1994) *AIDS Res. Hum. Retroviruses*, **10**, 1651–1658.
- Queen,C., Schneider,W., Selick,H., *et al.* (1989) *Proc. Natl Acad. Sci. USA*, **86**, 10029–10033.
- Rerks-Ngarm,S., Pitisuttithum,P., Nitayaphan,S., *et al.* (2009) *N. Engl. J. Med.*, **361**, 2209–2220. doi: 10.1056/NEJMoa0908492.
- Riechmann,L., Clark,M., Waldmann,H. and Winter,G. (1988) *Nature*, **332**, 323–327.
- Rodon,J., Garrison,M., Hammond,L., *et al.* (2008) *Cancer Chemother. Pharmacol.*, **62**, 911–919. doi: 10.1007/s00280-007-0672-8.
- Roguska,M., Pedersen,J., Keddy,C., *et al.* (1994) *Proc. Natl Acad. Sci. USA*, **91**, 969–973.
- Rosok,M., Yelton,D., Harris,L., *et al.* (1996) *J. Biol. Chem.*, **271**, 22611–22618.
- Sgro,C. (1995) *Toxicology*, **105**, 23–29. doi: 0300483X9503123W.
- Shoenfeld,Y. (1995) *Clin. Exp. Immunol.*, **101**(Suppl. 1), 26–28.
- Staelens,S., Desmet,J., Ngo,T., *et al.* (2006) *Mol. Immunol.*, **43**, 1243–1257.
- Stoiber,H., Frank,I., Spruth,M., *et al.* (1997) *Mol. Immunol.*, **34**, 855–863.
- Tan,P., Mitchell,D., Buss,T., Holmes,M., Anasetti,C. and Foote,J. (2002) *J. Immunol.*, **169**, 1119–1125.
- Trkola,A., Pomaes,A., Yuan,H., *et al.* (1995) *J. Virol.*, **69**, 6609–6617.
- Urlaub,G. and Chasin,L. (1980) *Proc. Natl Acad. Sci. USA*, **77**, 4216–4220.
- van Gunsteren,W.F., Billeter,S.R., Eising,A.A., Huenenberger,P.H., Krueger,P., Mark,A.E., Scott,W.R.P. and Tiron,I.G. (1996) *Biomolecular Simulation: The GROMOS96 Manual and User Guide*, VdF: Hochschulverlag AG, Zuerich, Switzerland.
- Whitelegg,N. and Rees,A. (2000) *Protein Eng.*, **13**, 819–824.

Molecular Simulations to Rationalize Humanized Ab2/3H6 Activity

Anita de Ruiter,^A Alexander Mader,^B Renate Kunert,^B
and Chris Oostenbrink^{A,C}

^AInstitute for Molecular Modeling and Simulation, BOKU–University of Natural Resources and Life Sciences, Muthgasse 18, 1190, Vienna, Austria.

^BDepartment of Biotechnology, Institute for Applied Microbiology, BOKU–University of Natural Resources and Life Sciences, Muthgasse 11, 1190 Vienna, Austria.

^CCorresponding author. Email: chris.oostenbrink@boku.ac.at

The murine anti-idiotypic antibody 3H6 (Ab2/3H6) is directed against the human 2F5 antibody, which is capable of neutralizing HIV-1. Recently, four humanized Ab2/3H6 models have been developed in order to reduce the risk of human anti-mouse antibody (HAMA) responses in case of administration to humans. In this study, molecular dynamics simulations were performed on these models as well as on the murine Ab2/3H6 in solution and bound to 2F5, in order to rationalize the differences in binding affinities of the models towards 2F5. Analysis of these simulations suggested that the orientation and dynamics of the residues TYR54 and TYR103 of the heavy chain of Ab2/3H6 play an important role in these differences. Subsequently, the contribution of these residues to the binding affinity was quantified by applying free energy calculations.

Manuscript received: 20 December 2010.

Manuscript accepted: 17 February 2011.

Introduction

Since the discovery of the human immunodeficiency virus type 1 (HIV-1) almost 30 years ago, extensive research has been performed in order to elicit broadly neutralizing antibodies. The glycoproteins gp120 and gp41 are the main immunogens of HIV-1, as they are part of the envelope and involved in the fusion of the viral membrane with the host cell plasma membrane.^[1,2] However, as these glycoproteins are so crucial to the virus, many protective mechanisms have evolved which reduce the immunogenicity.^[3,4] First of all, the glycoproteins contain only a few conserved regions. These regions might be exposed on the monomeric subunits, but are often buried in the interior of the envelope glycoprotein spike.^[5,6] Furthermore, a large part of gp120 is covered with carbohydrates, which are (for different reasons) less immunogenic compared with protein structures, again preventing gp120 from being recognized by antibodies.^[7,8] Despite these protective mechanisms, years of research has led to the identification of a few broadly neutralizing antibodies directed against HIV-1.^[7,9–14] One of them is the human monoclonal antibody (mAb) 2F5,^[15,16] which recognizes the membrane-proximal external region (MPER) on the gp41 envelope protein.^[17] The MPER is a highly conserved region that is important for the conformational change of gp41 required for membrane fusion.^[18,19] However, as this epitope on gp41 is only poorly immunogenic, the possibility of using an anti-idiotypic antibody (Ab2)^[20] to activate 2F5 was investigated. In 2002, a murine anti-idiotypic antibody, 3H6 (Ab2/3H6), was generated in order to mimic the gp41 epitope and thereby elicit 2F5 or 2F5-like production.^[21] Ab2/3H6 is

therefore an interesting vaccine candidate. Comparable to all other murine antibodies, the framework regions are expected to trigger an immunogenic response when administered to humans, the so called human anti-mouse antibody (HAMA) response.^[22] In order to prevent this, the framework regions of an antibody can be humanized, thereby preserving the complementarity determining regions (CDRs) that are responsible for the specific antigen binding. Mader et al. applied several of these humanization techniques, namely resurfacing, conservative or aggressive CDR-grafting, and superhumanization, which led to four different humanized Ab2/3H6 models.^[23] As the framework regions can influence the structure of the CDRs, the influence of the humanization on the binding affinity to 2F5 was determined by comparison to the murine Ab2/3H6. Mader et al. showed that the resurfaced (RS3H6) and the conservative CDR-grafted (GC3H6) models show similar binding affinity to 2F5, whereas the aggressive CDR-grafted (GA3H6) and the superhumanized models (SH3H6) show reduced and complete loss of binding affinity, respectively.^[23] In this study, molecular dynamics (MD) simulations of the murine Ab2/3H6 (in solution and bound to 2F5) as well as of the humanized 3H6 models (in solution) are performed in order to gain more insight into the causes of these differences. With MD simulations, one can obtain molecular level insight into not only the structural differences between the models, but also differences in their fluctuations and dynamics. Furthermore, free energy calculations are performed to gain quantitative information about the influence on the free energy of binding of two residues which appear to be important for binding from the initial MD simulations.

Table 1. Stability of the humanized and murine Ab2/3H6 during 1 ns MD simulations

Each model was simulated four times, each with different initial velocities (see Methods). The column RMSD gives the average and the maximum (in brackets) root mean square deviation in nm of the backbone atoms over the simulation. H-bonds states the average number of hydrogen bonds in the backbone, where a hydrogen bond is defined to be present when the angle between the donor hydrogen and acceptor atom is larger than 135° and the distance between the hydrogen and the acceptor atom is less than 0.25 nm. The remaining columns give the average percentage of the protein which is folded in the stated secondary structure, separate for the heavy (H) and light (L) chain

Model	Run	RMSD avg (max)	H-bonds avg	3-Helix		Turn		B-strand		B-bridge		Bend	
				L	H	L	H	L	H	L	H	L	H
GA3H6	1	1.97 (2.43)	97.4	1.0	2.9	3.7	5.4	44.6	47.7	1.5	1.2	23.4	20.9
	2	1.85 (2.30)	94.7	0.7	3.5	4.5	4.6	45.7	45.1	1.0	1.9	23.8	23.4
	3	2.25 (2.76)	93.5	0.2	2.3	4.4	4.8	43.4	46.7	1.0	1.8	25.2	21.8
	4	2.67 (3.21)	94.9	0.2	3.2	3.9	4.8	41.9	47.9	1.3	1.4	24.0	21.6
GC3H6	1	1.85 (2.29)	95.9	0.0	1.8	4.4	4.8	43.1	47.5	2.9	1.6	24.7	20.9
	2	2.48 (2.80)	95.6	0.1	1.4	4.2	4.7	44.2	46.0	1.5	2.0	25.7	21.4
	3	2.16 (2.74)	95.9	0.0	3.0	3.8	4.9	45.2	44.9	3.2	1.9	23.9	20.2
	4	2.73 (3.26)	93.9	0.1	1.8	4.1	4.8	46.0	47.5	1.4	1.6	25.3	20.9
RS3H6	1	2.61 (3.07)	91.0	0.0	1.6	2.9	2.4	44.6	45.1	1.8	2.0	24.1	20.5
	2	2.27 (2.63)	92.9	1.0	0.4	4.3	3.4	44.6	44.2	1.4	2.5	26.0	22.5
	3	2.45 (2.78)	92.7	0.0	0.5	3.3	3.2	43.4	44.1	2.3	3.7	24.0	21.2
	4	2.03 (2.63)	95.4	0.1	1.1	2.1	4.1	45.6	47.8	2.5	1.3	24.3	20.1
SH3H6	1	2.24 (2.78)	100.7	0.6	1.5	4.8	4.1	44.8	48.1	1.6	1.2	26.0	21.3
	2	2.33 (2.80)	93.4	1.2	3.0	4.0	5.3	46.5	41.3	2.1	1.2	25.2	20.3
	3	1.85 (2.29)	100.9	0.4	1.6	5.0	3.8	47.1	48.4	1.3	1.2	26.1	19.5
	4	2.67 (3.19)	98.1	1.6	1.9	3.8	4.4	47.7	44.9	1.7	2.2	23.8	19.5
3H6	1	1.92 (2.29)	84.6	1.4	3.7	4.1	5.6	37.4	43.5	2.3	1.9	26.5	22.6
	2	2.19 (2.60)	93.9	1.4	2.5	3.7	4.7	39.2	45.3	3.7	2.6	26.7	20.4
	3	2.44 (2.82)	89.1	1.0	2.5	4.1	5.6	33.3	44.4	2.8	2.4	25.3	21.3
	4	1.89 (2.25)	91.4	1.3	2.6	3.5	5.6	37.3	46.0	3.2	2.0	26.4	20.5

Results and Discussion

MD Simulations of Humanized Models

The results in Table 1 indicate the stability of the humanized and the murine Ab2/3H6 during the four repeats of the 1 ns MD simulations. At first the root mean square deviations (RMSDs) of the backbone atoms with respect to the energy minimized structures were evaluated. Only some minor differences between models and between runs of a single model were observed, but in general the RMSD values indicate stable simulations. The second measure used to evaluate the stability of the models is the average number of hydrogen bonds between backbone atoms. During the simulations of the humanized models, the number of hydrogen bonds remains almost constant, although there are some differences between the models. For example, more hydrogen bonds are observed in the backbone of SH3H6 with respect to RS3H6, indicating that SH3H6 might be slightly more stable. Surprisingly, the murine Ab2/3H6 simulations show fewer backbone hydrogen bonds than the humanized models. The remaining columns of Table 1 indicate the preservation of the secondary structure during the MD simulations. It can be seen that the average percentages of the secondary structures within the runs of the simulations are constant. The largest difference between the models is the lower percentage of β -strands in the light chain of the murine Ab2/3H6. Further investigation revealed that this is a result of a missing β -strand located at residues 10–13, which is near to and part of an unresolved loop (residues 12–18) that was constructed with Swiss PDB Viewer (SPDBV).^[24]

In order to gain insight into the structural differences between the humanized models which could explain the differences in the binding affinities to 2F5, the energy minimized

structures were aligned and are shown in Fig. 1. The largest differences between the humanized models can be seen in the loops with residues 52–56 and 100–108 (both Ab2/3H6 V_H). These regions are also known to be part of the CDRs 2 and 3, respectively. It is important to notice that even though the sequences of these loops are completely identical for all models, the structural orientations are quite different.

Root mean square fluctuations (RMSFs) of the backbone atoms of the humanized models and the murine Ab2/3H6 (both in solution and in crystal form) are shown in Fig. 2. For the majority of atoms, the RMSF values are small, indicating a stable backbone conformation. Regions of high and low fluctuations are also in agreement with the indicated secondary structure elements as observed in the crystal structure. The regions with highest fluctuations correspond to loops 10–18 and 38–43 of the light chain, the N-terminus of the heavy chain, and loop 102–108 of the heavy chain. The fluctuations of the backbone atoms in the crystal simulation are generally similar to the models, except for the loop 102–108 of the heavy chain. In this region, the humanized models show the largest fluctuations, followed by Ab2/3H6 in solution and the crystal simulation with the smallest fluctuations.

It is to be expected that the differences in binding affinity between the humanized Ab2/3H6 models towards 2F5 are caused by differences in the interface region. Residues of Ab2/3H6 are defined to be part of the interface when any of its atoms is within 0.4 nm of 2F5 in the X-ray structure of the complex. In order to obtain a more detailed view of the flexibility of the residues in the interface region, the RMSF values for all atoms of the interface residues are shown in Fig. 3. For the majority of these residues, there are no significant

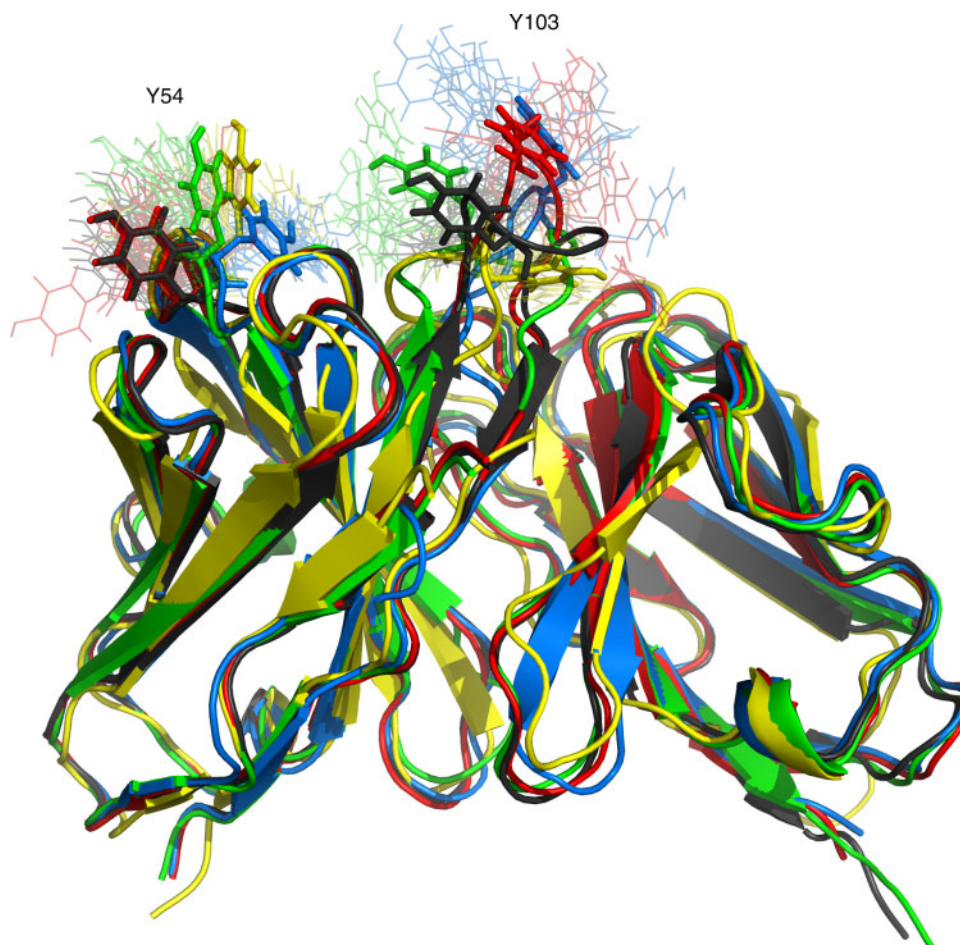


Fig. 1. Structures of GA3H6 (black), GC3H6 (red), RS3H6 (green), SH3H6 (blue), and murine Ab2/3H6 (yellow). The backbone structures after energy minimization are shown in cartoon representation. Shown in stick representation are the residues Y54 and Y103 after energy minimization. Lines represent the residues Y54 and Y103 after 200, 600, and 1000 ps of MD simulation, for each of the four runs of the simulations.

differences between the models. This is not the case, however, for TYR54 and TYR103 (both Ab2/3H6 V_H). Not surprisingly, the fluctuations of the TYR54 atoms are the smallest in the crystal simulation. In the murine Ab2/3H6 and RS3H6, the fluctuations are the largest, followed closely by GC3H6 and GA3H6. Fluctuations in SH3H6 are small, but not as small as in the crystal simulation.

A completely different pattern is seen for TYR103, where the largest fluctuations are observed for GA3H6, GC3H6, and SH3H6, with values up to 0.55 nm. RMSF values for RS3H6 are considerably lower. For the murine Ab2/3H6, TYR103 seems to have found a stable conformation in the free simulation as well as in the crystal simulation.

More information about the orientation and the possible influence on the binding affinity to 2F5 is obtained by calculating the solvent accessible surface area (SASA) of these residues (Fig. 4).^[25] For TYR54 the difference between the SH3H6 model and the other models is quite prominent. Especially obvious is the much smaller SASA for the OH of the SH3H6 model. For TYR103, the differences in SASA are not so obvious, but in general it can be said that it is most solvent accessible in SH3H6 and GC3H6, whereas it is mostly buried in the murine Ab2/3H6 (both bound and free).

In Fig. 1, the two tyrosine residues are shown after energy minimization (sticks) and after 200, 600, and 1000 ps of each of

the four repeats of the simulation (lines), giving a rough indication of the dynamics of these residues.

Combining all information obtained so far, it seems that both TYR54 and TYR103 play an important role in the differences in binding affinities between the different humanized Ab2/3H6 models. In the SH3H6 model, TYR54 has a stable conformation which is different from all other models and the murine Ab2/3H6. This conformation is stabilized by a hydrogen bond between ASN52 (ND2) and TYR54 (OH), which is on average present during ~90% of the simulation (data not shown). Although this particular hydrogen bond is not observed in the other models, there is another hydrogen bond between these two residues in the RS3H6 (~47%) and Ab2/3H6 (~79%) simulations. This hydrogen bond is between TYR54 (N) and ASN52 (OD1) and results in a different orientation of TYR54. Because the latter hydrogen bond is located at the backbone of TYR54, the side chain is still able to move relatively freely. No significant hydrogen bonds involving TYR54 were found during the simulations of the models GA3H6 and GC3H6. All in all, one can say that in SH3H6 TYR54 already has a strong intramolecular interaction and is, therefore, not available for hydrogen bonding with 2F5. Murine Ab2/3H6 and RS3H6 show a similar conformation for TYR54 which is partly stabilized with a hydrogen bond on the backbone, but leaves the side chain free to interact with 2F5. The fact that in SH3H6 TYR54 is not

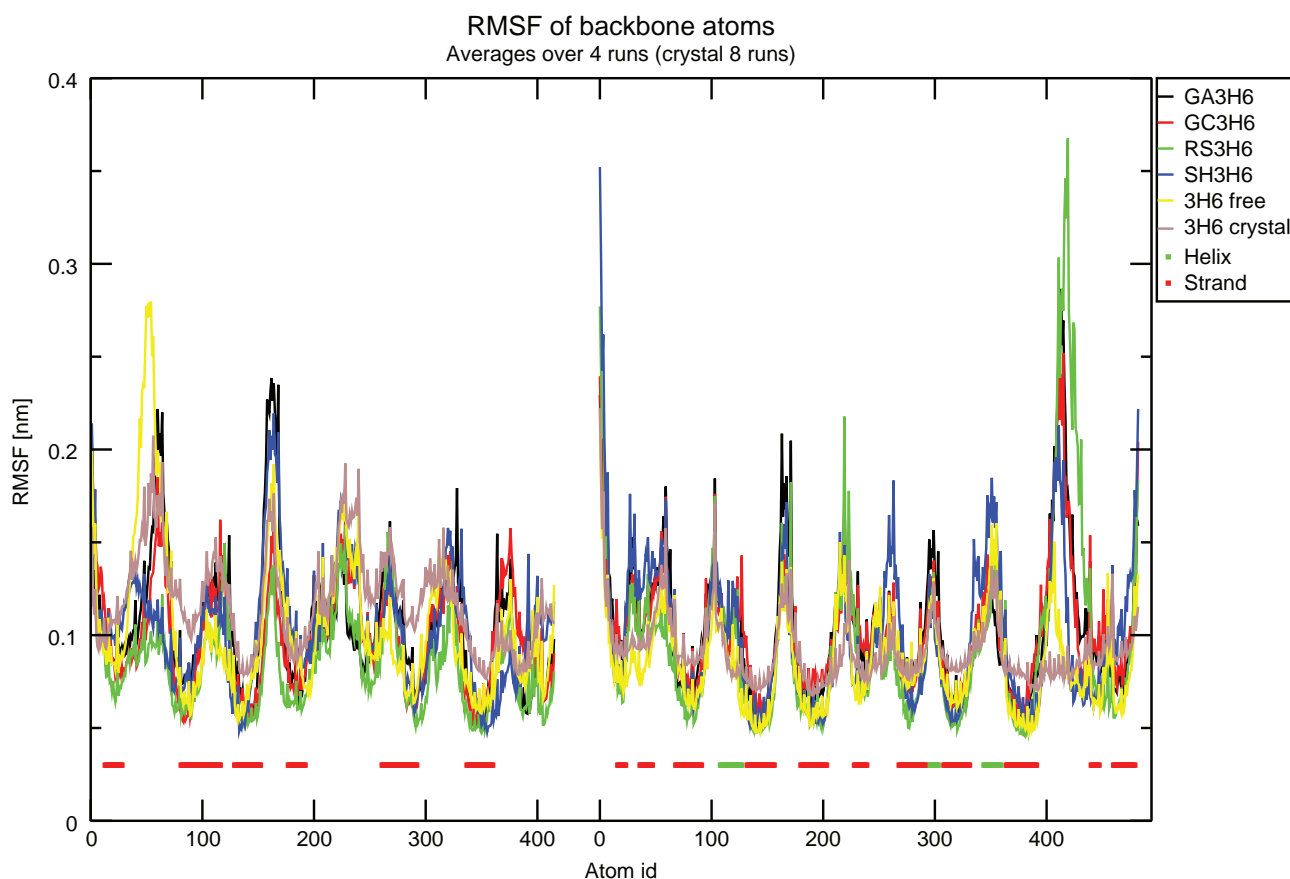


Fig. 2. Root mean square fluctuations (RMSFs) of the backbone atoms of GA3H6 (black), GC3H6 (red), RS3H6 (green), SH3H6 (blue), the murine Ab2/3H6 in solution (yellow), and murine Ab2/3H6 as part of the crystal (brown). Underneath the RMSF curves, the positions of the strands and helices as defined in the PDB file are indicated with red and green lines respectively. The graph is separated into two parts; on the left side V_L and on the right hand side V_H . For the humanized and the murine Ab2/3H6, the average RMSF is obtained from the RMSF values of four simulations of 1 ns for each model. For the 3H6 in the crystal simulation, RMSF values for each of the four copies in two simulations of 600 ps were calculated and averaged.

available for favourable interactions with 2F5 contributes to the lower binding affinity of SH3H6 for 2F5.

During the simulations of the models GA3H6, GC3H6, and SH3H6, TYR103 shows more flexibility than in the simulations of RS3H6 and murine Ab2/3H6. Furthermore, it has the smallest SASA in the murine Ab2/3H6, followed by RS3H6 and GA3H6. This indicates that in these models TYR103 is quite tightly packed to 3H6, whereas in GC3H6 and SH3H6, it is more directed towards the solvent. RS3H6 thus seems to show most resemblance with the murine Ab2/3H6. However, looking at the conformations of TYR103 which were sampled during the simulations (Fig. 1), it is clear that RS3H6 also does not sample the conformation which is present in murine Ab2/3H6, which is stabilized by a hydrogen bond with ASP50 of the light chain (also observed in the crystal simulation, see Table 2). Further structural analysis showed that the conformations sampled with RS3H6 will most likely not cause big clashes with backbone atoms of 2F5, whereas this is much more likely for SH3H6, for example. The loss of binding affinity of SH3H6 for 2F5 may thus partially be caused by the fact that TYR103 would cause clashes with backbone atoms of 2F5, or would need to move to a less favourable orientation. Because of the different orientation of TYR103 in RS3H6, it is quite likely that the cation- π interaction with 2F5, as seen in the crystal structure, is not preserved. It may, however, find some compensating interactions. Another factor that plays a role here is the loss of entropy

upon binding. As indicated by the high RMSF, the side chain of Y103 in the models GA3H6, GC3H6, and SH3H6 is very flexible. Upon binding to 2F5, the movement of this residue would be restricted and the entropy would be lost. This makes it less favourable for these models to bind to 2F5, with respect to RS3H6 and the murine Ab2/3H6 which show less flexibility to start with.

MD Simulation of 2F5 Ab2/3H6 Complex

Preliminary simulations of the dimer of the variable regions of 2F5 and Ab2/3H6 in solution indicated a widening of the interface region. For the thermodynamic cycles on which the free energy calculations are based (see below), it is crucial that the two proteins form a stable dimer interface. Therefore, the 2F5 Ab2/3H6 complex, including the constant regions, was simulated as a crystal with four copies of the complex for 600 ps, in two parallel simulations. The RMSD of the backbone atoms of the separate copies remained lower than 0.35 nm (data not shown), indicating a good dynamic stability of the complex. In Fig. 5 the structure of a single copy of the 2F5 Ab2/3H6 complex, consisting of the Fab regions of 2F5 and Ab2/3H6, is shown. Furthermore, a more detailed view of the interface region is given, in which several residues important for the interactions between 2F5 and Ab2/3H6 are indicated. Selected hydrogen bond occurrences for the atoms which are part of the interface, are shown in Table 2 (for a more extensive table, see

the Accessory Publication). The five hydrogen bonds that are most dominantly present during the MD simulations were also the ones identified in the crystal structure.^[26] Three of them (2F5^H:T67–3H6^H:T30, 2F5^H:N66–3H6^H:D31, and 3H6^H:G102–2F5^H:N66) are observed for all eight copies, 3H6^H:G104–2F5^H:N66 in six copies, and 2F5^H:T61–3H6^H:G102 in only five copies. This shows that although most of the interactions found in the crystal structure are preserved, there are some differences between simulations of the different copies of the complex.

Also shown in Table 2 are the observed hydrogen bonds between interface residues and other residues within the same antibody. Both in 2F5 and Ab2/3H6 there are several of these hydrogen bonds which are very stable. We focus on the interactions involving TYR54 and TYR103 of 3H6^H. There are three hydrogen bonds involved with TYR103, from which two (with 3H6^L:D50 and 3H6^H:S106) are observed in all eight copies and one (with 3H6^H:S100) in six copies of the complex. This indicates that TYR103 has a very stable conformation in the complex, which probably allows for the formation of a π -cation interaction with ARG60 (2F5^H) which was observed in the crystal structure (see also Fig. 5). The same hydrogen bonds were also observed in most (but not all) simulations of Ab2/3H6 in solution, but were missing in the simulations of the humanized models. For TYR54 one important hydrogen bond is found in seven copies of the complex, which is between the backbone atoms of 3H6^H:Y54 and 3H6^H:N52. Note that hydrogen bonds between these residues also played an important role in the differences between the humanized models, but then involved the side chain of ASN52.

Free Energy Calculations

In order to quantify the importance of the residues TYR54 and TYR103 for the binding affinity of Ab2/3H6 to 2F5, free energy calculations were performed. In Fig. 6 the free energy profiles of the mutations Y54A (left) and Y103A (right) in 3H6 (top) and in the 2F5:3H6 complex (bottom) are shown. Error estimates based on block averaging are shown as error bars.^[27]

Y54A

For the mutation Y54A in the simulation of the free murine Ab2/3H6, the free energy profile is smooth and has a free energy difference of $100.4 \pm 2.3 \text{ kJ mol}^{-1}$. Although the thermodynamic integration (TI) in the 2F5:3H6 complex required the prolongation of the sampling runs for $\lambda = 0.85$ and 0.9 up to 600 ps, the free energy profiles of the individual copies of the 2F5:3H6 complex are relatively smooth. The values of the free energy differences vary between 108.9 ± 2.7 and $117.3 \pm 2.3 \text{ kJ mol}^{-1}$, leading to an average of $114.0 \pm 2.9 \text{ kJ mol}^{-1}$. Making use of the thermodynamic cycle as described in the methods section, a relative free energy of binding of 13.6 kJ mol^{-1} is found, indicating that this mutation is unfavourable for binding. This confirms the hypothesis that Y54 is important for the binding affinity of Ab2/3H6 to 2F5.

Y103A

During initial TI simulations, there were some difficulties to equilibrate the system at higher lambda values. These problems turned out to be related to occasional changes in the dihedral angle ($N-C_{\alpha}-C_{\beta}-C_{\gamma}$) of TYR103. The reduced interactions of

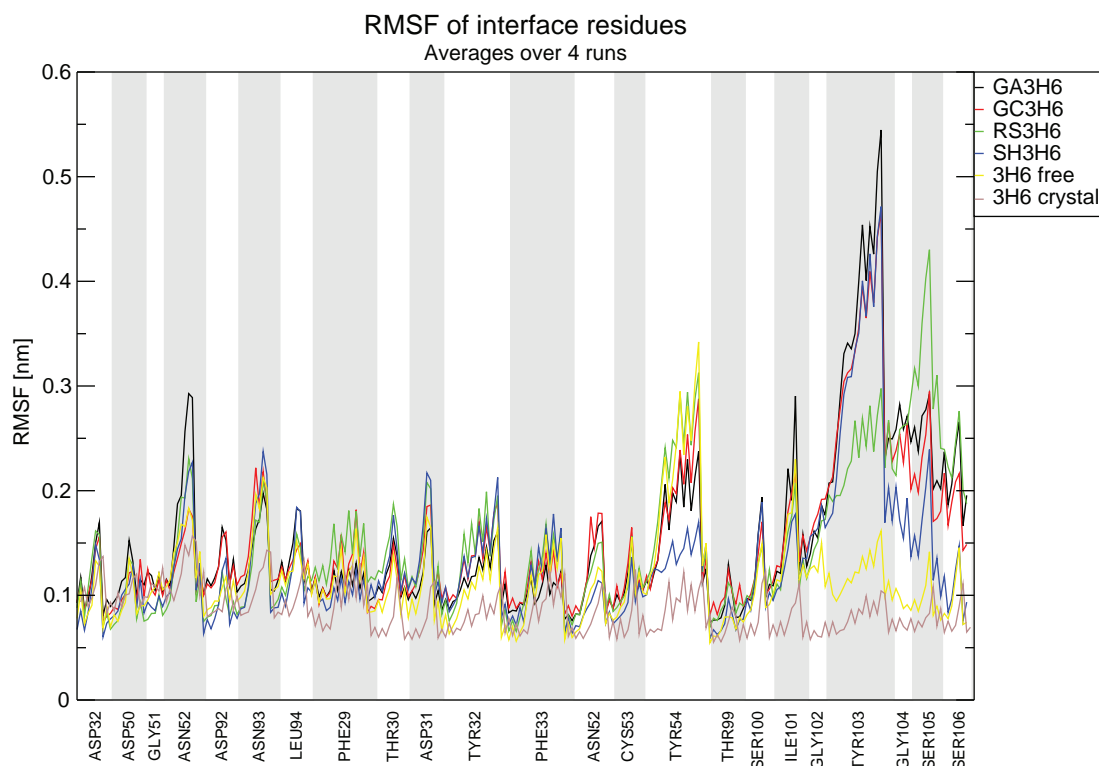


Fig. 3. Root mean square fluctuations (RMSFs) of residues of 3H6 defined as being part of the interface between 2F5 and 3H6 (residues of 3H6 with atoms within 0.4 nm of atoms of 2F5). Residues up to LEU94 are part of V_L , residues starting from PHE29 belong to V_H . Shown are the average values of RMSF (for description of the calculation, see caption of Fig. 2) for GA3H6 (black), GC3H6 (red), RS3H6 (green), SH3H6 (blue), murine Ab2/3H6 free (yellow), and murine Ab2/3H6 crystal (brown).

the perturbed atoms allows for such a large movement, as it is no longer restricted by neighbouring atoms. The jumps in the dihedral angle have a significant influence on the value of $\partial H/\partial \lambda$, as this value still depends on the positions of the side chain atoms. Because of the barrier in the dihedral angle potential of

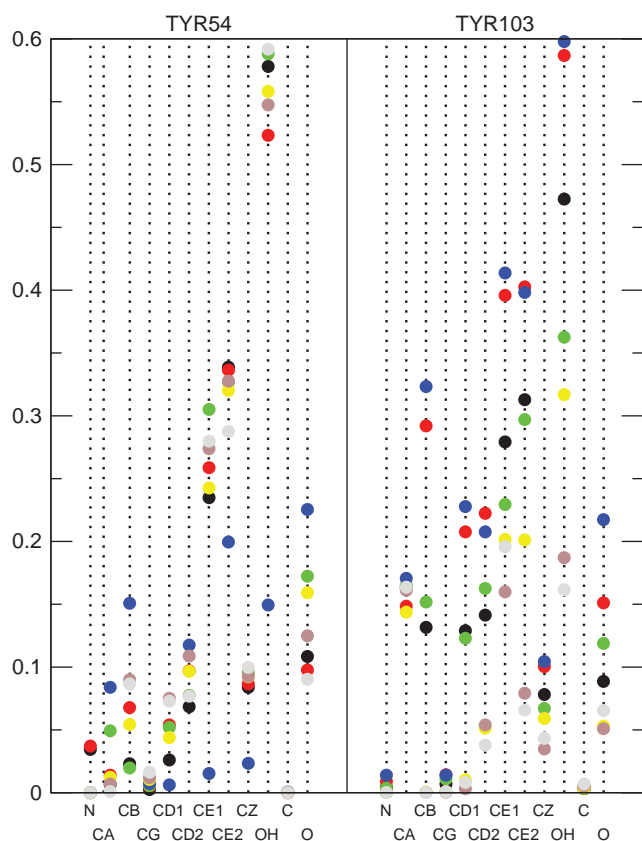


Fig. 4. Solvent accessible surface area in nm^2 per atom of TYR54 and TYR103, calculated according to Lee and Richards using a probe radius of 0.14 nm .^[25] Shown for GA3H6 (black), GC3H6 (red), RS3H6 (green), SH3H6 (blue), Ab2/3H6 (yellow), and Ab2/3H6 bound (1st simulation: brown, 2nd simulation: grey). Average over four simulations for the humanized models and free Ab2/3H6, average over four copies for the bound Ab2/3H6 (two crystal simulations). SASA values from the crystal simulations are calculated in the absence of 2F5.

5.92 kJ mol^{-1} , the jumps only occur occasionally and the simulations suffered from inadequate sampling. The TI calculations were, therefore, repeated during which this dihedral angle was perturbed to a dihedral angle type with a force constant of 0, allowing free rotation around this dihedral at $\lambda = 1$. This allows for adequate sampling of all orientations of the side chain of Y103 and should give rise to a more converged value of $\langle \partial H/\partial \lambda \rangle$.

Even with the perturbed dihedral angle, extra lambda points ($\lambda = 0.825$ and 0.875) and prolongation of the simulation at $\lambda = 0.15$ up to 600 ps, and at $\lambda = 0.8, 0.825$, and 0.85 up to a total of 1.2 ns, were required. Furthermore, the equilibration time for simulation at $\lambda = 0.8$ was prolonged up to 500 ps as it showed large fluctuations in $\partial H/\partial \lambda$ during this time. Despite these adjustments the free energy profile for Ab2/3H6 free in solution is still somewhat noisy at high lambda values (see Fig. 6, panel C), but slight modifications no longer have a large effect on the integrated free energy difference. Integrating this free energy profile leads to a free energy difference of $107.5 \pm 3.3 \text{ kJ mol}^{-1}$. In the complex simulation, sampling runs were required to be prolonged up to 600 ps at $\lambda = 0.1, 0.15, 0.8$, and 0.85 . Despite the larger system, the 2F5:3H6 crystal simulation shows smoother curves, giving rise to free energy differences between 111.5 and $123.1 \text{ kJ mol}^{-1}$ (with error estimates between 3.2 and 4.2 kJ mol^{-1}), leading to an average of $115.1 \pm 3.8 \text{ kJ mol}^{-1}$. The relative free energy of binding for the Y103A mutation is thus 7.6 kJ mol^{-1} . Although smaller than for Y54A, the difference is still significant, showing the importance of TYR103 for the binding affinity of Ab2/3H6 to 2F5. These results are in agreement with experimental data, where apparent binding affinities were determined with competition ELISA for the wild type Ab2/3H6 and several mutated variants.^[28] It was shown that the mutation Y103A (Y111A according to the numbering used in the paper of Gach et al.) results in complete loss of binding capacity to 2F5. In the same paper it was also shown that the mutant could not inhibit the neutralization potency of 2F5 with a concentration up to $100 \mu\text{g mL}^{-1}$ whereas the wildtype Ab2/3H6 extinguished the neutralizing potency of 2F5 at a concentration of $3.1 \mu\text{g mL}^{-1}$. From these values, a lower boundary to the relative free energies of binding may be estimated to be 8.6 kJ mol^{-1} , thus supporting the unfavourable free energy of binding for the mutation Y103A according to the free energy calculations.

Table 2. Average number of hydrogen bonds in the interface region during the 2F5/3H6 crystal simulation

For selected hydrogen bonds the acceptor and donor residues, the average number of hydrogen bonds between the residues over all eight copies (two simulations, each with four copies of the complex), the standard deviation of the average and the number of copies (#) for which the hydrogen bond is seen for more than 50% of the time are shown. The 'Atom' columns indicate whether the hydrogen bonds involve the backbone (bb) or side chain (sc) atoms. See the Accessory Publication for the complete table of hydrogen bonds which were observed more than 50% of the time in one of the eight copies

Chain	Donor		Acceptor		No. H-bonds		#
	Residue	Atom	Chain	Residue	Atom	Avg (stdev)	
2F5_H	THR67	sc	3H6_H	THR30	bb	0.98 (0.01)	8
2F5_H	ASN66	sc	3H6_H	ASP31	bb	0.92 (0.13)	8
3H6_H	GLY102	bb	2F5_H	ASN66	sc	0.79 (0.12)	8
3H6_H	GLY104	bb	2F5_H	ASN66	sc	0.71 (0.35)	6
2F5_H	TYR61	bb	3H6_H	GLY102	bb	0.41 (0.26)	5
3H6_H	ASN52	sc	2F5_H	THR67	bb	0.37 (0.26)	3
3H6_H	TYR103	sc	3H6_L	ASP50	sc	1.22 (0.14)	8
3H6_H	SER106	bb	3H6_H	TYR103	bb	0.71 (0.12)	8
3H6_H	TYR54	bb	3H6_H	ASN52	bb	0.70 (0.23)	7
3H6_H	TYR103	bb	3H6_H	SER100	bb	0.57 (0.28)	6

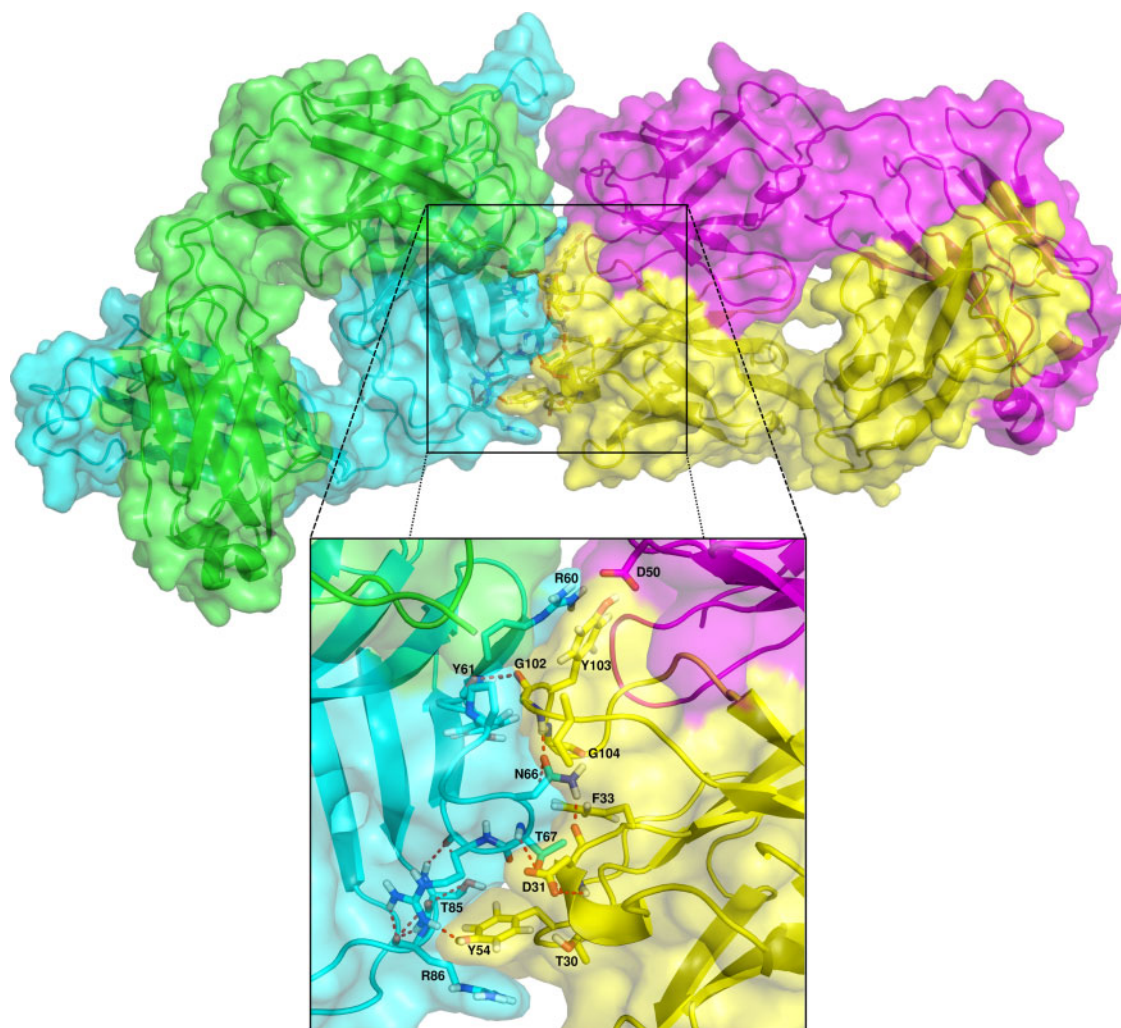


Fig. 5. (Top) Surface and cartoon representation of the 2F5:Ab2/3H6 complex including modelled loops after energy minimization, with 2F5^L (green), 2F5^H (cyan), 3H6^L (magenta), and 3H6^H (yellow). (Bottom) Close-up view of the interface region with side chains of amino acids important for interactions between 2F5 and 3H6 shown in stick representation. Backbone atoms of these amino acids are only shown when involved in hydrogen bonds. Hydrogen bonds within the interface region (residues with atoms within 0.4 nm of the other antibody) as present in the minimized structure are shown as red dashes.

Conclusions

MD simulations were performed for the four humanization models of Ab2/3H6, as well as for the murine Ab2/3H6 in solution and bound to 2F5. No major structural changes were observed during the simulations, which indicates the stability of the antibodies. TYR54 and TYR103 (located in the heavy chain of 3H6) were identified as residues which showed structural as well as dynamic differences between the different humanized models. These observations strongly suggest the influence of these residues on the binding affinities of the humanized antibodies. The lack of binding affinity of SH3H6 may be understood at a molecular level, whereas the reasons for the difference between the binding affinities of GA3H6 and GC3H6 are still not completely clear. Our results emphasise that humanization processes should not only preserve the sequences of the CDRs but also the structure and dynamic behaviour in these regions.

The importance of the residues TYR54 and TYR103 for the binding affinity of Ab2/3H6 to 2F5 was quantified using thermodynamic integration, leading to relative free energies of binding of 13.6 and 7.6 kJ mol⁻¹ for Y54A and Y103A, respectively. Whereas the influence of TYR103 has already been shown in experimental research, this is not the case for

TYR54. It will be interesting to experimentally determine the apparent binding affinity for the Y54A mutant as well, in order to confirm or refute our prediction of the importance of this residue for binding of Ab2/3H6 to 2F5. Furthermore, it may be possible to (partially) regain the binding affinity of SH3H6 by influencing the conformation and dynamics of TYR54 through a mutation like N52A. This mutation would disrupt the hydrogen bond between TYR54 (OH) and ASN52 (ND2), allowing TYR54 to adopt conformations similar to those observed in RS3H6 and murine Ab2/3H6. Such a mutation would also disrupt the hydrogen bond observed in RS3H6 and Ab2/3H6 (ASN52:OD1–TYR54:N) which seemed to stabilize a favourable conformation for binding. However, in the simulations of the complex, the hydrogen bond between these residues was predominantly between the backbone atoms, which would be preserved with the N52A mutation. As ASN52 is also part of CDR 3, such a mutation may directly influence the interaction with 2F5, but this interaction may not be crucial as it was only observed in three out of eight copies of the simulation (Table 2).

In summary, the various simulations of Ab2/3H6 and its humanized forms offer a molecular rationalization of

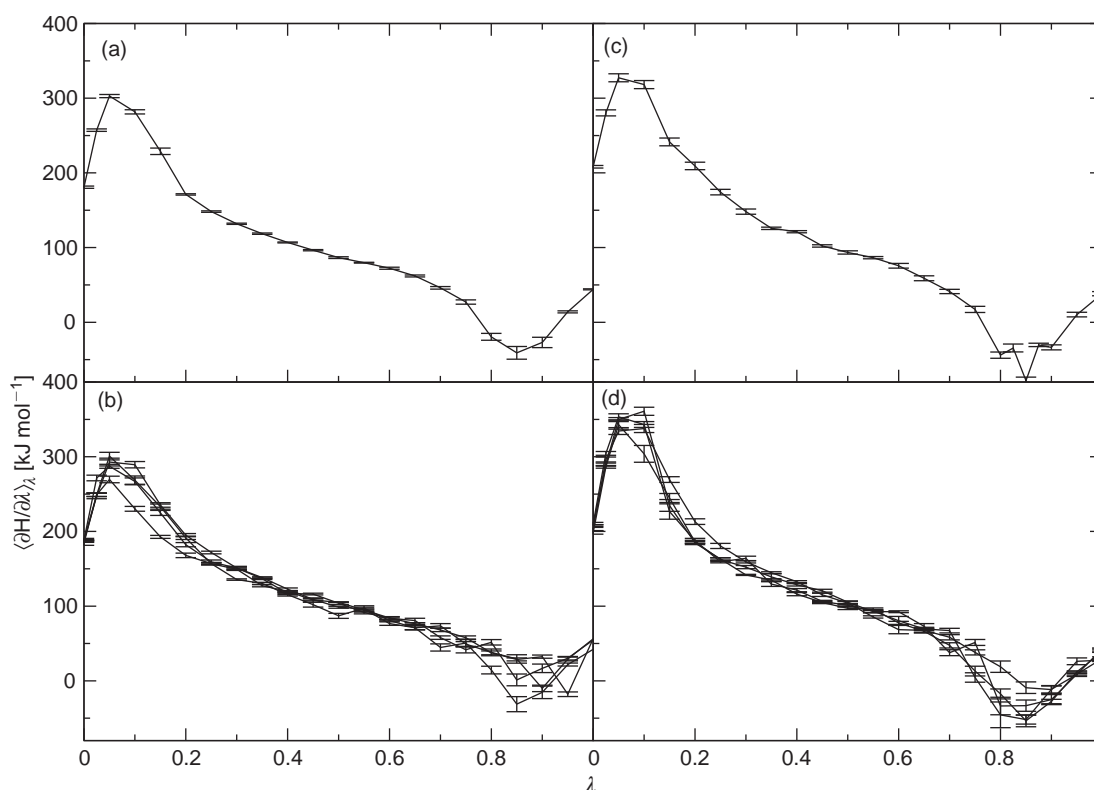


Fig. 6. Free energy profiles for the mutation Y54A in 3H6 (a) and in the crystal 2F5:3H6 (b), and the mutation Y103A in 3H6 (c) and in the crystal 2F5:3H6 (d). The individual curves correspond to different copies of the crystallographic unit cell (c and d). The error bars are error estimates calculated using block averaging.^[27]

experimental observations which are supported by free energy calculations. For one of the investigated mutations (Y103A), the calculations were validated by experimental data from point mutations, while for the Y54A mutation new experiments are suggested.

Experimental

Humanized Ab2/3H6

Energy minimizations and MD simulations were performed using the GROMOS05 simulation package^[29] in combination with the force field parameter set 53A6.^[30] The initial configurations of four humanized Ab2/3H6 homology models, named GA3H6, GC3H6, RS3H6, and SH3H6, were obtained as previously described.^[23] These models only consist of the variable regions of the heavy (V_H) and light chain (V_L) of the antibody. In order to relax the models, two steepest descent energy minimizations were performed. Backbone atoms were positionally restrained in the first minimization, but allowed to move freely in the second. Subsequently the models were solvated in periodic rectangular boxes using Simple Point Charge (SPC) water molecules.^[31] Applying a minimal solute–wall distance of 0.8 nm, this resulted in systems with 7738 to 9044 water molecules, depending on the model. No counter ions were added, leading to charges of $-2e$, $-3e$, $-8e$, and $-8e$ for GA3H6, GC3H6, RS3H6, and SH3H6, respectively. Another round of energy minimization was performed with position constraints on the solute atoms, to relax the solvent configurations.

Initial random velocities were generated from a Maxwell–Boltzmann distribution at 50 K. The systems were slowly heated with steps of 50 K, simulating for 20 ps at each temperature. Position restraints on the backbone atoms were applied with a force constant of $2.5 \times 10^4 \text{ kJ mol}^{-1} \text{ nm}^{-2}$ at a temperature of

50 K, and reduced ten-fold with each increase in temperature. The final equilibration step was a 40 ps simulation at 298 K without any position restraints. As soon as the position restraints were turned off, rototranslational constraints were switched on, thereby preventing rotation of the models within the water box.^[32] The equilibration phase was followed by a 1 ns simulation at 298 K. The temperature was kept constant using weak coupling^[33] with a relaxation time of 0.1 ps and separate temperature baths for solute and solvent atoms. Pressure was kept constant by applying isotropic scaling with a compressibility of $4.575 \times 10^{-4} (\text{kJ mol}^{-1} \text{ nm}^{-3})^{-1}$ and a relaxation time of 0.5 ps. All bond lengths were constrained using the SHAKE algorithm^[34] with a geometric accuracy of 1×10^{-4} , allowing for a time step of 2 fs. The long range interactions (van der Waals and electrostatic) were calculated using a triple range cut-off scheme. A pair-list was generated every fifth time step. At every step interactions within 0.8 nm were calculated, whereas interactions between 0.8 and 1.4 nm were evaluated only when the pair-list was generated and kept constant at intermediate time steps. Applying the reaction field method,^[35] the contribution of interactions beyond 1.4 nm was modelled as a homogeneous medium with a dielectric constant of 61, as appropriate for SPC water molecules.^[36]

Each production simulation was performed for 1 ns and coordinates were written to disk every 0.5 ps for later analysis. For each humanized Ab2/3H6 model, the equilibration and production simulations were conducted four times, each with different initial velocities.

2F5:Ab2/3H6 Complex

The crystal structure of the Fab' fragment of the antibody 2F5 and the Fab fragment of its anti-idiotypic antibody 3H6 (PDB code

3BQU)^[26] including the constant regions, were taken as initial configurations for the simulations. The following residues were missing in the crystal structure and were modelled in using Swiss PDB viewer (SPDBV)^[24]: 2F5^{heavy}: 112–115, 146–153, 209–213; 3H6^{light}: 12–18, 75–79, 105–107, 152–156, 200–202; 3H6^{heavy}: 140–144 (numbering according to the Protein Data Bank (PDB) file). After specifying the residues, SPDBV generated a list of possible configurations of the loop, from which the most suitable one was chosen based on the number of clashes, the energy calculated with the GROMOS force field, and visual inspection. Other missing residues, located at the N or C termini, were not added to the models. In order to simulate the complex as a crystal, four copies of the complex (including the sulfate ion present in the crystal structure) were subjected to symmetry transformations according to the crystallographic data. No further counter ions were added, leading to a total charge of +8e. In order to carefully relax the modelled residues, the first steepest descent energy minimization was applied with position constraints on all atoms except for the modelled ones and without using the SHAKE algorithm. Subsequent energy minimizations were performed with SHAKE turned on while keeping the position constraints and eventually without position constraints. Under periodic boundary conditions the four copies of the complex represented the crystallographic $P2_12_12_1$ unit cell. After solvation of the complexes in a rectangular box with the lengths as specified in the PDB file, 17 443 SPC water molecules were included, leading to a system consisting of ~87 000 atoms in total. The solvent was relaxed by another round of energy minimization with position constraints on the solute atoms. After a last energy minimization without any position constraints, random velocities were generated from a Maxwell–Boltzmann distribution at a temperature of 50 K. The same equilibration protocol was used as described for the humanized Ab2/3H6. After this, the crystal was simulated for 600 ps, in two parallel simulations, using centre of mass motion removal every 1000 steps.

3H6

For the simulation of the Ab2/3H6 in solution, the initial configuration was obtained from the crystal structure (PDB code 3BQU),^[26] from which the coordinates of 2F5 as well as the constant region of Ab2/3H6 were removed. This just left V_L and V_H of Ab2/3H6, which was equivalent to what was simulated for the humanized models. The sulfate ion present in the crystal structure was not included. The total charge of the system was -5e. The V_L and V_H regions contained two missing loops for which the models obtained with SPDBV (as described in the section above) were used. This was subjected to steepest descent energy minimization and subsequently solvated in a periodic rectangular box with a minimum solute-to-wall distance of 0.8 nm. SPC water molecules (8557) were added, which resulted in a total system size of ~28 000 atoms. Another round of energy minimization was applied with position constraints on the solute atoms in order to relax the solvent. The system was equilibrated using the same protocol as described for the humanization models. The equilibration and the 1 ns production simulations were performed four times, starting with different random seeds to create the initial velocities.

Thermodynamic Integration

TI is a method to calculate the free energy difference between two states of a system.^[37] In this method, the Hamiltonian as a function of the atomic positions, \mathbf{r} , and momenta, \mathbf{p} , is made

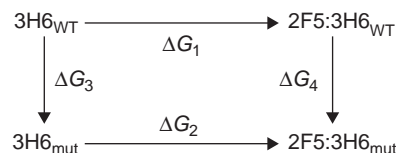


Fig. 7. Thermodynamic cycle for the calculation of the relative free energy of binding of murine Ab2/3H6 and mutated Ab2/3H6 to 2F5.

dependent on a coupling parameter λ , such that at $\lambda = 0$, the system is at state A, whereas at $\lambda = 1$, the system is at state B,

$$H(r, p) \rightarrow H(r, p; \lambda) \text{ with } H(r, p; 0) = H_A(r, p) \quad (1)$$

$$H(r, p; 1) = H_B(r, p)$$

MD simulations were performed at different λ values, thereby evaluating the ensemble average of the derivative of the Hamiltonian with respect to λ . Integration over these ensemble averages leads to the free energy difference between state A and B, as shown in Eqn 2.

$$\Delta G_{BA} = \int_0^1 \left\langle \frac{\partial H(\lambda)}{\partial \lambda} \right\rangle_{\lambda} d\lambda \quad (2)$$

Here, we aimed to gain insight into the influence of particular residues on the free energy of binding of 2F5 and 3H6. As simulating the actual binding process of 3H6 to 2F5 is computationally too demanding, the fact that free energy is a state function was exploited by defining a thermodynamic cycle as shown in Fig. 7.^[38] Since the free energy along the complete cycle must be zero, the relative free energy of binding ($\Delta G_2 - \Delta G_1$) could be obtained by calculating the other two legs of the cycle ($\Delta G_4 - \Delta G_3$). This required calculation of the free energy difference of the mutation of 3H6 while in solution and while bound to 2F5. In cases where the mutated state was not too different from that of the wildtype, these unphysical processes could be simulated using TI.

Two mutations in the heavy chain of 3H6 were evaluated in this way, namely Y54A (part of CDR 2) and Y103A (part of CDR 3). Mutating a tyrosine into an alanine residue involved the change of C_{β} from a CH_2 to a CH_3 and the removal of all other side chain atoms. Removal of atoms during a TI was implemented as mutations into so called dummy atoms, which did not have any non-bonded interactions but preserved the original masses. Atoms undergoing changes in their charge had a softness parameter of 0.5 nm^2 for the electrostatic interactions, and for the other atoms normal electrostatic interactions were used. The softness parameter for the van der Waals interactions was set to 0.5 for all mutated atoms.^[39]

A total of four TI calculations were performed; 3H6 Y103A, 2F5:3H6 Y103A, 3H6 Y54A, and 2F5:3H6 Y54A. The 2F5:3H6 complex was simulated as a crystal, performing the perturbations in each of the four copies simultaneously. The distances between the mutation sites within the crystal were well beyond the interaction cut-off. In the crystal simulation, the whole Fab regions were simulated (consisting of V_L , V_H , C_L , and C_{H1}), whereas the simulation of Ab2/3H6 in solution consisted of only the V_L and V_H regions. Despite these differences, the thermodynamic cycle could still be applied because the C_L and C_{H1} regions were outside of the cut-off range for the non-bonded interactions for Y54 and Y103. These constant regions were thus

not directly influencing the perturbations. Furthermore, the RMSD with respect to the initial positions for the variable regions of Ab2/3H6 showed a very similar behaviour for simulations in the crystal form compared with the simulations of just the variable regions in solution (data not shown). The indirect influence of the constant regions was, therefore, also believed to be limited.

Simulations were performed at lambda points between 0 and 1, with $\Delta\lambda = 0.05$, and at $\lambda = 0.025$. Based on the smoothness of the graph of the ensemble averages of $\partial H/\partial\lambda$, additional lambda points were added for individual TIs. At each lambda point (λ_i) a 100 ps equilibration run was started with the initial coordinates obtained from the equilibrated system at λ_{i-1} , followed by 400 ps sampling. At $\lambda = 0$, a longer equilibration run of 200 ps was performed. Sampling runs with high error estimates on the average derivative of the Hamiltonian were prolonged up to a maximum of 1.2 ns in order to increase sampling.

Accessory Publication

The Accessory Publication contains a more extensive version of Table 2, showing the hydrogen bond occurrences in the interface region during the 2F5/3H6 crystal simulation. The Accessory Publication is available on the journal's website.

Acknowledgements

Financial support of the Vienna Science and Technology Fund is gratefully acknowledged (A.d.R. and C.O.).

References

- S. A. Gallo, C. M. Finnegan, M. Viard, Y. Raviv, A. Dimitrov, S. S. Rawat, A. Puri, S. Durell, R. Blumenthal, *Biochim. Biophys. Acta* **2003**, *1614*, 36. doi:10.1016/S0005-2736(03)00161-5
- A. S. Dimitrov, S. S. Rawat, S. Jiang, R. Blumenthal, *Biochemistry* **2003**, *42*, 14150. doi:10.1021/BI035154G
- D. R. Burton, R. C. Desrosiers, R. W. Doms, W. C. Koff, P. D. Kwong, J. P. Moore, G. J. Nabel, J. Sodroski, I. A. Wilson, R. T. Wyatt, *Nat. Immunol.* **2004**, *5*, 233. doi:10.1038/NI0304-233
- R. Wyatt, J. Sodroski, *Science* **1998**, *280*, 1884. doi:10.1126/SCIENCE.280.5371.1884
- J. P. Moore, Q. J. Sattentau, R. Wyatt, J. Sodroski, *J. Virol.* **1994**, *68*, 469.
- J. Liu, A. Bartesaghi, M. J. Borgnia, G. Sapiro, S. Subramaniam, *Nature* **2008**, *455*, 109. doi:10.1038/NATURE07159
- M. B. Zwick, A. F. Labrijn, M. Wang, C. Spencehauer, E. O. Saphire, J. M. Binley, J. P. Moore, G. Stiegler, H. Katinger, D. R. Burton, P. W. H. I. Parren, *J. Virol.* **2001**, *75*, 10892. doi:10.1128/JVI.75.22.10892-10905.2001
- R. Wyatt, P. D. Kwong, E. Desjardins, R. W. Sweet, J. Robinson, W. A. Hendrickson, J. G. Sodroski, *Nature* **1998**, *393*, 705. doi:10.1038/31514
- M. B. Zwick, R. Jensen, S. Church, M. Wang, G. Stiegler, R. Kunert, H. Katinger, D. R. Burton, *J. Virol.* **2005**, *79*, 1252. doi:10.1128/JVI.79.2.1252-1261.2005
- H. Yu, D. Tudor, A. Alfsen, B. Labrosse, F. Clavel, M. Bomsel, *Retrovirology* **2008**, *5*, 93. doi:10.1186/1742-4690-5-93
- E. O. Saphire, P. W. H. I. Parren, R. Pantophlet, M. B. Zwick, G. M. Morris, P. M. Rudd, R. A. Dwek, R. L. Stanfield, D. R. Burton, I. A. Wilson, *Science* **2001**, *293*, 1155. doi:10.1126/SCIENCE.1061692
- J. S. Gach, P. G. Furtmüller, H. Quendler, P. Messner, R. Wagner, H. Katinger, R. Kunert, *J. Biol. Chem.* **2010**, *285*, 1122. doi:10.1074/JBC.M109.058792
- Y. Li, S. A. Migueles, B. Welcher, K. Svehla, A. Phogat, M. K. Louder, X. Wu, G. M. Shaw, M. Connors, R. T. Wyatt, J. R. Mascola, <http://www.nature.com/nm/journal/v13/n9/full/nm1624.html-a1#a1>, *Nat. Med.* **2007**, *13*, 1032. doi:10.1038/NM1624
- D. Corti, J. P. M. Langedijk, A. Hinz, M. S. Seaman, F. Vanzetta, B. M. Fernandez-Rodriguez, C. Silacci, D. Pinna, D. Jarrossay, S. Balla-Jhaghoorsingh, B. Willems, M. J. Zekveld, H. Dreja, E. O'Sullivan, C. Pade, C. Orkin, S. A. Jeffs, D. C. Montefiori, D. Davis, W. Weissenhorn, Á. McKnight, J. L. Heeney, F. Sallusto, Q. J. Sattentau, R. A. Weiss, A. Lanzavecchia, <http://www.plosone.org/article/info%3Adoi%2F10.1371%2Fjournal.pone.0008805-aff1#aff1>, *PLoS ONE* **2010**, *5*, e8805. doi:10.1371/JOURNAL.PONE.0008805
- A. Trkola, A. B. Pomales, H. Yuan, B. Korber, P. J. Maddon, G. P. Allaway, H. Katinger, C. F. Barbas, D. R. Burton, D. D. Ho, *J. Virol.* **1995**, *69*, 6609.
- M. Purtscher, A. Trkola, G. Gruber, A. Buchacher, R. Predl, F. Steindl, C. Tauer, R. Berger, N. Barrett, A. Jungbauer, H. Katinger, *AIDS Res. Hum. Retroviruses* **1994**, *10*, 1651. doi:10.1089/AID.1994.10.1651
- H. Stoiber, I. Frank, M. Spruth, M. Schwendinger, B. Mullauer, J. M. Windisch, R. Schneider, H. Katinger, I. Ando, M. P. Dierich, *Mol. Immunol.* **1997**, *34*, 855. doi:10.1016/S0161-5890(97)00108-9
- Z.-Y. J. Sun, K. J. Oh, M. Kim, J. Yu, V. Brusica, L. Song, Z. Qiao, J.-H. Wang, G. Wagner, E. L. Reinherz, *Immunity* **2008**, *28*, 52. doi:10.1016/J.IMMUNI.2007.11.018
- L. Song, Z.-Y. J. Sun, K. E. Coleman, M. B. Zwick, J. S. Gach, J.-H. Wang, E. L. Reinherz, G. Wagner, M. Kim, *Proc. Natl. Acad. Sci. USA* **2009**, *106*, 9057. doi:10.1073/PNAS.0901474106
- N. K. Jerne, J. Roland, P. A. Cazenave, *EMBO J.* **1982**, *1*, 243.
- R. E. Kunert, R. Weik, B. Ferko, G. Stiegler, H. Katinger, *AIDS* **2002**, *16*, 667. doi:10.1097/00002030-200203080-00020
- C. Sgro, *Toxicology* **1995**, *105*, 23. doi:10.1016/0300-483X(95)03123-W
- A. Mader, R. Kunert, *Protein Eng. Des. Sel.* **2010**, *23*, 947. doi:10.1093/PROTEIN/GZQ092
- N. Guex, M. C. Peitsch, *Electrophoresis* **1997**, *18*, 2714. doi:10.1002/ELPS.1150181505
- B. Lee, F. M. Richards, *J. Mol. Biol.* **1971**, *55*, 379. doi:10.1016/0022-2836(71)90324-X
- S. Bryson, J.-P. Julien, D. E. Isenman, R. Kunert, H. Katinger, E. F. Pai, *J. Mol. Biol.* **2008**, *382*, 910. doi:10.1016/J.JMB.2008.07.057
- M. P. Allen, D. J. Tildesley, *Computer Simulation of Liquids* **1987** (Oxford University Press: Oxford).
- J. S. Gach, H. Quendler, S. Strobach, H. Katinger, R. Kunert, *Mol. Immunol.* **2008**, *45*, 1027. doi:10.1016/J.MOLIMM.2007.07.030
- M. Christen, P. H. Hünenberger, D. Bakowies, R. Baron, R. Bürgi, D. P. Geerke, T. N. Heinz, M. A. Kastenholz, V. Kräutler, C. Oostenbrink, C. Peter, D. Trzesniak, W. F. van Gunsteren, *J. Comput. Chem.* **2005**, *26*, 1719. doi:10.1002/JCC.20303
- C. Oostenbrink, A. Villa, A. E. Mark, W. F. Van Gunsteren, *J. Comput. Chem.* **2004**, *25*, 1656. doi:10.1002/JCC.20090
- H. J. C. Berendsen, J. P. M. Postma, W. F. Van Gunsteren, J. Hermans, *Interaction Models for Water in Relation to Protein Hydration*, in *Intermolecular Forces* **1981**, pp. 331–342 (Reidel: Dordrecht, The Netherlands).
- H. Bekker, J. P. Van Den Berg, T. A. Wassenaar, *J. Comput. Chem.* **2004**, *25*, 1037. doi:10.1002/JCC.20050
- H. J. C. Berendsen, J. P. M. Postma, W. F. van Gunsteren, A. DiNola, J. R. Haak, *J. Chem. Phys.* **1984**, *81*, 3684. doi:10.1063/1.448118
- J.-P. Ryckaert, G. Cicciotti, H. J. C. Berendsen, *J. Comput. Phys.* **1977**, *23*, 327. doi:10.1016/0021-9991(77)90098-5
- I. G. Tironi, R. Sperb, P. E. Smith, W. F. van Gunsteren, *J. Chem. Phys.* **1995**, *102*, 5451. doi:10.1063/1.469273
- T. N. Heinz, W. F. van Gunsteren, P. H. Hünenberger, *J. Chem. Phys.* **2001**, *115*, 1125. doi:10.1063/1.1379764
- J. G. Kirkwood, *J. Chem. Phys.* **1935**, *3*, 300. doi:10.1063/1.1749657
- B. L. Tembre, J. A. Mc Cammon, *Comput. Chem.* **1984**, *8*, 281. doi:10.1016/0097-8485(84)85020-2
- T. C. Beutler, A. E. Mark, R. C. van Schaik, P. R. Gerber, W. F. van Gunsteren, *Chem. Phys. Lett.* **1994**, *222*, 529. doi:10.1016/0009-2614(94)00397-1

Evaluation of the Potency of the Anti-Idiotypic Antibody Ab2/3H6 Mimicking gp41 as a HIV-1 Vaccine in a Rabbit Prime/Boost Study

A. Mader, R. Kunert*

Department of Biotechnology, Institute for Applied Microbiology, BOKU – University of Natural Resources and Life Sciences, Muthgasse 11, A-1190 Vienna, Austria

* correspondent author: email: renate.kunert@boku.ac.at

Running title: anti-idiotypic antibody HIV-1 vaccine

Abstract

The HIV-1 envelope protein harbors several conserved epitopes that are recognized by broadly neutralizing antibodies. One of these neutralizing sites, the MPER region of gp41, is targeted by one of the most potent and broadly neutralizing antibodies, 2F5. Different vaccination strategies and a lot of efforts have been undertaken to induce MPER neutralizing antibodies but little success has been achieved so far. We tried to consider the alternative anti-idiotypic vaccination approach for induction of 2F5-like antibodies. The previously developed and characterized anti-idiotypic antibody Ab2/3H6 was expressed as antibody fragment fusion protein with C-terminally attached immunomodulators and used for immunization of rabbits to induce antibodies specific for HIV-1. Interestingly only those rabbits immunized with immunogens fused with the immunomodulators developed the HIV-1 specific antibodies. Anti-anti-idiotypic antibodies were further affinity purified using a two-step affinity purification protocol which revealed that only little amount of the total rabbit IgG fraction contained HIV-1 specific antibodies. The characterization of the induced anti-anti-idiotypic antibodies showed specificity for the HIV-1 envelope protein gp140 and the linear epitope of 2F5 GGGELDKWASL. Despite specificity for the linear epitope and the truncated HIV-1 envelope protein these antibodies were not able to exhibit any virus neutralization activities. These results suggest that Ab2/3H6 alone is might not be suitable as a vaccine, but the combination with other immunogens it could be beneficial for induction of HIV-1 nAbs.

Introduction

Currently 33 million people are living with human immunodeficiency virus type 1 (HIV-1) worldwide. In 2009 2.6 million people became newly infected and 1.8 million people died in the course of AIDS [1]. During the last decades several efforts to induce HIV-1 defending neutralizing antibodies (nAbs) have failed but still one key feature for successful defense of HIV-1 is to develop a vaccine which stimulates the humoral immune system specifically [2-4]. The potency of nAbs alone and in combination was demonstrated by passive immunization and viral challenge in non-human primate models [5-8]. One of the most potent neutralizing HIV-1 Abs identified so far is the monoclonal Ab (mAb) 2F5 [9-13] which binds with high affinity to the membrane proximal external region (MPER) of the virus envelope glycoprotein gp41 [14,15]. Therefore the specific induction of likewise broadly nAbs against the MPER (2F5-like Abs) is a major goal for Ab-based HIV-1 vaccine strategies. Despite a strong humoral response to gp41 during the course of HIV-1 infection is evident [16], approaches to elicit cross-clade nAbs against the MPER region failed so far although various immunogens like envelope proteins, plasmid DNA or recombinant viral vectors have been used [17-19].

An alternative method to induce nAbs is the anti-idiotypic (Id) approach. This approach is based on the idiotypic network theory postulated by Jerne about the Ab (Ab1) - anti-Id Ab (Ab2) – anti-anti-Id Ab (Ab3) cascade stimulation, whereby specific anti-Id Abs can serve as an "internal image" of the target antigen and can be used to induce Abs that can bind to the cognate antigen [20]. Anti-Id Abs have been proposed as vaccines for cancer immunotherapy and significant success has been achieved using anti-Id vaccines mimicking tumor-associated antigens in animal studies [21-24] as well as in clinical trials [25]. The anti-Id Ab Ab2/3H6 was developed at the Department of Biotechnology [26] and is directed against mAb 2F5. The chimeric as well as humanized version of Ab2/3H6 significantly inhibits the binding of mAb 2F5 to its synthetic epitope ELDKWA in an equimolar ratio and also decreases the *in vitro* neutralization potency of mAb 2F5 in a dose-related manner [27-29]. Ab2/3H6 is therefore estimated to mimic the epitope of mAb 2F5 and would be of great therapeutic interest as an anti-Id HIV-1

vaccine. To improve the potency of the anti-Id Ab we designed fusion proteins consisting of Ab2/3H6 Ab fragments (Ab2/3H6^{Fab}) and C-terminally attached polypeptides to induce T-cell responses against the virus.

One molecule with a wide range of biological activities is the immune stimulatory cytokine interleukin 15 (IL15). It is involved in the activation and proliferation of CD8+ T-cells and natural killer T-cells, the maintenance of CD8+ memory cells, and the differentiation and maturation of B cells [30,31]. Previous studies have shown that the incorporation of IL15 into vaccinia-based smallpox vaccine [32] or tuberculosis vaccine [33] induces high avidity, long lived antigen specific memory T-cells as well as persistent antigen specific Ab responses.

Other interesting immunostimulatory peptides are the so-called “promiscuous” T-cell epitopes from tetanus toxin (TT), measles virus, or E6 transforming protein [34,35]. It has been proposed that T-cells provide “help” to B cells under genetic control which can be provided by incorporation into an effective vaccine. Previous studies showed that co-immunization of the consensus cavealin-1 binding domain peptide with the T-cell epitope from TT increased the production of HIV-1 nAbs in a macaque prime/boost study [36].

Therefore we recombinantly expressed fusion proteins of Ab2/3H6^{Fabs} with the IL15 and alternatively an epitope of TT, respectively. In this study we immunized rabbits with the different Ab2/3H6^{Fabs} and evaluated the humoral immune response as well as the neutralization potency of the obtained Ab3s to those generated with Ab2/3H6^{Fab} only.

Material and Methods

Ethics statement

Serological tests of rabbits were performed at the Institute of Small Farm Animals, Animal Production Research Center, Nitra (Slovakia) in accordance with Slovak and EU regulations concerning animal experiments (Slovak national law 115/1995). Study approval was issued based on the study protocol by ethics committee of the Institute of Small Farm Animals, Animal Production Research Centre Nitra under the approval ID SK P 28004.

Construction of expression vectors

The Ab2/3H6^{Fab} expression vector, containing the murine variable regions of Ab2/3H6 (ABP04229, ABP04230) and the human constant CH1 and Ckappa regions was described previously [27]. The plasmid pcDNA3 (Invitrogen) containing the CMV promoter and the neomycin phospho-transferase gene (neo) was used as backbone for the coding region of the HC genes of Ab2/3H6^{Fab}-IL15 and -TT. pIRESdhfr [37] was used as backbone for the coding region of the Ab2/3H6 LC. The genes of Ab2/3H6^{Fab}-IL15 heavy chain (HC) and Ab2/3H6 light chain (LC) were synthesized by Geneart (Regensburg, Germany) including the *Gaussia* luciferase signal peptide [38] for both, the HC and LC. The sequence of the human IL15 (P40933) gene was obtained from the UniProtKB/Swiss-Prot database. The TT epitope (YSYFPSV) [39] was introduced by PCR amplification of Ab2/3H6^{Fab} HC sequence with the sense primer 5'-accctggtgaccgtgtcc-3' and antisense primer 5'-aggagcggccgcctatacagatggaaaatatgaataggcagatcctcctccgcc-3' containing a *NotI* restriction site for exchange of the IL15 tag.

Expression of Ab2/3H6^{Fab} variants in CHO cells

Stable cell lines were generated by co-transfection of corresponding HC and LC plasmids into CHO dhfr negative cells (ATCC CRL-9096; [40]). Clones were selected with Geneticin G418 (Fisher Scientific) and methotrexate (MTX) (Sigma) in combination with limiting dilution subcloning. Collected supernatants were concentrated by the Stirred cell 8200 with UF Discs Ultracel RC 10 kD (Millipore) before purification.

Purification of Ab2/3H6^{Fab} variants

Purification of all Ab2/3H6^{Fab} variants was performed on a BioLogic Duo Flow chromatography system (Biorad). Concentrated animal cell culture supernatant was diluted 1:2 in buffer A (20 mM Na₂HPO₄, pH 7.2) and filtered through a 0.22 µm syringe filter (Millipore). The UNO Q 1.3 ml anion exchange (AIX) column (Biorad) was equilibrated with 5 column volumes (cv) buffer A. Five millilitre of the concentrated sample were loaded onto the column using direct injection via the DuoFlow F40 pump at a flow rate of 1 ml/min corresponding to a linear velocity of 155.9 cm/h. The column was washed with buffer A until the optical density returned to base line. Ab2/3H6^{Fab}s were

eluted from the AIX column using a 3 step gradient of 20, 40 and 100 % of buffer B (20 mM Na₂HPO₄, 1 M NaCl pH 7.2) in buffer A in 5 cv at a flow rate of 1.0 ml/min (155.9 cm/h). Ten microlitres samples from the eluted AIX chromatography fractions were analysed by SDS-PAGE and NN-silver stain. Quantification of Ab2/3H6^{Fab} was done by double sandwich enzyme-linked immunosorbent assay (ELISA). Ab2/3H6^{Fab} containing fractions were further purified on a Superdex 75 prep grade Tricorn 10/300 column (GE) with PBS as mobile phase at a flow rate of 0.5 ml/min, corresponding to a linear velocity of 38.2 cm/h.

Animals and Immunization

Ab2/3H6^{Fab}, -IL15, and -TT preparations were used for the immunisation of New Zealand white rabbits. Six rabbits (groups of two rabbits per preparation) were immunised subcutaneously and intramuscularly with 0.1 mg of purified Ab2/3H6^{Fab} proteins emulsified in complete Freund's adjuvant and boosted two times with the same Fab preparations in incomplete Freund's adjuvant at three-week intervals. Pre-immune sera were collected one day prior the first immunization step. Terminal bleeding and sera preparation were done ten days after the third immunisation step.

Purification of antibody fractions from crude sera

Purification of rabbit IgG

Purification of rabbit IgG from crude sera was performed on an Äkta Purifier chromatography system (GE) with the UNOsphere SUPra Mini cartridge column (Biorad). IgGs were eluted from the Protein A column using a step gradient of 80 % of buffer B (100 mM Glycin pH 3.5) in buffer A (100 mM Glycin, 100 mM NaCl, pH 7.0). Quantification of rabbit IgG was done by double sandwich ELISA.

Purification of gp140/ELDKWA specific Ab3s

Ab3s were purified from rabbit IgG fractions using an affinity column coupled with recombinant gp140 (HIV-1 cladeA, 92/UG/037) [41] and the synthetic 2F5 epitope (GGGELDKWASL). The affinity matrix was prepared with the AminoLink Plus Immobilization Kit (Thermo Scientific) following the manufacturer's instructions. Briefly, a mixture of 1.5 mg of recombinant gp140 (UG37) combined with 0.5 mg synthetic

GGGELDKWASL (both Polymun Scientific, Inc) was coupled to the beads using the pH 10 coupling procedure. Pooled rabbit IgG fractions were diluted 1:2 with binding buffer and 2 ml batches were incubated with the conjugated beads for 1h at RT. The eluted fractions were pooled and concentrated using Amicon Ultra-15 3k columns (Millipore).

Evaluation of humoral immune response

ELISA

Rabbit IgG, Ab2/3H6^{Fab}-specificity and HIV-envelope specificity were analysed by ELISA. The 96-well microtiter plates (Nunc) were coated over night at 4°C with 1 µg/mL of anti-rabbit IgG (Sigma), Ab2/3H6^{Fab}, UG37 or GGGELDKWASL peptide, respectively. Plates were blocked with PBS containing 3% BSA and 0.1% Tween 20 (RT, 1 h) and incubated with serial twofold dilutions of heat inactivated serum samples or purified rabbit IgG (RT, 1 h). After washing with PBS containing 0.1% Tween 20 plates were incubated with peroxidase-conjugated anti-rabbit IgG antibody (Sigma) and unbound antibody was removed by further washing. Reactions were visualised with o-phenylenediamine and H₂O₂ (Merck).

Bio-layer Interferometry (BLI)

BLI, a label-free technology was used for determination of binding affinity of Ab3s in comparison to mAb 2F5. Kinetic measurements were performed with an Octet QK equipped with amine reactive (AR) biosensor tips (fortéBio). Sensor tips were loaded with 25 µg/mL of UG37 protein according to the manufacturer's instructions. The assay was performed at 30°C in PBS buffer with 1000 rpm agitation. Association and dissociation curves were recorded for the individual samples and data were processed and analyzed using the Octet data analysis software 6.4 (fortéBio).

Neutralization assay

Pseudotyped virions were generated in HEK293T (ATCC: CRL-11268) cells by co-transfection with HIV-1 Env plasmid SF162 (NIHARRRP; contributed by L. Stamatatos and C. Cheng-Mayer) and the HIV-1 Env-deleted backbone plasmid pSG3^{ΔEnv} (NIHARRRP; contributed by J. Kappes and X. Wu), as previously described [42]. Virions were added to the same volume of serially diluted mAbs (starting at 25 µg/mL) and

incubated for 1 h at 37°C. Then, freshly trypsinized TZM-bl reporter cells (NIHARRRP; contributed by J.Kappes and X.Wu) (10,000 cells in 100 µL growth medium supplemented with DEAE-dextran at a final concentration of 10 µg/mL) were added and the plates were incubated at 37°C. After 48 to 72 h incubation, the medium was removed and 50 µL lysis buffer (25 mM glycylglycin, 15 mM MgSO₄, 4 mM EDTA, 1% Triton X-100 in H₂O, pH 7.8) was added. Finally, 50 µL Bright-Glo reagent (Promega) was added and luminescence was measured using a luminometer (Tecan). All experiments were performed at least in duplicate. The IC₅₀ was calculated with GraphPad Prism 5.04 (GraphPad Software, Inc.) using a four parameter fit.

Results

Expression and purification of Ab2/3H6^{Fab} fusion proteins

To increase the specific anti-I_D immune response in a rabbit prime/boost regime two different Ab2/3H6^{Fab} fusion proteins were designed (Figure 1A). For the first fusion protein the sequence of the human IL15 was fused to the CH1 domain of Ab2/3H6^{Fab} and cloned into pcDNA3 to obtain the plasmid pAb2/3H6^{Fab}-IL15. For the second fusion protein the IL15 sequence in the vector pAb2/3H6^{Fab}-IL15 was replaced for the TT epitope sequence to obtain the expression plasmid pAb2/3H6^{Fab}-TT. Each plasmid in combination with pAb2/3H6LC was used to generate stable recombinant CHO cell lines. Approximately two mg of each of the recombinant Ab2/3H6^{Fab} variants were purified on a Q-Sepharose column followed by a SEC polishing step. The previously developed recombinant cell line expressing Ab2/3H6^{Fab} [27] was used for purification of Ab2/3H6^{Fab}. Purified proteins were analyzed by ELISA, SDS-PAGE and Western Blot (Figure 1B).

Humoral immune response in rabbits

New Zealand white rabbits were immunized with different Ab2/3H6^{Fab} variants in duplicates in a prime/boost regime. Ten days after the final boost animals were bled to death and serum was collected. Pre-immune sera and immune sera of all animals were screened for total rabbit IgG content ranging from 9 to 22 mg/ml per animal.

Immunization with the IL15 or TT fusion protein did not increase total IgG levels significantly compared to immunization with Ab2/3H6^{Fab}. Figure 2 shows that immunization with Ab2/3H6^{Fab}, Ab2/3H6^{Fab}-IL15 and Ab2/3H6^{Fab}-TT leads to 70%, 50% and 20% increase of total rabbit IgG compared to the pre-immune IgG levels, respectively. IgG was purified from rabbit sera to avoid unspecific binding of accompanied serum proteins. Samples from individual rabbits were coded accordingly: Fab-1 and Fab-2 for Ab2/3H6^{Fab} immunized animals; IL15-1 and IL15-2 for Ab2/3H6^{Fab}-IL15 immunized animals and TT-1 and TT-2 for Ab2/3H6^{Fab}-TT immunized animals.

Specificity against Ab2/3H6^{Fab} and HIV-1 epitopes

Ab2/3H6^{Fab} specificity of IgG fractions was estimated in an ELISA starting with a concentration of 10 µg/ml rabbit IgG. Fab-1, Fab-2, IL15-1, IL15-2 and TT-1 samples show a similar binding curve resulting in cut-off concentrations between 0.2 µg/ml and 0.5 µg/ml whereas the TT-2 sample shows weaker binding (Figure 3).

Additionally, the IgG samples were tested for the presence of HIV-1 specific Ab3s on UG37 coated ELISA plates with a starting concentration of 125 µg/ml rabbit IgG. Fab-1, Fab-2 and TT-1 did not bind at all to the HIV-1 envelope protein UG37 despite the immunized rabbits developed antibodies with high specificity for the immunogen Ab2/3H6^{Fab}. Nevertheless, the rabbit IgG samples IL15-1, IL15-2 and TT-2 showed significant specificity to UG37 as shown in Figure 3. Cut-off values are summarized in Table 1. Binding specificity towards the linear epitope GGGELDKWASL could not be evaluated because the control IgG fractions showed strong cross reactivity (data not shown).

This data demonstrate impressively that the polyclonal immune response of rabbits is highly specific for the applied antigen but only a limited amount of Abs are generated against the structure of Ab2/3H6 which mimicks the HIV-1 envelope.

Characterization of the affinity purified Ab3 pool

To further reduce unspecific binding Ab3s were isolated from a pool of rabbit IgG samples IL15-1, IL15-2 and TT-2 with a second affinity purification step, using a UG37/GGGELDKWASL coupled column. The results of the affinity purification step are

summarized in Table 2 and show that only 0.7 % of the rabbit IgG fraction contained UG37/GGELDKWASL binding Abs.

After affinity purification the Ab3 fraction was tested for specificity to UG37 and the linear epitope GGELDKWASL starting with 1 µg/ml rabbit IgG in ELISA. UG37 and GGELDKWASL specificity was estimated by cut-off values, resulting in more than the two-fold OD value of the control IgG fraction. In Figure 4A the concentrations of the purified Ab3 fraction are blotted against the obtained OD-values indicating a 10-fold stronger binding to UG37 (cut-off 42 ng/ml) than to the linear epitope GGELDKWASL (cut-off 400 ng/ml) (Figure 4B). In comparison mAb 2F5 exhibits a 2-fold weaker binding to UG37 (cut-off 15ng/ml) than to GGELDKWASL (cut-off 7 ng/ml) (data not shown). These differences might reflect different conformations of the 2F5 epitope in the UG37 protein and the linear peptide GGELDKWASL.

To confirm the ELISA data we compared the affinity of the UG37 specific Ab3 pool with the mAb 2F5 using UG37 coated sensor tips in a biolayer interferometry assay. The concentration of protein used for this assay was 400 nM and the assay was done in triplicates. Figure 5 displays the association and dissociation curves of mAb 2F5, the affinity purified Ab3 fraction and an unspecific IgG sample indicating specific binding and dissociation for both samples. The calculated k-values are summarized in Table 2. The binding properties of mAb 2F5 and the Ab3 pool to UG37 are comparable indicated by the k_{on} -values, but the affinity of mAb 2F5 to UG37 is stronger than of the Ab3 fraction caused by a 6-fold lower k_{off} -value. Therefore the overall calculated affinity of the Ab3 fraction described by the K_D -value is 6.6 –fold lower compared to the mAb 2F5. The different signal intensity measured in the assay can be explained by using identical concentrations of the monoclonal 2F5 and the polyclonal Ab3 sample.

Neutralization assay

To investigate the neutralization potency of the purified gp140 binding Ab3 fraction a TZM-bl Env-pseudotyped virus assay against the HIV-1 SF162 Env clone was performed. In this assay mAb 2F5 inhibits entry of the pseudotyped virus with an IC_{50} of 130 ng/ml. The purified Ab3s induced by immunization of rabbits with Ab2/3H6 shows no neutralization activity (data not shown).

Discussion

The global HIV pandemic is still expanding and thus the development of a preventive vaccine is of high priority. One approach is to elicit broadly nAbs (bnAb) against the MPER region that resemble similar potency as the mAb 2F5. In previous studies MPER-containing proteins [43,44] or MPER-containing peptides [45-47] failed to elicit bnAbs, eventually due to the poor immunogenicity of the MPER [19]. It was suggested that the native gp41 exodomain is structurally more complex than represented by the linear epitope [48,49] and thus incorrect conformation of MPER-based peptide immunogens result in suboptimal presentation of neutralizing epitopes [50,51]. Additionally, a so far unidentified part of a second epitope has been considered [52]. This possible second epitope could be an alpha-helix turn C-terminal of the core epitope DKW [53] or membrane compounds [54-56] which interact with the long CDR-H3 loop of mAb 2F5. This rather complex neutralizing epitope calls for an alternative vaccine approach and we decided to continue with anti-Id antibodies. In previous studies Ab2/3H6 showed promising results mimicking the gp41 epitope of mAb 2F5. Gach et al. demonstrated that Ab2/3H6 is able to inhibit the binding of mAb 2F5 to its synthetic epitope ELDKWA and induces Ab3s (2F5-like Abs) in a mouse immunization study [27,28]. However, in these former studies only binding assays against gp160 and the linear epitope ELDKWA were performed. To get a deeper insight into the binding mechanism of Ab2/3H6 to mAb 2F5 co-crystallization of Ab2/3H6 in complex with mAb 2F5 was performed. This study revealed that Ab2/3H6 only partly overlaps with the HIV-1 epitope on mAb 2F5 but does not center on the core epitope binding site of mAb 2F5. Thus the Ab was classified as a gamma-class anti-Id Ab [57]. However, since mAb 2F5 crystals were generated with a small peptide of the MPER only, the exact binding mechanism of mAb 2F5 to HIV remains elusive and the most critical paratope responsible for the neutralization activity of mAb 2F5 might not be identified yet.

In this study we aimed to induce 2F5-like Abs using an anti-Id network approach, instead of using MPER epitopes to elicit nAbs. We constructed Fab fusion proteins of Ab2/3H6 containing the molecular adjuvant IL15 or a “promiscuous” T-cell epitope of TT and administered them in a rabbit prime/boost regime. Total rabbit IgG levels, Ab2/3H6^{Fab}

and specificity for HIV-1 epitopes were measured in an ELISA showing that the use of IL15 and TT as immune stimulators do not significantly influence total rabbit IgG levels (Figure 2). However, after purification of rabbit IgG it could be demonstrated impressively that UG37 binding Abs (Ab3s) were induced significantly (Figure 3) in 50% of all animals. The binding assays with the 2F5 peptide epitope could not be exploited since the control IgG cross reacted with GGGELDKWASL. Therefore selected rabbit IgG samples were affinity purified using a UG37/GGGELDKWASL coupled column which resulted in less than 1 % of the rabbit IgG fraction (Table 2). This affinity enriched Ab3 fraction shows significant binding to UG37 and also considerable interaction with the synthetic linear 2F5 epitope GGGELDKWASL (Figure 4). Further affinity binding studies revealed that the obtained Ab3 fraction has only a 6.6-fold lower affinity to the UG37 protein compared to the mAb 2F5 (Table 3), indicating a similar binding strength of the Ab2/3H6 induced Ab3s like the original mAb 2F5. Since the neutralization assays failed to indicate that nAbs were generated in rabbits, we favour the hypothesis of a second epitope that is responsible for the neutralization potency of mAb 2F5. Additionally the long H3 loop of mAb 2F5 indicates that the Ab has experienced intensive somatic mutagenesis and it is questionable if a seven week prime/boost schedule can represent the maturation of the human immune system.

To conclude on this study, Ab2/3H6 shows the ability to induce Abs against the HIV-1 envelope protein UG37 as well as the synthetic epitope of mAb 2F5. Despite the induced Ab3s were not able to inhibit infection of TZM-bl cells in an Env-pseudotyped neutralization assay Ab2/3H6 at least mimicks part of the epitope of mAb 2F5 as demonstrated by ELISA and BLI affinity measurements.

After decades of intense research regarding the induction of 2F5-like Abs a potent immunogen that is able to induce bn 2F5-like Abs is still missing. Deciphering the complete and correct mechanism on how mAb 2F5 prevents gp41 to fuse with the host cell membrane is the major task in developing HIV-1 vaccines able to induce broadly neutralizing anti-MPER Abs. Unfortunately, the anti-Id approach using Ab2/3H6 does not lead to the desired outcome. Therefore Ab2/3H6 alone is not suitable as a vaccine, but the combination with other immunogens or membranes as adjuvants [58] might be beneficial for induction of HIV nAbs.

Acknowledgements

The authors thank Boris Ferko and Lubomir Ondruska from the Institute of Small Farm Animals (Slovakia), for immunization of rabbits and preparation of rabbit sera as well as Heribert Quendler for performing the neutralization assays. This work was supported by the Austrian Science Fund (FWF; www.fwf.ac.at); Project number: P20603-B13. The funders had no role in study design, data collection and analysis, decision to publish, or preparation of the manuscript.

Authors contribution

Conceived and designed the experiments: AM, RK Performed the experiments: AM
Analyzed the data: AM Wrote the paper: AM, RK

References

1. HIV/AIDS UJPo (2010) *Global Report: UNAIDS Report on the Global AIDS Epidemic: 2010*.
2. Plotkin S (2008) Vaccines: correlates of vaccine-induced immunity. *Clin Infect Dis* 47: 401-409.
3. Amanna IJ, Slifka MK (2009) Wanted, dead or alive: new viral vaccines. *Antiviral Res* 84: 119-130.
4. Zinkernagel RM (2003) On natural and artificial vaccinations. *Annu Rev Immunol* 21: 515-546.
5. Mascola JR, Stiegler G, VanCott TC, Katinger H, Carpenter CB, et al. (2000) Protection of macaques against vaginal transmission of a pathogenic HIV-1/SIV chimeric virus by passive infusion of neutralizing antibodies. *Nat Med* 6: 207-210.
6. Veazey RS, Shattock RJ, Pope M, Kirijan JC, Jones J, et al. (2003) Prevention of virus transmission to macaque monkeys by a vaginally applied monoclonal antibody to HIV-1 gp120. *Nat Med* 9: 343-346.
7. Hessel AJ, Rakasz EG, Poignard P, Hangartner L, Landucci G, et al. (2009) Broadly neutralizing human anti-HIV antibody 2G12 is effective in protection against mucosal SHIV challenge even at low serum neutralizing titers. *PLoS Pathog* 5: e1000433.
8. Hessel AJ, Rakasz EG, Tehrani DM, Huber M, Weisgrau KL, et al. (2010) Broadly neutralizing monoclonal antibodies 2F5 and 4E10 directed against the human immunodeficiency virus type 1 gp41 membrane-proximal external region protect against mucosal challenge by simian-human immunodeficiency virus SHIVBa-L. *J Virol* 84: 1302-1313.
9. Buchacher A, Predl R, Strutzenberger K, Steinfellner W, Trkola A, et al. (1994) Generation of human monoclonal antibodies against HIV-1 proteins; electrofusion and Epstein-Barr virus transformation for peripheral blood lymphocyte immortalization. *AIDS Res Hum Retroviruses* 10: 359-369.

10. Purtscher M, Trkola A, Gruber G, Buchacher A, Predl R, et al. (1994) A broadly neutralizing human monoclonal antibody against gp41 of human immunodeficiency virus type 1. *AIDS Res Hum Retroviruses* 10: 1651-1658.
11. Mehandru S, Wrin T, Galovich J, Stiegler G, Vcelar B, et al. (2004) Neutralization profiles of newly transmitted human immunodeficiency virus type 1 by monoclonal antibodies 2G12, 2F5, and 4E10. *J Virol* 78: 14039-14042.
12. Kunert R, Steinfeldner W, Purtscher M, Assadian A, Katinger H (2000) Stable recombinant expression of the anti HIV-1 monoclonal antibody 2F5 after IgG3/IgG1 subclass switch in CHO cells. *Biotechnol Bioeng* 67: 97-103.
13. Kunert R, R ker F, Katinger H (1998) Molecular characterization of five neutralizing anti-HIV type 1 antibodies: identification of nonconventional D segments in the human monoclonal antibodies 2G12 and 2F5. *AIDS Res Hum Retroviruses* 14: 1115-1128.
14. Stoiber H, Frank I, Spruth M, Schwendinger M, Mullauer B, et al. (1997) Inhibition of HIV-1 infection in vitro by monoclonal antibodies to the complement receptor type 3 (CR3): an accessory role for CR3 during virus entry? *Mol Immunol* 34: 855-863.
15. Stiegler G, Kunert R, Purtscher M, Wolbank S, Voglauer R, et al. (2001) A potent cross-clade neutralizing human monoclonal antibody against a novel epitope on gp41 of human immunodeficiency virus type 1. *AIDS Res Hum Retroviruses* 17: 1757-1765.
16. Opalka D, Pessi A, Bianchi E, Ciliberto G, Schleif W, et al. (2004) Analysis of the HIV-1 gp41 specific immune response using a multiplexed antibody detection assay. *J Immunol Methods* 287: 49-65.
17. Hu SL, Stamatatos L (2007) Prospects of HIV Env modification as an approach to HIV vaccine design. *Curr HIV Res* 5: 507-513.
18. Karlsson Hedestam GB, Fouchier RA, Phogat S, Burton DR, Sodroski J, et al. (2008) The challenges of eliciting neutralizing antibodies to HIV-1 and to influenza virus. *Nat Rev Microbiol* 6: 143-155.
19. Montero M, van Houten NE, Wang X, Scott JK (2008) The membrane-proximal external region of the human immunodeficiency virus type 1 envelope: dominant site of antibody neutralization and target for vaccine design. *Microbiol Mol Biol Rev* 72: 54-84, table of contents.

20. Jerne N (1974) Towards a network theory of the immune system. *Ann Immunol (Paris)* 125C: 373-389.
21. Ladjemi MZ, Chardes T, Cognac S, Garambois V, Morisseau S, et al. (2011) Vaccination with human anti-trastuzumab anti-idiotypic scFv reverses HER2 immunological tolerance and induces tumor immunity in MMTV.f.huHER2(Fo5) mice. *Breast Cancer Res* 13: R17.
22. Ramos AS, Parise CB, Travassos LR, Han SW, de Campos-Lima PO, et al. (2011) The idiotype (Id) cascade in mice elicited the production of anti-R24 Id and anti-anti-Id monoclonal antibodies with antitumor and protective activity against human melanoma. *Cancer Sci* 102: 64-70.
23. Lee G, Ge B (2010) Inhibition of in vitro tumor cell growth by RP215 monoclonal antibody and antibodies raised against its anti-idiotypic antibodies. *Cancer Immunol Immunother* 59: 1347-1356.
24. Wang JJ, Li YH, Liu YH, Song J, Guo FJ, et al. (2010) The ability of human bispecific anti-idiotypic antibody to elicit humoral and cellular immune responses in mice. *Int Immunopharmacol* 10: 707-712.
25. de Cerio AL, Zabalegui N, Rodríguez-Calvillo M, Inogés S, Bendandi M (2007) Anti-idiotypic antibodies in cancer treatment. *Oncogene* 26: 3594-3602.
26. Kunert R, Weik R, Ferko B, Stiegler G, Katinger H (2002) Anti-idiotypic antibody Ab2/3H6 mimics the epitope of the neutralizing anti-HIV-1 monoclonal antibody 2F5. *AIDS* 16: 667-668.
27. Gach J, Quendler H, Weik R, Katinger H, Kunert R (2007) Partial humanization and characterization of an anti-idiotypic antibody against monoclonal antibody 2F5, a potential HIV vaccine? *AIDS Res Hum Retroviruses* 23: 1405-1415.
28. Gach J, Quendler H, Strobach S, Katinger H, Kunert R (2008) Structural analysis and in vivo administration of an anti-idiotypic antibody against mAb 2F5. *Mol Immunol* 45: 1027-1034.
29. Mader A, Kunert R (2010) Humanization strategies for an anti-idiotypic antibody mimicking HIV-1 gp41. *Protein Eng Des Sel* 23: 947-954.
30. Waldmann TA (2006) The biology of interleukin-2 and interleukin-15: implications for cancer therapy and vaccine design. *Nat Rev Immunol* 6: 595-601.

31. Rodrigues L, Bonorino C (2009) Role of IL-15 and IL-21 in viral immunity: applications for vaccines and therapies. *Expert Rev Vaccines* 8: 167-177.
32. Perera LP, Waldmann TA, Mosca JD, Baldwin N, Berzofsky JA, et al. (2007) Development of smallpox vaccine candidates with integrated interleukin-15 that demonstrate superior immunogenicity, efficacy, and safety in mice. *J Virol* 81: 8774-8783.
33. Kolibab K, Yang A, Derrick SC, Waldmann TA, Perera LP, et al. (2010) Highly persistent and effective prime/boost regimens against tuberculosis that use a multivalent modified vaccine virus Ankara-based tuberculosis vaccine with interleukin-15 as a molecular adjuvant. *Clin Vaccine Immunol* 17: 793-801.
34. Panina-Bordignon P, Tan A, Termijtelen A, Demotz S, Corradin G, et al. (1989) Universally immunogenic T cell epitopes: promiscuous binding to human MHC class II and promiscuous recognition by T cells. *Eur J Immunol* 19: 2237-2242.
35. Kaumaya PT, Kobs-Conrad S, Seo YH, Lee H, VanBuskirk AM, et al. (1993) Peptide vaccines incorporating a 'promiscuous' T-cell epitope bypass certain haplotype restricted immune responses and provide broad spectrum immunogenicity. *J Mol Recognit* 6: 81-94.
36. Benferhat R, Martinon F, Krust B, Le Grand R, Hovanessian AG (2009) The CBD1 peptide corresponding to the caveolin-1 binding domain of HIV-1 glycoprotein gp41 elicits neutralizing antibodies in cynomolgus macaques when administered with the tetanus T helper epitope. *Mol Immunol* 46: 705-712.
37. Kunert R, Wolbank S, Stiegler G, Weik R, Katinger H (2004) Characterization of molecular features, antigen-binding, and in vitro properties of IgG and IgM variants of 4E10, an anti-HIV type 1 neutralizing monoclonal antibody. *AIDS Res Hum Retroviruses* 20: 755-762.
38. Knappskog S, Ravneberg H, Gjerdrum C, Trösse C, Stern B, et al. (2007) The level of synthesis and secretion of *Gaussia princeps* luciferase in transfected CHO cells is heavily dependent on the choice of signal peptide. *J Biotechnol* 128: 705-715.
39. Ho PC, Mutch DA, Winkel KD, Saul AJ, Jones GL, et al. (1990) Identification of two promiscuous T cell epitopes from tetanus toxin. *Eur J Immunol* 20: 477-483.

40. Urlaub G, Chasin L (1980) Isolation of Chinese hamster cell mutants deficient in dihydrofolate reductase activity. *Proc Natl Acad Sci U S A* 77: 4216-4220.
41. Jeffs SA, Goriup S, Kebble B, Crane D, Bolgiano B, et al. (2004) Expression and characterisation of recombinant oligomeric envelope glycoproteins derived from primary isolates of HIV-1. *Vaccine* 22: 1032-1046.
42. Li M, Gao F, Mascola JR, Stamatatos L, Polonis VR, et al. (2005) Human immunodeficiency virus type 1 env clones from acute and early subtype B infections for standardized assessments of vaccine-elicited neutralizing antibodies. *J Virol* 79: 10108-10125.
43. Zhang MY, Wang Y, Mankowski MK, Ptak RG, Dimitrov DS (2009) Cross-reactive HIV-1-neutralizing activity of serum IgG from a rabbit immunized with gp41 fused to IgG1 Fc: possible role of the prolonged half-life of the immunogen. *Vaccine* 27: 857-863.
44. Kim M, Qiao Z, Yu J, Montefiori D, Reinherz EL (2007) Immunogenicity of recombinant human immunodeficiency virus type 1-like particles expressing gp41 derivatives in a pre-fusion state. *Vaccine* 25: 5102-5114.
45. Wang Z, Liu Z, Cheng X, Chen YH (2005) The recombinant immunogen with high-density epitopes of ELDKWA and ELDEWA induced antibodies recognizing both epitopes on HIV-1 gp41. *Microbiol Immunol* 49: 703-709.
46. Joyce JG, Hurni WM, Bogusky MJ, Garsky VM, Liang X, et al. (2002) Enhancement of alpha -helicity in the HIV-1 inhibitory peptide DP178 leads to an increased affinity for human monoclonal antibody 2F5 but does not elicit neutralizing responses in vitro. Implications for vaccine design. *J Biol Chem* 277: 45811-45820.
47. Ho J, MacDonald KS, Barber BH (2002) Construction of recombinant targeting immunogens incorporating an HIV-1 neutralizing epitope into sites of differing conformational constraint. *Vaccine* 20: 1169-1180.
48. Lorizate M, Cruz A, Huarte N, Kunert R, Pérez-Gil J, et al. (2006) Recognition and blocking of HIV-1 gp41 pre-transmembrane sequence by monoclonal 4E10 antibody in a Raft-like membrane environment. *J Biol Chem* 281: 39598-39606.

49. Menendez A, Chow KC, Pan OC, Scott JK (2004) Human immunodeficiency virus type 1-neutralizing monoclonal antibody 2F5 is multispecific for sequences flanking the DKW core epitope. *J Mol Biol* 338: 311-327.
50. Ofek G, Tang M, Sambor A, Katinger H, Mascola J, et al. (2004) Structure and mechanistic analysis of the anti-human immunodeficiency virus type 1 antibody 2F5 in complex with its gp41 epitope. *J Virol* 78: 10724-10737.
51. Cardoso R, Zwick M, Stanfield R, Kunert R, Binley J, et al. (2005) Broadly neutralizing anti-HIV antibody 4E10 recognizes a helical conformation of a highly conserved fusion-associated motif in gp41. *Immunity* 22: 163-173.
52. Julien JP, Bryson S, Nieva JL, Pai EF (2008) Structural details of HIV-1 recognition by the broadly neutralizing monoclonal antibody 2F5: epitope conformation, antigen-recognition loop mobility, and anion-binding site. *J Mol Biol* 384: 377-392.
53. Bryson S, Julien JP, Hynes RC, Pai EF (2009) Crystallographic definition of the epitope promiscuity of the broadly neutralizing anti-human immunodeficiency virus type 1 antibody 2F5: vaccine design implications. *J Virol* 83: 11862-11875.
54. Alam SM, Morelli M, Dennison SM, Liao HX, Zhang R, et al. (2009) Role of HIV membrane in neutralization by two broadly neutralizing antibodies. *Proc Natl Acad Sci U S A* 106: 20234-20239.
55. Scherer EM, Leaman DP, Zwick MB, McMichael AJ, Burton DR (2010) Aromatic residues at the edge of the antibody combining site facilitate viral glycoprotein recognition through membrane interactions. *Proc Natl Acad Sci U S A* 107: 1529-1534.
56. Ofek G, McKee K, Yang Y, Yang ZY, Skinner J, et al. (2010) Relationship between antibody 2F5 neutralization of HIV-1 and hydrophobicity of its heavy chain third complementarity-determining region. *J Virol* 84: 2955-2962.
57. Bryson S, Julien J, Isenman D, Kunert R, Katinger H, et al. (2008) Crystal structure of the complex between the F(ab)' fragment of the cross-neutralizing anti-HIV-1 antibody 2F5 and the F(ab) fragment of its anti-idiotypic antibody 3H6. *J Mol Biol* 382: 910-919.
58. Maeso R, Huarte N, Julien JP, Kunert R, Pai EF, et al. (2011) Interaction of Anti-HIV Type 1 Antibody 2F5 with Phospholipid Bilayers and Its Relevance for the Mechanism of Virus Neutralization. *AIDS Res Hum Retroviruses*.

Figure legends

Figure 1. Design and purification of Ab2/3H6^{Fab} variants.

Three different Ab2/3H6^{Fab} preparations were developed for the immunization study. Panel **A.** displays **(a)** the Fab-fragment of Ab2/3H6 named Ab2/3H6^{Fab}. **(b)** human IL15 fused to Ab2/3H6^{Fab} named Ab2/3H6^{Fab}-IL15 and **(c)** a tetanus toxin epitope fused to Ab2/3H6^{Fab} named Ab2/3H6^{Fab}-TT. Panel **B.** shows the non-reduced SDS-gel on the left side and the Western Blot on the right side of purified Fabs. The lanes 1 represents Ab2/3H6^{Fab}-TT (49 kD); lane 2: Ab2/3H6^{Fab}-IL15 (61 kD); lane 3: Ab2/3H6^{Fab} (47 kD) and M represents the marker. The double band is significant for glycosylated Ab2/3H6. The gel was silver stained and the Western Blot was developed using an anti-human Fab specific antibody. Bands were visualized with NBT/BCIP.

Figure 2. Quantification of total IgG from rabbit sera.

Rabbit IgG from pre-immune (shaded bars) and immune sera (full bars) were quantified by sandwich ELISA. Data was averaged from two individual rabbits in each immunized group (Fab for Ab2/3H6^{Fab}, IL15 for Ab2/3H6^{Fab}-IL15 and TT for Ab2/3H6^{Fab}-TT immunized rabbits) and assayed in duplicates; error bars represents mean \pm standard deviation.

Figure 3. Binding of different immunized rabbit IgG fractions to Ab2/3H6^{Fab} and UG37.

Purified rabbit IgG fractions immunized with different Fab preparations and the pre-immune IgG fraction (control) were tested in a binding ELISA for Ab2/3H6^{Fab} and UG37 specificity. Diluted IgG fractions from individual rabbits (Fab for Ab2/3H6^{Fab}, IL15 for Ab2/3H6^{Fab}-IL15 and TT for Ab2/3H6^{Fab}-TT immunized rabbits) are blotted against the OD-value.

Figure 4. Binding of 2F5-like Ab fraction to UG37 and ELDKWA.

Affinity purified Ab3 fraction from pooled rabbit IgG fractions were tested in a binding ELISA for **A.** UG37 and **B.** ELDKWA specificity. Diluted Ab fraction is blotted against the

OD-value. For control the rabbit IgG fraction from the flow-through of the affinity purification step was used.

Figure 5. Affinity measurement of Ab3 fraction to UG37

Affinity purified Ab3 fraction, the negative control (rabbit IgG fraction from the flow-through of the affinity purification step) and mAb 2F5 were tested in a BLI assay for binding affinity to UG37. Binding curves of mAb 2F5 (red), Ab3 fraction (blue) and control fraction (green) are displayed. The assay was set up in triplicates. The data was fitted using the 1:1 model (solid lines).

Tables

Table 1. Cut-off values ($\mu\text{g/ml}$) calculated from ELISA data

Rabbit sample	Cut off values with different antigen	
	Ab2/3H6 ^{Fab(1)}	UG37 ⁽²⁾
Fab-1	0.3	>125
Fab-2	0.5	>125
IL15-1	0.5	21.0
IL15-2	0.2	7.0
TT-1	0.4	>125
TT-2	1.4	5.5

(1) estimated cut-off values resulting in more than the 5-fold OD-value

(2) estimated cut-off values resulting in more than the 2-fold OD-value

Table 2. Mass balance of Ab3 affinity purification

	total IgG [$\mu\text{g/ml}$]	Yield [% of rabbit IgG]
rabbit IgG	4500	-
Flow through	3810	84.6
Wash	154	3.4
Ab3 pool	31	0.7

The total rabbit IgG recovery after each run was approximately 89 %

Table 3. Summary of k-values for binding to UG37

Samples [c=400nM]	kon [1/Ms]	koff [1/s]	KD [nM]
mAb 2F5	1.66×10^{04}	3.09×10^{-04}	18.65
Ab3 fraction	1.56×10^{04}	1.91×10^{-03}	122.90
Control IgG fraction	n.d.	n.d.	n.d.

Figure 1

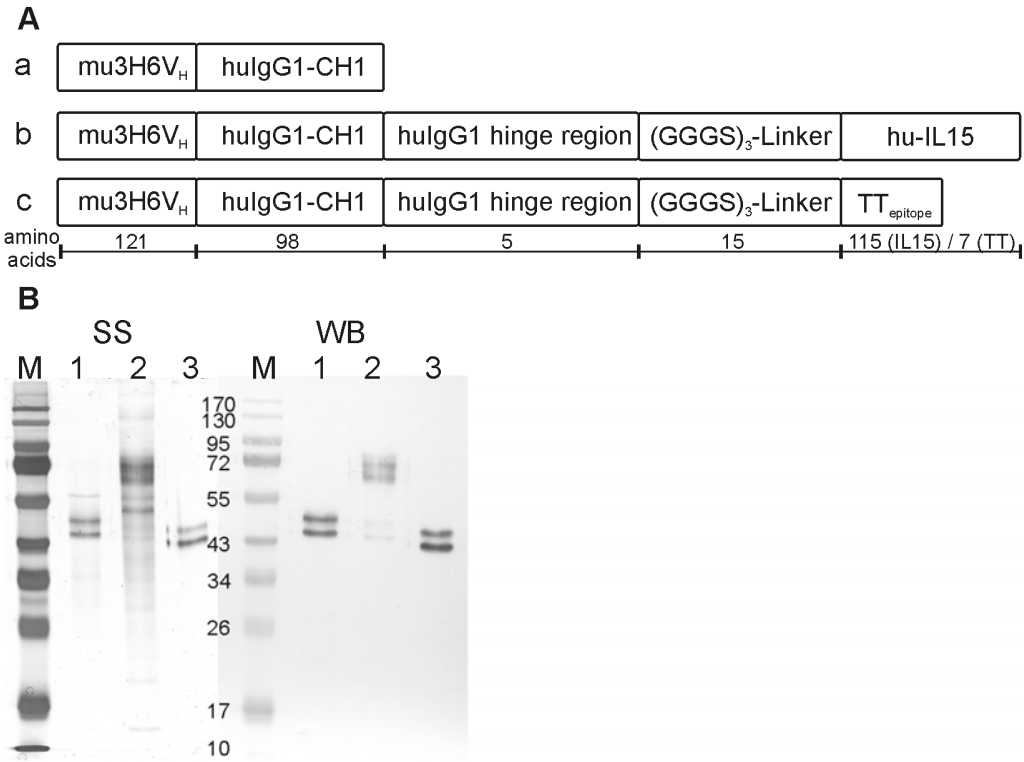


Figure 2

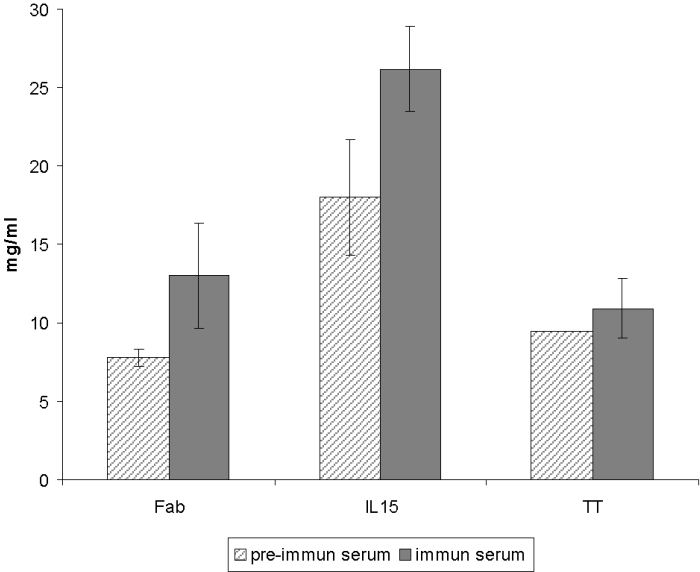


Figure 3

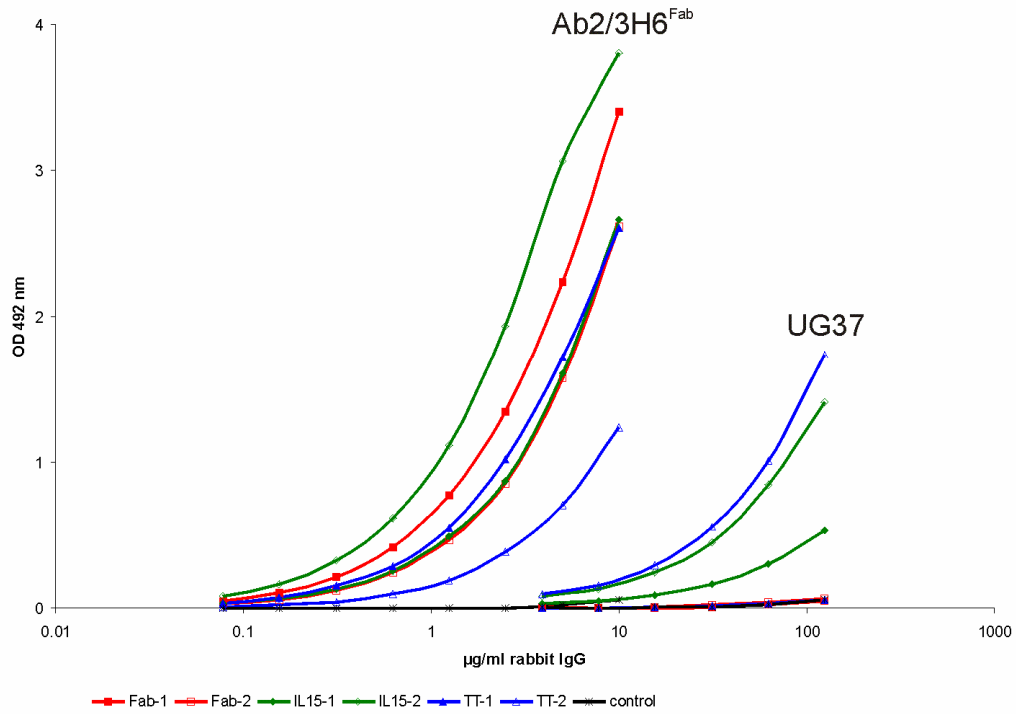


Figure 4

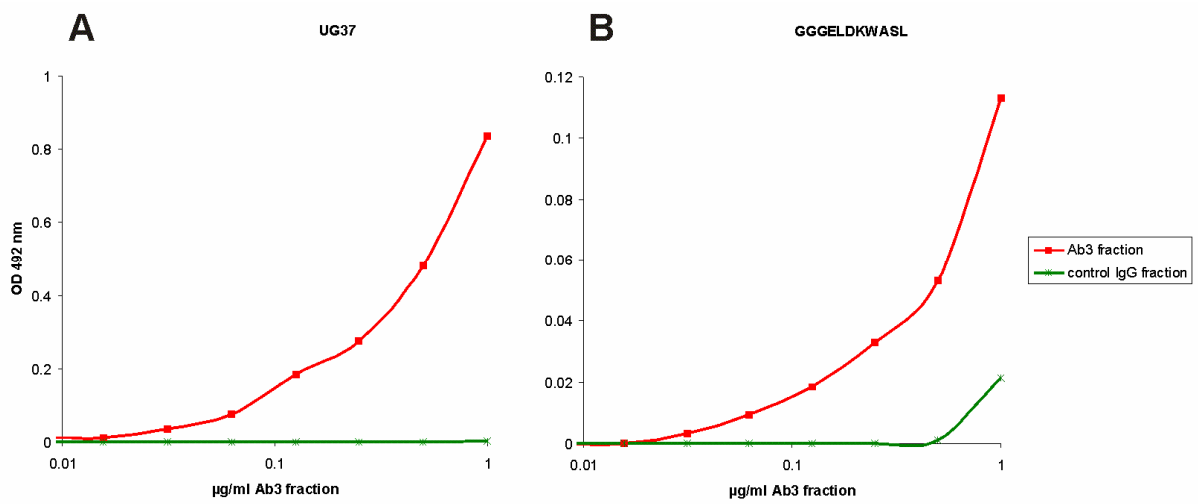


Figure 5

